frontiers | Research Topics

Omics research in canine and feline microbiome: implications for veterinary medicine and companion animal health

Edited by
Xu Wang, Qinghong Li and Rachel Pilla

Coordinated by
Alessandro Gramenzi

Published in
Frontiers in Microbiology
Frontiers in Veterinary Science

ISSN 1664-8714
ISBN 978-2-8325-7072-2
DOI 10.3389/978-2-8325-7072-2

Generative AI statement
Any alternative text (Alt text) provided alongside figures in the articles in this ebook has been generated by Frontiers with the support of artificial intelligence and reasonable efforts have been made to ensure accuracy, including review by the authors wherever possible. If you identify any issues, please contact us.

About Frontiers

Frontiers is more than just an open access publisher of scholarly articles: it is a pioneering approach to the world of academia, radically improving the way scholarly research is managed. The grand vision of Frontiers is a world where all people have an equal opportunity to seek, share and generate knowledge. Frontiers provides immediate and permanent online open access to all its publications, but this alone is not enough to realize our grand goals.

Frontiers journal series

The Frontiers journal series is a multi-tier and interdisciplinary set of open-access, online journals, promising a paradigm shift from the current review, selection and dissemination processes in academic publishing. All Frontiers journals are driven by researchers for researchers; therefore, they constitute a service to the scholarly community. At the same time, the *Frontiers journal series* operates on a revolutionary invention, the tiered publishing system, initially addressing specific communities of scholars, and gradually climbing up to broader public understanding, thus serving the interests of the lay society, too.

Dedication to quality

Each Frontiers article is a landmark of the highest quality, thanks to genuinely collaborative interactions between authors and review editors, who include some of the world's best academicians. Research must be certified by peers before entering a stream of knowledge that may eventually reach the public - and shape society; therefore, Frontiers only applies the most rigorous and unbiased reviews. Frontiers revolutionizes research publishing by freely delivering the most outstanding research, evaluated with no bias from both the academic and social point of view. By applying the most advanced information technologies, Frontiers is catapulting scholarly publishing into a new generation.

What are Frontiers Research Topics?

Frontiers Research Topics are very popular trademarks of the *Frontiers journals series*: they are collections of at least ten articles, all centered on a particular subject. With their unique mix of varied contributions from Original Research to Review Articles, Frontiers Research Topics unify the most influential researchers, the latest key findings and historical advances in a hot research area.

Find out more on how to host your own Frontiers Research Topic or contribute to one as an author by contacting the Frontiers editorial office: frontiersin.org/about/contact

Omics research in canine and feline microbiome: implications for veterinary medicine and companion animal health

Topic editors
Xu Wang — Auburn University, United States
Qinghong Li — Nestle Purina Research, United States
Rachel Pilla — University of Milan, Italy

Topic coordinator
Alessandro Gramenzi — University of Teramo, Italy

Citation
Wang, X., Li, Q., Pilla, R., Gramenzi, A., eds. (2025). *Omics research in canine and feline microbiome: implications for veterinary medicine and companion animal health*. Lausanne: Frontiers Media SA. doi: 10.3389/978-2-8325-7072-2

Table of contents

frontiers | Frontiers in Microbiology

TYPE Original Research
PUBLISHED 10 May 2024
DOI 10.3389/fmicb.2024.1337917

OPEN ACCESS

EDITED BY
Himel Mallick,
Cornell University, United States

REVIEWED BY
Yancong Zhang,
Broad Institute, United States
Thilini Nilusha Jayasinghe,
The University of Sydney, Australia

*CORRESPONDENCE
Xu Wang
xzw0070@auburn.edu

RECEIVED 13 November 2023
ACCEPTED 12 April 2024
PUBLISHED 10 May 2024

CITATION
Ma X, Brinker E, Lea CR, Delmain D, Chamorro ED, Martin DR, Graff EC and Wang X (2024) Evaluation of fecal sample collection methods for feline gut microbiome profiling: fecal loop vs. litter box.
Front. Microbiol. 15:1337917.
doi: 10.3389/fmicb.2024.1337917

Evaluation of fecal sample collection methods for feline gut microbiome profiling: fecal loop vs. litter box

Xiaolei Ma[1,2], Emily Brinker[3], Christopher R. Lea[4], Diane Delmain[4], Erin D. Chamorro[4], Douglas R. Martin[5,6], Emily C. Graff[2,5] and Xu Wang[2,5,7,8]*

[1]School of Life Sciences and Technology, Tongji University, Shanghai, China, [2]Department of Pathobiology, College of Veterinary Medicine, Auburn University, Auburn, AL, United States, [3]Department of Comparative Pathobiology, Cummings School of Veterinary Medicine, Tufts University, North Grafton, MA, United States, [4]Department of Clinical Sciences, College of Veterinary Medicine, Auburn University, Auburn, AL, United States, [5]Scott-Ritchey Research Center, College of Veterinary Medicine, Auburn University, Auburn, AL, United States, [6]Department of Anatomy, Physiology, and Pharmacology, College of Veterinary Medicine, Auburn University, Auburn, AL, United States, [7]Center for Advanced Science, Innovation, and Commerce, Alabama Agricultural Experiment Station, Auburn, AL, United States, [8]HudsonAlpha Institute for Biotechnology, Huntsville, AL, United States

Introduction: Microbial population structures within fecal samples are vital for disease screening, diagnosis, and gut microbiome research. The two primary methods for collecting feline fecal samples are: (1) using a fecal loop, which retrieves a rectal sample using a small, looped instrument, and (2) using the litter box, which collects stool directly from the litter. Each method has its own advantages and disadvantages and is suitable for different research objectives.

Methods and results: Whole-genome shotgun metagenomic sequencing were performed on the gut microbiomes of fecal samples collected using these two methods from 10 adult cats housed in the same research facility. We evaluated the influence of collection methods on feline microbiome analysis, particularly their impact on DNA extraction, metagenomic sequencing yield, microbial composition, and diversity in subsequent gut microbiome analyses. Interestingly, fecal sample collection using a fecal loop resulted in a lower yield of microbial DNA compared to the litterbox method ($p = 0.004$). However, there were no significant differences between the two groups in the proportion of host contamination ($p = 0.106$), virus contamination ($p = 0.232$), relative taxonomy abundance of top five phyla ($Padj > 0.638$), or the number of microbial genes covered ($p = 0.770$). Furthermore, no significant differences were observed in alpha-diversity, beta-diversity, the number of taxa identified at each taxonomic level, and the relative abundance of taxonomic units.

Discussion: These two sample collection methods do not affect microbial population structures within fecal samples and collecting fecal samples directly from the litterbox within 6 hours after defecation can be considered a reliable approach for microbiome research.

KEYWORDS

gut microbiota, fecal microbiome, stool sample collection, whole-genome shotgun metagenomic sequencing, microbial diversity

Introduction

Understanding the feline microbiome is essential in veterinary medicine, informing the diagnosis and treatment of conditions such as gastrointestinal disorders, obesity, and immune-mediated diseases (Day, 2016; Suchodolski, 2016; Ma et al., 2022). Additionally, research on the feline microbiome offers insights into zoonotic disease transmission and the transfer of beneficial microorganisms between cats and their owners (Overgaauw et al., 2020; Bhat, 2021). Thus, investigating the feline microbiome is crucial for advancing veterinary medicine and enhancing our understanding of human-animal interactions. The method of collecting fecal samples is crucial for obtaining accurate microbial profiles in microbiome studies (Wang et al., 2018; Watson et al., 2019; Tang et al., 2020; Jones et al., 2021), providing insights into microbial population structures and their correlations with health or disease. The two most commonly used methods for collecting feline fecal samples are: (1) the fecal loop method, which involves using a small plastic instrument with a looped end to collect a sample of the cat's stool from the rectum, and (2) the litter box approach, which involves collecting the cat's stool directly from the litter box. For the latter approach, it is vital to collect the sample immediately after the animal defecates to minimize the risk of environmental contamination of the microbiome. The fecal loop method provides a precise and sanitary collection technique, which minimizes the risk of cross-contamination and exposure of anaerobes to oxygen. However, this approach is often invasive and potentially uncomfortable or painful for cats. It should only be performed by veterinarians or experienced personnel who can insert the loop into the rectum and gently scoop out a small amount of feces. Moreover, sedation may be required prior to fecal loop collection, which can increase the time and cost involved in the process, particularly when dealing with multiple cats. The litter box method involves regularly monitoring the litter box, and promptly collecting the fresh stool with a clean and sterile container or scoop when the cat defecates. This approach is a non-invasive and cost-effective method commonly used in large-scale population studies, involving sample collection by cat owners. However, there is a greater risk of introducing environmental contaminations, which may affect the accuracy and completeness of the microbial community representation in the sample (Hale et al., 2016; Tal et al., 2017; Tap et al., 2019). Collecting fecal samples directly from the litter box may limit the information available to the clinician and researcher regarding fecal consistency (Sherding and Johnson, 2006). The choice of method depends on factors such as the specific research goals, the need for precision and sanitation, the invasiveness and discomfort for the cat, and the potential for environmental contamination.

Researchers should be mindful of the potential limitations and take steps to minimize environmental contamination and ensure timely sample collection. In addition to the conditions of the fecal sample, the stability of the microbial community within fecal samples is a critical aspect of microbiome research. This is particularly important when considering the method of sample collection, as gut microbial profiles are often linked to health status and have the potential to indicate the development of metabolic diseases, gastrointestinal disorders, and even cancer (Fukuda and Ohno, 2014; Parekh et al., 2015; Sanz et al., 2015; Quigley, 2017; Gopalakrishnan et al., 2018; Gorkiewicz and Moschen, 2018; Dabke et al., 2019; Li et al., 2019; Akbar et al., 2022). Using a fecal loop may reduce environmental contamination, but it also poses the risk of contaminating the sample with cells from the host's bowel wall or blood due to improper technique. Furthermore, it is important to note that using a fecal loop for sample collection may result in insufficient amounts of fecal material, which in turn could lead to an incomplete representation of the microbial community (Claassen-Weitz et al., 2020; Villette et al., 2021; Kennedy et al., 2023). Conversely, collecting fecal samples directly from the litter box may eliminate the risk of inadequate sample collection; however, it may also increase the likelihood of environmental contamination and the introduction of extraneous bacterial taxa into the samples. It is essential to note that fecal samples collected directly from litter boxes may not be collected promptly, which can lead to prolonged exposure to ambient conditions. Room temperature and oxygen levels are crucial environmental factors that influence the growth and survival of bacteria, potentially leading to changes in the composition of the gut microbiome. Research studies have shown that long-term storage at room temperature may alter the microbial diversity and community (Howell et al., 1996; Amir et al., 2017; Tal et al., 2017; Martin de Bustamante et al., 2021), leading to an inaccurate representation of the fecal microbiome. Oxygen levels significantly affect the growth and metabolic processes of both aerobic and anaerobic bacteria (Kennedy et al., 2023). This emphasizes consideration of environmental conditions when determining the optimal method for collecting cat fecal samples.

More than 10 previous studies have explored fecal collection and storage methods, examining variables such as temperature, storage duration at different temperatures, and the application of stabilizers like the OMNI-gene GUT kit, 95% ethanol, RNAlater, and other preservative solutions (Van der Waaij et al., 1994; Dominianni et al., 2014; Doukhanine et al., 2014; Flores et al., 2015; Loftfield et al., 2016; Song et al., 2016; Vogtmann et al., 2017; Wong et al., 2017; Burz et al., 2019; Conrads and Abdelbary, 2019; Papanicolas et al., 2019; Tap et al., 2019; Wu et al., 2019; Liang et al., 2020; Shalaby et al., 2020). While these studies have identified various methods to achieve stable microbial composition results, a universally accepted standard protocol has yet to emerge. This standard is crucial to the consistency, reliability, and comparability of results across studies. The majority of such studies concentrated on the methods of collecting and storing human fecal samples, while research on handling animal fecal samples is relatively limited. In the case of cats, the only prior study was our own research, which focused on the fecal loop collection method, specifically examining the use of lubricant versus no lubricant (Ma et al., 2022). This research is the first investigation into two fecal sample collection methods in cats, specifically examining the potential variances in gut microbiome composition resulting from the use of a fecal loop for collection compared to direct retrieval from a litter box. This research addresses a previously unexplored area by systematically comparing microbiome profiles derived from fecal samples collected via these two distinct methods. To assess the potential impact of various collection methods on the composition of the microbial community, we collected two sets of fecal samples from a group of cats housed in a controlled research environment. One set was collected using fecal loops, while the other was collected directly from the litter box. The collected samples underwent whole-genome shotgun metagenomic sequencing, followed by comprehensive analyses of

microbial diversity, composition, and abundance at all taxonomic and gene levels. Our study aimed to provide valuable insights into the impact of different fecal collection methods and to contribute to the development of standardized protocols for collecting fecal samples in feline microbiome research.

Materials and methods

Study animals

The Auburn University Institutional Animal Care and Use Committee (IACUC) approved the study. Four intact female and six intact male cats, raised and maintained at the Scott-Ritchey Research Center, Auburn University College of Veterinary Medicine (Auburn, AL, USA), were enrolled in this study (Table 1). The age range of the 10 adult cats is 2.7–7.0 years old, with a mean age of 4.4 years. All cats are housed in USDA and AAALAC accredited facilities in indoor wards with heating and air conditioning that allow compliance with federally mandated climate control parameters including an ambient temperature of ~72 degrees Fahrenheit, ranging from 64 to 84 degrees, with humidity between 30 and 70%. Cats were allowed *ad libitum* access to food and water. They were fed a Hill's Science Diet maintenance-formula dry food mixed with an equal amount of Friskies canned food. There was a rotation of the canned food protein sources (tuna, salmon, chicken, beef, and turkey) to increase enrichment. All cats were provided access to the same rotating protein source and there was no changes in diet throughout the study. The cats are born, raised, and housed in the colony and are maintained in these conditions throughout adulthood or until adoption. They were all cared for according to the principles outlined in the NIH Guide to the Care and Use of Laboratory Animals.

Sample size determination

To perform a systematic comparison of microbiome profiles generated from fecal samples collected using these two methods, we collected two sets of fecal samples from these cats. One set was obtained using fecal loops, while the other was collected directly from the litter box.

In total, 20 fecal samples were collected from 10 cats. Our previous work has discovered that that more than 90% of microbial genes and species are covered in a feline microbiome study when the sample size reaches eight (Ma et al., 2022). In this study, we performed rarefaction analyses on the 20 samples in this study at both the gene level (Supplementary Figure S1A) and the species levels (Supplementary Figure S1B), through random subsampling from 20 samples multiple times and plotting the average gene and species richness against different numbers of included samples using a customized R script (Supplementary Data S1).

Fecal sample collection and storage

Each cat was given 24 h to acclimate to a single housing environment. Afterward, each cat was provided with a fresh litter box and monitored every 2–6 h. After the cat defecated, the sample was immediately collected in a sterile 1.5 mL Eppendorf tube and stored at −80°C. The following morning, after collecting the fecal sample from the litterbox, the cat was sedated with intramuscular administration of medetomidine, ketamine, and butorphanol. A plastic fecal loop (Catalog number 7500, Covetrus, Dublin, OH, USA) was inserted into the rectum and descending colon to collect the fecal sample. The fecal loop was coated with mineral oil (Equate, Bentonville, AR, USA) as a lubricant, as described in our previous study (Ma et al., 2022). The samples were collected using 1.5 mL sterile Eppendorf tubes (Eppendorf, Hamburg, Germany) and immediately stored at −80°C (CryoCube F570, Eppendorf North America, Enfield, CT, USA) until analysis.

Whole-genome shotgun metagenomic sequencing

The Qiagen Allprep PowerFecal DNA/RNA kit (Qiagen, Redwood City, CA, USA) was used for microbial DNA extraction. For each cat, the weight of fecal specimens was measured (Table 2) before being placed into a Microbial Lysis Tube for homogenization using a

TABLE 1 Characteristics of study participants and fecal sample collection date/time.

Cat ID	Sex	Date of birth	Date of litterbox collection	Time of litterbox collection	Date of fecal loop collection	Time of fecal loop collection
9–1866	F	10/20/2015	10/4/2022	6:00	10/4/2022	13:00
944	F	3/17/2019	10/5/2022	14:00	10/10/2022	13:30
924	F	9/20/2018	9/27/2022	22:00	9/28/2022	8:20
960	F	1/25/2020	10/12/2022	12:00	10/13/2022	11:15
926	M	9/20/2018	9/28/2022	6:00	9/28/2022	12:00
936	M	1/21/2019	9/27/2022	18:00	9/28/2022	8:20
9–2033	M	5/5/2018	9/27/2022	6:00	9/28/2022	8:30
921	M	2/25/2018	10/4/2022	14:00	10/5/2022	14:00
9–2060	M	8/6/2018	9/28/2022	6:00	9/28/2022	12:00
9–1952	M	3/23/2017	9/28/2022	12:00	9/29/2022	15:00

F, Intact female; M, Intact male.

TABLE 2 Amount of fecal material collected and DNA yield from fecal samples.

Cat ID	Group	Weight of feces collected (mg)	DNA yield (μg)	Group	Weight of feces collected (mg)	DNA yield (μg)
9–1866	LB	205	238	FL	112	181
944	LB	208	165	FL	165	113
924	LB	212	121	FL	192	134
960	LB	201	156	FL	190	39.4
926	LB	198	138	FL	160	89.2
936	LB	215	202	FL	100	179
9–2033	LB	219	150	FL	201	79.4
921	LB	202	193	FL	165	65.4
9–2060	LB	216	290	FL	212	226
9–1952	LB	212	286	FL	176	144

LB, fecal collection by picking from litterbox; FL, fecal collection by using fecal loop.

PowerLyzer24 instrument (Qiagen, Redwood City, CA, USA). DNA extraction procedures were conducted for all fecal samples in the same batch to minimize technical variability. The DNA concentrations were measured using a Qubit 3.0 Fluorometer (Thermo Fisher Scientific, Waltham, MA, USA), and the A260/A280 absorption ratios were determined with a NanoDrop One C Microvolume Spectrophotometer (Thermo Fisher Scientific, Waltham, MA, USA). 500 ng of DNA from each sample was fragmented into 500-bp fragments using an M220 Focused-ultrasonicator (Covaris, Woburn, MA, USA). The WGS metagenomic libraries were prepared using the NEBNext Ultra II DNA Library Prep Kit for Illumina (New England BioLabs, Ipswich, MA, USA). TapeStation 4,200 (Agilent Technologies, Santa Clara, CA, USA) was utilized to evaluate the library size distributions. Subsequently, the final libraries were quantified using qPCR before being sequenced on an Illumina NovaSeq6000 sequencing platform in 150-bp paired-end mode by Novogene Corporation Inc. in Sacramento, CA, USA.

Bioinformatic processing of metagenomic data

A total of 1.02 billion raw metagenomic reads, or 153 Gigabases (Gbp) of sequences, were generated from the 20 metagenomes (Table 3). The sequencing depth of coverage was 9.59 ± 2.04 per sample. Trimmomatic (version 0.36) (Bolger et al., 2014) was utilized to remove adapter sequences and low-quality bases. Host and viral sequences were eliminated by aligning the high-quality reads to the feline reference genome Felis_catus_9.0 (Buckley et al., 2020) and the viral genome downloaded from National Center for Biotechnology Information (NCBI) using Burrows-Wheeler Aligner (BWA) (v0.7.17-r1188) (Li and Durbin, 2009). The virus reference consists of 5,540 high-quality complete viral genomes curated by NCBI, with a total genome length of 166.4 megabases (Mb). The remaining microbial reads were extracted using SAMtools (version 1.17) (Li et al., 2009) and aligned to the feline gut microbiome reference contigs assembled from 16 Illumina short-read metagenomics data (GCA_022675345.1; short-read reference assembly) (Ma et al., 2022). To investigate whether different microbiome references will affect our analysis and conclusion, we also aligned metagenomic reads to the feline gut microbiome contigs assembled from Pacific Biosciences HiFi long-read using $N = 8$ fecal samples (accession number: PRJNA1062788; long-read reference assembly). The read mapping percentages against both short-read and long-read assemblies are summarized in Table 3.

Taxonomy assignment and quantification of taxonomy abundance

Taxonomy assignments were performed on reference contigs (Loftfield et al., 2016) against the NCBI-NR database using Kaiju (v1.7.3) (Menzel et al., 2016) to determine taxonomy annotations at the phylum, class, order, family, genus, and species levels. More than 90% of the reference contigs were annotated with the NCBI (National Center for Biotechnology Information) taxonomy ID. Based on the BWA alignments, read counts were obtained using BEDTools (version 2.30.0) (Doukhanine et al., 2014) with the command 'bedtools coverage-f 0.9 -a region.bed -b reads.bam -counts' (Quinlan and Hall, 2010). The taxonomy counts table was generated by aggregating the read counts of all contigs with the same taxonomy annotation using a custom Perl script. The taxonomy counts were then normalized by the total number of mapped reads in a sample to quantify the relative abundance of each taxonomic unit.

Microbial diversity analyses

Alpha- and beta-diversity analyses were conducted on the microbial profiles at all taxonomic levels using the R package vegan (version 2.6–4) (Oksanen et al., 2013). The alpha diversity was assessed using the Shannon index (Shannon, 1997). The beta diversity was calculated based on the Bray-Curtis distance (Bray and Curtis, 1957) and visualized in the PCoA (Principal Coordinates Analysis) plot format. A permutational multivariate analysis of variance (PERMANOVA) test (Anderson, 2014) was performed to assess the centroids and dispersion of the LB (litter box) and FL (fecal loop) groups, based on the dissimilarity matrix.

TABLE 3 Whole-genome shotgun metagenomic sequencing yield, quality control, and alignment statistics.

Cat ID	Group	Total number of reads	% adapters & low-quality reads	% host sequences	% read alignment (reference 1)	% read alignment (reference 2)
9–1866	LB	42,054,216	2.23%	0.49%	96.82%	89.25%
944	LB	48,132,278	1.24%	0.08%	98.01%	92.79%
924	LB	46,459,964	0.72%	0.14%	97.81%	90.50%
960	LB	49,593,768	1.00%	0.30%	96.09%	87.73%
926	LB	55,893,016	0.95%	0.11%	98.41%	93.59%
936	LB	23,861,570	0.69%	2.48%	96.87%	86.83%
9–2033	LB	30,247,308	0.62%	2.49%	96.88%	86.84%
921	LB	47,944,568	0.75%	0.07%	97.84%	92.86%
9–2060	LB	68,800,896	0.63%	0.09%	98.41%	92.18%
9–1952	LB	49,365,474	0.61%	0.07%	98.52%	91.07%
9–1866	FL	42,659,160	0.75%	0.13%	93.65%	84.40%
944	FL	59,450,856	0.55%	0.66%	97.64%	88.93%
924	FL	58,907,188	0.53%	6.65%	97.83%	88.40%
960	FL	52,903,612	0.53%	3.48%	97.47%	90.17%
926	FL	61,076,576	0.62%	1.10%	97.90%	91.02%
936	FL	52,452,186	0.51%	1.31%	98.14%	87.30%
9–2033	FL	59,764,500	0.70%	38.98%	96.42%	85.48%
921	FL	53,357,488	0.49%	0.08%	97.09%	91.40%
9–2060	FL	63,409,540	0.51%	0.27%	98.41%	93.33%
9–1952	FL	56,489,430	0.51%	0.24%	98.28%	91.47%

LB, fecal collection by picking from litterbox; FL, fecal collection using fecal loop.
Reference 1: feline gut reference contigs from Illumina short-read metagenomic assembly (GCA_022675345.1).
Reference 2: feline gut reference contigs from Pacific Biosciences long-read metagenomic assembly (PRJNA1062788).

Microbial gene abundance analysis

Microbial gene predictions were performed on reference metagenomic contigs using MetaGeneMark (v3.38) (Zhu et al., 2010). The redundant genes were identified and combined using CD-HIT-est (v4.7) (Li and Godzik, 2006; Fu et al., 2012) with the criterion of global sequence identity exceeding 95%. To determine the gene abundance, per-gene read counts were extracted using "BEDtools coverage," and gene abundance was normalized by RPKM (Reads Per Kilobase gene model per Million reads).

Statistical analysis

The comparison of DNA yield, levels of host and viral contaminations, number of taxonomic units and microbial genes, alpha diversities, and relative abundance of each taxon between the LB and FL groups was conducted using the Wilcoxon signed-rank test (Bauer, 1972; Hollander et al., 2013) in the R software (R Core Team, 2013). For the multiple comparisons of the microbial profiles, we utilized the R package qvalue (Storey et al., 2015) to determine the false discovery rate. When the p-value was less than 0.05 or the q-value was less than 0.1, the null hypothesis was rejected. In addition to the pairwise nonparametric test, we also performed differential abundance testing using Analysis of Compositions of Microbiomes with Bias Correction (ANCOM-BC), which was implemented in the R package ANCOMBC (Lin and Peddada, 2020). To determine the differences in the variance, Levene's test of equality of variances (Brown and Forsythe, 1974; Carroll and Schneider, 1985) and the Brown–Forsythe test (Iachine et al., 2010) were performed. To estimate the correlation of taxonomy composition in fecal samples between the LB and FL groups, Spearman's rank correlation tests were conducted on the average relative abundance of taxa between the LB and FL groups using the "cor.test()" function from the stats R package (Table 4).

Results

Fecal sample collection using a fecal loop resulted in a lower DNA extraction yield compared to the litterbox method

The amount of fecal material per sample collected using a fecal loop (FL group) was significantly lower than that collected from the litter box approach ($p = 0.002$, Wilcoxon signed-rank test; Table 2). As a result, the DNA yield of the FL group (4.376 μg [2.905 μg – 5.848 μg, 95% CI]) was significantly lower than that of the LB group (6.787 μg [5.285 μg – 8.288 μg, 95% CI]) ($p = 0.004$, Wilcoxon signed-rank test; Figure 1A). This suggests that the fecal collection method using a fecal loop might result in a reduced amount of DNA for subsequent research.

TABLE 4 Correlation of taxonomic abundance at phylum, class, order, family, genus, and species level between fecal loop (FL) and litter box (LB) groups.

Taxonomy level	% of FL taxa identified in LB (short-read assembly)	FL-LB abundance correlation (short-read assembly)	% of FL taxa identified in LB (long-read assembly)	FL-LB abundance correlation (long-read assembly)
Phylum	95.83%	0.9573	100.0%	0.9912
Class	97.80%	0.9804	100.0%	0.9915
Order	98.97%	0.9789	100.0%	0.9914
Family	96.97%	0.9698	100.0%	0.9912
Genus	94.07%	0.9373	99.21%	0.9876
Species	89.83%	0.8974	99.65%	0.9794

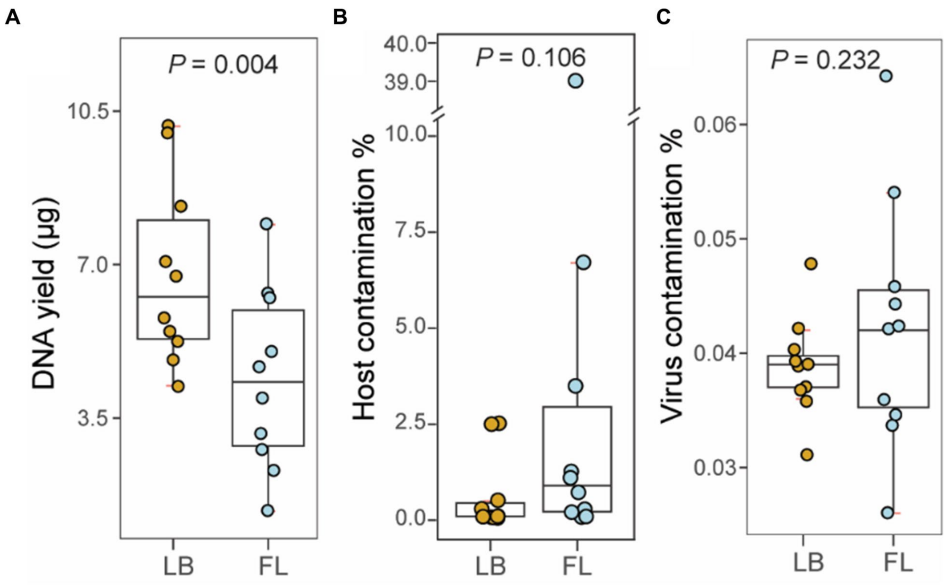

FIGURE 1
Metagenomic sequencing statistics from fecal samples collected by fecal loop (FL) and litter box (LB) approaches. **(A)** Boxplot of DNA yield (µg) extracted from fecal specimens in LB (brown) and FL (blue) groups. **(B)** Boxplot of percentage of host contamination in LB (brown) and FL (blue) groups. **(C)** Boxplot of percentage of viral contamination in LB (brown) and FL (blue) groups.

No significant difference was observed in the levels of contaminants in the WGS metagenomic sequencing data between the LB and FL groups

A total of 1.02 billion 150-bp reads (153.4 Gbp of sequences) were generated in total through whole-genome shotgun (WGS) metagenomic sequencing of 20 fecal DNA samples (51.1 million reads per sample; Table 3). On average, 0.76% of the adapter sequences and low-quality bases were trimmed and excluded from subsequent analysis. The level of feline sequence contamination was 8-fold higher in the FL group (5.290% [−3.306–13.886%, 95% CI]) than in the LB groups (0.631% [−0.073–1.337% 95%, CI]), but the difference did not reach statistical significance ($p = 0.11$, Wilcoxon signed-rank test; Figure 1B). The levels of viral contamination did not show a significant difference between the LB group (0.039% [0.036–0.042%, 95% CI]) and the FL group (0.042% [0.035–0.050%, 95% CI]) ($p = 0.232$, Wilcoxon signed-rank test; Figure 1C). However, there were higher variations in host and viral sequence contamination detected in FL samples, with marginal significance ($p = 0.05$, Levene's test of homogeneity of variance). When the Brown–Forsythe test was used, homogeneity of variances between the two groups cannot be rejected ($p = 0.25$).

No significant differences were found in the number of microbial taxa discovered in the fecal specimens from the LB and FL groups

From the WGS metagenomic data, a total of 127 phyla, 93 classes, 196 orders, 435 families, 1,892 genera, and 8,467 species were identified in 20 samples based on the short-read reference assembly. No significant difference was observed in the number of microbial taxa between the LB (79.8 taxa [73.0–86.6, 95% CI]) and FL groups (82.7 [77.5–87.9, 95% CI]) at the phylum ($p = 0.441$, Wilcoxon

signed-rank test), class (LB: 73.0 [67.7–78.3, 95% CI], FL: 72.1 [67.9–76.3, 95% CI], $p = 0.682$), order (LB: 151.5 [144.0–159.0, 95% CI], FL: 153.2 [146.5–159.9, 95% CI], $p = 0.959$), family (LB: 317.2 [300.2–334.2, 95% CI], FL: 327.7 [312.0–343.4, 95% CI], $p = 0.275$), genus (LB: 1093.9 [1007.2–1180.6, 95% CI], FL: 1146.2 [1069.5–1222.9, 95% CI], $p = 0.160$) and species levels (LB: 4074.3 [3709.4–4439.2, 95% CI], FL: 4288.0 [3985.3–4590.7, 95% CI], $p = 0.106$; Figure 2). The short-read assembly contains a large number of rare taxa, which greatly inflates the number of identified taxa due to ambiguity and false positives in taxonomic assignments. To address this issue, we aligned the metagenomic reads to an improved long-read feline gut microbiome assembly with enhanced metagenomic contig size and completeness. A total of 19 phyla, 35 classes, 63 orders, 104 families, 298 genera, and 936 species were identified using the long-read reference. When we repeated the analyses, we did not discover any significant differences in the number of microbial taxa between the groups either (Supplementary Figure S2).

No significant variation in microbial diversities was observed at all taxonomic levels between the LB and FL groups

Alpha-diversity, as measured by the Shannon index, and beta-diversity, assessed using the Bray-Curtis distance, were determined for microbial profiles in both the LB and FL groups (Figure 2). For alpha-diversity, no significant differences were detected between the LB and FL groups at the phylum (LB: 1.05 [1.02–1.08, 95% CI], FL: 1.10 [1.03–1.18, 95% CI]; $p = 0.064$), class (LB: 1.68 [1.56–1.79, 95% CI], FL: 1.74 [1.66–1.82, 95% CI]; $p = 0.275$), order (LB: 1.78 [1.65–1.91, 95% CI], FL: 1.83 [1.74–1.93, 95% CI]; $p = 0.432$), family (LB: 2.36 [2.21–2.50, 95% CI], FL: 2.41 [2.29–2.53, 95% CI]; $p = 0.492$), genus (LB: 2.58 [2.42–2.74, 95% CI], FL: 2.67 [2.54–2.80, 95% CI]; $p = 0.160$), and species levels (LB: 3.57 [3.42–3.73, 95% CI], FL: 3.57 [3.42–3.71, 95% CI]; $p = 0.846$; Figure 2). When additional alpha diversity metrics were examined, we failed to discover any significant differences in

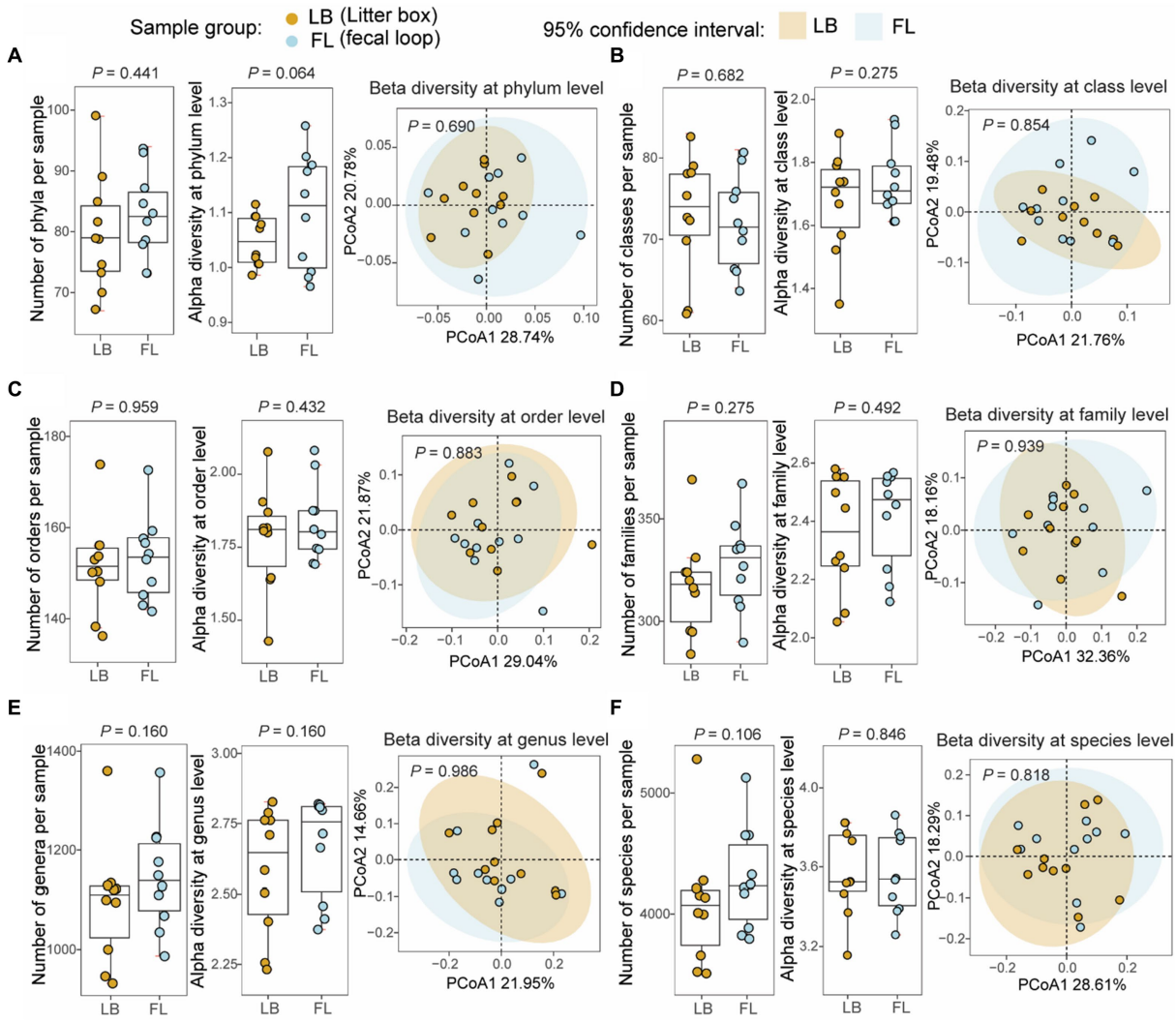

FIGURE 2
Microbial diversity analyses at different taxonomic levels from fecal samples collected by fecal loop (FL) and litter box (LB) approaches. Boxplots of non-redundant microbial taxa and alpha diversity (Shannon index) for each sample and principal coordinates analysis (PCoA) plot of beta diversity (Bray–Curtis dissimilarity) for microbial profiles from the LB (brown) and FL (blue) groups at **(A)** phylum, **(B)** class, **(C)** order, **(D)** family, **(E)** genus, and **(F)** species levels.

Simpson diversity index, richness, or Chao1 index between FL and LB ($p > 0.05$). Similarly, no significant changes were detected in beta-diversity analysis either ($p > 0.689$ for all taxonomic levels, PERMANOVA test; Figure 2) using both Bray-Curtis and Jaccard distance measures. When we use the long-read assembled reference contigs as the mapping reference, the results remain consistent (see Supplementary Figure S2).

Consistent relative taxonomic abundance in the microbiome quantified from fecal samples collected by LB and FL

Through Wilcoxon signed-rank tests on all taxonomic categories at the phylum level in the LB and FL groups, no significant difference was detected in the relative abundance of the top five most abundant phyla: Firmicutes (LB: 48.6% [42.6–54.6%, 95% CI] vs. FL: 47.5% [43.1–51.9%, 95% CI]; $P_{adj} = 1$), Actinobacteria (LB: 39.4% [30.8–47.9%, 95% CI] vs. FL: 37.7% [29.4–46.0%, 95% CI]; $P_{adj} = 1$), Bacteroidetes (LB: 8.1% [6.1–10.1%, 95% CI] vs. FL: 9.6% [5.3–14.0%, 95% CI]; $P_{adj} = 0.880$), Proteobacteria (LB: 0.9% [0.4–1.4%, 95% CI] vs. FL: 1.9% [0.6–3.3%, 95% CI]; $P_{adj} = 0.639$), and Fusobacteria (LB: 0% [0–0%, 95% CI] vs. FL: 0% [0–0%, 95% CI]; $P_{adj} = 0.639$; Figure 3A). Collectively, these five predominant phyla represented more than 97% of all phyla observed in both the LB and FL groups (97.6% [97.2–97.9%, 95% CI] vs. 97.5% [97.2–97.8%, 95% CI]; $p = 1$). When utilizing the long-read assembled feline gut microbiome contigs as the reference, the top five most abundant phyla remained consistent and maintained the same ranking order (Supplementary Figure S3A). Upon examining lower taxonomic units, there were no significant differences in the relative abundance between the LB and FL groups at the class, order, family, genus, or species levels ($P_{adj} > 0.909$ for short-read assembly, and $P_{adj} > 0.379$ for long-read assembly). Furthermore, in addition to pairwise nonparametric tests, we employed the ANCOM approach for detecting differential abundance as outlined in the Methods section. Our analysis did not reveal any taxa with a statistically significant difference in abundance between the LB and FL groups (FDR > 0.05; Supplementary Data S2), and 99.5% of the tested taxa exhibited an FDR = 1, suggesting remarkable concordance in microbial abundance between the two fecal sample collection methods.

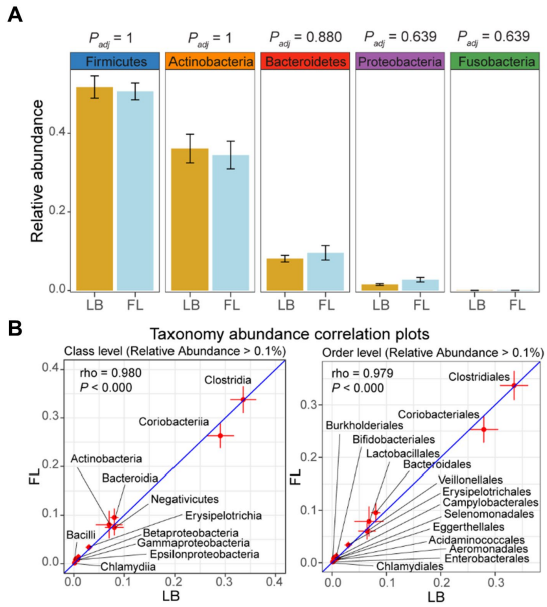

FIGURE 3
Relative abundance of major phyla and microbiome abundance (> 0.1%) correlation at class and order levels in the feline microbiome from samples collected by fecal loop (FL) and litter box (LB) approaches. **(A)** Boxplots of major phyla in LB (brown) and FL (blue) groups. **(B)** Correlation plots of microbes with high abundance (> 0.1%) at class and order levels. Each data point on the plot represents the averaged relative abundance of a particular taxon across samples within each group (FL on the *y*-axis and LB on the *x*-axis), and error bars indicate the standard error intervals around the mean for FL (vertical lines) and LB (horizontal lines) groups.

A strong correlation in taxonomic composition was observed among fecal samples in the LB and FL groups

When using the long-read assembled feline gut microbiome reference contigs, the LB and FL groups showed nearly perfect abundance correlation at phylum, class, order, and family levels, with Spearman's rank-order correlation coefficients greater than 0.99 (Table 4 and Supplementary Figure S3B; $p = 0.000$; Spearman's Rank-Order Correlation test). All taxa identified in the FL samples were also detected in the LB data (Table 4). At phylum, class, order, and family levels, results from short-read assembly demonstrated strong abundance correlations with lightly lower correlation coefficients, ranging from 0.957 and 0.980, with >95% taxa shared among FL and LB groups (Table 4 and Figure 3B). For the genus and species levels, the Spearman's correlation coefficients are 0.937 and 0.897, respectively (Table 4), which is presumably due to potential misannotations of shorter contigs in the short-read reference assembly at lower taxonomic units. For the long-read assembly with much greater contig completeness, abundance correlation coefficients remain remarkably high even at the genus ($\rho = 0.988$) and the species levels ($\rho = 0.979$; Table 4), with >99% of FL taxa also identified in LB samples, indicating excellent consistency in taxonomic abundance between the two fecal sample collection approaches.

The number, alpha diversity, and beta diversity of microbial genes are similar between the LB and FL groups

A total of 860,169 unique microbial genes were identified in the 20 metagenomes. Among these, 10 metagenomes from the LB group contained 796,138 nonredundant genes, while 10 metagenomes from the FL group contained 797,990 nonredundant genes (Figure 4A). Statistical analysis revealed no significant difference in the number of observed genes between fecal samples obtained from the fecal loop and litter box approaches ($p = 0.770$, Wilcoxon signed-rank test; Figure 4A). Additionally, the alpha diversity, as assessed by the Shannon index of observed genes, did not exhibit any significant difference between the two groups ($p = 1$, Wilcoxon signed-rank test; Figure 4B). Furthermore, the PCoA plot based on the Bray-Curtis distance matrix did not reveal any significant dissimilarities between

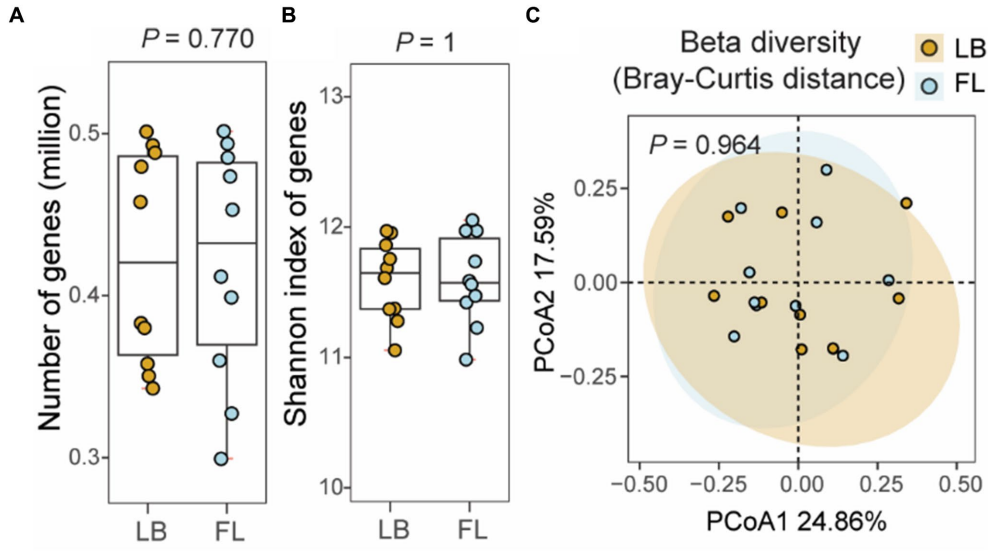

FIGURE 4
Number of non-redundant microbial genes and gene level diversity in the feline fecal microbiome from samples collected by fecal loop (FL) and litter box (LB) approaches. **(A)** Boxplot of the number of observed genes in the LB (brown) and FL (blue) groups. **(B)** Boxplot of Shannon index of genes identified in the LB (brown) and FL (blue) groups. **(C)** PCoA plot of beta diversity based on Bray-Curtis distance of the genes identified in the LB (brown) and FL (blue) groups.

the LB and FL groups, as indicated by the overlapping 95% confidence interval ellipses ($p = 0.964$, PERMANOVA test; Figure 4C). No significant differences were observed in the number, alpha diversity, and beta diversity of the microbial genes identified in the LB and FL groups when long-read assembled feline gut microbiome reference contigs were used as the references (Supplementary Figure S4).

Discussion

Fecal sample collection plays a crucial role in veterinary medicine for routinely diagnosing various health conditions, including parasitism (Verocai et al., 2020), enteropathogenic bacteria (Marks et al., 2011) and viruses (Sykes, 2014) in research for studying the gut microbiome. Establishing a gold standard for fecal sample collection is crucial for acquiring accurate, reliable, and reproducible microbiome data in a feasible manner. Such a standard safeguards the validity and consistency of microbiome research, facilitating the smooth transition of discoveries into clinical and therapeutic practices. Studies to optimize fecal sample collection techniques were mainly performed for humans, with no specific emphasis on investigating methods tailored for cats. Typically, there are two common methods of collecting feline fecal samples: from the litter box or from the rectum using a fecal loop. Each method possesses its own unique advantages and disadvantages. The fecal loop method is generally considered a more accurate approach for faithfully representing the gut microbiome, as it minimizes the risks of potential cross-contamination and exposure to the environment. However, inserting a fecal loop into the cat rectum requires experienced veterinary professionals to administer sedation, which may not be practical for all situations, particularly in cases where the cat is uncooperative, aggressive, or unable to tolerate sedation due to health concerns. In contrast, fecal samples collected from the litterbox are noninvasive, but more susceptible to environmental contamination, and the duration after defecation may cause bacterial growth to shift the microbiome composition (Vandeputte et al., 2016). Our aim was to conduct a thorough comparison of their impact on microbiome studies to assess whether the two collection methods could be interchangeable under certain circumstances. In this study, we demonstrated that there was no significant difference in the microbial profiles of fecal samples collected from the litter box compared to those collected using a fecal loop. No significant changes were observed in terms of alpha-diversity, beta-diversity, the number of taxa identified at each taxonomic level, and the relative abundances of taxonomic units. Collectively, these findings suggest that the microbiome composition of fecal samples collected using a fecal loop is the same as those collected directly from the litterbox within 6 h post-defecation. This indicates that collecting fecal samples directly from a clean litterbox in a timely manner can be considered a reliable method for feline microbiome studies.

The fecal loop collection approach resulted in a significantly lower DNA yield than the litterbox approach. Due to the uncertainty regarding whether sufficient feces can be collected from the colon in a single trial, the fecal loop method may cause missing data in the research or require multiple collections at different time points, which are not ideal for the experimental design. Consequently, the DNA yield was lower from fecal specimens collected using a fecal loop in this study. If consistent microbial DNA yield is a concern, the litter box approach will guarantee a superior DNA yield compared to the fecal loop approach.

Another disadvantage of using the fecal loop is the possibility of introducing host contaminations to the sample. Our results demonstrated that fecal samples collected using a fecal loop exhibited greater variability in the proportion of host contaminations compared to samples collected from the litter box, although this difference did not reach statistical significance. Notably, one of the fecal samples collected using a fecal loop in this study had a host contamination

level of 39%, making it difficult to estimate the necessary sequencing data to achieve the desired depth.

However, using a fecal loop to collect fecal samples remains indispensable for veterinary diagnosis. When fresh feces are needed for medical diagnosis, it is more appropriate to collect fresh fecal samples using a fecal loop in a clinical setting with trained personnel. This method enables the direct assessment of a presenting enteric complaint and the localization to the small, large, or mixed bowel based on fecal features (Sherding and Johnson, 2006), which may be challenging when relying on litter box samples exposed to unknown factors.

For citizen science projects or owner-participated research projects, the fecal loop collection approach is likely not feasible due to the requirement for access to sedation. In such cases, the litter box method is amenable to the participants as it only involves regularly monitoring the litter box. It supports the possibility of applying this feline fecal sample collection method in large-scale population microbiome studies when access to a veterinarian and medical facility is not feasible.

One limitation of our study is that we did not investigate the potential impact of extended room temperature exposure on the microbiome of the fecal samples. In our study, we monitored the litter box every 2 to 6 h to detect fecal deposits. The potential impact of prolonged exposure to room temperature on the composition of the microbiome in fecal samples is an area that requires further exploration.

Data availability statement

The datasets presented in this study can be found in online repositories. The names of the repository/repositories and accession number(s) can be found at: https://www.ncbi.nlm.nih.gov/, PRJNA1032714.

Ethics statement

The animal study was approved by Auburn University Institutional Animal Care and Use Committee. The study was conducted in accordance with the local legislation and institutional requirements.

Author contributions

XM: Data curation, Formal analysis, Investigation, Methodology, Validation, Visualization, Writing – original draft, Writing – review & editing. EB: Investigation, Methodology, Writing – original draft, Writing – review & editing. CL: Conceptualization, Funding acquisition, Resources, Supervision, Writing – review & editing. DD: Conceptualization, Funding acquisition, Resources, Supervision, Writing – review & editing. EC: Conceptualization, Funding acquisition, Resources, Supervision, Writing – review & editing. DM: Conceptualization, Funding acquisition, Resources, Supervision, Writing – review & editing. EG: Conceptualization, Funding acquisition, Investigation, Methodology, Resources, Supervision, Writing – original draft, Writing – review & editing. XW: Conceptualization, Data curation, Formal analysis, Funding acquisition, Investigation, Methodology, Project administration, Resources, Supervision, Writing – original draft, Writing – review & editing.

Funding

The author(s) declare that financial support was received for the research, authorship, and/or publication of this article. This study was supported by an Auburn University College of Veterinary Medicine Animal Health and Disease Research Program and an EveryCat Health Foundation award (EC22-023) to XW. XM was supported by an Elanco Animal Health Fellowship.

Acknowledgments

The feline colony was supported in part by the Auburn University Animal Health and Disease Research Grants and the Scott-Ritchey Research Center. We thank Auburn University Easley Cluster for the computational support of this work.

Conflict of interest

The authors declare that the research was conducted in the absence of any commercial or financial relationships that could be construed as a potential conflict of interest.

The author(s) declared that they were an editorial board member of Frontiers, at the time of submission. This had no impact on the peer review process and the final decision.

Publisher's note

Supplementary material

The Supplementary material for this article can be found online at: https://www.frontiersin.org/articles/10.3389/fmicb.2024.1337917/full#supplementary-material

References

Akbar, N., Khan, N. A., Muhammad, J. S., and Siddiqui, R. (2022). The role of gut microbiome in cancer genesis and cancer prevention. *Health Sci. Rev.* 2:100010. doi: 10.1016/j.hsr.2021.100010

Amir, A., McDonald, D., Navas-Molina, J. A., Debelius, J., Morton, J. T., Hyde, E., et al. (2017). Correcting for microbial blooms in fecal samples during room-temperature shipping. *Msystems* 2:e00199-16. doi: 10.1128/mSystems.00199-16

Anderson, M. J. (2014). Permutational multivariate analysis of variance (PERMANOVA). *Wiley Statsref*, 1–15.

Bauer, D. F. (1972). Constructing confidence sets using rank statistics. *J. Am. Stat. Assoc.* 67, 687–690. doi: 10.1080/01621459.1972.10481279

Bhat, A. H. (2021). Bacterial zoonoses transmitted by household pets and as reservoirs of antimicrobial resistant bacteria. *Microb. Pathog.* 155:104891. doi: 10.1016/j.micpath.2021.104891

Bolger, A. M., Lohse, M., and Usadel, B. (2014). Trimmomatic: a flexible trimmer for Illumina sequence data. *Bioinformatics* 30, 2114–2120. doi: 10.1093/bioinformatics/btu170

Bray, J. R., and Curtis, J. T. (1957). An ordination of the upland Forest communities of southern Wisconsin. *Ecol. Monogr.* 27, 325–349. doi: 10.2307/1942268

Brown, M. B., and Forsythe, A. B. (1974). Robust tests for the equality of variances. *J. Am. Statistical Assoc.* 69, 364–367. doi: 10.1080/01621459.1974.10482955

Buckley, R. M., Davis, B. W., Brashear, W. A., Farias, F. H., Kuroki, K., Graves, T., et al. (2020). A new domestic cat genome assembly based on long sequence reads empowers feline genomic medicine and identifies a novel gene for dwarfism. *PLoS Genet.* 16:e1008926. doi: 10.1371/journal.pgen.1008926

Burz, S. D., Abraham, A.-L., Fonseca, F., David, O., Chapron, A., Béguet-Crespel, F., et al. (2019). A guide for ex vivo handling and storage of stool samples intended for fecal microbiota transplantation. *Sci. Rep.* 9:8897. doi: 10.1038/s41598-019-45173-4

Carroll, R. J., and Schneider, H. (1985). A note on Levene's tests for equality of variances. *Stat. Probabil. Lett.* 3, 191–194. doi: 10.1016/0167-7152(85)90016-1

Claassen-Weitz, S., Gardner-Lubbe, S., Mwaikono, K. S., du Toit, E., Zar, H. J., and Nicol, M. P. (2020). Optimizing 16S rRNA gene profile analysis from low biomass nasopharyngeal and induced sputum specimens. *BMC Microbiol.* 20:113. doi: 10.1186/s12866-020-01795-7

Conrads, G., and Abdelbary, M. M. (2019). Challenges of next-generation sequencing targeting anaerobes. *Anaerobe* 58, 47–52. doi: 10.1016/j.anaerobe.2019.02.006

Dabke, K., Hendrick, G., and Devkota, S. (2019). The gut microbiome and metabolic syndrome. *J. Clin. Invest.* 129, 4050–4057. doi: 10.1172/JCI129194

Day, M. J. (2016). Cats are not small dogs: is there an immunological explanation for why cats are less affected by arthropod-borne disease than dogs? *Parasit. Vectors* 9, 1–9. doi: 10.1186/s13071-016-1798-5

Dominianni, C., Wu, J., Hayes, R. B., and Ahn, J. (2014). Comparison of methods for fecal microbiome biospecimen collection. *BMC Microbiol.* 14, 1–6. doi: 10.1186/1471-2180-14-103

Doukhanine, E., Bouevitch, A., Pozza, L., and Merino, C. (2014). OMNIgene® • GUT enables reliable collection of high quality fecal samples for GUT microbiome studies. *DNA Genotek*. PD-PR-0043. Available at: www.dnagenotek.com

Flores, R., Shi, J., Yu, G., Ma, B., Ravel, J., Goedert, J. J., et al. (2015). Collection media and delayed freezing effects on microbial composition of human stool. *Microbiome* 3, 1–11. doi: 10.1186/s40168-015-0092-7

Fu, L., Niu, B., Zhu, Z., Wu, S., and Li, W. (2012). CD-HIT: accelerated for clustering the next-generation sequencing data. *Bioinformatics* 28, 3150–3152. doi: 10.1093/bioinformatics/bts565

Fukuda, S., and Ohno, H. (2014). Gut microbiome and metabolic diseases. *Semin. Immunopathol.* 36, 103–114. doi: 10.1007/s00281-013-0399-z

Gopalakrishnan, V., Helmink, B. A., Spencer, C. N., Reuben, A., and Wargo, J. A. (2018). The influence of the gut microbiome on cancer, immunity, and cancer immunotherapy. *Cancer Cell* 33, 570–580. doi: 10.1016/j.ccell.2018.03.015

Gorkiewicz, G., and Moschen, A. (2018). Gut microbiome: a new player in gastrointestinal disease. *Virchows Arch.* 472, 159–172. doi: 10.1007/s00428-017-2277-x

Hale, V. L., Tan, C. L., Niu, K., Yang, Y., Cui, D., Zhao, H., et al. (2016). Effects of field conditions on fecal microbiota. *J. Microbiol. Methods* 130, 180–188. doi: 10.1016/j.mimet.2016.09.017

Hollander, M., Wolfe, D. A., and Chicken, E. (2013). *Nonparametric statistical methods*. Hoboken, New Jersey, United States: John Wiley & Sons.

Howell, J., Coyne, M. S., and Cornelius, P. (1996). Effect of sediment particle size and temperature on fecal bacteria mortality rates and the fecal coliform/fecal streptococci ratio. *J. Environ. Qual.* 25, 1216–1220. doi: 10.2134/jeq1996.00472425002500060007x

Iachine, I., Petersen, H. C., and Kyvik, K. O. (2010). Robust tests for the equality of variances for clustered data. *J. Stat. Comput. Simul.* 80, 365–377. doi: 10.1080/00949650802641841

Jones, J., Reinke, S. N., Ali, A., Palmer, D. J., and Christophersen, C. T. (2021). Fecal sample collection methods and time of day impact microbiome composition and short chain fatty acid concentrations. *Sci. Rep.* 11:13964. doi: 10.1038/s41598-021-93031-z

Kennedy, K. M., de Goffau, M. C., Perez-Muñoz, M. E., Arrieta, M.-C., Bäckhed, F., Bork, P., et al. (2023). Questioning the fetal microbiome illustrates pitfalls of low-biomass microbial studies. *Nature* 613, 639–649. doi: 10.1038/s41586-022-05546-8

Li, W., Deng, Y., Chu, Q., and Zhang, P. (2019). Gut microbiome and cancer immunotherapy. *Cancer Lett.* 447, 41–47. doi: 10.1016/j.canlet.2019.01.015

Li, H., and Durbin, R. (2009). Fast and accurate short read alignment with burrows–wheeler transform. *Bioinformatics* 25, 1754–1760. doi: 10.1093/bioinformatics/btp324

Li, W., and Godzik, A. (2006). Cd-hit: a fast program for clustering and comparing large sets of protein or nucleotide sequences. *Bioinformatics* 22, 1658–1659. doi: 10.1093/bioinformatics/btl158

Li, H., Handsaker, B., Wysoker, A., Fennell, T., Ruan, J., Homer, N., et al. (2009). The sequence alignment/map format and SAMtools. *Bioinformatics* 25, 2078–2079. doi: 10.1093/bioinformatics/btp352

Liang, Y., Dong, T., Chen, M., He, L., Wang, T., and Liu, X. (2020). Systematic analysis of impact of sampling regions and storage methods on fecal gut microbiome and metabolome profiles. *mSphere* 5:e00763-19. doi: 10.1128/mSphere.00763-19

Lin, H., and Peddada, S. D. (2020). Analysis of compositions of microbiomes with bias correction. *Nat. Commun.* 11:3514. doi: 10.1038/s41467-020-17041-7

Loftfield, E., Vogtmann, E., Sampson, J. N., Moore, S. C., Nelson, H., Knight, R., et al. (2016). Comparison of collection methods for fecal samples for discovery metabolomics in epidemiologic studies. *Cancer Epidemiol. Biomarkers Prev.* 25, 1483–1490. doi: 10.1158/1055-9965.EPI-16-0409

Ma, X., Brinker, E., Cao, W., Graff, E. C., and Wang, X. (2022). Effect of mineral oil as a lubricant to collect feces from cats for microbiome studies. *J. Vet. Intern. Med.* 36, 1974–1980. doi: 10.1111/jvim.16556

Ma, X., Brinker, E., Graff, E. C., Cao, W., Gross, A. L., Johnson, A. K., et al. (2022). Whole-genome shotgun metagenomic sequencing reveals distinct gut microbiome signatures of obese cats. *Microbiol. Spectr.* 10:e00837-22. doi: 10.1128/spectrum.00837-22

Marks, S. L., Rankin, S. C., Byrne, B. A., and Weese, J. S. (2011). Enteropathogenic Bacteria in dogs and cats: diagnosis, epidemiology, treatment, and control. *J. Vet. Intern. Med.* 25, 1195–1208. doi: 10.1111/j.1939-1676.2011.00821.x

Martin de Bustamante, M., Plummer, C., MacNicol, J., and Gomez, D. (2021). Impact of ambient temperature sample storage on the equine fecal microbiota. *Animals* 11:819. doi: 10.3390/ani11030819

Menzel, P., Ng, K. L., and Krogh, A. (2016). Fast and sensitive taxonomic classification for metagenomics with kaiju. *Nat. Commun.* 7, 1–9. doi: 10.1038/ncomms11257

Oksanen, J, Blanchet, FG, Kindt, R, Legendre, P, Minchin, PR, O'Hara, R.B., et al. (2013). Package 'vegan'. Community ecology package, version.

Overgaauw, P. A., Vinke, C. M., van Hagen, M. A., and Lipman, L. J. (2020). A one health perspective on the human–companion animal relationship with emphasis on zoonotic aspects. *Int. J. Environ. Res. Public Health* 17:3789. doi: 10.3390/ijerph17113789

Papanicolas, L. E., Choo, J. M., Wang, Y., Leong, L. E., Costello, S. P., Gordon, D. L., et al. (2019). Bacterial viability in faecal transplants: which bacteria survive? *EBioMedicine* 41, 509–516. doi: 10.1016/j.ebiom.2019.02.023

Parekh, P. J., Balart, L. A., and Johnson, D. A. (2015). The influence of the gut microbiome on obesity, metabolic syndrome and gastrointestinal disease. *Clin. Transl. Gastroenterol.* 6:e91. doi: 10.1038/ctg.2015.16

Quigley, E. M. (2017). Gut microbiome as a clinical tool in gastrointestinal disease management: are we there yet? *Nat. Rev. Gastroenterol. Hepatol.* 14, 315–320. doi: 10.1038/nrgastro.2017.29

Quinlan, A. R., and Hall, I. M. (2010). BEDTools: a flexible suite of utilities for comparing genomic features. *Bioinformatics* 26, 841–842. doi: 10.1093/bioinformatics/btq033

R Core Team. *R: A language and environment for statistical computing*. R Foundation for Statistical Computing, Vienna. (2013).

Sanz, Y., Olivares, M., Moya-Pérez, Á., and Agostoni, C. (2015). Understanding the role of gut microbiome in metabolic disease risk. *Pediatr. Res.* 77, 236–244. doi: 10.1038/pr.2014.170

Shalaby, A. G., Bakry, N. R., Mohamed, A. A., and Khalil, A. A. (2020). Evaluating Flinders technology associates card for transporting bacterial isolates and retrieval of bacterial DNA after various storage conditions. *Vet. World* 13, 2243–2251. doi: 10.14202/vetworld.2020.2243-2251

Shannon, C. E. (1997). The mathematical theory of communication. 1963. *MD Comput.* 14, 306–317.

Sherding, R. G., and Johnson, S. E. (2006). "Chapter 69- diseases of the intestines" in *Saunders manual of small animal practice (third edition)*. eds. S. J. Birchard and R. G. Sherding (Saint Louis: W.B. Saunders), 702–738.

Song, S. J., Amir, A., Metcalf, J. L., Amato, K. R., Xu, Z. Z., Humphrey, G., et al. (2016). Preservation methods differ in fecal microbiome stability, affecting suitability for field studies. *mSystems* 1, e00021–e00016. doi: 10.1128/mSystems.00021-16

Storey, J. D., Bass, A. J., Dabney, A., and Robinson, D. (2015). qvalue: Q-value estimation for false discovery rate control. *R package version 2.22.0*. Available at: github.com/jdstorey/qvalue (Accessed April 14, 2017).

Suchodolski, J. S. (2016). Diagnosis and interpretation of intestinal dysbiosis in dogs and cats. *Vet. J.* 215, 30–37. doi: 10.1016/j.tvjl.2016.04.011

Sykes, J. E. (2014). "Chapter 14- canine parvovirus infections and other viral Enteritides" in *Canine and feline infectious diseases*. ed. J. E. Sykes (Saint Louis: W.B. Saunders), 141–151.

Tal, M., Verbrugghe, A., Gomez, D. E., Chau, C., and Weese, J. S. (2017). The effect of storage at ambient temperature on the feline fecal microbiota. *BMC Vet. Res.* 13:256. doi: 10.1186/s12917-017-1188-z

Tang, Q., Jin, G., Wang, G., Liu, T., Liu, X., Wang, B., et al. (2020). Current sampling methods for gut microbiota: a call for more precise devices. *Front. Cell. Infect. Microbiol.* 10:151. doi: 10.3389/fcimb.2020.00151

Tap, J., Cools-Portier, S., Pavan, S., Druesne, A., Öhman, L., Törnblom, H., et al. (2019). Effects of the long-term storage of human fecal microbiota samples collected in RNAlater. *Sci. Rep.* 9:601. doi: 10.1038/s41598-018-36953-5

Van der Waaij, L., Mesander, G., Limburg, P., and Van der Waaij, D. (1994). Direct flow cytometry of anaerobic bacteria in human feces. *Cytometry* 16, 270–279. doi: 10.1002/cyto.990160312

Vandeputte, D., Falony, G., Vieira-Silva, S., Tito, R. Y., Joossens, M., and Raes, J. (2016). Stool consistency is strongly associated with gut microbiota richness and composition, enterotypes and bacterial growth rates. *Gut* 65, 57–62. doi: 10.1136/gutjnl-2015-309618

Verocai, G. G., Chaudhry, U. N., and Lejeune, M. (2020). Diagnostic methods for detecting internal parasites of livestock. *Vet. Clin. N. Am. Food Anim. Pract.* 36, 125–143. doi: 10.1016/j.cvfa.2019.12.003

Villette, R., Autaa, G., Hind, S., Holm, J. B., Moreno-Sabater, A., and Larsen, M. (2021). Refinement of 16S rRNA gene analysis for low biomass biospecimens. *Sci. Rep.* 11:10741. doi: 10.1038/s41598-021-90226-2

Vogtmann, E., Chen, J., Amir, A., Shi, J., Abnet, C. C., Nelson, H., et al. (2017). Comparison of collection methods for fecal samples in microbiome studies. *Am. J. Epidemiol.* 185, 115–123. doi: 10.1093/aje/kww177

Wang, Z., Zolnik, C. P., Qiu, Y., Usyk, M., Wang, T., Strickler, H. D., et al. (2018). Comparison of fecal collection methods for microbiome and metabolomics studies. *Front. Cell. Infect. Microbiol.* 8:301. doi: 10.3389/fcimb.2018.00301

Watson, E.-J., Giles, J., Scherer, B. L., and Blatchford, P. (2019). Human faecal collection methods demonstrate a bias in microbiome composition by cell wall structure. *Sci. Rep.* 9:16831. doi: 10.1038/s41598-019-53183-5

Wong, W. S., Clemency, N., Klein, E., Provenzano, M., Iyer, R., Niederhuber, J. E., et al. (2017). Collection of non-meconium stool on fecal occult blood cards is an effective method for fecal microbiota studies in infants. *Microbiome* 5, 1–11. doi: 10.1186/s40168-017-0333-z

Wu, W.-K., Chen, C.-C., Panyod, S., Chen, R.-A., Wu, M.-S., Sheen, L.-Y., et al. (2019). Optimization of fecal sample processing for microbiome study—the journey from bathroom to bench. *J. Formos. Med. Assoc.* 118, 545–555. doi: 10.1016/j.jfma.2018.02.005

Zhu, W., Lomsadze, A., and Borodovsky, M. (2010). Ab initio gene identification in metagenomic sequences. *Nucleic Acids Res.* 38:e132. doi: 10.1093/nar/gkq275

frontiers | Frontiers in Microbiology

TYPE Original Research
PUBLISHED 16 July 2024
DOI 10.3389/fmicb.2024.1426691

OPEN ACCESS

EDITED BY
Xu Wang,
Auburn University, United States

REVIEWED BY
Ziyao Zhou,
Sichuan Agricultural University, China
Lei Deng,
Massachusetts General Hospital and Harvard Medical School, United States

*CORRESPONDENCE
Gregory Kislik
✉ gkislik@g.ucla.edu

RECEIVED 03 May 2024
ACCEPTED 02 July 2024
PUBLISHED 16 July 2024

CITATION
Kislik G, Zhou L, Rubbi L and Pellegrini M (2024) Age-correlated changes in the canine oral microbiome.
Front. Microbiol. 15:1426691.
doi: 10.3389/fmicb.2024.1426691

Age-correlated changes in the canine oral microbiome

Gregory Kislik*, Lin Zhou, Liudmilla Rubbi and Matteo Pellegrini

Molecular Cell and Developmental Biology, University of California, Los Angeles (UCLA), Los Angeles, CA, United States

Introduction: Canine oral disease has been associated with significant changes in the oral microbiome rather than the presence or absence of individual species. In addition, most studies focus on a single age group of canines and as of yet, the relationship between canine microbiomes and age is poorly understood.

Methods: This study used a shotgun whole gene sequencing approach in tandem with the Aladdin Bioinformatics platform to profile the microbiomes of 96 companion dogs, with the sourmash-zymo reference database being used to perform taxonomic profiling.

Results: Findings showed significant age correlations among 19 species, including positive correlations among several *Porphyromonas* species and a negative correlation with *C. steedae*. Although a significant correlation was found between predicted and actual ages, ElasticNet Regression was unable to successfully predict the ages of younger canines based on their microbiome composition. Both microbiome samples and microbial species were successfully clustered by age group or age correlation, showing that the age-microbiome relationship survives dimensionality reduction. Three distinct clusters of microbial species were found, which were characterized by *Porphyromonas*, *Conchiformibius*, and *Prevotella* genera, respectively.

Discussion: Findings showed that the microbiomes of older dogs resembled those that previous literature attributed to dogs with periodontal disease. This suggests that the process of aging may introduce greater risks for canine oral disease.

KEYWORDS

whole genome sequencing, canine, microbiome, metagenomics, ElasticNet regression

Introduction

Microbiomes are the collection of all microorganisms that are found in an environment which are present in all eukaryotic organisms and live in symbiosis with the host. Different microbiomes can be found in the mouth, respiratory tract, urogenital tract and gastrointestinal tract as well as on the skin (Grzeskowiak et al., 2015; Malard et al., 2021). Besides being involved in metabolism, the microbiome is also deeply connected with the health and diseases of the host. At surfaces that are in contact with the external environment (e.g., skin, oral cavity or intestine), the community of diverse microorganisms prevents the establishment of potentially invasive pathogens. The microbiome is also critical in the development and maintenance of the host's immune system, which learns to recognize resident microorganisms and initiate inflammatory responses against invaders. Dysbiosis or drastic changes in the microbiome are often associated with diseases (Young, 2017; Deo and Deshmukh, 2019; Malard et al., 2021).

The canine oral microbiome is an enormously complex and diverse community within a host organism. Despite the variety of changes in the environment, the oral microbiome remains relatively stable over time and has coevolved with the host organism (Zaura et al.,

2014). Depending on the method of delivery (either vaginal or Cesarean section), most organisms acquire their oral microbiome during birth when the newborn is exposed to the mother's vaginal or gut flora (Zaura et al., 2014). The healthy canine microbiome is defined by common clades of aerobic bacteria, including species from *Actinomyces*, *Porphyromonas*, and *Campylobacter* (Niemiec et al., 2021).

Significant, microbiome-wide changes occur in canines with oral diseases. Periodontal disease is an inflammatory oral disease commonly seen among canines. Compared to a healthy canine oral microbiome, microbiomes of diseased oral cavities exhibit a shift towards anaerobic bacteria (Davis et al., 2013; Santibanez et al., 2021). The abundance of bacteria of the genus *Porphyromonas* increases more than two-fold in the oral microbiome of dogs with periodontal disease (Santibanez et al., 2021). Species including *Porphyromonas cangingivalis* can regulate the host immune response, exacerbating inflammation. Moreover, they can also contribute to the breakdown of the host gingival epithelium (Santibanez et al., 2021). Such oral diseases have been observed at high rates among more senior canines, with frequent oral dysbiosis being observed (Templeton et al., 2023).

Whole genome sequencing (WGS) has been shown to more accurately detect broader microbiome diversity compared to existing 16S amplicon methods (Lewis et al., 2021). A previous study on the metagenomes of aging dogs was able to effectively use WGS to measure longitudinal alpha diversity changes in senior companion dogs (Templeton et al., 2023). However, canine microbiome changes across age groups are not well characterized. Understanding compositional changes related to physical traits will be important for establishing benchmarks when comparing the microbial flora of healthy and diseased dogs where age, sex and weight may be a relevant variable. Age and weight have both previously been correlated with the progression of periodontal disease in canines (Carreira et al., 2015). However, their oral flora was not examined, which leaves both age and weight as possible confounders in the origin of canine periodontal disease. Understanding this relationship will be important for determining how these factors influence canine oral health and its decline. Given previous findings that both periodontal dysfunction and microbial changes are common among aging dogs, it was hypothesized that aging will have a significant relationship with bacterial species associated with oral disease. A longitudinal analysis was not possible due to sampling limitations, but single-factor level correlations could still be used to perform a cross-sectional analysis. This study uses shotgun WGS to characterize metagenomic differences across dogs of varying ages, weights and sexes.

Results

Metagenome composition

Whole genome shotgun sequencing was performed on 96 dogs from the study Rubbi et al. (2022) and profiled using the shotgun taxonomy profiling pipeline on the Aladdin Bioinformatics Platform, which conducted quality assurance and microbiome identification. The kmers species composition is shown in Figure 1A. The majority of kmers belonged to *Canis lupus*. The canine microbiome contained 102 species with more than 0.1% abundance of all kmers belonging to microbial species. The distribution of bacterial abundances across all samples is shown in Figure 1B. Among samples of lower ages, *Conchiformibius* tends to be the dominant genus, while at higher ages *Porphyrmonas* becomes more abundant. The *Moraxella* clade becomes more common in middle age but is less abundant among dogs near the extremes of the age spectrum. The change in abundance of species with significant age correlations is shown in Figure 1C. The abundance of *C. steedae* decreases substantially with increasing age and several *Porphyromonas* species increase over time.

Species correlated with age

Pearson correlations between all microbial species, age, sex and weight were computed (Supplementary Figure S1). The correlation matrix of microbial species that exhibit a significant correlation with age is shown in Figure 2. The correlation of microbiome composition with weight and sex is also included in Figure 2. Of the 102 species detected, 19 of them were found to be significantly correlated with age ($p < 0.05$, FDR adjusted). Supplementary Table S1 displays the species' abundances, age and Simpson's Index (calculated with the whole microbiome) of each sample. A significant correlation ($p = 0.0013$) was found between Simpson's Index and age with a coefficient of 0.014016 (standard error: 0.004228), indicating that alpha diversity increased with age. Of the 19 species found to be significantly correlated with age, six belonged to the genus *Porphyromonas*, which all displayed positive Pearson correlations. Four species (*M. sp002224245*, *F. canicola*, *C. steedae*, and *C. haemoglobinophilus*) had negative correlations with age. The change in abundance of species that had significant age correlations with $p < 0.001$ and age is shown in Figure 3. Notably, *C. steedae* has a significant negative correlation with age and quickly decreases with increasing age. Of the 19 species that showed a correlation with age, none showed a significant correlation with sex and only three showed a significant correlation with weight: *Tannerella forsythia*, *Campylobacter sp012978815*, and *Porphyromonas crevioricanis*.

Canine microbiome samples and microbial species cluster by age group

To visualize the relationships between samples in a lower dimensional space, uniform manifold approximation and projection (UMAP) was performed using cosine distance. UMAP analysis was performed twice, once with all species considered and again with only species with significant age correlations. Afterward, k-means clustering was performed to identify groups of similar samples. Silhouette scores were used to find the optimal number of clusters. Although seven clusters were found to be optimal in the UMAP of all samples, the number was reduced to four to remain consistent with the UMAP of only species with significant age correlations. The UMAP and age distributions of all samples when considering all microbial species are shown in Figures 4A,C and of samples when considering only significantly age-correlated species are in Figures 4B,D. Wilcoxon tests were performed to compare age distributions. When all species were considered, Cluster 4 was found to have a significantly different age distribution than Clusters 1, 2, and 3. Clusters 1, 2, and 3 were not found to have significantly different ages from each other. When considering only significantly age-correlated species, Cluster 1 was found to be significantly different from Clusters 2 and 3, but not Cluster 4. Cluster 4 was found to have a significantly different age distribution than Clusters 2 and 3. Cluster 2 was not significantly different from Cluster 3.

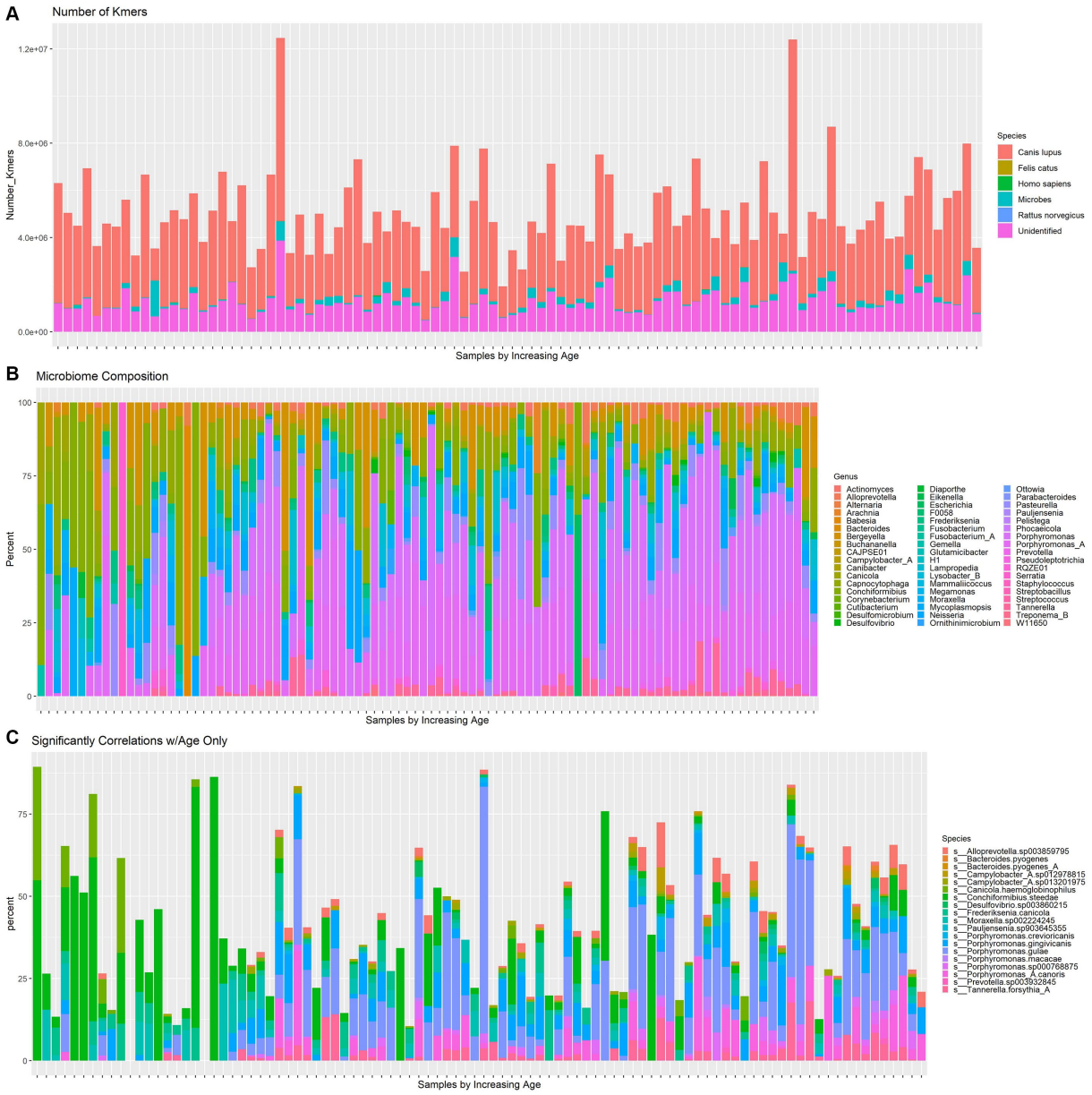

FIGURE 1
(A) Number of kmers corresponding to dog (*Canis lupus*), cat (*Felis catus*), human (*Homo Sapiens*), microbial, brown rat (*Rattus norvegicus*) and unrecognized species in each dog. Samples increase by age left to right. **(B)** Relative abundance of all microbial species with at least 0.01% abundance which shows changes in alpha diversity over time. Samples increase by age left to right. **(C)** Relative abundance of species which have a significant ($p < 0.05$, FDR adjusted) age correlation. Samples increase by age left to right.

Next, the similarity between bacterial species was investigated. Although the Silhouette score indicated that two clusters were optimal, three were used to better resolve different groups of species. From the species UMAP, we identified three clusters (Figure 5A). Clusters 1 and 3 had higher age correlations than Cluster 2, while Cluster 1 and 3 were not shown to have significantly different age correlations between each other (Figure 5B). The distribution of abundances showed a similar pattern where the species in Cluster 2 had a significantly different abundance from those in Clusters 1 and 3. However, the species in Clusters 1 and 3 did not have significantly different abundances (Figure 5C). We sought to investigate the phylogenetic distribution of bacterial species in each cluster. The sunburst plot displays the taxonomy of all species colored by cluster (Figure 5D). Notably, the family Bacteroidaceae contained most Cluster 3 bacteria. Cluster 1 contained most *Porphyromonas* species in addition to all of the detected *Desulfomicrobium*, *Desulfovibrio*, and *Treponema_B* species. Phylum Firmicutes was contained entirely in Cluster 2.

Age prediction based on microbiome

To investigate whether the microbial composition of a canine could be used to predict its age, ElasticNet regression was performed using the abundance of microbial species as features and the age of the dog as the

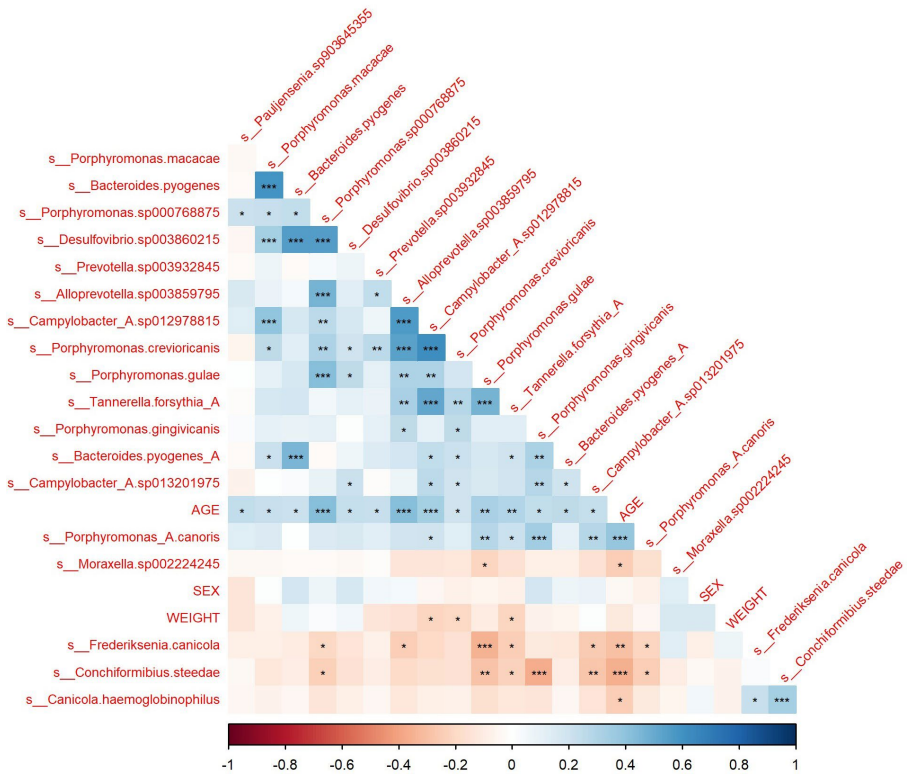

FIGURE 2
Correlation matrix of species with significant age correlation with sex and weight. *<0.05, **<0.01, ***<0.001.

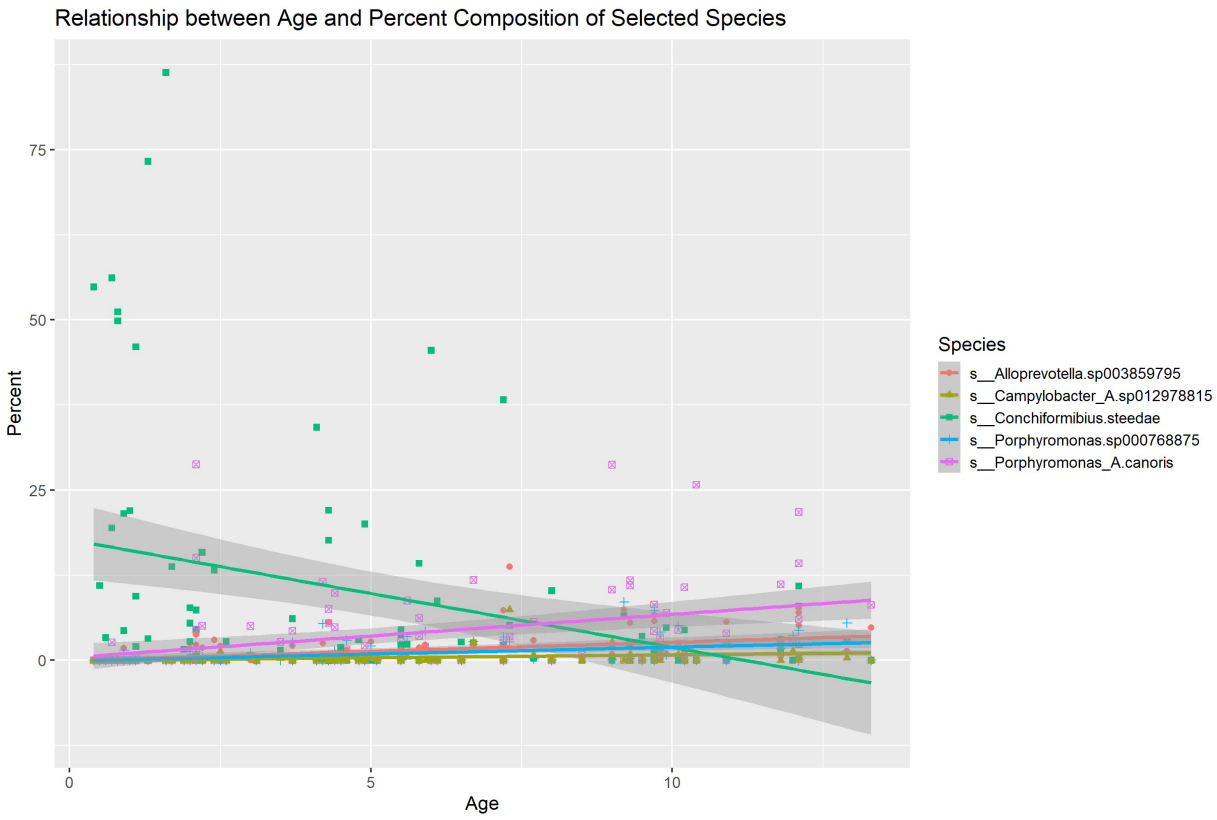

FIGURE 3
Linear regression describing the change in abundance of species with age correlations with $p < 0.001$.

10.3389/fmicb.2024.1426691

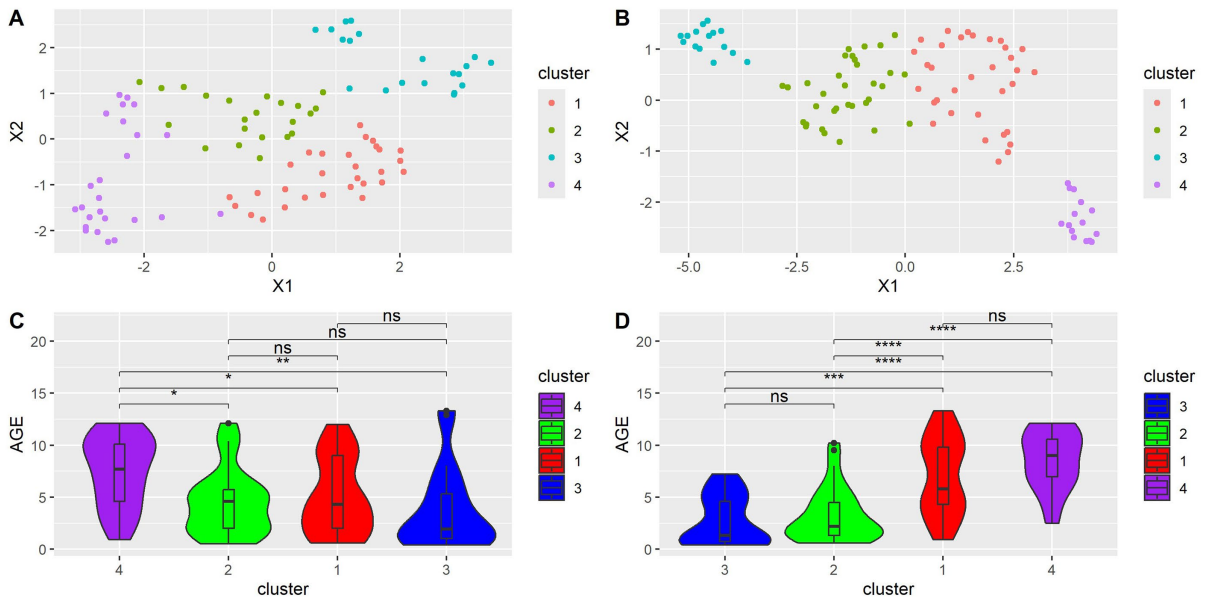

FIGURE 4
(A) UMAP dimension reduction on all species. Each point represents a sample. **(B)** UMAP dimension reduction on species with significant age correlation. Each point represents a sample. **(C)** Violin plots showing differences in age distribution across clusters for **(A)**. Wilcoxon test, FDR adjusted. *<0.05, **<0.01, ***<0.001. **(D)** Violin plot showing differences in age distribution across clusters for **(B)**. Wilcoxon test, FDR adjusted. *<0.05, **<0.01, ***<0.001.

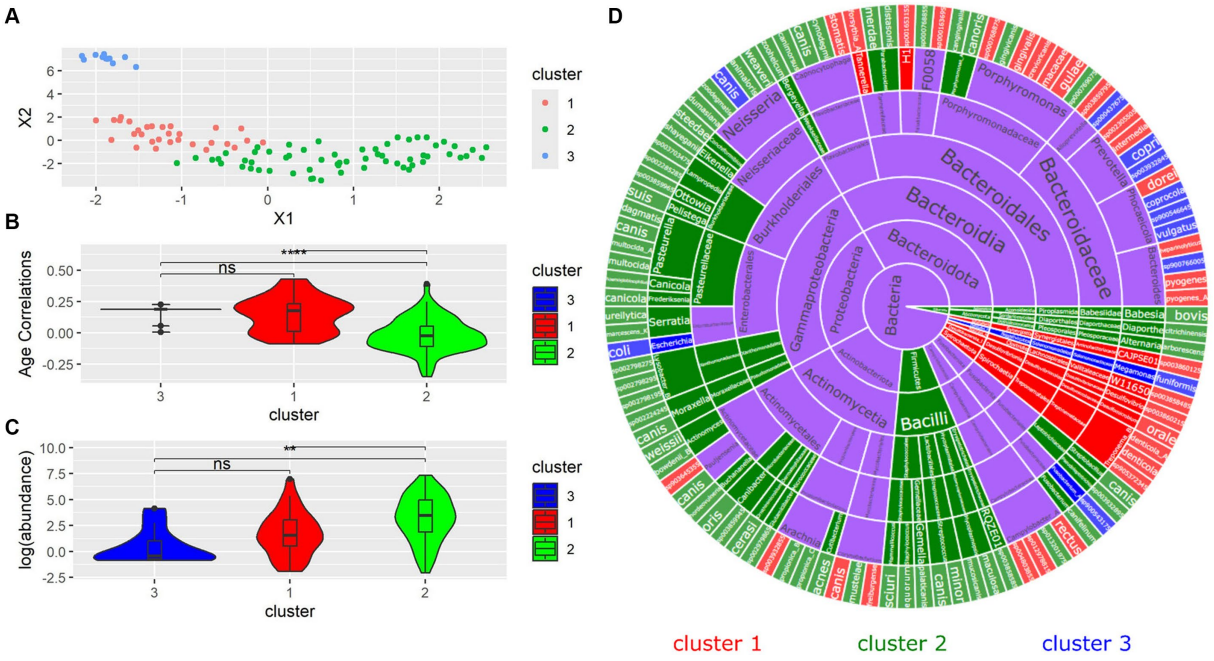

FIGURE 5
(A) UMAP dimension reduction on all samples. Each point represents a species. **(B)** Differences in distribution of age correlations for each cluster. **(C)** Log(abundances) across each cluster. **(D)** Sunburst plot of all microbial species separated by cluster.

response. Twenty-fold grid cross-validation was performed to find optimal hyperparameters. This cross-validation method tests a range of alpha (orders of magnitude between 1×10^{-5} and 100) and l1 ratio (0.2, 0.4, 0.6, or 0.8) combinations to select the ones with the highest accuracy: an alpha of 10 and an l1 ratio of 0.2 were chosen. The results of this cross-validation method are in Supplementary Table S2. Fourteen species had

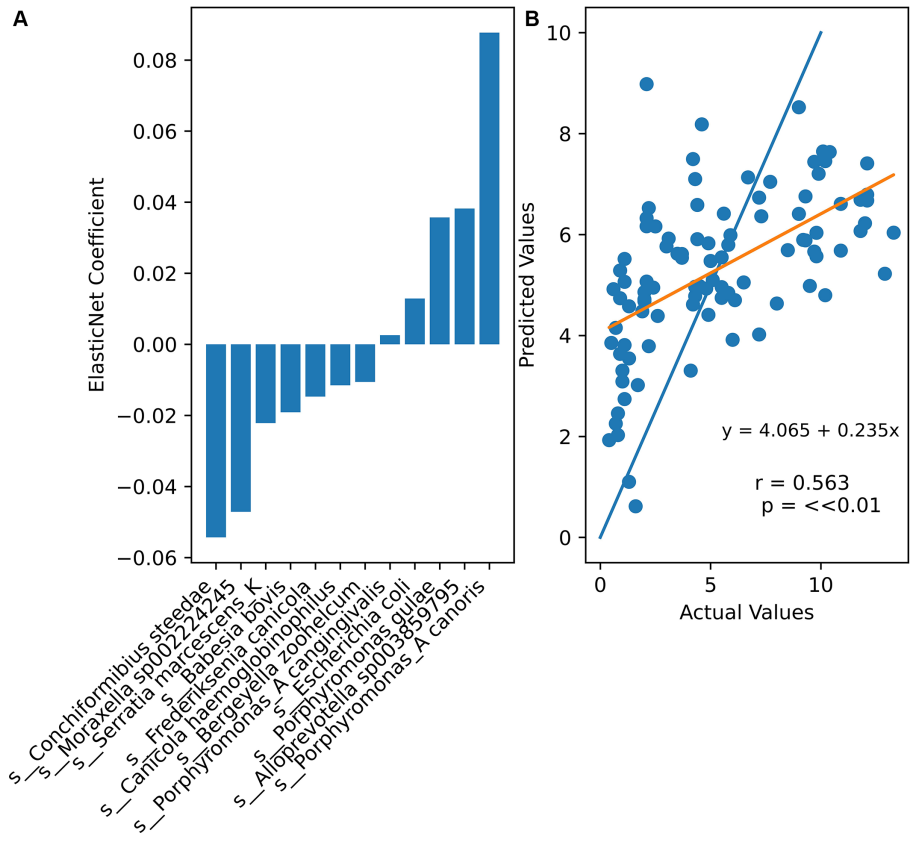

FIGURE 6
(A) Non-zero ElasticNet regression coefficients (alpha = 10, l1 ratio = 0.2). **(B)** Comparison between actual sample ages and ElasticNet predicted ages. Orange line represents the least squares regression line through all points. Blue line is ideal actual = predicted age.

non-zero coefficients (Figure 6). Although a significant correlation was found between the actual and predicted ages, higher real ages were often underestimated, while lower real ages were often overestimated by ElasticNet. The mean squared error of the model was 9.77, meaning that the model tended to predict within ± 3.13 years of the dogs' actual ages.

Discussion

Simpson's Index was found to be positively correlated with age. This is congruent with findings in Templeton et al. (2023), which observed significant increases in bacterial alpha diversity. In human subjects, alpha diversity, as measured by the Shannon index, has been observed to be significantly higher among those with chronic gingivitis and Stage I periodontitis (Kharitonova et al., 2021). This may suggest that the canine's ability to regulate its oral flora is diminished with age. This may also support that the microbiomes of aging canines resemble those who have periodontal disease. We found that the genus *Porphyromonas* shows a significant positive correlation with age. Species of the genus *Porphyromonas* have been previously observed to be enriched in the oral microbiome of dogs with periodontal disease (Santibanez et al., 2021). *P. gulae* and *P. gingivalis* are both associated with the progression of the disease (Hajishengallis and Lambris, 2012; Nomura et al., 2020). *P. gulae* has been established as part of the core oral bacteriome of dogs with periodontal disease (Niemiec et al., 2021). As an opportunistic pathogen, *P. gingivalis* is capable of subverting a host's innate immune response and even remodeling the periodontal microbiota (Hajishengallis and Lambris, 2012). It has been observed that in small dog breeds, *P. gulae* likely causes oral disease through the formation of FimA proteins (Yasuda et al., 2024). These proteins polymerize to form fimbriae, which greatly increase *P. gulae* virulence and allow for more rapid formation of biofilms in the gingival margins. This leads to inflammation and eventual tooth decay and loss (Yasuda et al., 2024). The pathogenicity of *P. gingivalis* is largely due to gingipains, which cleave T-cell receptors, immunoglobulins, as well as extracellular matrix components (Bostanci and Belibasakis, 2012). This allows *P. gingivalis* to evade immune response and accumulate to form a biofilm, which leads to periodontitis and dental decay.

By contrast, species from several phyla show negative correlations with age (Santibanez et al., 2021). A prior study compared the relative abundances of various microbial species between the oral microbiomes of healthy dogs and dogs with mild periodontitis through 16S rRNA gene sequencing. In their findings, reductions in *C. steedae* were found to be associated with both gingivitis and periodontitis. Similarly, *C. steedae* abundance had a significant negative correlation with age, suggesting that older dogs have microbiomes more similar to dogs with oral disease. Thus, the oral

microbiome of older dogs resembles the periodontal microbiome. Overall, the significant difference in relative abundances of several microbial species between younger and older dogs may be explained by the fact that periodontal disease is more prevalent in older dogs (Nomura et al., 2020). It is also possible that the observed results are a product of natural shifts in oral microbiomes as a result of age. Previous literature has suggested that there may be a genetic predisposition to oral disease and that some breeds may lack resistance to potentially pathogenic strains of bacteria (Wallis and Holcombe, 2020; Wallis et al., 2021). Differences in the longevity of different breeds may also play a role, as those with longer lifespans may accumulate additional subgingival plaque and be at higher risk for periodontal disease. Additional investigation is needed to understand potential genetic risk factors for oral dysbiosis. Understanding potential genetic risk factors or differences in oral dysbiosis among different breeds could help to guide future efforts to prevent the development of canine periodontal disease as veterinarians would be better able to recommend prophylactic action to dog owners. Because samples were collected without medical examination, the disease state of the canines cannot be confirmed. Future research may seek to confirm this possible relationship found in this study by conducting regular health checks in a longitudinal design.

The use of k-means clustering showed that taxonomically unrelated species could be grouped based on similarities in age correlations. Clustering was able to distinguish between clades traditionally associated with canine periodontal disease. Cluster 1 largely contained *Treponema*, *Desulfomicrobium* and many *Porphyromonas* species, which are associated with canine periodontal disease (Harvey, 1998; Riggio et al., 2011). Cluster 3 was characterized by *Prevotella* species, which are similarly implicated in canine periodontal disease and are frequently found in canine plaque and periodontal pockets (Stephan et al., 2008). *N. canis* was also found in Cluster 3, which has been found in canine mandibular abscesses (Cantas et al., 2011). Both *Porphyromonas* and *Prevotella* are associated with human periodontal disease (Stephan et al., 2008). *Conchiformibius* and *Actinomyces*, found in Cluster 2, have been associated with oral health, and declining abundance with worsening oral health (Watanabe et al., 2023). Clusters 1 and 3 both possessed significantly higher age correlations than Cluster 2, suggesting that k-means clustering is able to distinguish between groups associated with both age and disease.

Various approaches have been used to predict human ages using gut microbiome data (Seo et al., 2023). However, there has been no concerted effort to predict canine ages based on their microbiomes. This study was able to predict dogs' actual ages within 3.13 years of their actual age by using ElasticNet regression, a regularized model. The largest negative coefficient in the ElasticNet model belonged to *Conchiformibius steedae*, which further supports the conclusion that increased age is associated with the decline of beneficial oral flora. Three *Porphyrmonas* species possessed positive coefficients, suggesting that their abundances are positively associated with age. *Porphyromonas* has also been associated with increased periodontal disease severity (Watanabe et al., 2023). While still nascent, being able to predict age and health status based on microbiome composition may be useful for identifying risk factors and deviations from normal aging and canine health. Future studies may look into improving the accuracy of predictive methods and comparing machine learning and regression models, as well as performing longitudinal analyses to better control for microbial changes over time and their relationship to disease progression.

Methods

Whole genome sequencing and processing

DNA was extracted from the buccal swabs using the vendor-supplied protocol. Buccal swabs were incubated overnight at 50 degrees Celsius before DNA Extraction. 100 ng of extracted DNA was used for Whole Genome Sequencing (WGS) library preparation. Fragmented DNA was subject to end repair, dA-tailing and adapter ligation using the NEBNext Ultra II Library prep kit using dual unique index adapters (IDT). Libraries were subject to PCR amplification using KAPA HiFi Uracil+(Roche) with the following conditions: 2 min at 98°C; 14 cycles of (98°C for 20 s; 60°C for 30 s; 72°C for 30 s); 72°C for 5 min; hold at 4°C. Library QC was performed using the High-Sensitivity D1000 Assay on a 2200 Agilent TapeStation. Pools of 96 libraries were sequenced on a NovaSeq X Plus (10b lane) as paired-end 150 bases (Rubbi et al., 2022). The mean number of reads was 3,612,534 per canine. The Aladdin Bioinformatics Shotgun Platform, which uses the qiime2 reference databases, was used to process the sequence data, profile taxa and conduct quality assurance (Ewels et al., 2016; Chen et al., 2018; Bolyen et al., 2019). Aladdin uses FastQC to conduct quality assurance by measuring the frequency of duplicated reads as well as G-C content and removing sequences of extreme length (Chen et al., 2018). Sourmash identifies the kmers composition of the samples by comparing kmers to the sourmash-zymo database (Ewels et al., 2016). Sourmash performs taxonomic profiling by creating the smallest possible list of matches to its reference database based on existing k-mers, which are profiled. This smallest possible metagenome is compiled using the method described in Irber et al. (2022), in which containment of a sample hash within the larger reference is calculated using the smallest possible elements from the sample. After finding the match in the reference genome with the highest containment, the match is removed from the sample's query and the process is repeated. Abundances are estimated using the Jaccard containment of the matched genome within the whole sample metagenome. Qiime2 was used to visualize the composition barplot (Bolyen et al., 2019).

Correlation and UMAP analysis

The generation of correlation matrices, violin plots, bar plots and scatter plots was done in RStudio version 2023.6.0.421 using the corrr and ggplot2 packages (Wickham, 2016; Kuhn et al., 2022; Posit Team, 2023). The UMAP package was used to perform dimensionality reduction using the procedure described in McInnes et al. (2018). All *p*-values were corrected for using the false discovery rate method for multiple comparisons.

Age regression model

Jupyter Notebooks were used to generate sunburst plots and the bar and scatter plots for ElasticNet regression using the plotly and

sklearn packages (Pedregosa et al., 2011; Plotly Technologies Inc., 2015; Kluyver et al., 2016). Grid Cross Validation tests a range of possible hyperparameters in order to find the optimal settings for ElasticNet regression. For alpha, orders of magnitude between 1×10^{-5} and 100 were tested and for l1 ratio the following values were tested: 0.2, 0.4, 0.6, or 0.8. Twenty fold Grid Cross Validation found optimal hyperparameters: l1 ratio = 0.2 and an alpha = 10. The results of all combinations of hyperparameters are available in Supplementary Table S2. These hyperparameters were used by ElasticNet regression to predict dogs' ages based on their microbiome. A Pearson correlation and associated p-value were computed to measure the effectiveness of the prediction.

Data availability statement

The datasets presented in this study can be found in online repositories. The names of the repository/repositories and accession number(s) can be found at: https://www.ncbi.nlm.nih.gov/, PRJNA1106914.

Ethics statement

Ethical approval was not required for the studies involving animals in accordance with the local legislation and institutional requirements because the method of data collection (buccal swab) is non-invasive and did not need ethical approval. Written informed consent was obtained from the owners for the participation of their animals in this study.

Author contributions

GK: Formal analysis, Investigation, Visualization, Writing – original draft, Writing – review & editing. LZ: Conceptualization, Writing – original draft, Writing – review & editing. LR: Data curation, Writing – original draft, Writing – review & editing. MP: Conceptualization, Data curation, Project administration, Supervision, Writing – original draft, Writing – review & editing.

Funding

The author(s) declare that no financial support was received for the research, authorship, and/or publication of this article.

Conflict of interest

The authors declare that the research was conducted in the absence of any commercial or financial relationships that could be construed as a potential conflict of interest.

Publisher's note

Supplementary material

The Supplementary material for this article can be found online at: https://www.frontiersin.org/articles/10.3389/fmicb.2024.1426691/full#supplementary-material

SUPPLEMENTARY FIGURE S1
Correlation matrix of all species, age, weight, and sex.

SUPPLEMENTARY TABLE S1
Age, Simpson's index of all species in the sample, and relative abundance of species with significant age correlations.

SUPPLEMENTARY TABLE S2
Grid cross validation results.

References

Bolyen, E., Rideout, J. R., Dillon, M. R., Bokulich, N. A., Abnet, C. C., Al-Ghalith, G. A., et al. (2019). Reproducible, interactive, scalable and extensible microbiome data science using QIIME 2. *Nat. Biotechnol.* 37, 852–857. doi: 10.1038/s41587-019-0209-9

Bostanci, N., and Belibasakis, G. N. (2012). *Porphyromonas gingivalis*: an invasive and evasive opportunistic oral pathogen. *FEMS Microbiol. Lett.* 333, 1–9. doi: 10.1111/j.1574-6968.2012.02579.x

Cantas, L., Pekarkova, M., Kippenes, H. S., Brudal, E., and Sorum, H. (2011). First reported isolation of *Neisseria canis* from a deep facial wound infection in a dog. *J. Clin. Microbiol.* 49, 2043–2046. doi: 10.1128/JCM.02610-10

Carreira, L. M., Dias, D., and Azevedo, P. (2015). Relationship between gender, age, and weight and the serum ionized calcium variations in dog periodontal disease evolution. *Top. Companion Anim. Med.* 30, 51–56. doi: 10.1053/j.tcam.2015.07.001

Chen, S., Zhou, Y., Chen, Y., and Gu, J. (2018). fastp: an ultra-fast all-in-one FASTQ preprocessor. *Bioinformatics* 34, i884–i890. doi: 10.1093/bioinformatics/bty560

Davis, I. J., Wallis, C., Deusch, O., Colyer, A., Milella, L., Loman, N., et al. (2013). A cross-sectional survey of bacterial species in plaque from client owned dogs with healthy gingiva, gingivitis or mild periodontitis. *PLoS One* 8:e83158. doi: 10.1371/journal.pone.0083158

Deo, P. N., and Deshmukh, R. (2019). Oral microbiome: unveiling the fundamentals. *J. Oral Maxillofac. Pathol.* 23, 122–128. doi: 10.4103/jomfp.JOMFP_304_18

Ewels, P., Magnusson, M., Lundin, S., and Käller, M. (2016). MultiQC: summarize analysis results for multiple tools and samples in a single report. *Bioinformatics* 32, 3047–3048. doi: 10.1093/bioinformatics/btw354

Grzeskowiak, L., Endo, A., Beasley, S., and Salminen, S. (2015). Microbiota and probiotics in canine and feline welfare. *Anaerobe* 34, 14–23. doi: 10.1016/j.anaerobe.2015.04.002

Hajishengallis, G., and Lambris, J. D. (2012). Complement and dysbiosis in periodontal disease. *Immunobiology* 217, 1111–1116. doi: 10.1016/j.imbio.2012.07.007

Harvey, C. E. (1998). Periodontal disease in dogs. Etiopathogenesis, prevalence, and significance. *Vet. Clin. North Am. Small Anim. Pract.* 28, 1111–1128, vi. doi: 10.1016/s0195-5616(98)50105-2

Irber, L., Brooks, P. T., Reiter, T., Pierce-Ward, N. T., Hera, M. R., Koslicki, D., et al. (2022). Lightweight compositional analysis of metagenomes with FracMinHash and minimum metagenome covers. *BioRxiv* 475838. doi: 10.1101/2022.01.11.475838

Kharitonova, M., Vankov, P., Abdrakhmanov, A., Mamaeva, E., Yakovleva, G., and Ilinskaya, O. (2021). The composition of microbial communities in inflammatory periodontal diseases in young adults Tatars. *AIMS Microbiol.* 7, 59–74. doi: 10.3934/microbiol.2021005

Kluyver, T., Ragan-Kelley, B., Perez, F., Granger, B., Bussonnier, M., Frederic, J., et al. (2016). "Jupyter notebooks – a publishing format for reproducible computational

workflows" in Positioning and power in academic publishing: players, agents and agendas. eds. F. Loizides and B. Schmidt (IOS Press), 87–90.

Kuhn, M., Jackson, S., and Cimentada, J. (2022). Corrr: correlations in R. Available at: https://github.com/tidymodels/corrr; https://corrr.tidymodels.org.

Lewis, S., Nash, A., Li, Q., and Ahn, T. H. (2021). Comparison of 16S and whole genome dog microbiomes using machine learning. *BioData Mining* 14:41. doi: 10.1186/s13040-021-00270-x

Malard, F., Dore, J., Gaugler, B., and Mohty, M. (2021). Introduction to host microbiome symbiosis in health and disease. *Mucosal Immunol.* 14, 547–554. doi: 10.1038/s41385-020-00365-4

McInnes, L., Healy, J., Saul, N., and Großberger, L. (2018). UMAP: uniform manifold approximation and projection. *J. Open Source Softw.* 3:861. doi: 10.21105/joss.00861

Niemiec, B. A., Gawor, J., Tang, S., Prem, A., and Krumbeck, J. A. (2021). The bacteriome of the oral cavity in healthy dogs and dogs with periodontal disease. *Am. J. Vet. Res.* 83, 50–58. doi: 10.2460/ajvr.21.02.0027

Nomura, R., Inaba, H., Yasuda, H., Shirai, M., Kato, Y., Murakami, M., et al. (2020). Inhibition of Porphyromonas gulae and periodontal disease in dogs by a combination of clindamycin and interferon alpha. *Sci. Rep.* 10:3113. doi: 10.1038/s41598-020-59730-9

Pedregosa, F., Varoquaux, G., Gramfort, A., Michel, V., Thirion, B., Grisel, O., et al. (2011). Scikit-learn: machine learning in Python. *J. Mach. Learn. Res.* 12, 2825–2830. doi: 10.48550/arXiv.1201.0490

Plotly Technologies Inc. (2015). Collaborative data science. Montréal, QC: Plotly Technologies Inc.

Posit Team (2023). RStudio: Integrated development environment for R. PBC, Boston, MA: Posit Software.

Riggio, M. P., Lennon, A., Taylor, D. J., and Bennett, D. (2011). Molecular identification of bacteria associated with canine periodontal disease. *Vet. Microbiol.* 150, 394–400. doi: 10.1016/j.vetmic.2011.03.001

Rubbi, L., Zhang, H., Feng, J., He, C., Kurnia, P., Ratan, P., et al. (2022). The effects of age, sex, weight, and breed on canid methylomes. *Epigenetics* 17, 1497–1512. doi: 10.1080/15592294.2022.2069385

Santibanez, R., Rodriguez-Salas, C., Flores-Yanez, C., Garrido, D., and Thomson, P. (2021). Assessment of changes in the Oral microbiome that occur in dogs with periodontal disease. *Vet. Sci.* 8:291. doi: 10.3390/vetsci8120291

Seo, S. H., Na, C. S., Park, S. E., Kim, E. J., Kim, W. S., Park, C., et al. (2023). Machine learning model for predicting age in healthy individuals using age-related gut microbes and urine metabolites. *Gut Microbes* 15:2226915. doi: 10.1080/19490976.2023.2226915

Stephan, B., Greife, H. A., Pridmore, A., and Silley, P. (2008). Activity of pradofloxacin against Porphyromonas and Prevotella spp. implicated in periodontal disease in dogs: susceptibility test data from a European multicenter study. *Antimicrob. Agents Chemother.* 52, 2149–2155. doi: 10.1128/AAC.00019-08

Templeton, G. B., Fefer, G., Case, B. C., Roach, J., Azcarate-Peril, M. A., Gruen, M. E., et al. (2023). Longitudinal analysis of canine Oral microbiome using whole genome sequencing in aging companion dogs. *Animals* 13:3846. doi: 10.3390/ani13243846

Wallis, C., and Holcombe, L. J. (2020). A review of the frequency and impact of periodontal disease in dogs. *J. Small Anim. Pract.* 61, 529–540. doi: 10.1111/jsap.13218

Wallis, C., Saito, E. K., Salt, C., Holcombe, L. J., and Desforges, N. G. (2021). Association of periodontal disease with breed size, breed, weight, and age in pure-bred client-owned dogs in the United States. *Vet. J.* 275:105717. doi: 10.1016/j.tvjl.2021.105717

Watanabe, A., Okada, J., Niwa, R., Inui, Y., Ito, K., Shimokawa, Y., et al. (2023). Profiling of bacterial communities associated with periodontal disease severity in dog subgingival plaque. *bioRxiv*. doi: 10.1101/2023.09.13.557668

Wickham, H. (2016). ggplot2: Elegant graphics for data analysis. New York: Springer-Verlag.

Yasuda, J., Yasuda, H., Nomura, R., Matayoshi, S., Inaba, H., Gongora, E., et al. (2024). Investigation of periodontal disease development and *Porphyromonas gulae* FimA genotype distribution in small dogs. *Sci. Rep.* 14:5360. doi: 10.1038/s41598-024-55842-8

Young, V. B. (2017). The role of the microbiome in human health and disease: an introduction for clinicians. *BMJ* 356:j831. doi: 10.1136/bmj.j831

Zaura, E., Nicu, E. A., Krom, B. P., and Keijser, B. J. (2014). Acquiring and maintaining a normal oral microbiome: current perspective. *Front. Cell. Infect. Microbiol.* 4:85. doi: 10.3389/fcimb.2014.00085

frontiers | Frontiers in Veterinary Science

TYPE Original Research
PUBLISHED 02 September 2024
DOI 10.3389/fvets.2024.1405470

OPEN ACCESS

EDITED BY
Shuai Liu,
China Agricultural University, China

REVIEWED BY
Rachel Pilla,
University of Milan, Italy
Jia Xu,
Jinhua Polytechnic, China

*CORRESPONDENCE
Holly H. Ganz
holly@animalbiome.com

RECEIVED 22 March 2024
ACCEPTED 09 August 2024
PUBLISHED 02 September 2024

CITATION
Rojas CA, Park B, Scarsella E, Jospin G, Entrolezo Z, Jarett JK, Martin A and Ganz HH (2024) Species-level characterization of the core microbiome in healthy dogs using full-length 16S rRNA gene sequencing.
Front. Vet. Sci. 11:1405470.
doi: 10.3389/fvets.2024.1405470

Species-level characterization of the core microbiome in healthy dogs using full-length 16S rRNA gene sequencing

Connie A. Rojas, Brian Park, Elisa Scarsella, Guillaume Jospin, Zhandra Entrolezo, Jessica K. Jarett, Alex Martin and Holly H. Ganz*

AnimalBiome, Oakland, CA, United States

Despite considerable interest and research in the canine fecal microbiome, our understanding of its species-level composition remains incomplete, as the majority of studies have only provided genus-level resolution. Here, we used full-length 16S rRNA gene sequencing to characterize the fecal microbiomes of 286 presumed healthy dogs living in homes in North America who are devoid of clinical signs, physical conditions, medication use, and behavioral problems. We identified the bacterial species comprising the core microbiome and investigated whether a dog's sex & neuter status, age, body weight, diet, and geographic region predicted microbiome variation. Our analysis revealed that 23 bacterial species comprised the core microbiome, among them *Collinsella intestinalis*, *Megamonas funiformis*, *Peptacetobacter hiranonis*, *Prevotella copri*, and *Turicibacter sanguinis*. The 23 taxa comprised 75% of the microbiome on average. Sterilized females, dogs of intermediate body sizes, and those exclusively fed kibble tended to harbor the most core taxa. Host diet category, geographic region, and body weight predicted microbiome beta-diversity, but the effect sizes were modest. Specifically, the fecal microbiomes of dogs fed kibble were enriched in several core taxa, including *C. intestinalis*, *P. copri*, and *Holdemanella biformis*, compared to those fed raw or cooked food. Conversely, dogs on a raw food diet exhibited higher abundances of *Bacteroides vulgatus*, *Caballeronia sordicola*, and *Enterococcus faecium*, among others. In summary, our study provides novel insights into the species-level composition and drivers of the fecal microbiome in healthy dogs living in homes; however, extrapolation of our findings to different dog populations will require further study.

KEYWORDS

canine fecal microbiome, core microbiome, dogs, PacBio, 16S rRNA gene sequencing, diet, geography, body weight

Introduction

Research on the gut microbiome, particularly over the past 20 years has led to the recognition that bacteria and other microbes inhabiting the gastrointestinal tract are not just passive travelers and instead interact with the host in ways that can have a profound effect on health (1). These microbial communities in animals are complex, characteristic, and reflect the host's diet, phylogenetic history, and other ecological factors (2–4). Of particular interest

to human and animal health are studies examining whether there is a core microbiome that comprises essential groups of bacteria found in most healthy individuals (5), that may be functionally important to the host. There is some evidence to suggest that functional redundancy is common in microbial communities, and entire groups of bacteria may have overlapping functions such that in some cases one or more groups can stand in for another (6). However, in certain cases, there may be less redundancy in functions that are more specialized within these microbial communities. For example, it has been observed that *Peptacetobacter hiranonis* (formerly *Clostridium hiranonis*) is the primary or perhaps only bacterial species performing bile acid metabolism in domestic dogs (7, 8) and its elimination or depletion resulting from antibiotic use leaves the gut microbiome with reduced ability to perform this function (9).

A challenge for assessing the impact of disease, medications, and probiotics on the gut microbiome arises from a lack of a consensus on the definition of what comprises a "normal" or "healthy" core microbiome (10). Microbiome studies differ in the prevalence and abundance thresholds used to determine the core, as well as the taxonomic unit at which the core is being defined (e.g., at level of genera, species, or family) (5). Others may forgo taxonomy altogether and focus on core functional genes (5). Additionally, the criteria used to define a "healthy" from a "not healthy" individual are also contentious. The size, homogeneity, and descriptive characteristics of the host group may also influence the study's findings. However, despite these challenges, efforts made to characterize the core microbiome of a diverse study population can be insightful and expand our understanding of the microbiome in that host species.

In this study, we screened the microbiomes of over 3,000 pet dogs (*Canis lupus familiaris*) living in homes in North America and focused on a curated subset of this group ($n = 286$) to provide a taxonomically and statistically defined core microbiome associated with health. Previous research has established the importance of the gut microbiome in canine health, yet significant gaps remain in identifying the precise bacterial species that constitute a healthy canine gut microbiome. Many past studies have relied on short-read sequencing technologies, which offer limited taxonomic resolution. Here, we employed full-length 16S rRNA gene sequencing (V1-V9) using PacBio technology to overcome these limitations and gain species-level insights. Long-read sequencing, particularly PacBio technology, has been shown to enhance the resolution and accuracy of microbiome analyses, deepening our understanding of the microbial communities present (11). Despite these advantages, the application of full-length 16S rRNA gene sequencing in dogs remains unexplored. Additionally, while factors like diet, body condition, probiotics, and antibiotics have already been studied for their impact on microbiome variation, their effects using full-length sequencing technology have not yet been examined.

Our curated subset of dogs were reported to be healthy by their owners ($n = 230$) or via veterinarian records ($n = 56$), and met strict criteria that included having no physical conditions and clinical signs, and no usage of daily medications or antibiotics, given that these contribute to gut dysbiosis in healthy dogs (12). With this dataset, we investigated whether factors such as sex & neuter status, age, body weight, diet, and geographic region significantly predicted microbiome alpha- or beta-diversity. In addition, although probiotic use is common in healthy dogs and dogs with chronic enteropathy (13), we aimed here to understand the bacterial composition of the fecal microbiome that is reflective of a less managed state. Thus, our healthy reference set excluded dogs that consumed probiotics. However, we conducted additional analyses to compare the fecal microbiomes of dogs in this reference set with those of dogs given bacterial probiotics ($n = 86$) who would have otherwise met the criteria for inclusion in the reference set. Collectively, our comparisons sheds light on the effects of important factors on the canine gut microbiome, providing valuable insights for the field of veterinary medicine.

Methods

Sample and metadata collection

Fecal samples were collected from 3,754 dogs, although samples from only 286 dogs (7.61% of samples) were the focus of this study (see section below). Of these 286 dogs, 230 were owned by customers of AnimalBiome, a private company offering microbiome testing services for companion animals, and 56 were enrolled in AnimalBiome's stool bank program, which provides screened fecal material for veterinary purposes. Pet owners were instructed to collect a small amount of their dog's fecal sample and place it in a 2 mL screw cap tube containing 70% molecular-grade ethanol. Pet parents were instructed to use the provided clean gloves, wooden sticks, and bags for fecal collection to avoid contamination.

Pet owners then shipped the fecal samples to AnimalBiome's facilities in Oakland, CA and provided pertinent information about their dogs, including name, date of birth, body weight, body condition, spay or neuter status, breed, diet, medication and supplement use, current clinical signs, health diagnoses, and physical conditions via an online survey. Owners also documented the fecal consistency and color of the submitted samples.

Criteria for defining the healthy dataset

For a dog to qualify for the healthy reference set, the following strict criteria needed to be met: body condition scores 4–6 (inclusive), no antibiotics given within the previous 12 months, no other medications reported currently in use, no bacterial probiotics, no AnimalBiome Gut Restore supplements, no clinical signs, no physical conditions, and no fecal descriptions that included the word "blood." An additional 86 dogs met the aforementioned criteria with the exception of bacterial probiotics, and their microbiomes were compared to those of the healthy reference set to assess the impact of probiotics on the microbiome. For descriptive statistics regarding our reference set (see Table 1).

The 56 dogs that were part of AnimalBiome's stool donor program met additional criteria and were clinically verified to be healthy via medical history records, veterinary visits, and monthly screenings of parasites and pathogens.

DNA extraction and full-length 16S rRNA amplicon gene sequencing

Genomic DNA was extracted from canine fecal samples using the QIAGEN DNeasy Powersoil Pro Isolation Kit on the QIAcube HT

TABLE 1 Characteristics of the pet dogs that comprised the healthy reference set ($n = 286$).

Characteristic	Subcategory	*N* (%)
Age, in years*	Median & (range)	4 (0.6–11)
Body condition score	Median & (range)	5 (4–6)
Body weight (kg)*	Median & (range)	21.2 (1.8–67.1)
Body weight category	<6 kg	30 (10%)
	6–10 kg	33 (12%)
	10–25 kg	114 (40%)
	25–45 kg	99 (34%)
	45 kg +	10 (4%)
Sex & Neuter Status*	Female intact	27 (9%)
	Female sterilized	102 (36%)
	Male intact	40 (14%)
	Male sterilized	117 (41%)
Breed (broad)	Shepherd	33 (12%)
	Poodle (& mixes)	30 (10%)
	Retriever	28 (10%)
	Terrier	23 (8%)
	Mix (unknown breeds)	19 (7%)
	Other (Husky, PitBull, Collie, Bulldog, etc.)	153 (53%)
Diet*	Kibble only	85 (30%)
	Raw food only	76 (27%)
	Cooked food only	45 (16%)
	Other (combinations of kibble, raw, cooked)	80 (27%)
Geographic region*	USA West	111 (39%)
	USA MidWest	22 (8%)
	USA South	28 (10%)
	USA Northeast	37 (13%)
	Canada	7 (2%)
	North America (unknown location)	81 (28%)

Fecal samples from two-hundred and eighty-six dogs comprised the healthy reference set and had their microbiomes analyzed in this study. The dogs were privately owned and resided in North America.
An * indicates that this factor was included in statistical models that analyzed microbiome composition, alpha-diversity, and beta-diversity.

instrument (QIAGEN, CA, USA). Amplification of the full-length 16S rRNA gene was achieved using primers 27F (5′-AGRGTTYGATYMTGGCTCAG-3′) and 1492R (5′-RGYTACCTTGTTACGACTT-3′), which were tailed with 16-bp asymmetric barcode sequences. The PCR mixture comprised 12.5 µL of KAPA HiFi HotStart ReadyMix PCR (KAPA Biosystems, MA, USA), 3 µL of each primer (at 2.5 µM), 2 µL of template DNA, and 4.5 µL of PCR-grade water. PCR conditions included an initial denaturation at 95°C for 3 min, followed by 25 cycles of denaturation at 95°C for 30 s, annealing at 57°C for 30 s, and a final extension at 72°C for 60 s. Full-length 16S rRNA purified amplicons were sequenced on a PacBio Sequel IIe platform (Pacific Biosciences, CA, USA). The sequenced amplicons were compared against the ZymoBIOMICS Microbial Community DNA Standard positive control (Zymo Research, Irvine, CA) and a negative control (PCR-grade water) to ensure QC and no contamination.

Although samples spanned multiple sequencing runs, this did not affect microbiome composition (PERMANOVA Bray-Curtis $F = 0.9$, $R^2 = 0.003$, $p = 0.54$; Aitchison $F = 1.35$, $R^2 = 0.004$, $p = 0.09$) and samples from the same run did not cluster together (Supplementary Figure S1). Each run always had the same number of samples and the number of reads per sample was extremely consistent across runs.

Bioinformatic processing of PacBio CSS reads

Raw PacBio reads were converted to HiFi reads for each sample using the SMRT Analysis software (v.11.0.0.146107). The resulting reads underwent quality trimming, denoising, dereplication, and chimera removal using the dada2 plugin within QIIME 2 (14), following the protocol outlined by Anderson et al. (15). Specifically, reads shorter than 1,300 bp and longer than 1,600 bp after adapter trimming were removed, the pseudo-pooling method was used for denoising, the maximum number of expected errors was set to 3, and the pooling method was used for chimera detection. After processing with DADA2, a table of ASV counts for each sample was produced. Samples average 7,026 sequences post-processing.

For ASV taxonomic assignment, we employed the Naive Bayes trained sklearn classifier (16) within QIIME 2, utilizing our manually curated version of the Silva (v.138.1 NR99) reference database (17) as detailed in Anderson et al. (15) and in AnimalBiome's pipeline for classifying PacBio full-length 16S rRNA HiFi reads.[1] The confidence threshold was set to 0.7, which has been shown to perform the best for the naive Bayes classifier (16). These taxonomic labels were further refined using stringent VSEARCH (18) classification also within QIIME2. This dual hybrid approach enabled greater specificity in the taxonomic labels (e.g., if an ASV was assigned Genus-level classification by sklearn but VSEARCH assigned it to Species with 100% confidence, then we retained the species-level call) and confidence in these assignments. ASVs not classified at the Family level were filtered from the dataset. For ASVs unclassified at the species level, we appended "unclassified" to their existing taxonomic label.

The table of ASV counts was aggregated at the species level and imported into the R statistical software program (v.4.3.0) for subsequent statistical analyses and visualizations.

Statistical analysis

The primary objective of this study was to identify the bacterial species comprising the core microbiome of dogs in the healthy reference set. To achieve this, we determined the prevalence of each bacterial taxon by dividing the number of samples containing that taxon by the total sample size. Additionally, we computed various

1 https://github.com/AnimalBiome/AB_FlexTax/tree/main

descriptive statistics on taxon relative abundances including the mean, median, minimum (excluding 0 s), maximum, standard deviation, and percentiles (0.025, 0.1, 0.9, 0.975). Bacterial species with a prevalence of at least 33.333% and mean relative abundance >0.5% were designated as part of the core. This allowed us to capture highly prevalent taxa, as well as highly abundant taxa, and extract patterns of insight that are reflective of our study population. Additionally, because the core was being defined at the level of bacterial species and not broader bacterial genera, we deemed these thresholds appropriate. For statistical analysis, two core microbiome metrics were computed: (i) the number of core taxa, and (ii) the core microbiome sum, representing the proportion of the microbiome composed of core taxa.

The secondary objective was to identify host factors correlated with the core microbiome metrics, and microbiome alpha- and beta-diversity in this healthy reference set. Four types of statistical models were constructed: (i) a model that included sex & neuter status, age (years), and body weight (kg) as predictor variables, (ii) another model that specified diet as the sole predictor variable and excluded dogs with combined diets such as "Kibble & Raw," (iii) a third model that had USA geographic region (West, Midwest, Northeast, South) as the only predictor, and filtered dogs residing in Canada or in unknown North American locations, and (iv) a fourth model that compared the fecal microbiomes of dogs in the reference set that are part AnimalBiome's stool donor program with those that are not.

For both alpha- and beta-diversity analyses, microbiome data from dogs in the healthy reference set were subsampled to 3,500 reads per sample to account for uneven sequencing depth and minimize the risk of falsely detecting or rejecting group differences (19). This resulted in the exclusion of 24 samples. Although this sequence count cutoff might seem low compared to studies using Illumina short-read sequencing (150 or 250 bp amplicons), it is appropriate and robust for studies utilizing full-length 16S rRNA gene PacBio HiFi reads (1,600 bp), where throughput is lower but reads are longer. The longer sequences allow for a greater proportion of reads assigned to the species level compared to Illumina sequencing (11).

We computed three alpha-diversity metrics [Chao 1 Richness (log), Shannon Diversity, and Gini-Simpson's index (1- Simpson's Index)] using the *phyloseq* package (v.1.44.0) (20). Generalized additive models (GAMs) from the *mgcv* package (v.1.8–42) (21) correlated microbiome alpha-diversity or core microbiome metrics with the host factors of interest, as outlined in the above paragraph. In these GAMs, the two continuous predictors—age and body weight—were included as smooth terms, while all others were listed as linear terms. Hypothesis testing on the GAMs was conducted using Wald tests of significance from the *mgcv* package. Post-hoc comparisons were done with the *emmeans* (v.1.8.7) (22) and *multcomp* (v.1.4–23) (23) packages.

For beta-diversity analyses, rarefied microbiome data at the species level were converted to proportions for Bray-Curtis distances or applied a Center Log Ratio transformation for Aitchison distances. Both types of distances were estimated with the *phyloseq* package. Permutational Multivariate Analyses of Variance (PERMANOVAs) from the *vegan* package (v.2.6–4) (24) assessed the marginal effects of host predictor variables on Bray-Curtis and Aitchison distances, following the four models described earlier in this section. Post-hoc comparisons were done with the *pairwise Adonis* package (v0.4.1) (25) which employs Tukey tests.

Lastly, differential abundance testing was done with the *LinDA* package (v0.1.0) (26) to identify the bacterial species that were enriched in the fecal microbiomes of dogs according to their sex-neuter status, age, body weight, diet, or geographic region. The prevalence cutoff was set to 20%, winsorization cutoff (quantile) to 0.97, alpha to 0.05, and p.value adjustment as "FDR." All figures included in this manuscript were constructed with the *ggplot2* package (v.3.4.2) (27).

One additional statistical test was conducted that compared the fecal microbiomes of dogs in the healthy reference set ($n = 286$), with those from dogs receiving bacterial probiotics ($n = 86$) that would otherwise qualify to be in the healthy reference set. Statistical models in the forms of GAMs or PERMANOVAs specified rarefied microbiome alpha-diversity, beta-diversity, or core microbiome metrics as the dependent variable and bacterial probiotic intake (True/False) as the independent variable.

Results

Characteristics of healthy dogs

The dogs that formed part of the reference set ($N = 286$, Table 1) were verified to be healthy ($N = 56$) or were presumed to be healthy ($N = 230$), and had a median age of 4 yrs., median body weight of 21.2 kg, and median body condition score of 5. They tended to be medium- to large-size dogs, with 40% found in the 10–25 kg category and another 34% placed in the 25–45 kg category (Table 1). 70% of dogs were spayed or neutered (36% females, 41% males). The most common breeds were Australian and German Shepherds (12%), Goldendoodles and Poodles (10%), Golden Retrievers and Labrador Retrievers (10%), and Terriers (8%). About 30% of dogs were fed only dry kibble, another 27% ate only raw food, and 16% were fed only cooked food, with the remaining dogs (27%) consuming a combination of the aforementioned diets (Table 1). 70% of dogs in the reference set resided in known locations in the USA (39% came from the West coast, 13% from the Northeast, 10% from the South, and 8% from the Midwest), 2% resided in Canada, and for the remaining participants (28%), their specific North American location or region was unknown.

As mentioned, 56 dogs in the reference set (20% of dataset) were part of AnimalBiome's stool donor program and thus, were verified to be healthy via medical records, veterinary visits, and monthly monitoring of parasites and pathogens. This presented a unique opportunity to examine how the microbiomes of clinically validated healthy dogs compared to those from presumed healthy dogs. We found that the microbiomes of stool donors were richer than the microbiomes of presumed healthy dogs (GAM LRT Chao 1 Richness $F = 3.67$, $p = 0.056$; Shannon Diversity $F = 1.5$, $p = 0.22$; Gini-Simpson index $F = 1.83$, $p = 0.038$). Donors had a slightly greater number of core taxa ($\bar{x}$: 15.64 taxa) than did non-stool donors ($\bar{x}$: 13.29 taxa) (Figure 1A); donors also had more of their microbiome comprised by core taxa (80.8% of their microbiome) than did non-stool donors (73.9% of their microbiome) (GAM LRT Core taxa number $F = 14.96$, $p = 0.001$; Core Sum $F = 4.13$, $p = 0.04$). Lastly, donors have marginally distinct fecal microbiomes from those of apparently healthy dogs (PERMANOVA Bray-Curtis $R^2 = 0.019$, $p = 0.001$; Aitchison $R^2 = 0.024$, $p = 0.001$) (Figure 1B). This implies that, as anticipated, some

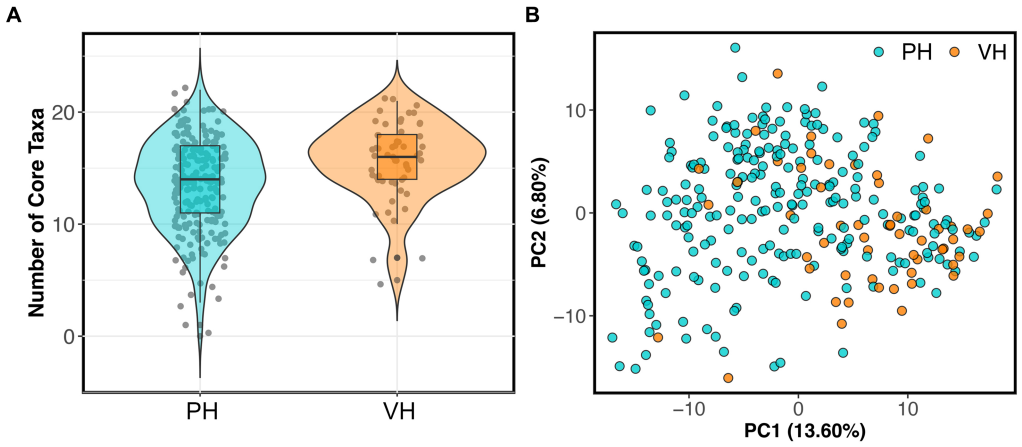

FIGURE 1
Fecal microbiomes differ between verified healthy and presumed healthy dogs. Dogs in the healthy reference set were categorized as "verified healthy" (VH) if they were verified to be healthy via medical records, veterinary visits, and monthly parasite screenings, or "presumed healthy" (PH) if they were not and were reported to be healthy by their owners. **(A)** Number of core taxa for verified healthy vs. presumed healthy dogs. **(B)** PCoA ordination based on Aitchison distances showing the clustering of verified healthy vs. presumed healthy microbiomes.

presumed healthy dogs may not possess the same level of health as perceived by their owners, or that the screening criteria for clinically validated dogs may favor a narrower spectrum of microbiome compositions.

Core fecal microbiome of healthy dogs

Twenty-three bacterial species formed part of the core microbiome in verified healthy and presumed healthy dogs (Table 2, Figure 2, and Supplementary Table S1). These were taxa that were found in at least 1 of 3 dogs that formed part of the healthy reference and had a mean relative abundance >0.5% across the dataset. This was an appropriate cutoff for a core defined at the bacterial species-level. Additionally, given the large variability found in the surveyed canine microbiomes, a stricter cutoff would not have been informative or representative of our data.

The bacterial core species with the highest prevalence (>60%) were: *Blautia hansenii*, *Ruminococcus gnavus*, *Faecalimonas umbilicata*, unclassified *Blautia*, unclassified *Fusobacterium*, *Collinsella intestinalis*, *Megamonas funiformis*, *Peptacetobacter hiranonis*, *Blautia marasmi*, and unclassified *Lachnoclostridium* (Table 2). Other bacterial species that were found at slightly lower prevalences but were also part of the core included *Escherichia coli*, *Prevotella copri*, *Romboutsia ilealis*, *Sutterella stercoricanis*, *Turicibacter sanguinis*, and *Streptococcus lutetiensis*. Of the 23 core bacterial taxa, the ones found at the highest relative abundances in dogs were *Megamonas funiformis* (11.2% mean relative abundance), *Streptococcus lutetiensis* (9.4%), unclassified *Fusobacterium* (6.5%), *Clostridium perfringens* (5.3%), *Collinsella intestinalis* (4.8%), and *Faecalimonas umbilicata* (4.4%) (Figure 2).

On average, the core microbiome represented the overall canine microbiome well and made up 75% of the sequences detected in a sample. However, the presence and relative abundances of core taxa were widely variable among dogs, with some dogs having some core taxa but not others. Interestingly, 10% of dogs in the dataset appeared to harbor a completely different set of bacteria that were not part of the core (Supplementary Figure S2). These dogs instead harbored high abundances of *Bacteroides vulgatus*, *Bifidobacterium pseudocatenulatum*, and *Lactobacillus acidophilus*, among others (Supplementary Figure S2).

Effects of sex-neuter status, age, body weight, diet, and geography on the microbiome

Next, we examined the impact of sex-neuter status, age (yrs), body weight (kg), diet, and geographic region on the core microbiome and on microbiome alpha-diversity and beta-diversity of presumed healthy and verified healthy dogs. Overall, the fecal microbiomes of sterilized females had marginally more core taxa ($\bar{x}$:14.2) than the microbiomes of intact males ($\bar{x}$:12.72) (GAM Tukey test $p < 0.05$, Figure 3A, and Supplementary Table S2). Dogs of intermediate body weights had more core taxa than small or large dogs (GAM $p < 0.05$, Figure 3C, and Supplementary Table S2). Dogs fed kibble tended to have slightly more core taxa in their microbiomes ($\bar{x}$:15.1) than dogs fed raw food ($\bar{x}$:13.3) or cooked food ($\bar{x}$:12.9) (GAM Tukey test $p < 0.05$) (Figure 3D). However, the total percentage of the fecal microbiome composed of core taxa was not associated with sex & neuter status, body weight, or diet. This core metric was significantly associated with age; there was a modest decline in the proportion of the microbiome made up of core taxa as the dog aged (GAM $p < 0.05$) (Figure 3B and Supplementary Table S2). Lastly, dogs residing in different geographic regions within the USA did not differ significantly in the number or sum of their core microbiome taxa.

Microbiome alpha-diversity was significantly correlated with all host factors examined except age and geographic region (GAM, $p < 0.05$, Figures 4A–D, and Supplementary Table S3). Specifically, the microbiomes of intact females ($\bar{x}$ Chao1 Richness: 33.94) were more diverse than the microbiomes of sterilized males ($\bar{x}$: 29.29) (Tukey test $p < 0.05$, Figure 4A). Microbiome alpha-diversity was highest in dogs of intermediate body weights (20–45 kg) (GAM $p < 0.05$, Figure 4C).

TABLE 2 Twenty-three bacterial species comprise the core microbiome in healthy dogs.

Bacterial species	Prev.	Mean	Median	Min*	Max	Stdev	Low10pct	Pct50	High90pct	High97.5pct
Blautia hansenii	0.867	3.656	1.008	0.045	50.525	7.048	0.000	1.008	10.260	22.576
Ruminococcus gnavus	0.846	3.101	0.970	0.049	68.980	6.746	0.000	0.970	7.947	23.084
Faecalimonas umbilicata	0.832	4.430	0.874	0.020	50.997	8.311	0.000	0.874	12.328	28.769
Blautia UC	0.797	3.948	1.287	0.022	51.346	7.174	0.000	1.287	11.727	29.979
Fusobacterium UC 1	0.766	6.558	2.259	0.032	46.319	9.333	0.000	2.259	18.702	34.324
Collinsella intestinalis	0.745	4.877	1.714	0.037	46.192	7.514	0.000	1.714	14.671	26.654
Megamonas funiformis	0.671	11.270	1.441	0.024	80.080	17.837	0.000	1.441	37.305	62.057
Fusobacterium UC 2	0.654	2.520	0.283	0.017	41.563	5.863	0.000	0.283	6.423	22.214
Peptacetobacter hiranonis	0.654	3.274	0.475	0.031	47.203	6.327	0.000	0.475	9.412	21.417
Blautia marasmi	0.636	0.642	0.225	0.018	7.525	1.104	0.000	0.225	2.038	3.848
Lachnoclostridium UC	0.605	0.758	0.135	0.019	20.325	2.010	0.000	0.135	1.729	5.744
Blautia caecimuris	0.573	0.864	0.093	0.031	13.586	1.917	0.000	0.093	2.354	7.551
Clostridium perfringens	0.510	5.328	0.040	0.032	95.001	12.995	0.000	0.040	18.875	46.342
Romboutsia UC	0.493	1.035	0.000	0.029	30.672	2.979	0.000	0.000	2.613	11.264
Blautia glucerasea	0.462	1.083	0.000	0.020	36.227	3.388	0.000	0.000	2.378	11.972
Turicibacter sanguinis	0.441	1.551	0.000	0.032	52.813	5.268	0.000	0.000	3.501	14.519
Romboutsia ilealis	0.416	1.300	0.000	0.038	55.220	4.735	0.000	0.000	2.974	14.949
Bacteroides UC	0.409	1.930	0.000	0.025	48.088	5.481	0.000	0.000	4.909	18.855
Escherichia coli	0.402	1.030	0.000	0.025	48.403	3.760	0.000	0.000	2.478	10.002
Holdemanella biformis	0.395	2.093	0.000	0.032	73.689	6.319	0.000	0.000	6.181	15.669
Allobaculum stercoricanis	0.392	1.329	0.000	0.024	38.850	4.160	0.000	0.000	3.209	11.478
Prevotella copri	0.350	3.331	0.000	0.034	75.757	8.934	0.000	0.000	11.139	30.045
Streptococcus lutetiensis	0.336	9.444	0.000	0.020	91.673	22.138	0.000	0.000	47.421	78.048

UC, unclassified; prev., prevalence; pct, percentile.
*The minimum value excludes 0 s; true minimum value is 0 which is not informative.

Dogs that consumed a cooked food diet ($\bar{x}$ Shannon Diversity: 1.71) had less diverse fecal microbiomes than dogs that consumed kibble ($\bar{x}$: 2) or raw food ($\bar{x}$: 2.04) (Tukey test $p < 0.05$, Figure 4D).

All of the factors examined in this study significantly predicted fecal microbiome beta-diversity (PERMANOVAs $p < 0.05$, Figures 5A–E, and Supplementary Table S4), but the effect sizes were low. A dog's diet accounted for the largest variance in the microbiome (5%), followed by geographic region (2.2%), body weight (1.8%), sex and neuter status (1.1%), and age (1.1%) (Supplementary Table S4). In an ordination plot, none of the host factors examined formed defined clusters which suggests that fecal microbiomes of dogs are likely influenced by a multitude of host factors. No one host factor alone can predict the composition of canine fecal microbiomes, even in healthy individuals that do not have any physical conditions, were not taking medications, and were of similar body conditions.

Nevertheless, we conducted post-hoc comparisons to determine which groups of dogs differed in their beta-diversity. The microbiomes of dogs fed kibble were modestly different from those of dogs fed raw food (Bray-Curtis Tukey test $F = 6.61$, $R^2 = 0.043$, $p = 0.001$; Aitchison Tukey test $F = 7.01$, $R^2 = 0.046$, $p = 0.001$) or cooked food (Bray-Curtis

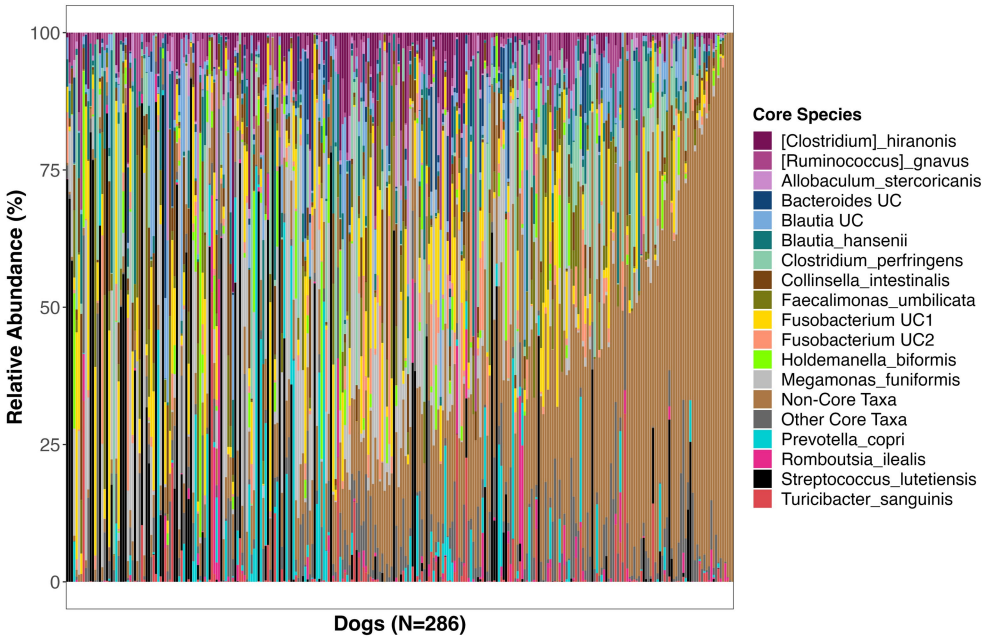

FIGURE 2
Relative abundances of bacterial species comprising the core microbiome in healthy dogs. These bacterial species were found in at least 33% of dogs at a mean relative abundance >0.5%. UC, unclassified.

Tukey test $F = 3.89$, $R^2 = 0.031$, $p = 0.001$; Aitchison Tukey test $F = 5.42$, $R^2 = 0.043$, $p = 0.001$). Regarding geographic region, minor differences were found between the microbiomes of dogs living in the western USA and dogs living in the Midwest (Bray-Curtis Tukey test $F = 1.63$, $R^2 = 0.013$, $p = 0.05$) or Northeast (Aitchison Tukey test $F = 1.57$, $R^2 = 0.011$, $p = 0.05$) (Figure 5E). The microbiomes of intact females were slightly different from the microbiomes of sterilized males (Aitchison Tukey test $F = 1.75$, $R^2 = 0.013$, $p = 0.02$).

One additional statistical comparison was conducted to determine whether the intake of bacterial probiotics impacted the microbiome. For this, the fecal microbiomes of dogs in the healthy reference set ($n = 286$) were compared with the fecal microbiomes of dogs that received bacterial probiotics ($n = 86$) and would otherwise qualify to be part of the healthy reference set. The two groups did not differ in terms of their core species (GAM LRT Core sum $F = 0.004$, $p = 0.94$; Core number $F = 0.92$, $p = 0.33$) or alpha-diversity (GAM LRT Chao 1 Richness $F = 0.218$, $p = 0.641$; Shannon Diversity $F = 0.078$, $p = 0.78$; Gini-Simpson index $F = 0.002$, $p = 0.964$). The two groups differed marginally in terms of their beta-diversity (PERMANOVA Bray-Curtis $R^2 = 0.003$, $p = 0.19$; Aitchison $R^2 = 0.004$, $p = 0.052$).

Identifying bacterial species that are enriched in the fecal microbiomes of dogs

Given that microbiome beta-diversity was moderately associated with sex & neuter status, age, body weight, diet, and geographic region, we sought to identify the bacterial species that could underlie those differences.

Differential abundance testing revealed that the abundances of six bacterial species, among them *Prevotella copri*, *Alloprevotella rava*, and *Bacteroides coprocola* decline with age, but the opposite was true for *Escherichia coli* abundances (LinDA p.adjusted <0.05, Figure 6A, and Supplementary Table S5). Sixteen bacterial species were more abundant in the fecal microbiomes of large dogs compared to smaller dogs. These species were *Megamonas funiformis*, *Collinsella intestinalis*, *Sutterella stercoricanis*, *Turicibacter sanguinis*, *Bacteroides plebeius*, and *Collinsella tanakaei*, among others (LinDA p.adjusted <0.05, Figure 6B, and Supplementary Table S5). Differential abundance testing was not able to single out any particular bacterial species as varying significantly between intact females and sterilized males (LinDA p.adjusted >0.05, Supplementary Table S5).

Compared to dogs fed only kibble, the fecal microbiomes of dogs fed raw food were enriched in 15 bacterial species, including *Bacteroides vulgatus*, *Caballeronia sordidicola*, *Enterococcus faecium*, *Erysipelatoclostridium ramosum*, three *Blautia* sp. and two *Clostridium* sp. (LinDA p.adjusted <0.05, Figure 7A, and Supplementary Table S6). A diet of only kibble enriched for *Collinsella intestinalis*, *Turicibacter sanguinis*, *Megamonas funiformis*, *Holdemanella biformis*, and *Prevotella copri*, among others (LinDA p.adjusted <0.05, Figures 7A,B). Dogs fed cooked food had an overrepresentation of two bacterial species: *Faecalimonas umbilicata* and *Clostridium perfringens* compared to dogs fed kibble (LinDA p.adjusted <0.05, Figure 7B). No differentially abundant bacteria taxa were detected between the fecal microbiomes of dogs that consumed cooked food compared to raw food (LinDA p.adjusted >0.05).

Lastly, dogs residing in the western USA tended to harbor larger abundances of *Enterococcus faecium* and *Escherichia coli* than dogs that lived in the Northeast region of the USA (LinDA p.adjusted <0.05). No differences in fecal bacterial abundances were identified between dogs living in western USA and dogs living in the Midwest.

10.3389/fvets.2024.1405470

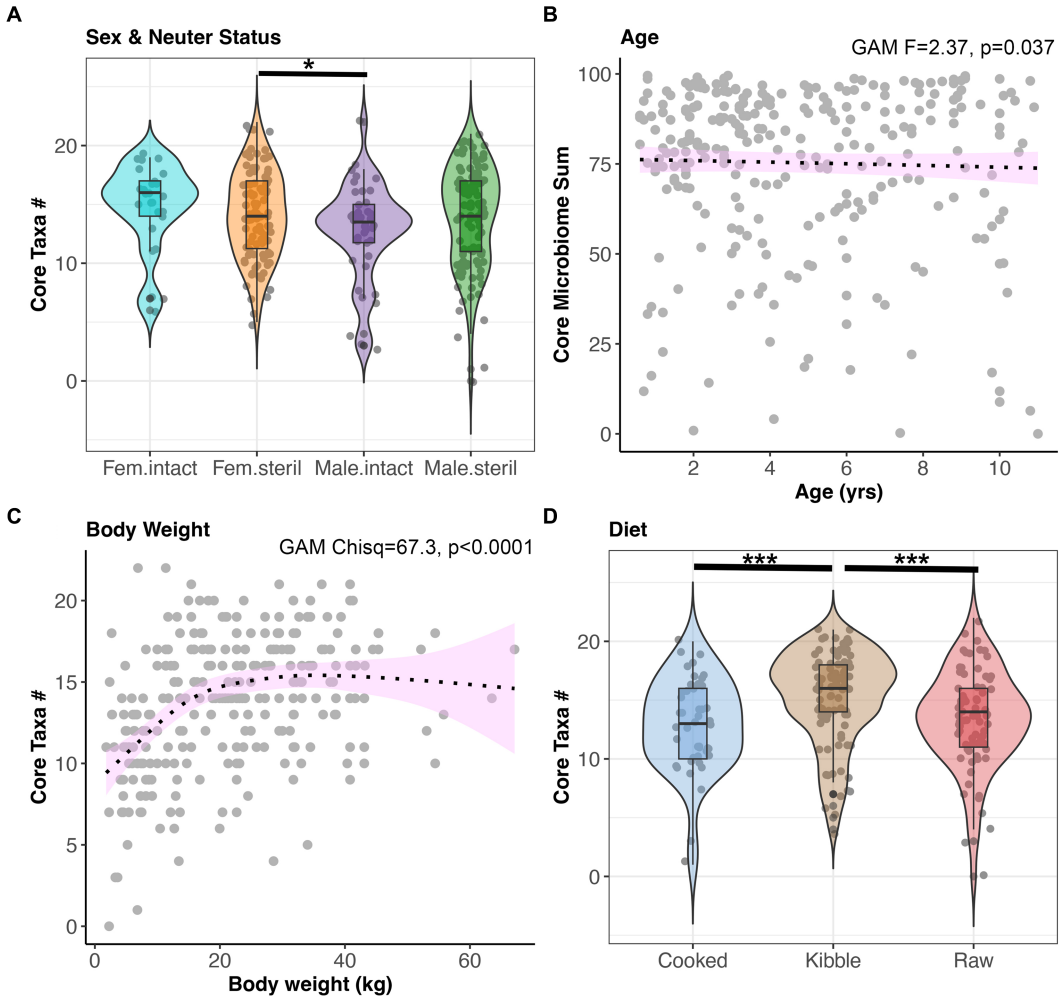

FIGURE 3
The number of core taxa present in canine fecal microbiomes varies with sex & neuter status, age, body weight, and diet. All dogs that were part of the dataset had BCS 4–6, and no history of antibiotics, medications, bacterial probiotics, and physical conditions. **(A)** Number of core taxa (max 23) for each Sex-Neuter category. **(B)** Proportion of the microbiome made up of core taxa regressed against age, with smooth curve overlaid to illustrate relationship between x and y. **(C)** Number of core taxa plotted against body weight in kg. **(D)** Number of core taxa for each diet category. *$p < 0.05$, **$p < 0.01$, ***$p < 0.0001$.

Discussion

To date, knowledge of the bacterial species comprising the core fecal microbiome in healthy dogs is limited. Here, we used full-length 16S rRNA gene sequencing to gain novel insights into the bacterial species residing in the healthy canine gut. Specifically, we profiled the fecal microbiomes of 286 total healthy dogs—56 verified to be healthy and 230 presumed to be healthy—and identified a core microbiome comprising 23 bacterial species, which included both well-established beneficial taxa like *Peptacetobacter hiranonis* and those belonging to genera traditionally associated with pathogenicity, such as *Escherichia coli* and *Streptococcus lutetiensis*. Host factors such as diet, age, body weight, sex & neuter status, and geographic region predicted microbiome variation.

It is important to emphasize that our study only evaluated a handful of host factors but other factors such as lifestyle, access to the outdoors, exercise frequency, and breed could also be significantly impacting microbiome variation. Additionally, our reference set of dogs all lived in homes in North America and were selected from a larger pool of dogs based on our chosen criteria. The study's findings could change if the selection criteria are adjusted. We encourage future studies to examine whether the same patterns are observed for dogs in other continents or dogs residing in different living environments.

Nevertheless, even with these limitations, our study provides novel information regarding the composition and variation of canine fecal microbiomes, and demonstrates the utility of full-length 16S rRNA gene sequencing in microbiome research.

Core microbiome species of healthy canines

Across 286 verified healthy or presumed healthy dogs, a core group of 23 bacterial species was detected, among them *Megamonas funiformis*, *Peptacetobacter hiranonis*, *Blautia hansenii*, *Escherichia coli*,

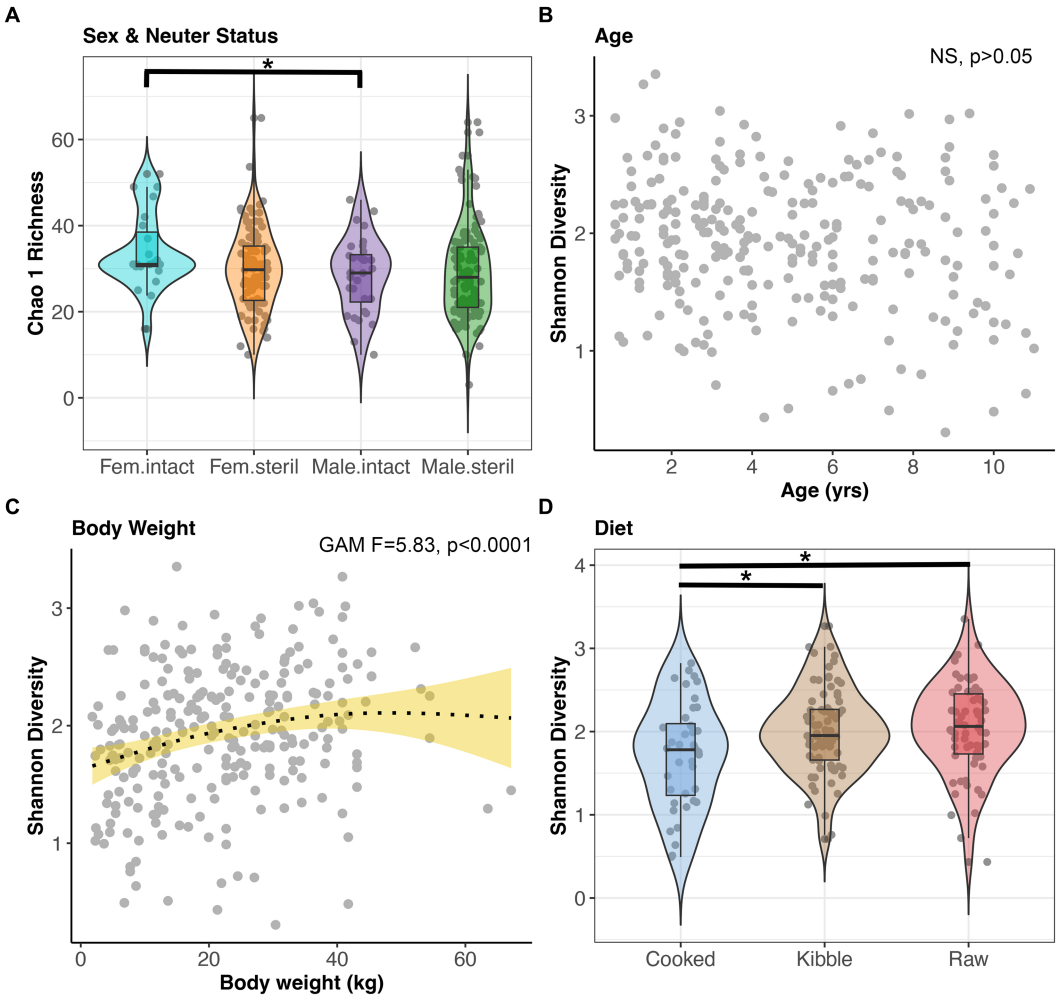

FIGURE 4
Microbiome alpha-diversity varies with dog sex & neuter status, age, body weight, and diet. **(A)** Chao 1 Richness by Sex-Neuter status (Female intact, Female sterilized, Male intact, Male sterilized). **(B,C)** Shannon diversity plotted against age in years or body weight in kg, with smooth curve overlaid to illustrate relationship between x and y. **(D)** Shannon diversity for each diet category. *$p < 0.05$, **$p < 0.01$, ***$p < 0.0001$.

Turicibacter sanguinis, *Prevotella copri*, *Sutterella stericoris*, *Streptococcus lutetiensis*, and unclassified *Fusobacterium*.

The core species belong to genera commonly found in the fecal microbiomes of dogs and cats. Likewise, in a dataset of 96 dogs from 9 different breeds, the most abundant bacterial genera were *Fusobacterium*, *Bacteroides*, *Prevotella*, *Blautia*, and *Lactobacillus* (28). Similarly, another study focusing on Maltese, Miniature Schnauzers, and Poodles found *Lactobacillus*, *Megamonas*, *Streptococcus*, *Blautia*, *Prevotella*, and *Escherichia* as the predominant bacterial groups (29).

However, much less is known beyond genus-level, as few canine microbiome studies have reported findings at a finer level of resolution. A recently published study did find that *Streptococcus lutetiensis*, *Collinsella intestinalis*, *Peptacetobacter hiranonis*, *Turicibacter sanguinis*, and *Blautia hansenii* were predominant in the fecal microbiomes of dogs receiving a low protein, low fiber diet and yeast probiotic (30). Another study surveying the microbiomes of 78 healthy dogs using shotgun metagenomic sequencing and qPCR reported the following three bacterial species as being part of the core (>78% prevalence): *Ruminococcus gnavus*, *P. hiranonis*, and *P. copri* (31). The remainder of the core was not defined at the species-level but contained genera represented in our dataset, e.g., *Blautia*, *Streptococcus*, and *Fusobacterium* (31). Their core also contained *Bifidobacterium* and *Lactobacillus* which were more rare in our dataset, likely due to differences in sequencing technologies and study populations.

Among the bacterial species detected in the core, *Peptacetobacter hiranonis*, is known for its beneficial effects on canine gut health. These anaerobes are the main group of microbes that dehydroxylate primary bile acids (PBAs) into secondary bile acids (SBAs) in the mammalian gut (32, 33). PBAs facilitate the emulsification of dietary fats and aid in the digestion and absorption of lipids; however, when conjugated, they can also be toxic to bacteria (34, 35). SBAs are involved in lipid metabolism, cell autophagy and immune system activation (36–38), but when low, are a biomarker of dysbiosis. Dogs with chronic enteropathies, inflammatory bowel disease, or antibiotic-induced dysbiosis (9, 39–41) have substantially reduced abundances of *P. hiranonis* and lower levels of SBAs compared to healthy dogs. Restoration of *P. hiranonis* abundances via the administration of prebiotics, synbiotics, or fecal transplants may restore bile acid metabolism and decrease dysbiosis (40, 42).

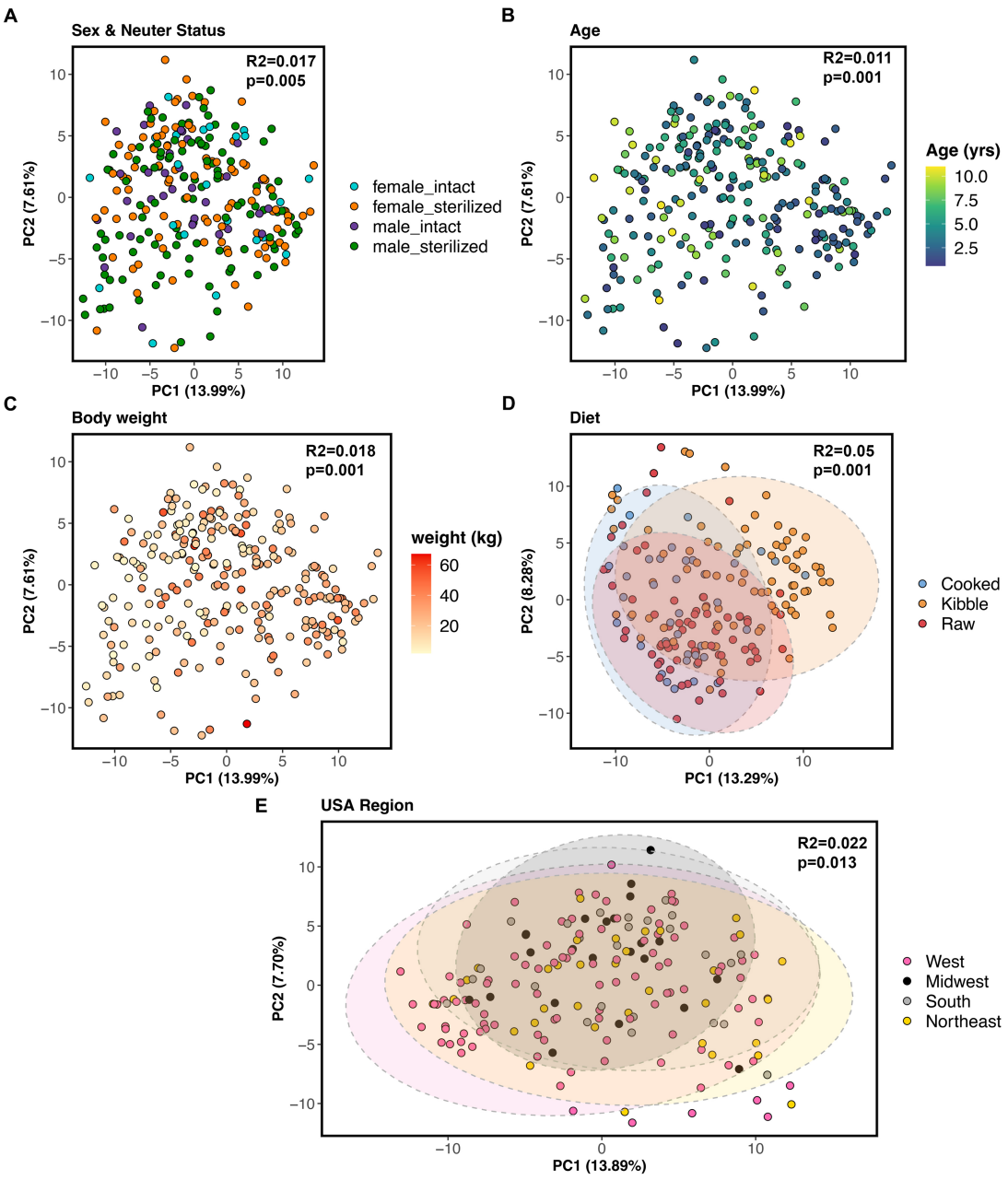

FIGURE 5
Host correlates of fecal microbiome beta-diversity in healthy dogs. PCoA ordinations based on Aitchison distances color coded by **(A)** sex & neuter status, **(B)** age (yrs), **(C)** body weight (kg), **(D)** diet, or **(E)** geographic region. PERMANOVA R^2 and *p*-values are shown.

Prevotella copri is another beneficial microbe known for its role in producing short-chain fatty-acids (SFCAs) in the gut, primarily succinate, acetate, and formate from the fermentation of carbohydrates (43–45). SCFAs serve as rich energy sources for other microbes or for host colonocytes (46), exhibit anti-inflammatory effects (47), and protect the mucosal intestinal barrier (48). Dogs with acute hemorrhagic diarrhea syndrome have lower abundances of *P. copri* compared to healthy controls, and administering colonoscopic fecal microbiota transplants (FMTs) to these dogs increases their *P. copri* levels (49). In mice, administration of *P. copri* via oral gavage improves glucose tolerance in individuals consuming a high-fiber, low-fat diet (50).

Less is known about other canine core microbiome species such as *Turicibacter sanguinis*. In mice, the absence of *Turicibacter* spp. in the gut is associated with increased susceptibility to severe *Citrobacter rodentium* infection and colonization with *T. sanguinis* provides protection from disease (51). Shotgun metagenomic analyses suggest that *T. sanguinis* may also be involved in bile acid, lipid, and steroid metabolism and the regulation of systemic triglyceride levels (52, 53). Dogs with gastrointestinal diseases including chronic enteropathy, acute and chronic diarrhea, and inflammatory bowel disease have lower abundances of *Faecalibacterium*, *Turicibacter*, *Blautia*, *Fusobacterium*, and *P. hiranonis*, and higher abundances of *Escherichia coli* compared

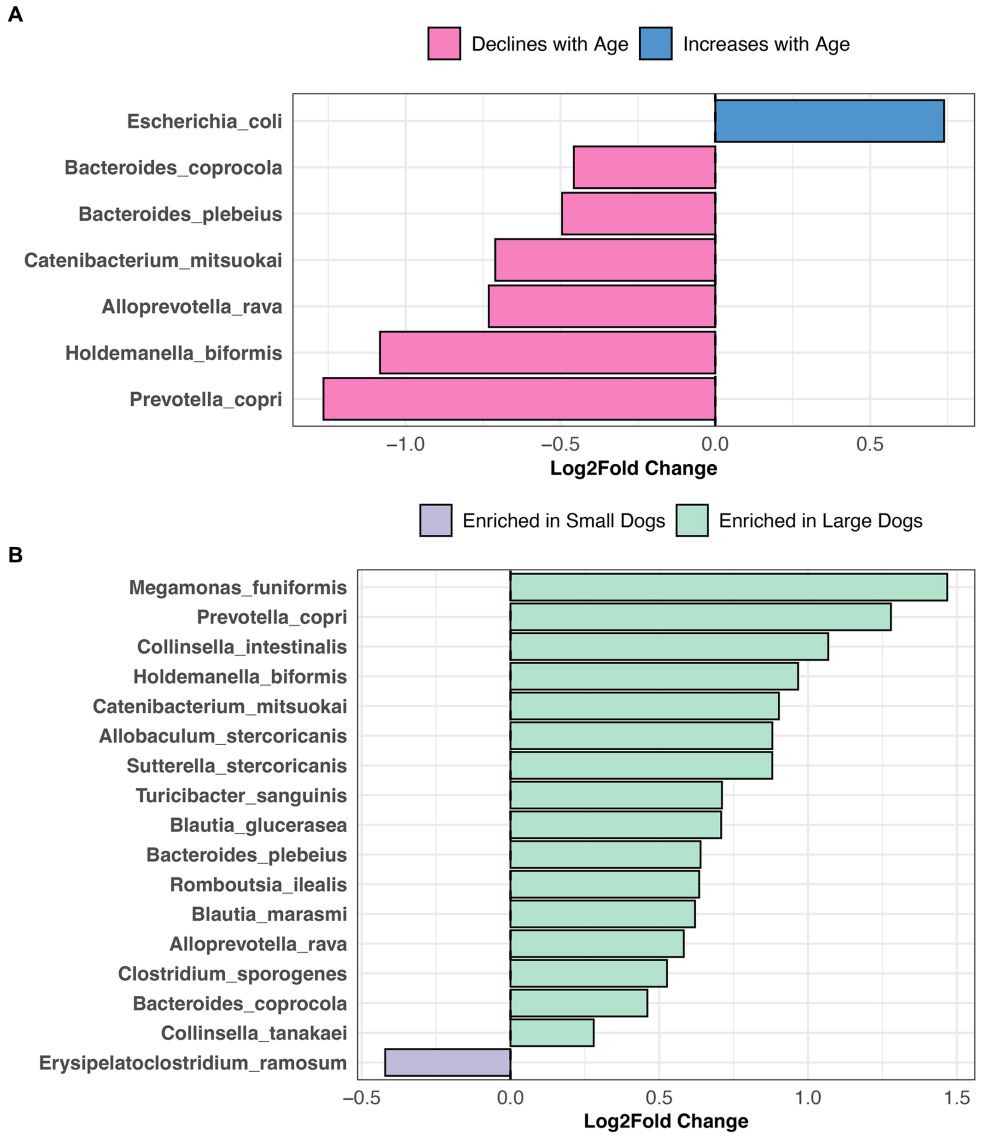

FIGURE 6
Bacterial species enriched in the microbiomes of young dogs and large dogs. Results from LinDA differential abundance analyses performed at the bacterial species level. **(A,B)** The LinDA model included age (yrs) and body weight (kg) as continuous variables, and sex & neuter status as a categorical variable, though no statistically significant taxa emerged for the categorical predictor.

to healthy dogs (54). However, more research is needed to uncover the potential impacts of *T. sanguinis* on canine health and the microbiome.

The presence of *Escherichia coli* in the gut is not always associated with disease. More than 700 serotypes of *E. coli* have been identified across humans, domestic mammals, and wild mammals (55, 56), and only a small fraction contain the virulence factors (57) that cause infections. In a recent study, 38 *E. coli* isolates were recovered from the fecal samples of healthy dogs, and these formed a distinct phylogenetic group from *E. coli* isolates recovered from dogs with diarrhea (58). Another study reported over 69 unique *E. coli* isolates collected from the feces of 183 healthy dogs (59). While some of the isolates demonstrated resistance against antibiotics, this in itself does not imply virulence or disease-causing potential. In the absence of clinical symptoms, *E. coli* appears to be a natural resident of the canine fecal microbiome and our work supports that. However, overgrowth of *E. coli* can indicate a microbiome imbalance, which could have functional consequences for the host.

It may be surprising that a *Streptococcus* species (*S. lutetiensis*) was prevalent in the microbiomes of presumed healthy dogs in our study. Pathogenic *Streptococcus* spp. (e.g., *S. equi* subsp. *zooepidemicus*) (60) are well documented but commensal (e.g., *S. canis*) and potentially beneficial Streptococci (e.g., *S. dentisani*) also exist (61). *S. lutetiensis* has been isolated from healthy dogs administered oligofructose and inulin (62), but is also found in high proportions in the microbiomes of dogs with lymphoma compared to healthy dogs (63). These findings suggest that the role of *S. lutetiensis* in canine health is complex and warrants further investigation. Significant taxonomic changes and genomic similarities among *Streptococcus* spp. add another layer of complexity. Taxonomic misidentifications have prompted researchers to place *S. lutetiensis* within the broader *Streptococcus bovis* group,

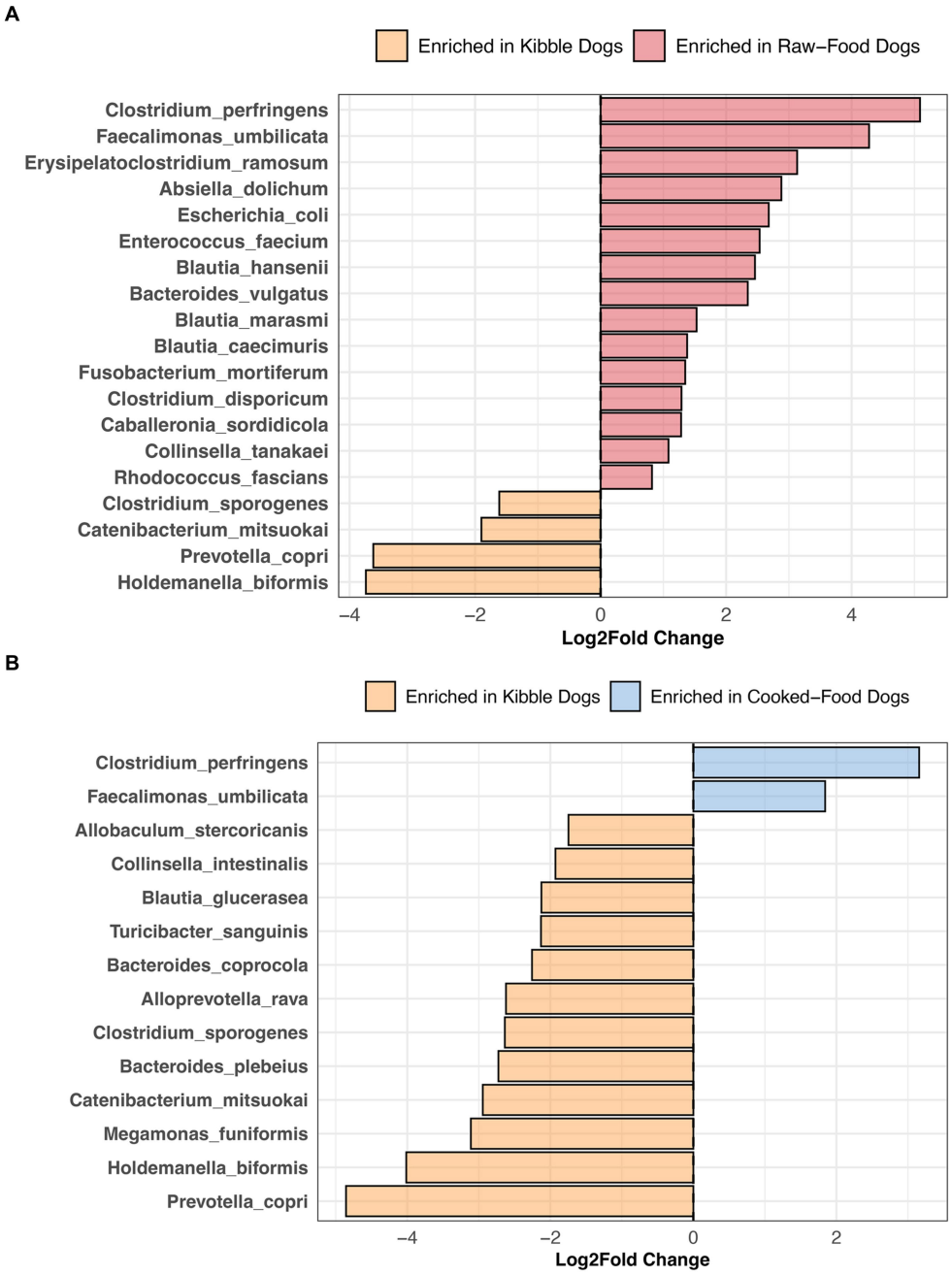

FIGURE 7
Bacterial species enriched in the microbiomes of dogs according to their diet category. Results from LinDA differential abundance analyses performed at the bacterial species level. The LinDA model included diet category (Kibble, Raw, or Cooked) as the dependent variable. **(A)** Dogs fed Kibble vs. Dogs fed Raw food. **(B)** Dogs fed Kibble vs. Dogs fed Cooked food. No bacterial taxa were differentially abundant between dogs fed cooked food compared to raw food, hence why these plots are not displayed.

alongside four other species of *Streptococcus* (64, 65). We encourage future work to isolate and characterize *S. lutetiensis* isolates from healthy dogs to broaden our understanding of their roles.

Host correlates of microbiome variation in healthy canines

We detected a core group of bacteria in healthy dogs, but their abundances varied among individuals. Some of this variation was associated with host age, spay-neuter status, body weight, diet, probiotic use, and geographic region, although the effect sizes were low. Perhaps other factors that we did not examine (e.g., breed, exercise frequency, urban vs. rural, host genetics) could be accounting for variation. There could also be latent interactions among the host factors themselves (e.g., are intact dogs more likely to be raw-fed, and smaller dogs less likely to be exercised?), that could be complicating our findings. Yet another possibility is that the microbiome is complex and host-associated factors alone cannot capture its variation.

Age-related effects on the microbiome have been observed in companion animals. In healthy cats, aging reduces the number of core taxa in the fecal microbiome (66), similarly, in this study, the proportion of the microbiome composed of core taxa decreased with age. Microbiome beta-diversity also shifts with age. In Beagles, the microbiome differs between pre-weanling, weanling, young, aged, and senile individuals (67), particularly in the abundances of *Lactobacillus* spp. and *Bifidobacterium* spp. Another study conducted across 288 shelter cats found that older cats harbored greater abundances of *Clostridium baratii*, *Turicibacter* spp., and *Campylobacter* than younger cats (68).

Spay & neuter status was also significantly associated with microbiome variation. Differences were mainly detected between sterilized females (or males) and intact males (or females). These findings align with recent research that surveyed the fecal microbiomes of 132 dogs and reported distinct clustering between intact individuals of both sexes and sterilized individuals of both sexes (69). Sterilized female dogs also have vaginal microbiomes that are distinct from those of intact females (70).

Our study found evidence that body weight was predictive of microbiome variation, with diversity highest at intermediate weights. Similarly, a meta-analysis of body size on canine digestive physiology reported a negative correlation between body weight and the relative abundances of *Proteobacteria* for some of the studies they examined (71). Broader patterns of microbiome variation with canine and feline body condition (72–74) and obesity (75–77) have also been reported.

We found that slight differences were detected between the microbiomes of dogs in the western USA and dogs in the Midwest or Northeast, echoing findings from a study (78) that surveyed the fecal microbiomes of 192 dogs from the Western and Midwestern parts of the USA. The study attributed microbiome patterns to regional differences in the degree of urbanization and diversity of pet food available. Geographic disparities in the lifestyles of owners and their pets, noise pollution, weather, and socialization practices could also underpin these differences.

Interestingly, we observed that the fecal microbiomes of dogs in the reference set were marginally distinct from those of dogs that received bacterial probiotics. Bacterial probiotics have been shown to influence microbiome composition in humans with obesity (79), cats or dogs with chronic diarrhea (80, 81), and healthy dogs (82–84), but they have also been shown to have no effect (85–88).

Influence of diet on the canine gut microbiome

Our work showed that diet accounted for the most variation in the microbiome. Particular differences were found between dogs fed kibble and dogs fed raw food or cooked food. The three diets vary significantly in their nutrient composition, and bioavailability of these nutrients (89) which inevitably shapes the fecal microbiome and favors microbes that are able to utilize the digested components. Kibble diets for example, comprise a blend of cereal grains and meats, and contain lower levels of protein and fat compared to some raw meat-based diets, also known as Biologically Appropriate Raw Food (BARF) diets. RMBDs consist primarily of uncooked meat, although fiber-rich ingredients may be added. To complicate things even further, even within a diet category such as kibble, nutrient profiles can vary significantly.

In our study, dogs fed RMBDs were enriched in *Clostridium perfringens*, *Bacteroides vulgatus*, *Enterococcus faecium*, *Caballeronia sordicola*, and *Collinsella tanakei*, among others compared to dogs that consumed kibble. Other studies have also reported higher abundances of *C. perfringens* in the fecal microbiomes of dogs fed a BARF diet compared to a commercial diet (90–92). *C. perfringens* are proteolytic bacteria adapted to breaking down protein into smaller components (93); hence, their abundance in high-protein diets. In broiler chickens, the levels of *C. perfringens* present in the ileum and cecum increase as the level of crude protein in their fishmeal-based diet also increases (94).

Enterococcus faecium and *Bacteroides vulgatus* were also enriched in the fecal microbiomes of dogs consuming RMBDs compared to kibble. Some strains of *E. faecium* (e.g., SF68) have been recognized for their potential probiotic benefits in dogs, aiding in specific immune functions (95) and diarrhea prevention (96). Similarly, *B. vulgatus* may be potentially beneficial in the gut. *B. vulgatus* is known to produce the fatty acids acetate, propionate, butyrate, and lactate (97, 98). They possess bile acid hydrolases (99, 100) that deconjugate primary bile acids.

Dogs primarily fed kibble were enriched in *Prevotella copri*, *Catenibacterium mitsuokai*, *Holdemanella biformis*, *Megamonas funiformis*, and *Bacteroides coprocola*, among others. Similarly, the fecal microbiomes of dogs fed kibble were enriched in bacteria from the genus *Megamonas*, *Faecalibacterium*, and *Catenibacterium* compared to dogs fed raw food (101). The fecal microbiomes of captive red wolves on a kibble diet are enriched in *Catenibacterium mitsuokai*, *Holdemanella* spp., and *Prevotella* spp. compared to red wolves fed a whole meat, wild, or mixed diet (102). Although *Holdemanella biformis* has shown to ameliorate hyperglycemia and restore gluconeogenesis in obese mice (103), its effects in dogs remain unexplored.

Interestingly, differential abundance testing failed to identify any bacterial species that were significantly associated with a cooked food versus raw food diet, perhaps the impact of cooking may vary depending on the food type. A study noted that while the gut microbiomes of mice fed raw versus cooked meat exhibited similar microbiome compositions and functions (104), the opposite was observed for mice fed cooked versus raw tubers.

Future directions

While our study provides valuable insights regarding the healthy canine fecal microbiome, many open questions remain. The impact of other host lifestyle variables and geographic regions outside of North America should be examined. Seasonal variations in the microbiome or the influence of factors such as time of day and host circadian rhythms could be interesting to study. Our study did not include a longitudinal component or assess the stability of the healthy canine microbiome, but this is a priority for our future investigations. Additionally, we did not conduct metagenomic sequencing, which could offer deeper insights into the functional capabilities of the microbiome but encourage other studies to pursue this avenue of research.

Conclusion

Our approach leverages full-length 16S rRNA gene sequencing and offers novel species-level insights into the fecal microbiome of verified healthy and presumed healthy dogs. Our findings highlight the prevalence of bacteria such as *Peptacetobacter hiranonis*, *Prevotella copri*, *Escherichia coli*, and *Streptococcus lutetiensis* in the microbiome and their potential impact on gut health. Specific microbial cocktails containing some of these core bacterial species could be developed to support pet health. Additionally, we identified age, spay-neuter status, body weight, diet and geographic region as modest predictors of microbiome variation, contributing to our understanding of the factors possibly interacting with the fecal microbiome in dogs.

Data availability statement

These data were generated using a proprietary reference database that was created through curating public data. Due to its commercial value, raw PacBio Hifi sequences, sample metadata, and microbiome data are only available upon request for academic research by emailing the corresponding author, HG, holly@animalbiome.com. Tables showing the output from all statistical tests are in the Supplementary materials.

Ethics statement

IACUC approval was not necessary for this descriptive study because fecal samples are considered a waste material and were obtained in a non-invasive manner and involved no interventions. Study protocols were conducted in accordance with the local legislation and institutional requirements. Written informed consent was obtained from the owners for the participation of their animals in this study.

Author contributions

CR: Conceptualization, Data curation, Formal analysis, Investigation, Methodology, Project administration, Software, Supervision, Validation, Visualization, Writing – original draft, Writing – review & editing. BP: Conceptualization, Data curation, Methodology, Project administration, Software, Validation, Writing – review & editing. ES: Methodology, Project administration, Resources, Software, Supervision, Validation, Writing – review & editing. GJ: Conceptualization, Data curation, Methodology, Project administration, Software, Validation, Writing – review & editing. ZE: Methodology, Project administration, Resources, Supervision, Validation, Writing – review & editing. JJ: Conceptualization, Data curation, Investigation, Methodology, Writing – review & editing. AM: Conceptualization, Investigation, Resources, Writing – review & editing. HG: Conceptualization, Funding acquisition, Investigation, Project administration, Resources, Supervision, Writing – original draft, Writing – review & editing.

Funding

The author(s) declare financial support was received for the research, authorship, and/or publication of this article. This work was supported by AnimalBiome and by 169 backers on Kickstarter.

Acknowledgments

We thank the dogs and dog owners for their participation in this study. We are grateful for the help provided by Carlton Osborne, Mary Jo Seminoff, Kari Goodman, Jana Botelho, and Anthony Russell in designing, creating, and fulfilling the DoggyBiome project on Kickstarter, as well as the Kickstarter backers whose generous contributions allowed us to launch this research. We also thank Jonathan Eisen and Jennifer Gardy for serving as science advisors.

Conflict of interest

CR, BP, ES, GJ, ZE, JJ, AM, and HG are employees of AnimalBiome, a pet health company that maintains a veterinary canine and feline stool bank.

The authors declare that this study received funding from AnimalBiome. The funder was involved in the study design, collection, analysis, interpretation of data, and the writing of this article.

Publisher's note

Supplementary material

The Supplementary material for this article can be found online at: https://www.frontiersin.org/articles/10.3389/fvets.2024.1405470/full#supplementary-material

References

1. Clemente JC, Ursell LK, Parfrey LW, Knight R. The impact of the gut microbiota on human health: an integrative view. *Cell*. (2012) 148:1258–70. doi: 10.1016/j.cell.2012.01.035

2. Dethlefsen L, McFall-Ngai M, Relman DA. An ecological and evolutionary perspective on human-microbe mutualism and disease. *Nature*. (2007) 449:811–8. doi: 10.1038/nature06245

3. Groussin M, Mazel F, Sanders JG, Smillie CS, Lavergne S, Thuiller W, et al. Unraveling the processes shaping mammalian gut microbiomes over evolutionary time. *Nat Commun*. (2017) 8:14319. doi: 10.1038/ncomms14319

4. Ley RE, Hamady M, Lozupone C, Turnbaugh PJ, Ramey RR, Bircher JS, et al. Evolution of mammals and their gut microbes. *Science*. (2008) 320:1647–51. doi: 10.1126/science.1155725

5. Neu AT, Allen EE, Roy K. Defining and quantifying the core microbiome: challenges and prospects. *Proc Natl Acad Sci U S A*. (2021) 118:51. doi: 10.1073/pnas.2104429118

6. Louca S, Polz MF, Mazel F, Albright MBN, Huber JA, O'Connor MI, et al. Function and functional redundancy in microbial systems. *Nat Ecol Evol*. (2018) 2:936–43. doi: 10.1038/s41559-018-0519-1

7. Rowe JC, Winston JA. Collaborative metabolism: gut microbes play a key role in canine and feline bile acid metabolism. *Vet Sci China*. (2024) 11:94. doi: 10.3390/vetsci11020094

8. Correa Lopes B, Chen CC, Sung CH, Ishii PE, Medina LFDC, Gaschen FP, et al. Correlation between Peptacetobacter hiranonis, the baiCD gene, and secondary bile acids in dogs. *Animals*. (2024) 14:216. doi: 10.3390/ani14020216

9. Pilla R, Gaschen FP, Barr JW, Olson E, Honneffer J, Guard BC, et al. Effects of metronidazole on the fecal microbiome and metabolome in healthy dogs. *J Vet Intern Med*. (2020) 34:1853–66. doi: 10.1111/jvim.15871

10. Éliás AJ, Barna V, Patoni C, Demeter D, Veres DS, Bunduc S, et al. Probiotic supplementation during antibiotic treatment is unjustified in maintaining the gut microbiome diversity: a systematic review and meta-analysis. *BMC Med*. (2023) 21:262. doi: 10.1186/s12916-023-02961-0

11. Buetas E, Jordán-López M, López-Roldán A, D'Auria G, Martínez-Priego L, De Marco G, et al. Full-length 16S rRNA gene sequencing by PacBio improves taxonomic resolution in human microbiome samples. *BMC Genomics*. (2024) 25:310. doi: 10.1186/s12864-024-10213-5

12. Pilla R, Suchodolski JS. The role of the canine gut microbiome and metabolome in health and gastrointestinal disease. *Front Vet Sci*. (2019) 6:498. doi: 10.3389/fvets.2019.00498

13. Pilla R, Guard BC, Steiner JM, Gaschen FP, Olson E, Werling D, et al. Administration of a synbiotic containing *Enterococcus faecium* does not significantly alter fecal microbiota richness or diversity in dogs with and without food-responsive chronic enteropathy. *Front Vet Sci*. (2019) 6:277. doi: 10.3389/fvets.2019.00277

14. Bolyen E, Rideout JR, Dillon MR, Bokulich NA, Abnet CC, Al-Ghalith GA, et al. Reproducible, interactive, scalable and extensible microbiome data science using QIIME 2. *Nat Biotechnol*. (2019) 37:852–7. doi: 10.1038/s41587-019-0209-9

15. Anderson JG, Rojas CA, Scarsella E, Entrolezo Z, Jospin G, Hoffman SL, et al. The oral microbiome across oral sites in cats with chronic gingivostomatitis, periodontal disease, and tooth resorption compared with healthy cats. *Animals*. (2023) 13:3544. doi: 10.3390/ani13223544

16. Bokulich NA, Kaehler BD, Rideout JR, Dillon M, Bolyen E, Knight R, et al. Optimizing taxonomic classification of marker-gene amplicon sequences with QIIME 2's q2-feature-classifier plugin. *Microbiome*. (2018) 6:90. doi: 10.1186/s40168-018-0470-z

17. Quast C, Pruesse E, Yilmaz P, Gerken J, Schweer T, Yarza P, et al. The SILVA ribosomal RNA gene database project: improved data processing and web-based tools. *Nucleic Acids Res*. (2013) 41:D590–6. doi: 10.1093/nar/gks1219

18. Rognes T, Flouri T, Nichols B, Quince C, Mahé F. VSEARCH: a versatile open source tool for metagenomics. *PeerJ*. (2016) 4:e2584. doi: 10.7717/peerj.2584

19. Schloss PD. Waste not, want not: revisiting the analysis that called into question the practice of rarefaction. *mSphere*. (2023):e00355–23. doi: 10.1128/msphere.00355-23

20. McMurdie PJ, Holmes S. Phyloseq: an R package for reproducible interactive analysis and graphics of microbiome census data. *PLoS One*. (2013) 8:e61217. doi: 10.1371/journal.pone.0061217

21. Wood SN. Fast stable restricted maximum likelihood and marginal likelihood estimation of semiparametric generalized linear models. *J R Stat Soc Series B Stat Methodol*. (2010) 73:3–36. doi: 10.1111/j.1467-9868.2010.00749.x

22. Lenth RV. emmeans: estimated marginal means, aka least-squares means. (2023). Available at: https://CRAN.R-project.org/package=emmeans

23. Hothorn T, Bretz F, Westfall P. Simultaneous inference in general parametric models. *Biom J*. (2008) 50:346–63. doi: 10.1002/bimj.200810425

24. Oksanen J, Simpson GL, Blanchet FG, Kindt R, Legendre P, Minchin PR, et al. vegan: community ecology package. (2022). Available at: https://CRAN.R-project.org/package=vegan

25. Martinez Arbizu P. pairwiseAdonis: pairwise multilevel comparison using Adonis. R package version 0.4 1. (2020)

26. Zhou H, He K, Chen J, Zhang X. LinDA: linear models for differential abundance analysis of microbiome compositional data. *Genome Biol*. (2022) 23:95. doi: 10.1186/s13059-022-02655-5

27. Villanueva RAM, Chen ZJ. ggplot2: elegant graphics for data analysis (2nd ed.). *Measurement*. (2019) 17:160–7. doi: 10.1080/15366367.2019.1565254

28. You I, Kim MJ. Comparison of gut microbiota of 96 healthy dogs by individual traits: breed, age, and body condition score. *Animals*. (2021) 11:2432. doi: 10.3390/ani11082432

29. Reddy KE, Kim H-R, Jeong JY, So K-M, Lee S, Ji SY, et al. Impact of breed on the fecal microbiome of dogs under the same dietary condition. *J Microbiol Biotechnol*. (2019) 29:1947–56. doi: 10.4014/jmb.1906.06048

30. Bastos TS, Souza CMM, Legendre H, Richard N, Pilla R, Suchodolski JS, et al. Effect of yeast *Saccharomyces cerevisiae* as a probiotic on diet digestibility, fermentative metabolites, and composition and functional potential of the fecal microbiota of dogs submitted to an abrupt dietary change. *Microorganisms*. (2023) 11:506. doi: 10.3390/microorganisms11020506

31. Sung C-H, Pilla R, Chen C-C, Ishii PE, Toresson L, Allenspach-Jorn K, et al. Correlation between targeted qPCR assays and untargeted DNA shotgun metagenomic sequencing for assessing the fecal microbiota in dogs. *Animals*. (2023) 13:2597. doi: 10.3390/ani13162597

32. Kitahara M, Takamine F, Imamura T, Benno Y. *Clostridium hiranonis* sp. nov., a human intestinal bacterium with bile acid 7alpha-dehydroxylating activity. *Int J Syst Evol Microbiol*. (2001) 51:39–44. doi: 10.1099/00207713-51-1-39

33. Isaiah A. *Clostridium hiranonis*, a bile acid 7α-dehydroxylating bacterium in dogs. (2018). Available at: https://oaktrust.library.tamu.edu/handle/1969.1/188939

34. Begley M, Gahan CGM, Hill C. The interaction between bacteria and bile. *FEMS Microbiol Rev*. (2005) 29:625–51. doi: 10.1016/j.femsre.2004.09.003

35. Islam KBMS, Fukiya S, Hagio M, Fujii N, Ishizuka S, Ooka T, et al. Bile acid is a host factor that regulates the composition of the cecal microbiota in rats. *Gastroenterology*. (2011) 141:1773–81. doi: 10.1053/j.gastro.2011.07.046

36. de Aguiar Vallim TQ, Tarling EJ, Edwards PA. Pleiotropic roles of bile acids in metabolism. *Cell Metab*. (2013) 17:657–69. doi: 10.1016/j.cmet.2013.03.013

37. Mroz MS, Lajczak NK, Goggins BJ, Keely S, Keely SJ. The bile acids, deoxycholic acid and ursodeoxycholic acid, regulate colonic epithelial wound healing. *Am J Physiol Gastrointest Liver Physiol*. (2018) 314:G378–87. doi: 10.1152/ajpgi.00435.2016

38. Chen ML, Takeda K, Sundrud MS. Emerging roles of bile acids in mucosal immunity and inflammation. *Mucosal Immunol*. (2019) 12:851–61. doi: 10.1038/s41385-019-0162-4

39. Comito R, Porru E, Interino N, Conti M, Terragni R, Gotti R, et al. Metabolic bile acid profile impairments in dogs affected by chronic inflammatory enteropathy. *Meta*. (2023) 13:980. doi: 10.3390/metabo13090980

40. Whittemore JC, Price JM, Moyers T, Suchodolski JS. Effects of synbiotics on the fecal microbiome and metabolomic profiles of healthy research dogs administered antibiotics: a randomized, controlled trial. *Front Vet Sci*. (2021) 8:665713. doi: 10.3389/fvets.2021.665713

41. Giaretta PR, Rech RR, Guard BC, Blake AB, Blick AK, Steiner JM, et al. Comparison of intestinal expression of the apical sodium-dependent bile acid transporter between dogs with and without chronic inflammatory enteropathy. *J Vet Intern Med*. (2018) 32:1918–26. doi: 10.1111/jvim.15332

42. Chaitman J, Ziese A-L, Pilla R, Minamoto Y, Blake AB, Guard BC, et al. Fecal microbial and metabolic profiles in dogs with acute diarrhea receiving either fecal microbiota transplantation or Oral metronidazole. *Front Vet Sci*. (2020) 7:192. doi: 10.3389/fvets.2020.00192

43. Franke T, Deppenmeier U. Physiology and central carbon metabolism of the gut bacterium *Prevotella copri*. *Mol Microbiol*. (2018) 109:528–40. doi: 10.1111/mmi.14058

44. Yeoh YK, Sun Y, Ip LYT, Wang L, Chan FKL, Miao Y, et al. Prevotella species in the human gut is primarily comprised of *Prevotella copri*, Prevotella stercorea and related lineages. *Sci Rep*. (2022) 12:9055. doi: 10.1038/s41598-022-12721-4

45. Liu T, Xiao Y, Ren Y, Su L. The interactional role of host and microbiota in diseases and intervention strategies of traditional Chinese medicine. *Front Media*. (2023) 2023:179. doi: 10.3389/978-2-8325-2913-3

46. Ruppin H, Bar-Meir S, Soergel KH, Wood CM, Schmitt MG Jr. Absorption of short-chain fatty acids by the colon. *Gastroenterology*. (1980) 78:1500–7. doi: 10.1016/S0016-5085(19)30508-6

47. Tedelind S, Westberg F, Kjerrulf M, Vidal A. Anti-inflammatory properties of the short-chain fatty acids acetate and propionate: a study with relevance to inflammatory bowel disease. *World J Gastroenterol*. (2007) 13:2826–32. doi: 10.3748/wjg.v13.i20.2826

48. Ma J, Piao X, Mahfuz S, Long S, Wang J. The interaction among gut microbes, the intestinal barrier and short chain fatty acids. *Anim Nutr*. (2022) 9:159–74. doi: 10.1016/j.aninu.2021.09.012

49. Gal A, Barko PC, Biggs PJ, Gedye KR, Midwinter AC, Williams DA, et al. One dog's waste is another dog's wealth: a pilot study of fecal microbiota transplantation in dogs with acute hemorrhagic diarrhea syndrome. *PLoS One*. (2021) 16:e0250344. doi: 10.1371/journal.pone.0250344

50. Kovatcheva-Datchary P, Nilsson A, Akrami R, Lee YS, De Vadder F, Arora T, et al. Dietary fiber-induced improvement in glucose metabolism is associated with increased abundance of Prevotella. *Cell Metab*. (2015) 22:971–82. doi: 10.1016/j.cmet.2015.10.001

51. Hoek KL, McClanahan KG, Latour YL, Shealy N, Piazuelo MB, Vallance BA, et al. Turicibacterales protect mice from severe *Citrobacter rodentium* infection. *Infect Immun*. (2023) 91:e0032223. doi: 10.1128/iai.00322-23

52. Kemis JH, Linke V, Barrett KL, Boehm FJ, Traeger LL, Keller MP, et al. Genetic determinants of gut microbiota composition and bile acid profiles in mice. *PLoS Genet*. (2019) 15:e1008073. doi: 10.1371/journal.pgen.1008073

53. Lynch JB, Gonzalez EL, Choy K, Faull KF, Jewell T, Arellano A, et al. Gut microbiota Turicibacter strains differentially modify bile acids and host lipids. *Nat Commun*. (2023) 14:3669. doi: 10.1038/s41467-023-39403-7

54. Félix AP, Souza CMM, de Oliveira SG. Biomarkers of gastrointestinal functionality in dogs: a systematic review and meta-analysis. *Anim Feed Sci Technol*. (2022) 283:115183. doi: 10.1016/j.anifeedsci.2021.115183

55. Ingle DJ, Valcanis M, Kuzevski A, Tauschek M, Inouye M, Stinear T, et al. In silico serotyping of *E. coli* from short read data identifies limited novel O-loci but extensive diversity of O:H serotype combinations within and between pathogenic lineages. *Microb Genom*. (2016) 2:e000064. doi: 10.1099/mgen.0.000064

56. Jang J, Hur H-G, Sadowsky MJ, Byappanahalli MN, Yan T, Ishii S. Environmental *Escherichia coli*: ecology and public health implications—a review. *J Appl Microbiol*. (2017) 123:570–81. doi: 10.1111/jam.13468

57. Karmali MA, Gannon V, Sargeant JM. Verocytotoxin-producing *Escherichia coli* (VTEC). *Vet Microbiol*. (2010) 140:360–70. doi: 10.1016/j.vetmic.2009.04.011

58. Karahutová L, Mandelík R, Bujňáková D. Antibiotic resistant and biofilm-associated *Escherichia coli* isolates from diarrheic and healthy dogs. *Microorganisms*. (2021) 9:1334. doi: 10.3390/microorganisms9061334

59. Wedley AL, Maddox TW, Westgarth C, Coyne KP, Pinchbeck GL, Williams NJ, et al. Prevalence of antimicrobial-resistant *Escherichia coli* in dogs in a cross-sectional, community-based study. *Vet Rec*. (2011) 168:354. doi: 10.1136/vr.d1540

60. Priestnall SL, Erles K, Brooks HW, Cardwell JM, Waller AS, Paillot R, et al. Characterization of pneumonia due to *Streptococcus equi* subsp. zooepidemicus in dogs. *Clin Vaccine Immunol*. (2010) 17:1790–6. doi: 10.1128/CVI.00188-10

61. Esteban-Fernández A, Ferrer MD, Zorraquín-Peña I, López-López A, Moreno-Arribas MV, Mira A. In vitro beneficial effects of Streptococcus dentisani as potential oral probiotic for periodontal diseases. *J Periodontol*. (2019) 90:1346–55. doi: 10.1002/JPER.18-0751

62. Vanhoutte T, Huys G, De Brandt E, Fahey GC Jr, Swings J. Molecular monitoring and characterization of the faecal microbiota of healthy dogs during fructan supplementation. *FEMS Microbiol Lett*. (2005) 249:65–71. doi: 10.1016/j.femsle.2005.06.003

63. Mahiddine FY, You I, Park H, Kim MJ. Microbiome profile of dogs with stage IV multicentric lymphoma: a pilot study. *Vet Sci China*. (2022) 9:409. doi: 10.3390/vetsci9080409

64. Putnam NE, Youn J-H, Wallace MA, Luethy PM, Burnham C-AD, Butler-Wu S, et al. Comparative evaluation of current biochemical-, sequencing-, and proteomic-based identification methods for the *Streptococcus bovis* group. *J Clin Microbiol*. (2023) 61:e0171222. doi: 10.1128/jcm.01712-22

65. Dekker JP, Lau AF. An update on the *Streptococcus bovis* group: classification, identification, and disease associations. *J Clin Microbiol*. (2016) 54:1694–9. doi: 10.1128/JCM.02977-15

66. Ganz HH, Jospin G, Rojas CA, Martin AL, Dahlhausen K, Kingsbury DD, et al. The kitty microbiome project: defining the healthy fecal "core microbiome" in pet domestic cats. *Vet Sci*. (2022) 9:635. doi: 10.3390/vetsci9110635

67. Masuoka H, Shimada K, Kiyosue-Yasuda T, Kiyosue M, Oishi Y, Kimura S, et al. Transition of the intestinal microbiota of dogs with age. *Biosci Microbiota Food Health*. (2017) 36:27–31. doi: 10.12938/bmfh.BMFH-2016-021

68. Kittson MA, Tanprasertsuk J, Burnham CM, Honaker RW, Jones RB, Trivedi S, et al. Fecal microbiome associations with age, body condition score, and stool consistency in domestic cats (*Felis catus*) living in an animal shelter. Res Sq [preprint] (2023) doi: 10.21203/rs.3.rs-3478102/v1

69. Scarsella E, Stefanon B, Cintio M, Licastro D, Sgorlon S, Dal Monego S, et al. Learning machine approach reveals microbial signatures of diet and sex in dog. *PLoS One*. (2020) 15:e0237874. doi: 10.1371/journal.pone.0237874

70. Rota A, Corrò M, Patuzzi I, Milani C, Masia S, Mastrorilli E, et al. Effect of sterilization on the canine vaginal microbiota: a pilot study. *BMC Vet Res*. (2020) 16:455. doi: 10.1186/s12917-020-02670-3

71. Deschamps C, Humbert D, Zentek J, Denis S, Priymenko N, Apper E, et al. From Chihuahua to saint-Bernard: how did digestion and microbiota evolve with dog sizes. *Int J Biol Sci*. (2022) 18:5086–102. doi: 10.7150/ijbs.72770

72. Thomson P, Santibáñez R, Rodríguez-Salas C, Flores-Yañez C, Garrido D. Differences in the composition and predicted functions of the intestinal microbiome of obese and normal weight adult dogs. *PeerJ*. (2022) 10:e12695. doi: 10.7717/peerj.12695

73. Chun JL, Ji SY, Lee SD, Lee YK, Kim B, Kim KH. Difference of gut microbiota composition based on the body condition scores in dogs. *Hanguk Tongmul Chawon Kwahakhoe Chi*. (2020) 62:239–46. doi: 10.5187/jast.2020.62.2.239

74. Kim H, Seo J, Park T, Seo K, Cho H-W, Chun JL, et al. Obese dogs exhibit different fecal microbiome and specific microbial networks compared with normal weight dogs. *Sci Rep*. (2023) 13:723. doi: 10.1038/s41598-023-27846-3

75. Handl S, German AJ, Holden SL, Dowd SE, Steiner JM, Heilmann RM, et al. Faecal microbiota in lean and obese dogs. *FEMS Microbiol Ecol*. (2013) 84:332–43. doi: 10.1111/1574-6941.12067

76. Rojas CA, Marks SL, Borras E, Lesea H, McCartney MM, Coil DA, et al. Characterization of the microbiome and volatile compounds in anal gland secretions from domestic cats (*Felis catus*) using metagenomics and metabolomics. *Sci Rep*. (2023) 13:19382. doi: 10.1038/s41598-023-45997-1

77. Forster GM, Stockman J, Noyes N, Heuberger AL, Broeckling CD, Bantle CM, et al. A comparative study of serum biochemistry, metabolome and microbiome parameters of clinically healthy, normal weight, overweight, and obese companion dogs. *Top Companion Anim Med*. (2018) 33:126–35. doi: 10.1053/j.tcam.2018.08.003

78. Jha AR, Shmalberg J, Tanprasertsuk J, Perry L, Massey D, Honaker RW. Characterization of gut microbiomes of household pets in the United States using a direct-to-consumer approach. *PLoS One*. (2020) 15:e0227289. doi: 10.1371/journal.pone.0227289

79. Naumova N, Alikina T, Tupikin A, Kalmykova A, Soldatova G, Vlassov V, et al. Human gut microbiome response to short-term Bifidobacterium-based probiotic treatment. *Indian J Microbiol*. (2020) 60:451–7. doi: 10.1007/s12088-020-00888-1

80. Lee T-W, Chao T-Y, Chang H-W, Cheng Y-H, Wu C-H, Chang Y-C. The effects of *Bacillus licheniformis*—fermented products on the microbiota and clinical presentation of cats with chronic diarrhea. *Animals*. (2022) 12:2187. doi: 10.3390/ani12172187

81. Xu H, Zhao F, Hou Q, Huang W, Liu Y, Zhang H, et al. Metagenomic analysis revealed beneficial effects of probiotics in improving the composition and function of the gut microbiota in dogs with diarrhoea. *Food Funct*. (2019) 10:2618–29. doi: 10.1039/C9FO00087A

82. Tanprasertsuk J, Jha AR, Shmalberg J, Jones RB, Perry LM, Maughan H, et al. The microbiota of healthy dogs demonstrates individualized responses to synbiotic supplementation in a randomized controlled trial. *Anim Microbiome*. (2021) 3:36. doi: 10.1186/s42523-021-00098-0

83. Ciaravolo S, Martínez-López LM, Allcock RJN, Woodward AP, Mansfield C. Longitudinal survey of fecal microbiota in healthy dogs administered a commercial probiotic. *Front Vet Sci*. (2021) 8:664318. doi: 10.3389/fvets.2021.664318

84. Rossi G, Pengo G, Galosi L, Berardi S, Tambella AM, Attili AR, et al. Effects of the probiotic mixture Slab51® (SivoMixx®) as food supplement in healthy dogs: evaluation of fecal microbiota, clinical parameters and immune function. *Front Vet Sci*. (2020) 7:613. doi: 10.3389/fvets.2020.00613

85. Hutchins RG, Bailey CS, Jacob ME, Harris TL, Wood MW, Saker KE, et al. The effect of an oral probiotic containing lactobacillus, bifidobacterium, and bacillus species on the vaginal microbiota of spayed female dogs. *J Vet Intern Med*. (2013) 27:1368–71. doi: 10.1111/jvim.12174

86. Bell SE, Nash AK, Zanghi BM, Otto CM, Perry EB. An assessment of the stability of the canine oral microbiota after probiotic administration in healthy dogs over time. *Front Vet Sci*. (2020) 7:616. doi: 10.3389/fvets.2020.00616

87. Jensen AP, Bjørnvad CR. Clinical effect of probiotics in prevention or treatment of gastrointestinal disease in dogs: a systematic review. *J Vet Intern Med*. (2019) 33:1849–64. doi: 10.1111/jvim.15554

88. Lucchetti B, Lane SL, Koenig A, Good J, Suchodolski JS, Brainard BM. Effects of a perioperative antibiotic and veterinary probiotic on fecal dysbiosis index in dogs. *Can Vet J*. (2021) 62:240–6.

89. Saar R, Dodd S. Small animal microbiomes and nutrition. New Jersey: John Wiley & Sons (2023). 384 p.

90. Schmidt M, Unterer S, Suchodolski JS, Honneffer JB, Guard BC, Lidbury JA, et al. The fecal microbiome and metabolome differs between dogs fed bones and raw food (BARF) diets and dogs fed commercial diets. *PLoS One*. (2018) 13:e0201279. doi: 10.1371/journal.pone.0201279

91. Kim J, An J-U, Kim W, Lee S, Cho S. Differences in the gut microbiota of dogs (*Canis lupus familiaris*) fed a natural diet or a commercial feed revealed by the Illumina MiSeq platform. *Gut Pathog*. (2017) 9:68. doi: 10.1186/s13099-017-0218-5

92. Viegas FM, Ramos CP, Xavier RGC, Lopes EO, Júnior CAO, Bagno RM, et al. Fecal shedding of Salmonella spp., Clostridium perfringens, and Clostridioides difficile in dogs fed raw meat-based diets in Brazil and their owners' motivation. *PLoS One*. (2020) 15:e0231275. doi: 10.1371/journal.pone.0231275

93. Cozzani I, Barsacchi R, Dibenedetto G, Saracchi L, Falcone G. Regulation of breakdown and synthesis of L-glutamate decarboxylase in *Clostridium perfringens*. *J Bacteriol*. (1975) 123:1115–23. doi: 10.1128/jb.123.3.1115-1123.1975

94. Drew MD, Syed NA, Goldade BG, Laarveld B, Van Kessel AG. Effects of dietary protein source and level on intestinal populations of *Clostridium perfringens* in broiler chickens. *Poult Sci*. (2004) 83:414–20. doi: 10.1093/ps/83.3.414

95. Benyacoub J, Czarnecki-Maulden GL, Cavadini C, Sauthier T, Anderson RE, Schiffrin EJ, et al. Supplementation of food with *Enterococcus faecium* (SF68) stimulates immune functions in young dogs. *J Nutr*. (2003) 133:1158–62. doi: 10.1093/jn/133.4.1158

96. Bybee SN, Scorza AV, Lappin MR. Effect of the probiotic *Enterococcus faecium* SF68 on presence of diarrhea in cats and dogs housed in an animal shelter. *J Vet Intern Med*. (2011) 25:856–60. doi: 10.1111/j.1939-1676.2011.0738.x

97. Lück R, Deppenmeier U. Genetic tools for the redirection of the central carbon flow towards the production of lactate in the human gut bacterium Phocaeicola (Bacteroides) vulgatus. *Appl Microbiol Biotechnol*. (2022) 106:1211–25. doi: 10.1007/s00253-022-11777-6

98. Clausen U, Vital S-T, Lambertus P, Gehler M, Scheve S, Wöhlbrand L, et al. Catabolic network of the fermentative gut bacterium Phocaeicola vulgatus (phylum Bacteroidetes) from a physiologic-proteomic perspective. *Microb Physiol*. (2024) 34:88–107. doi: 10.1159/000536327

99. Xu M, Lan R, Qiao L, Lin X, Hu D, Zhang S, et al. *Bacteroides vulgatus* ameliorates lipid metabolic disorders and modulates gut microbial composition in hyperlipidemic rats. *Microbiol Spectr*. (2023) 11:e0251722. doi: 10.1128/spectrum.02517-22

100. Kawamoto K, Horibe I, Uchida K. Purification and characterization of a new hydrolase for conjugated bile acids, chenodeoxycholyltaurine hydrolase, from *Bacteroides vulgatus*. *J Biochem*. (1989) 106:1049–53. doi: 10.1093/oxfordjournals.jbchem.a122962

101. Xu J, Becker AAMJ, Luo Y, Zhang W, Ge B, Leng C, et al. The fecal microbiota of dogs switching to a raw diet only partially converges to that of wolves. *Front Microbiol*. (2021) 12:701439. doi: 10.3389/fmicb.2021.701439

102. Bragg M, Freeman EW, Lim HC, Songsasen N, Muletz-Wolz CR. Gut microbiomes differ among dietary types and stool consistency in the captive red wolf (*Canis rufus*). *Front Microbiol*. (2020) 11:590212. doi: 10.3389/fmicb.2020.590212

103. Romaní-Pérez M, López-Almela I, Bullich-Vilarrubias C, Rueda-Ruzafa L, Gómez Del Pulgar EM, Benítez-Páez A, et al. Holdemanella biformis improves glucose tolerance and regulates GLP-1 signaling in obese mice. *FASEB J*. (2021) 35:e21734. doi: 10.1096/fj.202100126R

104. Carmody RN, Bisanz JE, Bowen BP, Maurice CF, Lyalina S, Louie KB, et al. Cooking shapes the structure and function of the gut microbiome. *Nat Microbiol*. (2019) 4:2052–63. doi: 10.1038/s41564-019-0569-4

frontiers | Frontiers in Microbiology

TYPE Original Research
PUBLISHED 12 September 2024
DOI 10.3389/fmicb.2024.1455839

OPEN ACCESS

EDITED BY
Qinghong Li,
Nestle Purina Research, United States

REVIEWED BY
Michael Super,
Harvard University, United States
Latifa Bousarghin,
University of Rennes 1, France

*CORRESPONDENCE
Elena Dalle Vedove
✉ elena.dallevedove@nilitaly.com

RECEIVED 27 June 2024
ACCEPTED 06 August 2024
PUBLISHED 12 September 2024

CITATION
Dalle Vedove E, Benvenga A, Nicolai G, Massimini M, Giordano MV, Di Pierro F and Bachetti B (2024) Antibiotic-induced dysbiosis in the SCIME™ recapitulates microbial community diversity and metabolites modulation of *in vivo* disease. *Front. Microbiol.* 15:1455839. doi: 10.3389/fmicb.2024.1455839

Antibiotic-induced dysbiosis in the SCIME™ recapitulates microbial community diversity and metabolites modulation of *in vivo* disease

Elena Dalle Vedove[1]*, Alessia Benvenga[1], Gianluca Nicolai[1], Marcella Massimini[2], Maria Veronica Giordano[3], Francesco Di Pierro[4,5] and Benedetta Bachetti[1]

[1]R&D Division, C.I.A.M. Srl, Ascoli Piceno, Italy, [2]Department of Veterinary Medicine, University of Teramo, Teramo, Italy, [3]Endovet Professional Association, Roseto degli Abruzzi, Italy, [4]Department of Medicine and Surgery, University of Insubria, Varese, Italy, [5]Scientific and Research Department, Velleja Research, Milan, Italy

Establishing the context: Intestinal dysbiosis is a significant concern among dog owners, and the gut health of pets is an emerging research field. In this context, the Simulator of the Canine Intestinal Microbial Ecosystem (SCIME™) was recently developed and validated with *in vivo* data.

Stating the purpose/introducing the study: The current study presents a further application of this model by using amoxicillin and clavulanic acid to induce dysbiosis, aiming to provoke changes in microbial community and metabolite production, which are well-known markers of the disease *in vivo*.

Describing methodology: Following the induction of dysbiosis, prebiotic supplementation was tested to investigate the potential for microbiota recovery under different dietary conditions.

Presenting the results: The results showed that antibiotic stimulation in the SCIME™ model can produce significant changes in microbial communities and metabolic activity, including a decrease in microbial richness, a reduction in propionic acid production, and alterations in microbial composition. Additionally, changes in ammonium and butyric acid levels induced by the tested diets were observed.

Discussing the findings: This alteration in microbial community and metabolites production mimicks *in vivo* canine dysbiosis patterns. A novel dynamic *in vitro* model simulating canine antibiotic-induced dysbiosis, capable of reproducing microbial and metabolic changes observed *in vivo*, has been developed and is suitable for testing the effects of nutritional changes.

KEYWORDS

gut disease, dog, intestinal microbiota, *in vitro* alternative to animal testing, prebiotics

1 Introduction

Gastrointestinal diseases are one of the primary reasons why dog owners in Western countries visit veterinarians (Hubbard et al., 2007; Nationwide Mutual Insurance Company, 2023). Similar to humans, intestinal disorders in dogs often correlate with an alteration in the intestinal microbiota, termed dysbiosis (Guard et al., 2015; Suchodolski, 2016). Dysbiosis in the gut can manifest as changes in

microbial composition (e.g., microbial richness, bacteria ratio) and alterations in metabolites production (e.g., decreased synthesis of short-chain fatty acids or increased production of putrefaction markers, such as ammonia; Suchodolski, 2022). The modulation of the intestinal microbial community and its metabolic function is of growing interest, and new *in vitro* models are valuable for advancing knowledge in this area without necessitating animal testing. Recently, within veterinary medicine, considerable attention has been directed toward strategies aimed at modulating the composition and metabolism of the canine intestinal microbial population as a potential new approach to enhancing canine health (Pinna and Biagi, 2014).

In this context, the Simulator of the Canine Intestinal Microbial Ecosystem (SCIME™), was developed and validated as an alternative to *in vivo* trials (Duysburgh et al., 2020). SCIME™ is a semi-dynamic *in vitro* model designed to simulate the canine gastrointestinal tract, focusing on the intestinal microbiota (Duysburgh et al., 2020). A standard SCIME™ setup consists of reactors that simulate the stomach, small intestine, and proximal (PC) and distal colon (DC) of dogs (Duysburgh et al., 2020). Once stabilization of colonic microbiota occurs, the simulated canine microbial community composition closely resembles the *in vivo* situation (Duysburgh et al., 2020). Moreover, a primary advantage of the simulator, compared to *in vivo* studies, is that by strictly controlling the environmental factors, it can provide mechanistic insights on how treatments work (Duysburgh et al., 2021).

In addition to the study of healthy microbiota, *in vitro* models can be useful to reproduce pathologic conditions, such as dysbiosis. Currently, the SCIME™ has been exclusively utilized for simulating intestinal microbiota in healthy conditions, whereas its human counterpart, the SHIME® (the Simulator of the Human Intestinal Microbial Ecosystem) has been adapted and is already extensively employed to mimic intestinal dysbiosis (Ichim et al., 2018; El Hage et al., 2019; Marzorati et al., 2020; Duysburgh et al., 2021). In the present study, broad-spectrum antibiotics were used to induce microbial dysbiosis, as previously reported in the literature, where experiments were conducted using the SHIME® model (Marzorati et al., 2017, 2020; Ichim et al., 2018; El Hage et al., 2019; Duysburgh et al., 2021). Amoxicillin-clavulanic acid was selected owing to its frequent usage as an antimicrobial agents in gastrointestinal disease in dogs and cats, and its association with gastro-intestinal disorders and antibiotic-associated diarrhea, which are reported as side effects (German et al., 2010; Jones et al., 2014; Mancabelli et al., 2021; Zoetis UK Limited, 2024). This study aims to investigate the feasibility of *in vitro* replication of a condition that mimics, in terms of taxonomic and biodiversity characteristics, the dysbiosis observed in dogs under various circumstances, including antibiotic administration (regardless of diarrheal symptoms) and other instances such as episodes of diarrhea due to gastroenteritis, functional gastrointestinal disorders, or Inflammatory Bowel Disease (IBD).

The primary objective of the current study was to investigate whether the administration of a specific dose of Amoxicillin-clavulanic acid to a dog with a healthy canine microbiota (eubiosis) could determine dysbiosis and induce alterations in metabolites production, the same markers indicative of dysbiosis *in vivo*. Moreover, industrial diets often lack essential nutrients such as fibers and several studies have shown the potential efficacy of prebiotics in nutrition, especially in mitigating the deleterious effect of antimicrobial treatments on the intestinal microbiota by facilitating faster restoration of gut homeostasis through eubiosis (Sanders et al., 2019). For this reason, an ancillary objective of the experiment was to assess the potential of the microbiota recovery under different dietary conditions. To achieve these goals, the SCIME™ was utilized coupled with 16S-targeted Illumina sequencing and metabolomics analysis.

2 Materials and methods

2.1 Fecal sample collection

Fecal samples for SCIME™ inoculum were collected in closed containers in the presence of an Oxoid™ AnaeroGen™ bag (Oxoid, Basingstoke, Great Britain), to remove all oxygen from the environment, and stored at 4°C until further processing. Samples were homogenized in anaerobic phosphate buffer, containing 8.8 g/L K_2HPO_4, 6.8 g/L KH_2PO_4, 0.1 g/L sodium thioglycolate, and 0.015 g/L sodium dithionite (20% w/v), and fecal supernatant was collected upon centrifugation and immediately used. As shown in Supplementary Table 1, to account for biological variability, fecal samples of six different clinical healthy adult dog donors were used to inoculate the distal colonic compartments of the SCIME™. Dog breeds involved in the experiment included Toy Poodle, Springer Spaniel, Cane Corso, Labrador Retriever, Jack Russell Terrier and a mixed-breed dog. All dogs were privately owned, lived in various home environments, and were fed various commercial diets. None of the dogs had a history of gastrointestinal signs or received antibiotics for at least 6 months prior to fecal samples collection. All healthy dogs lived in Ascoli Piceno, Italy. All dogs were neutered female; four were adult and two mature. All animal procedures were carried out in accordance with national guidelines.

2.2 Simulator of the canine microbial ecosystem

The configuration of the SCIME™ reactor was adapted from the SHIME® model (ProDigest, Ghent, Belgium and Ghent University, Ghent, Belgium) as previously described by Duysburgh et al. (2020) and Verstrepen et al. (2021). The set-up used in this study consisted of a stomach/small intestine (St-SI) vessel and two distal colon (DC) vessels (non-treated arm and treated arm) for two canine donors in parallel, per run. Three runs including 2 donors/run were performed, to account for biological variability. In this trial, proximal colon (PC) vessel was not used because the number of donors per run was prioritized over the number of colons, as it was done in previous experiment using the SHIME® (El Hage et al., 2019). The selection of the DC vessel over the PC vessel was based on its characterization by a microbial community abundant in species with specific metabolic functions, such as protein degradation, therefore more interesting outputs were expected (Duysburgh et al., 2020). The experimental setup for one run is shown in Figure 1.

Briefly, for each run, the set-up consisted of two pairs of three double-jacketed vessels connected via peristaltic pumps and operated under strictly anaerobic condition. These vessels simulate the stomach and small intestine (St-Si, simulated in one

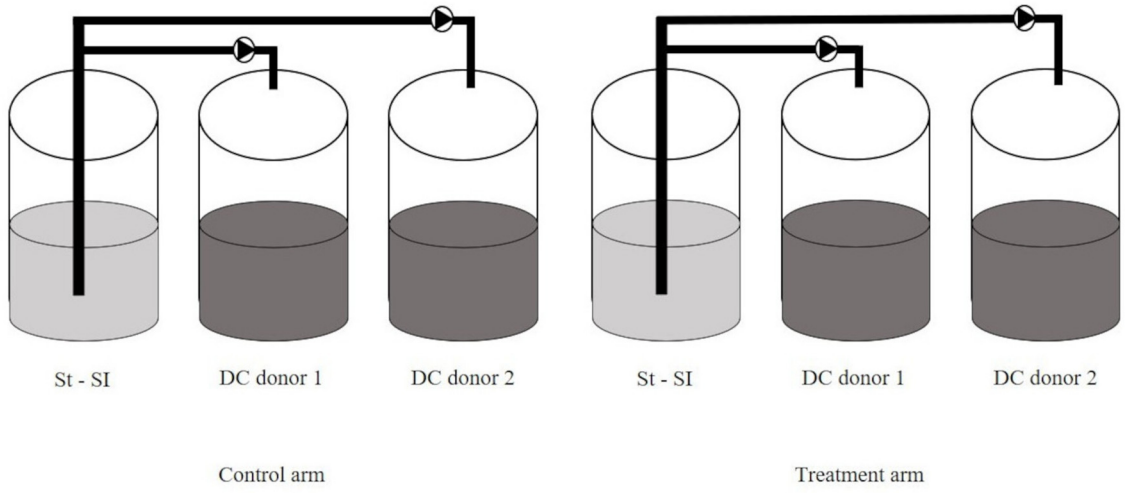

FIGURE 1
SCIME^{TM} reactor setup. Schematic overview of the Simulator of the Canine Intestinal Microbial Ecosystem (SCIME^{TM}) simulating the canine gastrointestinal tract (St, Stomach; SI, Small Intestine; DC, Distal Colon). Two donors were used per run and three runs were performed.

compartment by modifying conditions over time). For the reasons mentioned above, the colon vessels were limited to the distal colon (DC, pH 6.5–6.9). To simulate the gut microbiome, the distal colon vessels were inoculated with microbiota isolated from a fecal sample originating from healthy dogs with no history of antibiotic treatment in the 6 months prior to sample collection, as previously described.

The first vessel (St-SI) was fed with a nutritional medium (indicated as SCIME^{TM} "Feed") prepared by dissolving commercial dog petfood (composition shown in Table 1) at 9 g/L in gastric juice [1.5 g/L yeast extract, 4 g/L special peptone (Oxoid), 4 g/L mucin, and 0.5 g/L L-cystein (Sigma-Aldrich)].

The commercial diet was previously grinded and, after homogenization, the feed was autoclaved, mixed and decanted after 10′ of sedimentation. Twice daily, the St-SI reactor was filled with 140 mL Feed and 60 mL pancreatic juice [12.5 g/L $NaHCO_3$, 2 g/L oxgall (Difco), and 0.9. g/L pancreatin (Applichem)], resulting in a final concentration of 6.3 g of dog feed/L. The colon reactors were continuously stirred with constant volume (DC: 167 mL) and pH control. The pH controllers, peristaltic pumps for liquid transfer and flushing equipment were incorporated in an automated setup controlled by LabVIEW software (SHIME®, ProDigest). The system was run at 39°C under anaerobic conditions with daily flushing with nitrogen gas. The experimental schedule is schematically shown in Figure 2.

There was a 2-week stabilization period to allow the microbiota to adapt to the *in vitro* environment, followed by a 2-week control period during which stability in the microbiome was established and baseline parameters were measured. At the completion of the control period, there was a 1-week pre-treatment period (Dysbiosis week). Amoxicillin: Potassium Clavulanate (2:1; TOKU-E; 45 ppm, twice daily) was added to each colon vessel for 3 days to induce dysbiosis of the microbiota. This antibiotic dosage was determined based on previous experiments run with SHIME® (Duysburgh et al., 2021) and considering both the daily dosage recommended for dogs (Zoetis UK Limited, 2024) and the absorption rate (Kung and Wanner, 1994; The European Agency for the Evaluation of Medicinal Products, 1996). During week 1–5, both the non-treated arm and treated arm were given Feed including standard petfood. During week 6, the non-treated arm continued to be fed with Feed including standard petfood (non-treated group), while the treated arm was switched to Feed with prebiotic-enriched petfood instead (treated group). The composition of the two commercial diets used in the experiment are shown in Table 1.

2.3 Sample collection

Sampling of each distal colon vessel was performed three times per week during the stabilization period, control period, dysbiosis and treatment period. Specifically, sampling was conducted on Monday, Wednesday, Friday during stabilization, control and treatment period, while during the dysbiosis week, sampling occurred on Tuesday, Wednesday, and Thursday, which were the 3 days of the antibiotic treatment. Liquid samples for subsequent analysis of microbial metabolic activity were immediately frozen at −20°C, while pelleted cells (5 min, 9,000 g) originating from 1 mL liquid sample were frozen at −20°C for subsequent molecular analysis.

2.4 Microbial metabolic activity

The parameters used to assess the activity of the gut microbiota in the colons were monitored three times per week from the stabilization period onwards. Levels of short-chain fatty acids (SCFAs, acetate, propionate and butyrate) and branched-chain fatty acids (BCFAs, isobutyrate, isovalerate, and isocaproate) were quantified with gas chromatography (GC) coupled to flame ionization detection (FID). After the addition of 2-methyl hexanoic acid as an internal standard, 2.0 mL of sample was extracted with diethyl ether. The extracts were analysed using an Agilent 7890B GC gas chromatograph (Agilent, Santa Clara, CA, United States), equipped with a GC DB-FATWAX Ultra inert capillary column

TABLE 1 Dog feeds composition and analytical components.

Standard petfood	Prebiotic-enriched petfood
Composition: Dehydrated chicken protein (28%), rice (28%), maize (26%), chicken fat (7%), dehydrated fish protein, dried beet pulp (4%), fish oil (2%), sodium chloride, dried brewer's yeast (0.3%).	**Composition:** Derivatives of vegetable origin [of which dried beet pulp (4%), cellulose (2.5%), dried chicory (0.5%), yucca (0.1%)], processed chicken proteins (19%), animal fat, dried gelatine (1.25%), brewer's yeast [of which, mannan-oligosaccharides (MOS; 0.5%), beta-glucans (0.5%)], hydrolysed collagen (0.75%), dried apple pulp.
Additives per kg: Nutritional additives: Vitamin A 10,000 IU; Vitamin D3 1,000 IU; Vitamin E 100 mg; Vitamin C 100 mg; Niacin 25 mg; Calcium D-pantothenate 10 mg; Vitamin B2 5 mg; Vitamin B6 4 mg; Vitamin B1 3 mg; Biotin 0.25 mg; Folic acid 0.30 mg; Vitamin B12 0.04 mg; Choline chloride 1,500 mg; Zinc (zinc oxide): 86.7 mg; Zinc (zinc sulfate monohydrate): 43.7 mg; Manganese (manganous sulfate monohydrate): 48.8 mg; Iron [iron (II) sulfate monohydrate]: 14.5 mg; Iron [iron (II) carbonate]: 28.9 mg; Copper [copper (II) sulfate pentahydrate]: 12.8 mg; Iodine (anhydrous calcium iodate): 1.56 mg; Selenium (sodium selenite): 0.101 mg; DL-Methionine, technically pure 1,500 mg.	**Additives per kg:** Technological additives: antioxidants, preservatives—Organoleptic additives: tannic acid (410 mg).
Analytical components: crude protein 25.00%; crude fat 12.00%; crude fibers 2.00%; raw ash 6.50%; Calcium 1.20%; Phosphorus 0.90%.	**Analytical components:** crude protein: 16.50%, crude fat: 3.50%, crude fiber: 3.50%, raw ash: 2.50%

During weeks 1–5 both non-treated arm and treated arm were given standard petfood, included in SCIME^{TM} Feed. During week 6, non-treated arm was still fed with standard petfood, while treated arm was switched to prebiotic-enriched petfood.

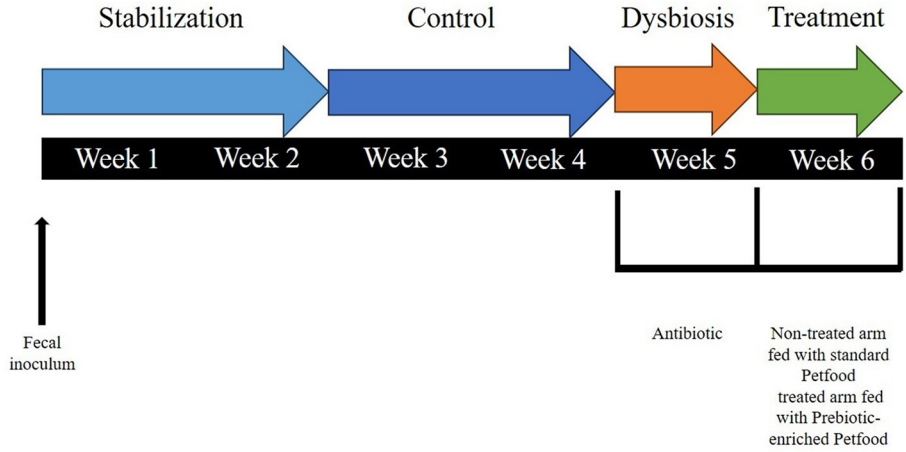

FIGURE 2
Schematic representation of the experimental setup for each run, including the experimental periods, i.e., stabilization period (2 weeks), control period (CTRL; 2 weeks), dysbiosis period (AB; 3 days), and treatment period (TR; 1 week).

(length: 30 m; Inner diameter: 0.32 mm; Film thickness 0.25 μm, Agilent, Santa Clara, CA, United States), a flame ionization detector and a split injector. The injection volume was 1 μL and the column temperature profile was set from 110 to 160°C, with a temperature increase of 6°C min−1. Helium was used as the carrier gas and the injector and detector temperatures of the were both 200°C. The procedure was adapted from what previously described by Ghyselinck et al. (2020).

Ammonium analysis was performed by steam distillation adapted from what was previously described by De Wiele et al. (2004). Using a Kjelmaster K-375 (BÜCHI, Flawil, Swizerland), ammonium in the sample was liberated as ammonia by the distillation in an alkalin medium (by addition of 32% NaOH). The released ammonia was captured from the sample into a boric acid mixed indicator solution, creating an ammonium-borate complex. The ammonium in the distillate was determined by titration with HCl.

2.5 Microbial community composition

The microbial community composition was determined through Illumina sequencing (16S rRNA) and performed by an external laboratory (Genprobio, Cadorago, Italy). Frozen samples from the three runs were shipped to the laboratory under frozen conditions where they were preserved at −20°C, until processed. Next generation 16S rRNA gene amplicon sequencing of V3 region was performed, using the primers 341F (CCATCTCATCCCTGCGTGTCTCCGAC) and 519R (CCTCTCTATGGGCAGTCGGTGAT), with the procedure described by Milani et al. (2013). Results were delivered in the form of relative abundances for each sample to the level of genera, prediction of relative abundances in term of species and alpha diversity curves. Since also raw data was delivered, other analyses were run using QIIME2 (Bolyen et al., 2019).

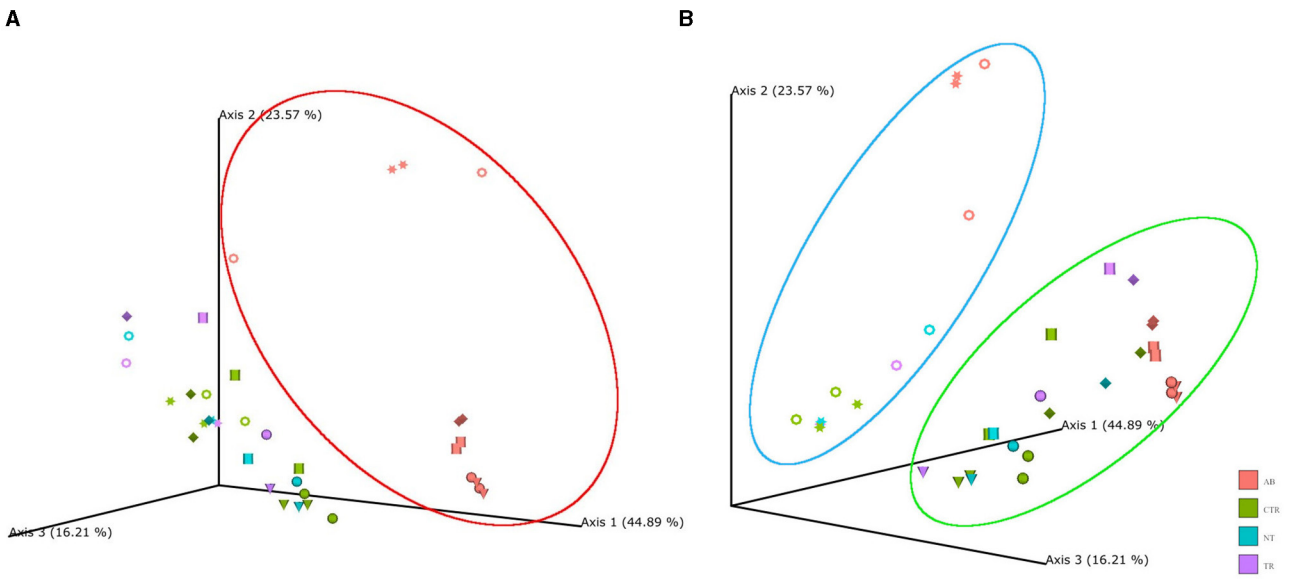

FIGURE 3
Principal coordinate analysis (PCoA) plot based on weighted UniFrac distances. PCoA was used to plot beta diversity of SCIME^{TM} samples. The colors are associated with the group (AB, antibiotics; CTR, control; NT, non-treated arm; TR, treated arm), while the shapes are associated with the donors (Ring = D1, Cylinder = D2, Sphere = D3, Cone = D4, Star = D5, Diamond = D6). **(A)** Shows that AB group clustered in red circle. **(B)** Shows that in the blue circle there are donors 1 and 5, while the rest are clustered in the green circle.

2.6 Statistical analysis

Statistical analysis was performed through R software (3.6.3, 2020) and Excel [Microsoft Corporation. (2018). Microsoft Excel. Retrieved from https://office.microsoft.com/excel].

To test the significance of metabolites and relative bacteria abundances, and to account for the correlation between repeated measurements on the same subject, a mixed-effect model was used, which considered as fixed effect the following groups: control period (CTR), antibiotic stimulation (AB), and non-treated arm (NT) and treated arm (TR) during the treatment period. The donor was considered as random effect. To test the differences among groups, the Tukey contrasts *post-hoc* test was used.

3 Results

3.1 Microbial community composition

In beta diversity PCoA plots (Figure 3A) based on weighted UniFrac analysis, the samples associated with antibiotic stimulation (AB) are distinctly clustered apart from the other groups. It is noteworthy that PCoA based on other metrics (such as Jaccard, Bray-Curtis, and unweighted UniFrac) show the same AB cloud of samples separated from the rest also depict a distinct cluster of antibiotic-stimulated samples separated from the rest (data not shown). PCoA plots were constructed to compare the groups across the weeks and revealing that samples related to the antibiotic stimulation can be identified as a cluster (red contour, Figure 3A) separated from the other samples. This represents healthy microbiota before antibiotic stimulation and bacterial communities one week after its end, both in the non-treated arm (standard petfood) and the treated arm (prebiotic-enriched petfood). Samples from control week and one week after the end of antibiotic stimulation overlap. Moreover, two additional clusters can be identified, both in PCoA plots based on weighted UniFrac metrics; in Figure 3B samples belonging to donors 1 and 5 (identified with circle and star shapes) and to donors 2, 3, 4, and 6 clustered separately. Furthermore, the PCoA plots show that all samples taken during dysbiosis week (AB) tend to move to the same direction in the graph regardless of the diversity of donors and microbiota.

PERMANOVA was used to determine factors that explained variance in bacterial community. The input of PERMANOVA was the weighted UniFrac distance matrix of 16s rRNA data and, the test was run in qiime2 environment. This test indicates that the differences among the groups were statistically significant (p-value = 0.001, num. of permutations = 999). The subsequent pairwise test shows that the differences between AB group and the others were statistically significant (AB vs. CTR p-value = 0.001; AB vs. NT p-value = 0.001; AB vs. TR p-value = 0.001). To test whether significant PERMANOVA results were based on location or dispersion effects, the PERMDISP routine was applied to evaluate the homogeneity of multivariate dispersions among groups. Since PERMDISP test did not show any significant difference (p-value = 0.64, num. of permutations = 999), it can be assessed that the significant differences highlighted by the PERMANOVA test cannot be ascribed to the variance within group, but to the antibiotic effect.

Figure 4 illustrates the rarefaction curves for observed species (represented by OTUs, operational taxonomic units) and Shannon index.

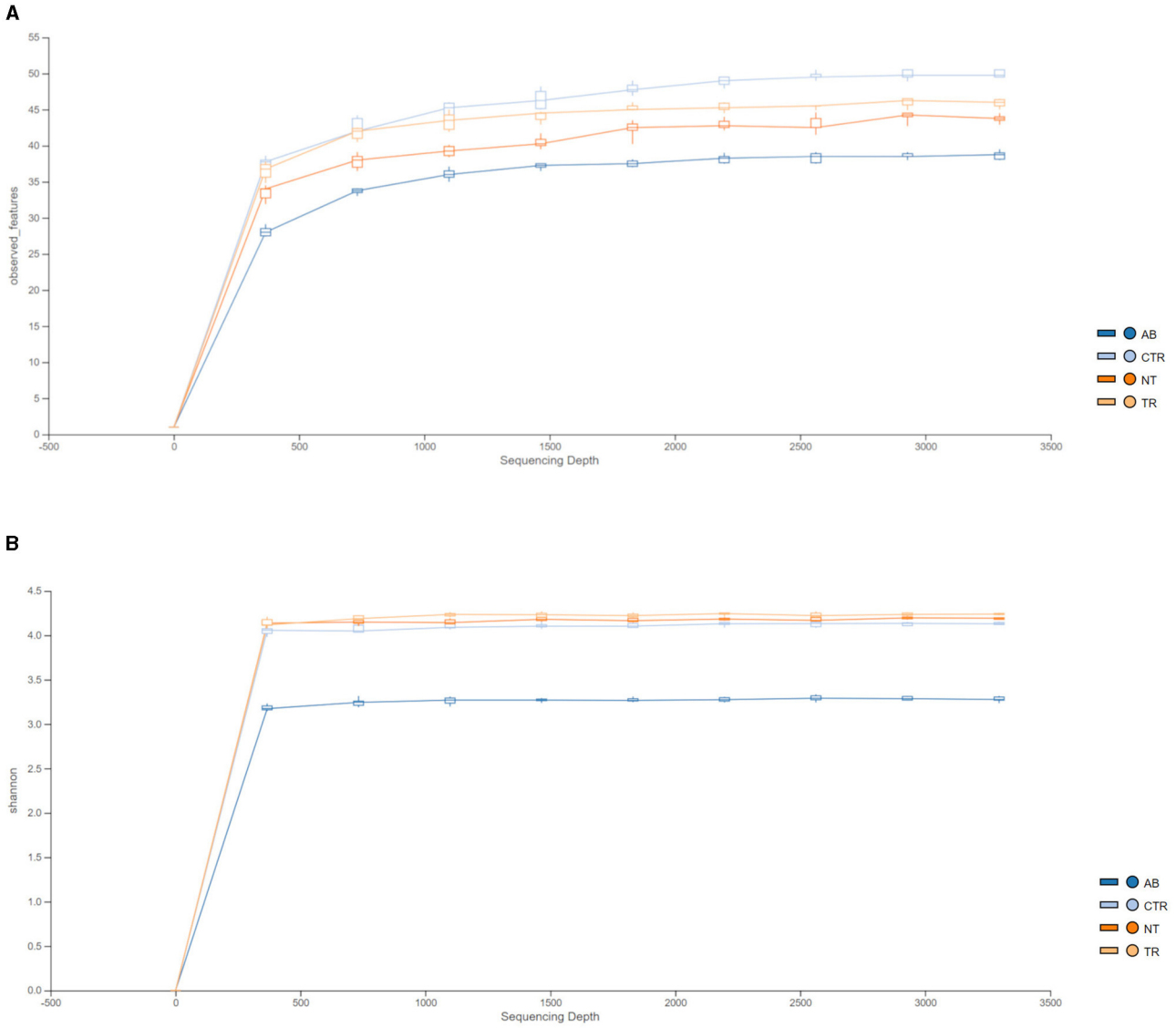

FIGURE 4
Rarefaction curves of 16 S rRNA gene sequences, expressed as OTUs **(A)** and Shannon index **(B)** separated by groups. Different colors represent different groups (AB = antibiotic stimulation, CTR = control period, NT = non-treated microbiota, TR = treated microbiota).

Figure 4A shows that observed species decreased in the dysbiosis week (AB) compared to the control week (CTR). Furthermore, one week after the end of antibiotic stimulation, the number of observed species had increased both in the non-treated arm and in the treated arm compared to the dysbiosis period. In addition, Figure 4A shows that OTUs in the treated arm were greater than in the non-treated arm, but the curve is still lower compared to the previous healthy microbiota (control period).

Figure 4B displays the rarefaction curves for the Shannon index. The curve for dysbiosis week (AB) is significantly decreased compared to the curve for control week and to the curves for treated and non-treated microbiota. The Shannon index was used to assess species richness. As shown in Figure 4B, lower values of the index were observed in the antibiotic stimulation group, as expected. Indeed, a Kruskal-Wallis test, performed on all groups, revealed a significant difference (p-value = 0.006); further differences among groups were elucidated with a *post-hoc* test (pairwise t-test; Figure 5). There are significant differences in all groups when compared to the antibiotic stimulation (AB vs. CTR p-value = 0.003; AB vs. NT p-value = 0.009; AB vs. TR p-value = 0.019). OTU and Chao1 were also evaluated as alpha diversity indexes, they behaved similarly to Shannon index (Supplementary Table 2).

Figures 6, 7 and Tables 2, 3 summarize differences in bacterial groups between groups. The groups are control (CTR), antibiotic stimulation (AB), prebiotic-enriched feed, labeled "treated" (TR), and normal feed, labeled "non-treated" (NT). Sequences belonging to the phyla Bacillota and Bacteroidota were significantly decreased after antibiotic stimulation, compared to control weeks ($p < 0.001$ and <0.001, respectively). Conversely, sequences belonging to the phyla Fusobacteria and Pseudomonadota were significantly

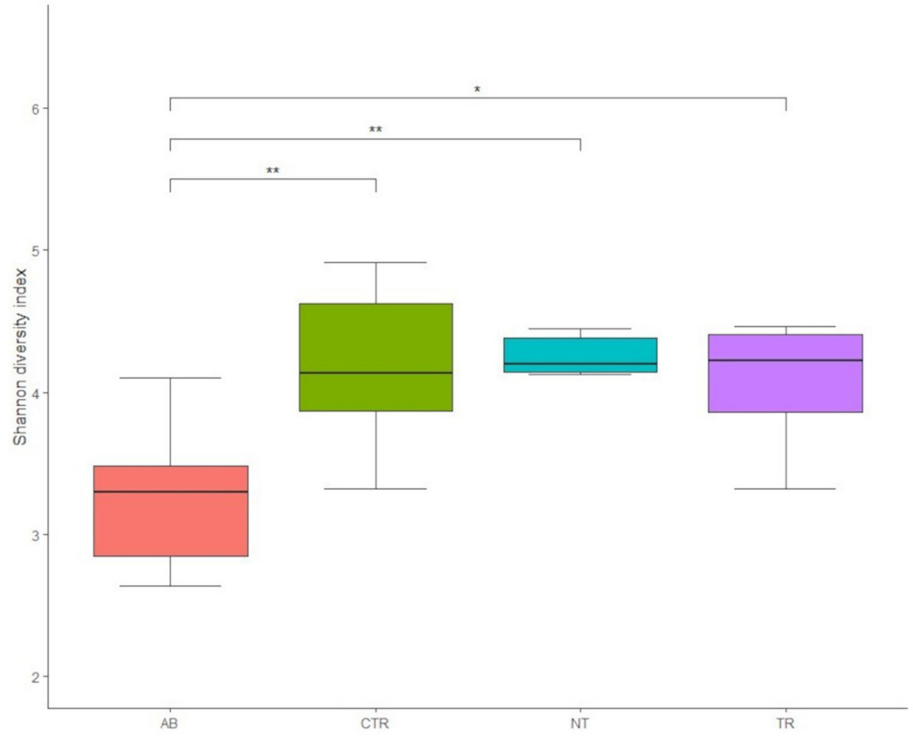

FIGURE 5
Boxplots of Shannon diversity index values of groups (AB = antibiotic stimulation, CTR = control period, NT = non-treated microbiota, TR = treated microbiota). There are significant differences (marked with asterisks) between all weeks when compared to the antibiotic week; the lowest value of the index is found in the antibiotic week.

increased after antibiotic trigger, compared to control weeks ($p <$ 0.001 and <0.001, respectively). Moreover, sequences belonging to the genus *Megamonas* and *Alloprevotella* significantly decreased after antibiotic stimulation, compared to control weeks ($p < 0.001$ and 0.0545, respectively). Conversely, sequences belonging to the genus *Fusobacterium*, *Shigella*, *Pseudomonas*, and *Parasutterella* were significantly increased after antibiotic trigger, compared to the control weeks ($p < 0.001 = 0.0426$, 0.00910, 0.0395, respectively).

One week after the end of antibiotic stimulation, no significant differences were identified between samples from treated or non-treated arm when evaluating bacterial groups. However, sequences belonging to the phyla Bacillota ($p < 0.001$ both TR and NT) and Bacteroidota ($p = 0.01019$ and $p = 0.00487$, TR and NT, respectively) were significantly increased after antibiotic stimulation compared to the previous week, both in treated and non-treated arms. Conversely, sequences belonging to the phyla Fusobacteria ($p < 1e^{-04}$ both TR and NT) and Pseudomonadota ($p = 0.00987$ and $p = 0.00499$, TR and NT, respectively) were both significantly decreased after antibiotic stimulation compared to the previous antibiotic week, both in treated and untreated arms. At genus level, *Megamonas* increased in both treated and non-treated arm ($p < 0.001$, both), while *Pseudomonas* ($p = 0.00486$ and $p = 0.00635$ TR and NT, respectively) and *Parasutterella* ($p = 0.02529$ and $p = 0.04430$ TR and NT, respectively) decreased in in both treated and non-treated arm. Some differences in microbial communities at genus level can be seen comparing samples taken during antibiotic week to those ones taken during the following week. For example, sequences belonging to genus *Prevotella* ($p = 0.00364$) and *Bacteroides* ($p = 0.00163$) significantly increased in treated arm compared to the previous antibiotic week. Additional significant differences can be seen for *Alloprevotella*, *Phascolarctobacterium*, *Sutterella*, *Lysinibacillus*, and *Catenibacterium*, as shown in Table 3, despite the low relative abundance of these genera (Table 2).

3.2 Metabolic activity analysis

Antibiotic stimulation significantly altered SCFAs levels. Plotting the most important SCFAs (Supplementary Figure 1) produced by the intestinal microbiota, a decrease of metabolites concentration is observed following the antibiotic stimulation. The major changes were observed for acetic acid, propionic acid and BCFAs, but a substantial reduction in butyric acid levels was also evident. The effect of the antibiotic, in all donors, on the production of metabolites, generated different distributions compared to other groups. Metabolites concentrations expressed in percentages for SCFAs and mg/L for ammonium are reported in Table 4.

Consistently, the TR and NTR groups had significantly higher Acetate and Propionate concentrations compared to the AB group (for Acetate AB-TR p-value $= 3.22e^{-05}$ and AB-NTR p-value =

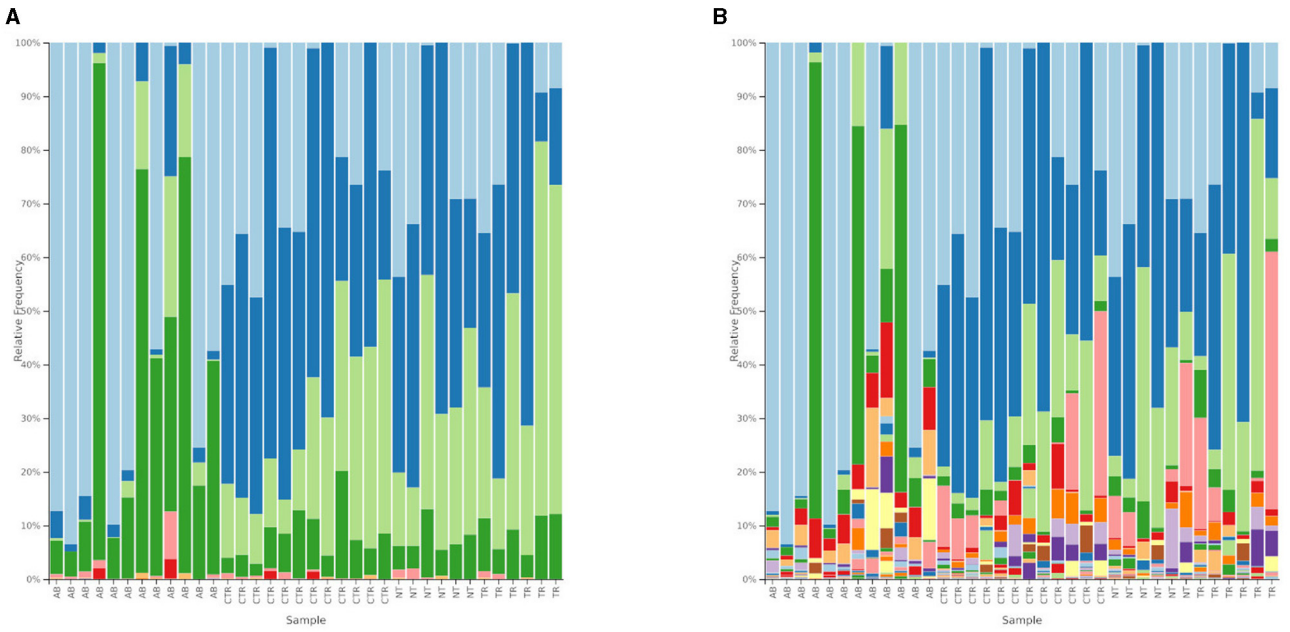

FIGURE 6
Relative abundances of bacterial composition. **(A)** Shows bacterial composition at phylum level. Light blue = Fusobacteria; blue = Bacillota; light green = Bacteroidota; green = Pseudomonadota; pink = Actinomycetota; red = Synergistes; light orange = Desulfobacterota. The groups are reported on the x-axis named as AB = antibiotic stimulation, CTR = control period, NT = non-treated microbiota, TR = treated microbiota. **(B)** Shows bacterial composition at genus level. Legend of the 10 most abundant genus: light blue = *Fusobacterium*; blue = *Megamonas*; light green = *Bacteroides*; green = *Escherichia-Shigella*; pink = *Prevotella*; red = *Pseudomonas*; light orange = *Parasutterella*; orange = *Alloprevotella*; light purple = *Phascolarctobacterium*; purple = *Sutterella*; light yellow = *Delftia*. The groups are reported on the x-axis named as AB = antibiotic stimulation, CTR = control period, NT = non-treated microbiota, TR = treated microbiota.

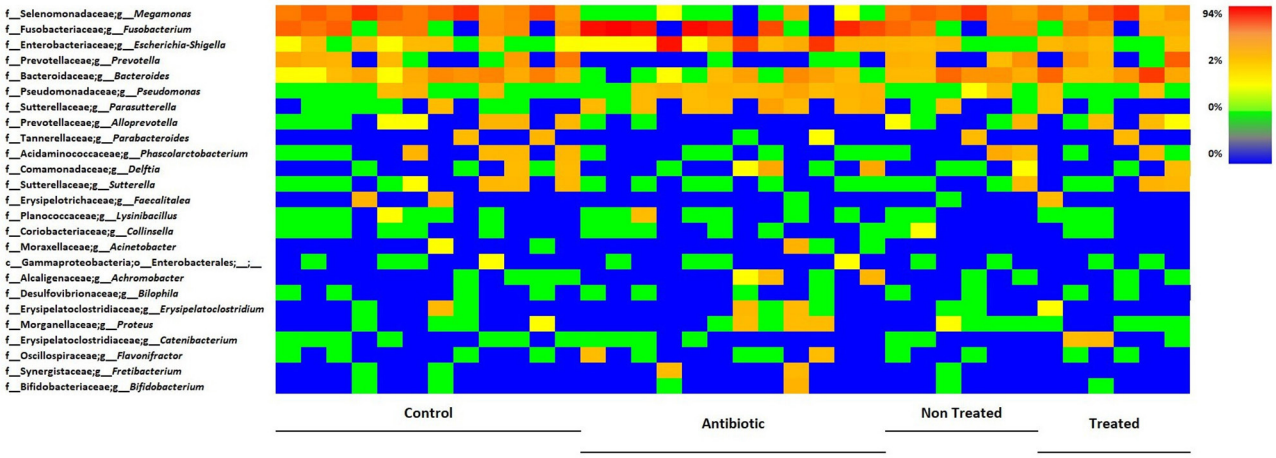

FIGURE 7
Heatmap illustrating the relative abundance of predominant bacterial genera in samples, divided by group. Each line reports the changes in relative abundance of a bacterial genus, among experimental groups, each column represents the bacteria relative abundances of a sample.

$6.47e^{-05}$, for Propionate AB -TR p-value = $<1e^{-06}$ and AB-NTR p-value = $<1e^{-06}$). BCFAs levels were significantly higher in NTR than in AB (p-value < 0.001), while they were almost unaltered in the other groups.

It is important to highlight that the TR group had significantly higher butyric acid levels compared to the CTR (p-value = 0.00115) and NTR (p-value = 0.01669), indicating that the treatment with the prebiotic seems to help with a faster recovery of the butyrate production.

Similarly, the fecal ammonium concentration (Supplementary Figure 2) decreased significantly following the antibiotic stimulation (CTR-AB, p-value < 0.001) while the NTR and TR groups had higher ammonium concentrations than the AB group, consistently with what is expected after finishing

the antibiotic administration. The TR group had lower ammonium concentrations compared to the CTR (p-value = 0.00105) and the NTR (p-value = 0.02410) groups, suggesting a significant effect of the treatment, while the ammonium concentration of NTR did not show significant differences compared to the control, even though it showed higher values. The statistical test results are summarized in Table 5.

4 Discussion

The aim of this research was to develop an *in vitro* model to mimic a condition that reproduces in taxonomic and biodiversity terms the dysbiosis that occurs in dogs in real life following antibiotic administration, but also in cases of other intestinal issues such as episodes of diarrhea. Due to similarities between SHIME® and SCIME™, some human experimental setups were adapted to meet the canine antibiotic-induced dysbiosis pattern. Although *in vivo* trials are the golden standard of studying disease processes, testing ingredients or even products for effectiveness, they are often too long and expensive (Nixon et al., 2019). In addition, despite their clinical importance, *in vivo* trials often do not succeed in unveiling how treatment mechanisms of action influence microbiota composition and functions (Duysburgh et al., 2021). Moreover, nowadays pet owners and consumers are very sensitive to the issue of animal testing and claims such as "Cruelty Free" or "Not Tested on Animals," and international agencies as FDA (Food and Drug Administration) and EFSA (European Food Safety Authority) support the development and use of alternatives to whole-animal testing (FDA, 2022; EFSA, 2024). Likewise, European legislation for the protection of pets is very rigid and aims to reduce the use of dogs as laboratory animals, encouraging the development and validation of *in vitro* models instead (Council directive 2010/63/EU, 2010). In this context, the main objective of the current study was to investigate if the administration of a selected amount of broad-spectrum antibiotic to a healthy canine microbiota could trigger dysbiosis and induce changes on the level of the same markers that occur *in vivo*. This would establish if an *in vitro* model could help to prevent or reduce the use of dogs as laboratory animals.

Regarding the simulated microbial community composition, it was observed that samples taken after antibiotic administration were significantly different from those taken during the previous control week, which was considered a "healthy" microbiota condition (eubiosis). The results showed significant changes in microbial communities and activity, similar to data observed in fecal samples from dogs with acute diarrhea, which is often coupled with intestinal dysbiosis, such as decreased microbial richness, lower SCFAs production and altered microbial composition (Guard et al., 2015). In this regard, rarefaction curves and alpha diversity data showed that during antibiotic stimulation, the bacterial diversity in all vessels was significantly lower compared to the control week. Lower alpha diversity (Shannon and Chao1 index) is a marker of dysbiosis and gastrointestinal diseases (Félix et al., 2022) and this pattern is also seen *in vivo* when sequencing fecal sample of dogs with acute diarrhea compared to healthy ones (Suchodolski et al., 2012; Guard et al., 2015; Chaitman et al., 2020). In addition to the reduction of microbial richness, antibiotic administration also impacted the metabolic activity of canine microbiota, as observed *in vivo*. SCFAs are the major metabolic products of anaerobic fermentation by microbial communities that colonize the mammalian gut (Louis and Flint, 2017) and a reduction of SCFAs production is associated with dysbiosis and many canine disease processes (Suchodolski, 2016). During dysbiosis week, triggered by antibiotic treatment, a significant reduction of propionate production in all donors was observed, reproducing the same trend observed in fecal samples of dogs with acute diarrhea (Guard et al., 2015; Félix et al., 2022). Guard et al. speculated that the decreased fecal propionic acid could possibly be due to lower production and/or increased absorption into the gut epithelium during stages of acute diarrhea. In the current *in vitro* model, since the absorption is excluded, the decreased propionic acid can be correlated to the decrease of microbial richness due to antibiotic treatment. Propionate plays a key role in canine gut wellness (Minamoto et al., 2019) and many studies report a lower concentration of propionate in the feces of dogs with dysbiosis compared to healthy animals (Guard et al., 2015; Félix et al., 2022). The main propionate-producing bacteria belong to Bacteroidota and Bacillota (Negativicutes class), which produce propionate through the succinate pathway, from sugar fermentation (Louis and Flint, 2017). During dysbiosis week the reduced propionate production can be correlated with the decreased abundance phylum Bacteroidota and Bacillota and this result overlaps with the data observed *in vivo* (Bell et al., 2008; Suchodolski et al., 2012; Guard et al., 2015). Moreover, the decreased propionate synthesis may be due to the decreased abundance of bacteria belonging to Negativicutes, such as *Megamonas*, which was strongly impacted by antibiotic treatment in all donors. Guard et al. (2015) found out that, along the general reduction of SCFAs concentration, the proportion of butyric acid was significantly increased in fecal samples from dogs with acute diarrhea, compared to healthy dogs. In the current *in vitro* model, comparing control week and antibiotic week, the concentration of butyrate significantly decreased. For this fatty acid, a strong donor dependent variability was found, as seen in Supplementary Figure 1. In this regard, in donors 2, 3, 4, and 6, the production of butyrate increased, while it decreased in donor 1 and 5. Donors 2, 3, 4, and 6 had a typical canine microbial community, mainly composed by Bacillota, Fusobacteria, Bacteroidota, Pseudomonadota, and Actinomycetota (Pilla and Suchodolski, 2020). Conversely, in donors 1 and 5 the abundance of Fusobacteria was very low and the microbial community composition was more similar to human gut microbiota, where some species belonging to Fusobacteriaceae family are even correlated with colorectal cancer (Nawab et al., 2023). We can speculate that the difference in microbial communities, both in healthy dogs and in those with a dysbiosis condition, can be related to the individual dog's habits and surroundings. For instance, *Fusobacterium* abundance is increased in dogs spending time outdoors and it is also reported that pets and pet owners can share some taxa (Song et al., 2013). Conversely, the increased butyrate concentration may be due to the increased abundance of *Fusobacterium* spp., which can produce butyrate from peptide and amino acid fermentation through glutamate and lysine degradation pathways (Louis and Flint, 2017) and the phylum Fusobacteria was also increased in dogs with acute hemorrhagic diarrhea (Suchodolski et al., 2012). Obviously, these

TABLE 2 Percentages of the most abundant bacterial groups.

Phylum	CTR	AB	NT	TR
Bacillota	44.93 (20.34–76.62)	2.61 (1.02–24.4)	40.87 (24.13–69.24)	37.72 (9.22–71.42)
Fusobacteria	25.16 (0–47.47)	66.42 (0.00–93.5)	29.09 (0.00–43.67)	8.84 (0–35.50)
Pseudomonadota	7.23 (2.27–20.07)	26.91 (4.70–92.6)	5.70 (4.25–12.79)	9.59 (4.18–12.15)
Bacteroidota	19.7 (6.34–47.33)	1.23 (0–26.12)	25.37 (10.83–43.62)	34.15 (13.09–69.69)
Actinomycetota	0.21 (0–1.25)	0.37 (0.00–8.79)	0.12 (0.00–1.97)	0.00 (0–1.22)
Desulfobacterota	0 (0–0.64)	0 (0.00–1.08)	0 (0.00–0.61)	0 (0.00–0.26)
Synergistes	0 (0–1.49)	0 (0.00–3.69)	0 (0.00–0.04)	0 (0.00–0.00)

Median (min-max) in percent is shown. The groups are reported named as (AB = antibiotic stimulation, CTR = control period, NT = non-treated microbiota, TR = treated microbiota). The abbreviation "unclass." denotes an unclassified taxonomy within the respective taxonomic group.

data have to be considered as preliminary since this study was performed using only six donors, and the results should be confirmed with a larger number of donors. Other microbiota metabolites, such as acetate, BCFAs and ammonia, tended to decrease during dysbiosis week. Their lower concentration can be generally related to lower Shannon and Chao1 index. It can be speculated that the lower alpha diversity mimics the reduction of bacteria during dysbiosis, because of the increased stool frequency (Vázquez-Baeza et al., 2016). The lower acetate production can be related to the decreased abundance of members of Bacillota (mainly *Megamonas*, but also *Fecalitalea* and *Phascolarctobacterium*) and Bacteroidota (*Alloprevotella* and *Prevotella* 9). The lower BCFAs concentration can be linked to the decreased abundance of *Bacteroides*. Moreover, during dysbiosis week a significant increase of Pseudomonadota, especially in donors with lower abundance of *Fusobacterium*, was observed. Pseudomonadota typically occur in small number in gut microbiota and fecal samples and their increase is often associated with dysbiosis and gastrointestinal diseases (Pilla and Suchodolski, 2020).

Having challenged the microbiota with antibiotic treatment, the current study investigated, as secondary outcome, whether a change in the SCIME^{TM} feed preparation (supposed to reproduce a change in the diet) could have any effect in microbiota recovery. In this regard, the aim of this second part of the experiment was to evaluate if a higher amount of prebiotic ingredient in the nutritional medium could induce a better recovery of microbiota, since it is known that the microbiota may not fully recover after an episode of acute diarrhea (Chaitman et al., 2020). Some studies have shown the potential of prebiotic ingredients in limiting the destructive effect of antibiotic treatments on the intestinal microbiota by promoting faster recovery of gut homeostasis (Sanders et al., 2019). In this regard, a petfood with a higher amount of prebiotic ingredients was chosen in the second part of the experiment. It is generally assumed that dietary changes and complementary feeds are a more natural alternative to conventional pharmacological approach to intestinal issues, as it also happens for dermatological disorders (Marchegiani et al., 2020). It has been widely suggested that complementary feeds containing prebiotic, probiotic and symbiotic ingredients can modulate gut microbiota and could potentially prevent acute diarrhea in dogs at risk or shorten the duration of the dysbiosis (Mekonnen et al., 2020). In this context, pet owners are becoming increasingly aware of the quality and effectiveness of the dietetic formulas and complementary feeds on the market (ASSALCO, 2023).

One week after the end of antibiotic administration, alpha diversity index significantly increased compared to the previous control week, in both arms of the experiment. This behavior can be explained as recovery from the dysbiosis trigger: moreover, rarefaction curves plotting OTUs data (Figure 5) show that a greater number of species was detected in the treated arm than in non-treated arm. This positive trend can be due to the higher amount and variety of fibers included in the prebiotic-enriched petfood, compared to standard petfood (compositions showed in Table 2). In fact, reduced richness, common during acute dysbiosis, can facilitate the invasion of pathogens, that could colonize niches otherwise occupied by the endogenous microbiota (Britton and Young, 2012). The data obtained from treatment week indicated that the administration of both nutritional mediums improved the conditions in each colonic vessel, compared to the previous week. It was found that treatment negatively impacted ammonium production (compared to the CTR p-value = 0.00105 and the NTR: p-value = 0.02410): ammonia has been linked with proteolytic fermentation and is a potentially harmful microbiota metabolite, correlated to foul fecal odor and colon carcinogenesis (Lin and Visek, 1991; Félix et al., 2010). Decreased ammonia production can be correlated to the lower percentage of crude protein and the inclusion of *Yucca schidigera* in the prebiotic-enriched feed, since this plant is known to reduce fecal oudors and ammonia (Cheeke, 2000; Vierbaum et al., 2019).

In the two groups, no strong differences were observed. The little differences observed in standard feed and prebiotic-enriched feed can be explained by the little difference in their composition: a higher concentration of prebiotics or a longer duration of the treatment could have given different results. As seen in PCoA plots (Figure 6A) sample results overlap those from control week and microbial community analysis showed high inter-individual variation. During treatment week, the sample was taken one week after the end of antibiotic trigger. It can be speculated that, in this *in vitro* model recovery occurs quite quickly and more differences in microbial communities could be seen sampling more often (e.g., every day between the last day of the antibiotic trigger). In addition, this result can be

10.3389/fmicb.2024.1455839

TABLE 3 *P*-values of the most abundant bacteria at phylum and genus level, obtained from multiple comparisons of means (Tukey contrasts) *post-hoc* test.

	Comparison					
Phylum	CTR-AB	AB-NTR	AB-TR	CTR-NTR	CTR-TR	NTR-TR
Bacillota	<0.001	<0.001	<0.001			
Fusobacteria	<0.001	<0.001	<0.001			
Pseudomonadota	<0.001	0.00499	0.00987			
Bacteroidota	<0.001	0.00487	0.01019			
Actinomycetota						
Desulfobacteria						
Synergistota						
Unclass. bacteria						
Unassigned						
Verrucomicrobiota						
Unassigned						
Genus	CTR-AB	AB-NTR	AB-TR	CTR-NTR	CTR-TR	NTR-TR
Megamonas	<0.001	<0.001	<0.001			
Fusobacterium	<0.001	<0.001	<0.001			
Shigella	0.0426					
Prevotella			0.00364			
Bacteroides			0.00163			
Pseudomonas	0.00910	0.00635	0.00486			
Parasutterella	0.0395	0.04430	0.02529			
Alloprevotella	0.0545	0.04119				
Parabacteroides						
Phascolarctobacterium		0.0203				
Delftia						
Sutterella			0.00795			
Faecalitalea						
Acinetobacter						
Lysinibacillus			0.0458			
Collinsella						
Enterobacterales						
Achromobacter	0.0379					
Bilophila						
Erysipelatoclostridium						
Proteus						
Catenibacterium			0.00317		0.00862	
Flavonifractor	0.0389					
Fretibacterium						

The groups are reported named as AB = antibiotic stimulation, CTR = control period, NT = non-treated microbiota, and TR = treated microbiota.

explained by the similar composition of the two nutritional mediums: both commercial diets include prebiotic ingredients (they share dried beet pulp and dried brewer's yeast) and the relative abundance of commercial feed in the nutritional medium is low (0.9%). Regarding SCFAs, it was found that the acetate and propionate increase during the week after antibiotic stimulation, but there is no difference between groups, that were given either standard petfood or prebiotic-enriched petfood. Conversely, it

TABLE 4 Percentages of the most common microbiota metabolites, SCFAs, BCFAs, and ammonium.

Group	Acetic acid (mmol/ml)	Propionic acid (mmol/ml)	Butyric acid (mmol/ml)	BCFAs (mmol/ml)	Ammonium (mg/L)
CTR	2.11 (3.74–7.14)	11.13 (6.67–18.01)	6.03 (3.54–7.82)	2.54 (2.14–3.66)	613.38 (487.1–703.58)
AB	2.67 (0.35–6.69)	1.34 (0.2–12.7)	8.07 (0.37–22.42)	2.02 (0.04–5.8)	432.98 (234.53–739.67)
NTR	3.75 (2.71–6.14)	10.39 (5.68–17.52)	6.59 (3.31–8.17)	2.6 (1.84–3.36)	586.32 (487.1–757.71)
TR	3.56 (2.91–6.78)	10.99 (6.09–20.22)	8.7 (4.03–11.77)	2.11 (1.82–2.76)	509.65 (432.98–595.34)

Median (min-max)* in percent is shown. The groups are reported labeled as AB = antibiotic stimulation, CTR = control period, NT = non-treated microbiota, and TR = treated microbiota.

TABLE 5 Significances of the main SCFAs concentrations obtained from multiple comparisons of means (Tukey contrasts) *post-hoc* test.

	Comparisons					
Metabolite	CTR-AB	AB-NT	AB-TR	CTR-NT	CTR-TR	NT-TR
Acetic acid	***↓	***↑	***↑			
Butyric acid	*↑				**↑	*↑
Propionic acid	***↓	***↑	***↑			
BCFAs	***↓	***↑				
Ammonium	***↓	***↑	*↑		**↓	*↓

The groups are reported named as AB = antibiotic stimulation, CTR = control period, NT = non-treated microbiota, and TR = treated microbiota. Each column represents the comparison between groups, the asterisks represent the multiple comparisons of means (Tukey contrasts) *post-hoc* test significance (*** = $0 < p$-value < 0.001, ** = $0.01 < p$-value < 0.01, * = $0.01 < p$-value < 0.05), while the arrows tell whether the metabolite concentration increases (↑) or decreases (↓) in the comparison.

was found that treatment positively impacted butyrate production compared to the CTR (p-value = 0.00115) and NTR (p-value = 0.01669). This can be explained by the higher amount of fibers in prebiotic-enriched feed. Butyrate is known to decrease the permeability of the intestinal epithelial lining by increasing the expression of tight junction proteins and reinforcing colonic defense barriers by increasing antimicrobial peptide levels and mucin production (Cook and Sellin, 1998; Wong et al., 2006; Antharam et al., 2013). It can be speculated that the increase in butyrate production may prevent over-growth of pathogens after an acute dysbisosis event.

As a limitation to this study, this *in vitro* work did not include a parallel *in vivo* validation, as happened for the validation of the SCIME™ model (Duysburgh et al., 2020). An additional *in vivo* validation would be favorable. Recent studies, such as the work of Argentini et al. (2022), confirm the rational of using *in vitro* models to reproduce microbial changes that would occur *in vivo* following antibiotic use.

Another limitation of the current work is that only a small number of animals were enrolled, partly due to cost and time restrictions. Also, all dogs, while all living in Ascoli Piceno (Italy), were on different diets and housed in different environments that were not controlled. Differing environments may influence intestinal microbiota. A larger number of enrolled donors would give more insights about microbiota modulation, due to the physiological interindividual variability in microbial communities. Anyway, we decided to select 6 donors for the study, based on literature research and previous publications where SCIME™ (Duysburgh et al., 2020; Verstrepen et al., 2021) and SHIME® (Deyaert et al., 2023; Duysburgh et al., 2024) have been used. The SCIME™ model, as well as the SHIME® and other chemostat models, allows the creation of an environment with highly reproducible and physiological conditions for the intestinal microbiota, by the means of a fecal inoculation of the system. In our case, by inoculating the system with the fecal material of 6 donors and considering only the distal colon (since we were interested in the effect of the antibiotic on the terminal part of the GI tract) we were able to introduce another variable in the system (prebiotic-enriched petfood compared to standard petfood). This because we had two replicates of the distal colon for each donor. This study can be considered a preliminary test and future experiments involving a larger sample size are needed to confirm or confute the results.

Another limitation of the study was that only a single antibiotic was used and it was known to cause dysbiosis. As stated in the abstract and introduction, the primary outcome of the study was to evaluate if SCIME™ could be used to mimic intestinal dysbiosis, as previously done employing SHIME®. For this reason, an already known trigger of dysbiosis *in vivo* was selected. In particular, fewer antibiotic are available as veterinary drugs for dogs, compared to those for human, and amoxicillin-clavulanic acid is one of them (Synulox, Clavobay, and Clavaseptin). Since information about therapeutical dosage and ADME are necessary to calculate the dose to administer to SCIME™, it was mandatory to select an antibiotic approved for dogs. Moreover, we decided to use only one antibiotic as a trigger after studying the latest papers (El Hage et al., 2019; Duysburgh et al., 2021). In addition, in a recent work from El Hage et al. a similar experimental setup (one antibiotic, six donors) was used (El Hage et al., 2019).

As the current study mainly focused on the validation of an acute dysbiosis model, especially in the distal colon region, it could be interesting to extend the setup to the conventional SCIME™

reactor, including proximal colon. Moreover, to further understand the effect of dysbiosis on canine microbiota, the inclusion of mucosal compartment could be useful (Verstrepen et al., 2021).

5 Conclusions

In conclusion, a dynamic *in vitro* model simulating canine antibiotic-induced dysbiosis was developed, with a focus on the distal colon-associated microbial community and its metabolites. The current study discovered that it is possible to mimic *in vitro* a condition that reproduces in taxonomic and biodiversity terms the dysbiosis that occurs in dogs in real life following antibiotic administration (whether it causes diarrhea or not) and during other conditions where, regardless of whether or not dogs received antibiotics, episodes of diarrhea occur (whether due to gastroenteritis, functional gastrointestinal disorders or IBD). Moreover, this new SCIME^{TM} setup facilitated the reproduction of microbial and metabolic changes seen *in vivo* in fecal samples obtained from dogs with acute diarrhea, such as lower microbial diversity and decreased concentration of propionate.

The main goal of this work is that, upon inducing dysbiosis with antibiotic administration, the simulated canine microbiota reproduced the same patterns seen *in vivo* in cases of antibiotic-induced dysbiosis, indicating an interesting application potential in research related to canine gastrointestinal health and petfood development, and preventing the use of *in vivo* testing.

Data availability statement

The original contributions presented in the study are publicly available. This data can be found here: https://doi.org/10.6084/m9.figshare.26863042.v1.

Author contributions

ED: Conceptualization, Data curation, Investigation, Methodology, Writing – original draft, Writing – review & editing. AB: Investigation, Visualization, Writing – review & editing. GN: Data curation, Writing – review & editing. MM: Investigation, Validation, Writing – review & editing. MG: Visualization, Writing – review & editing. FD: Visualization, Writing – review & editing. BB: Conceptualization, Data curation, Investigation, Methodology, Project administration, Writing – original draft, Writing – review & editing.

Funding

The author(s) declare financial support was received for the research, authorship, and/or publication of this article. This study received funding from C.I.A.M. Srl. The funder has the following involvement with the study: the writing of this article and the decision to submit it for publication.

Acknowledgments

This investigation was supported by C.I.A.M. Srl.

Conflict of interest

ED, AB, GN, and BB were employed by C.I.A.M. Srl. FD was employed by Velleja Research.

The remaining authors declare that the research was conducted in the absence of any commercial or financial relationships that could be construed as a potential conflict of interest.

Publisher's note

Supplementary material

The Supplementary Material for this article can be found online at: https://www.frontiersin.org/articles/10.3389/fmicb.2024.1455839/full#supplementary-material

References

3.6.3, R. D. C. T. (2020). *A Language and Environment for Statistical Computing*. R Foundation for Statistical Computing. Available at: https://www.R-project.org (accessed March 25, 2024).

Antharam, V. C., Li, E. C., Ishmael, A., Sharma, A., Mai, V., Rand, K. H., et al. (2013). Intestinal dysbiosis and depletion of butyrogenic bacteria in *Clostridium difficile* infection and nosocomial diarrhea. *J. Clin. Microbiol.* 51, 2884–2892. doi: 10.1128/JCM.00845-13

Argentini, C., Mancabelli, L., Alessandri, G., Tarracchini, C., Barbetti, M., Carnevali, L., et al. (2022). Exploring the ecological effects of naturally antibiotic-insensitive bifidobacteria in the recovery of the resilience of the gut microbiota during and after antibiotic treatment. *Appl. Environ. Microbiol.* 88:22. doi: 10.1128/aem.00522-22

ASSALCO (2023). *Alimentazione e cura degli animali da compagnia Pet in Italia: 15 anni di cambiamenti in famiglia e in società*. XV edizione Rapporto Assalco – Zoomark 2022. Available at: https://www.zoomark.it/media/zoomark/pressrelease/2023/rapporto_assalco_-_zoomark_2022_-_sintesi.pdf

Bell, J. A., Kopper, J. J., Turnbull, J. A., Barbu, N. I., Murphy, A. J., and Mansfield, L. S. (2008). Ecological characterization of the colonic microbiota of normal and diarrheic dogs. *Interdiscip. Perspect. Infect. Dis.* 2008, 1–17. doi: 10.1155/2008/149694

Bolyen, E., Rideout, J. R., Dillon, M. R., Bokulich, N. A., Abnet, C. C., Al-Ghalith, G. A., et al. (2019). Reproducible, interactive, scalable and extensible microbiome data science using QIIME 2. *Nat. Biotechnol.* 37, 852–857. doi: 10.1038/s41587-019-0209-9

Britton, R. A., and Young, V. B. (2012). Interaction between the intestinal microbiota and host in *Clostridium difficile* colonization resistance. *Trends Microbiol.* 20, 313–319. doi: 10.1016/j.tim.2012.04.001

Chaitman, J., Ziese, A. L., Pilla, R., Minamoto, Y., Blake, A. B., Guard, B. C., et al. (2020). Fecal microbial and metabolic profiles in dogs with acute diarrhea receiving either fecal microbiota transplantation or oral metronidazole. *Front. Vet. Sci.* 7:192. doi: 10.3389/fvets.2020.00192

Cheeke, P. R. (2000). "Actual and potential applications of Yucca Schidigera and Quillaja Saponaria Saponins in human and animal nutrition," in *Saponins in Food, Feedstuffs and Medicinal Plants. Proceedings of the Phythochemical Society of Europe, Vol. 45*, eds. W. Oleszek, and A. Marston, (Dordrecht: Springer). doi: 10.1007/978-94-015-9339-7_25

Cook, S. I., and Sellin, J. H. (1998). Review article: short chain fatty acids in health and disease. *Aliment. Pharmacol. Ther.* 12, 499–507. doi: 10.1046/j.1365-2036.1998.00337.x

Council directive 2010/63/EU (2010). Council directive 2010/63/EU on the protection of animals used for scientific purposes (2010). *Off. J.* L276, 4849.

De Wiele, T., Van Boon, N., Possemiers, S., Jacobs, H., and Verstraete, W. (2004). Prebiotic effects of chicory inulin in the simulator of the human intestinal microbial ecosystem. *FEMS Microbiol. Ecol.* 51, 143–153. doi: 10.1016/j.femsec.2004.07.014

Deyaert, S., Moens, F., Pirovano, W., van den Bogert, B., Klaassens, E. S., Marzorati, M., et al. (2023). Development of a reproducible small intestinal microbiota model and its integration into the SHIME® -system, a dynamic *in vitro* gut model. *Front. Microbiol.* 13:1054061. doi: 10.3389/fmicb.2022.1054061

Duysburgh, C., Govaert, M., Guillemet, D., and Marzorati, M. (2024). Co-supplementation of baobab fiber and arabic gum synergistically modulates the *in vitro* human gut microbiome revealing complementary and promising prebiotic properties. *Nutrients* 16:1570. doi: 10.3390/nu16111570

Duysburgh, C., Ossieur, W. P., De Paepe, K., Van den Abbeele, P., Vichez-Vargas, R., Vital, M., et al. (2020). Development and validation of the Simulator of the Canine Intestinal Microbial Ecosystem (SCIME)1. *J. Anim. Sci.* 98:skz357. doi: 10.1093/jas/skz357

Duysburgh, C., Van den Abbeele, P., Morera, M., and Marzorati, M. (2021). *Lacticaseibacillus rhamnosus* GG and *Saccharomyces cerevisiae* boulardii supplementation exert protective effects on human gut microbiome following antibiotic administration *in vitro*. *Benef. Microbes* 12, 365–379. doi: 10.3920/BM2020.0180

EFSA (2024). *Alternatives to Animal Testing*. EFSA European Food Safety Authority. Available at: https://www.efsa.europa.eu/en/topics/topic/alternatives-animal-testing (accessed April 8, 2024).

El Hage, R., Hernandez-Sanabria, E., Calatayud Arroyo, M., Props, R., and Van de Wiele, T. (2019). Propionate-producing consortium restores antibiotic-induced dysbiosis in a dynamic *in vitro* model of the human intestinal microbial ecosystem. *Front. Microbiol.* 10:1206. doi: 10.3389/fmicb.2019.01206

FDA (2022). *Focus Area: Novel Technologies to Improve Predictivity of Non-clinical Studies and Replace, Reduce, and Refine Reliance on Animal Testing*. Available at: https://www.fda.gov/science-research/focus-areas-regulatory-science-report/focus-area-novel-technologies-improve-predictivity-non-clinical-studies-and-replace-reduce-and (accessed February 15, 2024).

Félix, A. P., Netto, M. V. T., Murakami, F. Y., de Brito, C. B. M., de Oliveira, S. G., and Maiorka, A. (2010). Digestibilidade e características das fezes de cães suplementados com *Bacillus subtilis* na dieta. *Ciencia Rural* 40, 2169–2173. doi: 10.1590/S0103-84782010005000166

Félix, A. P., Souza, C. M. M., and de Oliveira, S. G. (2022). Biomarkers of gastrointestinal functionality in dogs: a systematic review and meta-analysis. *Anim. Feed Sci. Technol.* 283:115183. doi: 10.1016/j.anifeedsci.2021.115183

German, A. J., Halladay, L. J., and Noble, P. J. M. (2010). First-choice therapy for dogs presenting with diarrhoea in clinical practice. *Vet. Record* 167, 810–814. doi: 10.1136/vr.c4090

Ghyselinck, J., Verstrepen, L., Moens, F., Van den Abbeele, P., Said, J., Smith, B., et al. (2020). A 4-strain probiotic supplement influences gut microbiota composition and gut wall function in patients with ulcerative colitis. *Int. J. Pharm.* 587:119648. doi: 10.1016/j.ijpharm.2020.119648

Guard, B. C., Barr, J. W., Reddivari, L., Klemashevich, C., Jayaraman, A., Steiner, J. M., et al. (2015). Characterization of microbial dysbiosis and metabolomic changes in dogs with acute diarrhea. *PLoS ONE* 10:127259. doi: 10.1371/journal.pone.0127259

Hubbard, K., Skelly, B. J., Mckelvie, J., and Wood, J. L. N. (2007). Risk of vomiting and diarrhoea in dogs. *Vet. Record* 161, 755–757. doi: 10.1136/vr.161.22.755

Ichim, T. E., Kesari, S., and Shafer, K. (2018). Protection from chemotherapy- and antibiotic-mediated dysbiosis of the gut microbiota by a probiotic with digestive enzymes supplement. *Oncotarget* 9, 30919–30935. doi: 10.18632/oncotarget.25778

Jones, P. H., Dawson, S., Gaskell, R. M., Coyne, K. P., and Tierney Setzkorn, C. (2014). Surveillance of diarrhoea in small animal practice through the Small Animal Veterinary Surveillance Network (SAVSNET). *Vet. J.* 201, 412–418. doi: 10.1016/j.tvjl.2014.05.044

Kung, K., and Wanner, M. (1994). Bioavailability of different forms of amoxycillin administered orally to dogs. *Vet. Record* 135, 552–554.

Lin, H. C., and Visek, W. J. (1991). Large intestinal pH and ammonia in rats: dietary fat and protein interactions. *J. Nutr.* 121, 832–843. doi: 10.1093/jn/121.6.832

Louis, P., and Flint, H. J. (2017). Formation of propionate and butyrate by the human colonic microbiota. *Environ. Microbiol.* 19, 29–41. doi: 10.1111/1462-2920.13589

Mancabelli, L., Mancino, W., Lugli, G. A., Argentini, C., Longhi, G., Milani, C., et al. (2021). Amoxicillin-clavulanic acid resistance in the genus bifidobacterium. *Appl. Environ. Microbiol.* 87:20. doi: 10.1128/AEM.03137-20

Marchegiani, A., Fruganti, A., Spaterna, A., Vedove, E. D., Bachetti, B., Massimini, M., et al. (2020). Impact of nutritional supplementation on canine dermatological disorders. *Vet. Sci.* 7:20038. doi: 10.3390/vetsci7020038

Marzorati, M., Van den Abbeele, P., Bubeck, S. S., Bayne, T., Krishnan, K., Young, A., et al. (2020). *Bacillus subtilis* HU58 and *Bacillus coagulans* SC208 probiotics reduced the effects of antibiotic-induced gut microbiome dysbiosis in an M-SHIME® model. *Microorganisms* 8, 1–15. doi: 10.3390/microorganisms8071028

Marzorati, M., Vilchez-Vargas, R., Bussche, J., Vanden Truchado, P., Jauregui, R., El Hage, R. A., et al. (2017). High-fiber and high-protein diets shape different gut microbial communities, which ecologically behave similarly under stress conditions, as shown in a gastrointestinal simulator. *Mol. Nutr. Food Res.* 61:150. doi: 10.1002/mnfr.201600150

Mekonnen, S. A., Merenstein, D., Fraser, C. M., and Marco, M. L. (2020). Molecular mechanisms of probiotic prevention of antibiotic-associated diarrhea. *Curr. Opin. Biotechnol.* 61, 226–234. doi: 10.1016/j.copbio.2020.01.005

Milani, C., Hevia, A., Foroni, E., Duranti, S., Turroni, F., Lugli, G. A., et al. (2013). Assessing the fecal microbiota: an optimized ion torrent 16S rRNA gene-based analysis protocol. *PLoS ONE* 8:739. doi: 10.1371/journal.pone.0068739

Minamoto, Y., Minamoto, T., Isaiah, A., Sattasathuchana, P., Buono, A., Rangachari, V. R., et al. (2019). Fecal short-chain fatty acid concentrations and dysbiosis in dogs with chronic enteropathy. *J. Vet. Intern. Med.* 2019:15520. doi: 10.1111/jvim.15520

Nationwide Mutual Insurance Company (2023). *Dermatitis, Otitis Externa Continue to Top Common Conditions That Prompt Veterinary Visits*. Available at: https://news.nationwide.com/dermatitis-otitis-externa-top-common-conditions-vet-visits/ (accessed January 17, 2024).

Nawab, S., Bao, Q., Ji, L. H., Luo, Q., Fu, X., Fan, S., et al. (2023). The pathogenicity of *Fusobacterium nucleatum* modulated by dietary fibers-a possible missing link between the dietary composition and the risk of colorectal cancer. *Microorganisms* 11:82004. doi: 10.3390/microorganisms11082004

Nixon, S. L., Rose, L., and Muller, A. T. (2019). Efficacy of an orally administered anti-diarrheal probiotic paste (Pro-Kolin Advanced) in dogs with acute diarrhea: a randomized, placebo-controlled, double-blinded clinical study. *J. Vet. Intern. Med.* 33, 1286–1294. doi: 10.1111/jvim.15481

Pilla, R., and Suchodolski, J. S. (2020). The role of the canine gut microbiome and metabolome in health and gastrointestinal disease. *Front. Vet. Sci.* 6:498. doi: 10.3389/fvets.2019.00498

Pinna, C., and Biagi, G. (2014). The utilisation of prebiotics and synbiotics in dogs. *Ital. J. Anim. Sci.* 13, 169–178. doi: 10.4081/ijas.2014.3107

Sanders, M. E., Merenstein, D. J., Reid, G., Gibson, G. R., and Rastall, R. A. (2019). Probiotics and prebiotics in intestinal health and disease: from biology to the clinic. *Nat. Rev. Gastroenterol. Hepatol.* 16, 605–616. doi: 10.1038/s41575-019-0173-3

Song, S. J., Lauber, C., Costello, E. K., Lozupone, C. A., Humphrey, G., Berg-Lyons, D., et al. (2013). Cohabiting family members share microbiota with one another and with their dogs. *Elife* 2013:458. doi: 10.7554/eLife.00458

Suchodolski, J. S. (2016). Diagnosis and interpretation of intestinal dysbiosis in dogs and cats. *Vet. J.* 215, 30–37. doi: 10.1016/j.tvjl.2016.04.011

Suchodolski, J. S. (2022). Analysis of the gut microbiome in dogs and cats. *Vet. Clin. Pathol.* 50, 6–17. doi: 10.1111/vcp.13031

Suchodolski, J. S., Markel, M. E., Garcia-Mazcorro, J. F., Unterer, S., Heilmann, R. M., Dowd, S. E., et al. (2012). The fecal microbiome in dogs with acute diarrhea and idiopathic inflammatory bowel disease. *PLoS ONE* 7:e51907. doi: 10.1371/journal.pone.0051907

The European Agency for the Evaluation of Medicinal Products (1996). *Committee for Veterinary Medicinal Products Clavulanic Acid Summary Report*. EMEA/MRL/152/96. Available at: https://www.ema.europa.eu/en/documents/mrl-report/clavulanic-acid-summary-report-1-committee-veterinary-medicinal-products_en.pdf

Vázquez-Baeza, Y., Hyde, E. R., Suchodolski, J. S., and Knight, R. (2016). Dog and human inflammatory bowel disease rely on overlapping yet distinct dysbiosis networks. *Nat. Microbiol.* 1:177. doi: 10.1038/nmicrobiol.2016.177

Verstrepen, L., Van den Abbeele, P., Pignataro, G., Ribecco, C., Gramenzi, A., Hesta, M., et al. (2021). Inclusion of small intestinal absorption and simulated mucosal surfaces further improve the Mucosal Simulator of the Canine Intestinal Microbial

Ecosystem (M-SCIME^{TM}). *Res. Vet. Sci.* 140, 100–108. doi: 10.1016/j.rvsc.2021.08.011

Vierbaum, L., Eisenhauer, L., Vahjen, W., and Zentek, J. (2019). *In vitro* evaluation of the effects of *Yucca schidigera* and inulin on the fermentation potential of the faecal microbiota of dogs fed diets with low or high protein concentrations. *Arch. Anim. Nutr.* 73, 399–413. doi: 10.1080/1745039X.2019.1616498

Wong, J. M. W., De Souza, R., Kendall, C. W. C., Emam, A., and Jenkins, D. J. A. (2006). Colonic health: fermentation and short chain fatty acids. *J. Clin. Gastroenterol.* 15, 235–243. doi: 10.1097/00004836-200603000-00015

Zoetis UK Limited (2024). *Synulox Palatable Tablets Datasheet*. Available at: https://www.noahcompendium.co.uk/?id=-458486 (accessed March 18, 2024).

frontiers | Frontiers in Microbiology

TYPE Original Research
PUBLISHED 11 October 2024
DOI 10.3389/fmicb.2024.1433175

OPEN ACCESS

EDITED BY
Qinghong Li,
Nestle Purina Research, United States

REVIEWED BY
Jenessa Winston,
The Ohio State University, United States
Erin Beth Perry,
Southern Illinois University Carbondale, United States

*CORRESPONDENCE
Federica Cagnasso
federica.cagnasso@unito.it

RECEIVED 15 May 2024
ACCEPTED 24 September 2024
PUBLISHED 11 October 2024

CITATION
Cagnasso F, Suchodolski JS, Borrelli A, Borella F, Bottero E, Benvenuti E, Ferriani R, Tolbert MK, Chen C-C, Giaretta PR and Gianella P (2024) Dysbiosis index and fecal concentrations of sterols, long-chain fatty acids and unconjugated bile acids in dogs with inflammatory protein-losing enteropathy.
Front. Microbiol. 15:1433175.
doi: 10.3389/fmicb.2024.1433175

Dysbiosis index and fecal concentrations of sterols, long-chain fatty acids and unconjugated bile acids in dogs with inflammatory protein-losing enteropathy

Federica Cagnasso[1]*, Jan S. Suchodolski[2], Antonio Borrelli[1], Franca Borella[1], Enrico Bottero[3], Elena Benvenuti[3], Riccardo Ferriani[3], M. Katherine Tolbert[2], Chih-Chun Chen[2], Paula R. Giaretta[2] and Paola Gianella[1]

[1]Department of Veterinary Sciences, University of Turin, Grugliasco, Italy, [2]Gastrointestinal Laboratory, Department of Small Animal Clinical Sciences, Texas A&M University, College Station, TX, United States, [3]Associazione Professionale Endovet, Rome, Italy

Introduction: Canine protein-losing enteropathy (PLE) is a syndrome characterized by gastrointestinal loss of proteins. While fecal microbiome and metabolome perturbations have been reported in dogs with chronic enteropathy, they have not been widely studied in dogs with PLE. Therefore, the study aims were to investigate gut microbiome and targeted fecal metabolites in dogs with inflammatory PLE (iPLE) and evaluate whether treatment affects these changes at short-term follow-up.

Methods: Thirty-eight dogs with PLE and histopathological evidence of gastrointestinal inflammation and 47 healthy dogs were enrolled. Fecal samples were collected before endoscopy (T0) and after one month of therapy (T1). Microbiome and metabolome alterations were investigated using qPCR assays (dysbiosis index, DI) and gas chromatography/mass spectrometry (long-chain fatty acids, sterols, unconjugated bile acids), respectively.

Results: Median (min-max) DI of iPLE dogs was 0.4 (−5.9 to 7.7) and was significantly higher ($p < 0.0001$) than median DI in healthy dogs [−2.0 (−6.0 to 5.3)]. No significant associations were found between DI and selected clinicopathological variables. DI did not significantly differ between T0 and T1. In iPLE dogs, at T0, myristic, palmitic, linoleic, oleic, cis-vaccenic, stearic, arachidonic, gondoic, docosanoic, erucic, and nervonic acids were significantly higher ($p < 0.0001$) than healthy dogs. In iPLE dogs, oleic acid ($p = 0.044$), stearic acid ($p = 0.013$), erucic acid ($p = 0.018$) and nervonic acid ($p = 0.002$) were significantly decreased at T1. At T0, cholesterol and lathosterol ($p < 0.0001$) were significantly higher in iPLE dogs compared to healthy dogs, while total measured phytosterols were significantly lower ($p = 0.001$). No significant differences in total sterols, total phytosterols and total zoosterols content were found at T1, compared to T0. At T0, total primary bile acids and total secondary bile acids

did not significantly differ between healthy control dogs and iPLE dogs. No significant differences in fecal bile acid content were found at T1.

Discussion: Dysbiosis and lipid metabolism perturbations were observed in dogs with iPLE. Different therapeutic protocols lead to an improvement of some but not all metabolome perturbations at short-term follow-up.

KEYWORDS

canine, fecal long-chain fatty acids, fecal sterols, fecal bile acids, dysbiosis

1 Introduction

Protein-losing enteropathy (PLE) is a complex and challenging syndrome, characterized by chronic gastrointestinal signs and abnormal loss of proteins through the gastrointestinal tract (Jergens and Heilmann, 2022; Allenspach and Iennarella-Servantez, 2021; Green and Kathrani, 2022; Craven and Washabau, 2019). Numerous gastrointestinal diseases including inflammatory enteropathy, lymphangiectasia, and neoplasia, if severe enough, can result in PLE (Craven and Washabau, 2019). The diagnosis of the intestinal disorder causing PLE is time-consuming, the management is challenging, and the prognosis is guarded, with death occurring in > 50% of dogs with inflammatory PLE (Allenspach and Iennarella-Servantez, 2021; Green and Kathrani, 2022; Craven and Washabau, 2019). Therefore, a timely and early diagnosis and therapeutic intervention are desirable.

At present, the pathogenesis of PLE is not fully understood and appears to be multifactorial (Jergens and Heilmann, 2022; Craven and Washabau, 2019). Several markers have been described as negative prognostic factors of PLE, including hypocobalaminemia, increased CRP, and elevated CCECAI, although they are inconsistently observed during the course of the disease and are not pathognomonic (Allenspach and Iennarella-Servantez, 2021). It is suspected that in the context of a multifactorial pathogenesis and a complex and intricate disease, the population of dogs affected by PLE may vary in terms of clinical and pathological aspects, also in relation to the severity and extent of mucosal damage.

The gut microbiome plays an important role in preserving the intestinal mucosal barrier function, educating the immune system, driving inflammation, and affecting most physiologic functions through the production of metabolites (Tizard and Jones, 2018; Pilla and Suchodolski, 2020). Indeed, a dysfunctional microbiome, as observed in many acute and chronic gastrointestinal diseases, is associated with dysbiosis (Jergens and Heilmann, 2022; Allenspach and Iennarella-Servantez, 2021; Green and Kathrani, 2022). Recently, a quantitative PCR-based assay, namely the dysbiosis index (DI), was developed to assess shifts in the microbiome in fecal samples of dogs (AlShawaqfeh et al., 2017). It quantifies the fecal abundance of seven core bacteria and combines them into a single numeric value that accurately predicts global shifts in the canine microbiome as assessed by metagenomic sequencing (Sung et al., 2023a). The selected taxa of the DI that are frequently altered in a subset of dogs with chronic enteropathies have important metabolic functions for the host (AlShawaqfeh et al., 2017).

The intestinal metabolome is the biochemical environment representing a symbiosis between the host and the microbiota, broadly reflecting the health of the gastrointestinal tract (Pilla and Suchodolski, 2020; Bauset et al., 2021). The host provides a nutrient-rich environment, and the microbiota performs functions and produces metabolites. Chronic inflammatory enteropathy alters the fecal and serum metabolome, such as bile acids, amino acids, short- and long-chain fatty acids, vitamins, and their derivatives (Minamoto et al., 2015). Sterols and long-chain fatty acids are two important lipidic macronutrients that play different essential functions for the organism, such as energy production and storage, cellular membrane structure composition, and regulation of different biological processes, including the inflammation pathway (Piotrowska et al., 2021; Weng et al., 2019; Ma et al., 2019). Bile acids (BAs) play a key role in lipid absorption and metabolism and intestinal inflammatory processes. Primary conjugated bile acids are converted in the large intestine into secondary unconjugated bile acids, which exhibit beneficial properties for the intestinal functions and interact with the gut immune system (Pilla and Suchodolski, 2020; Ward et al., 2017; Kang et al., 2019).

Altered fecal concentrations of long-chain fatty acids, sterols, and bile acids have been observed in humans, cats, and dogs with gastrointestinal disease (Piotrowska et al., 2021; Ma et al., 2019; Blake et al., 2019; Marsilio et al., 2021; Sung et al., 2023b; Galler et al., 2022a; Galler et al., 2022b; Pilla et al., 2021). In particular, a subset of dogs with chronic inflammatory enteropathy have decreased fecal secondary bile acid concentrations compared to healthy dogs (Blake et al., 2019; Galler et al., 2022b; Honneffer, 2017; Xu et al., 2016; Ziese and Suchodolski, 2021), while a subset of Yorkshire terriers with chronic inflammatory enteropathy have increased fecal long-chain fatty acids, along with decreased plant sterol sitostanol (Galler et al., 2022b).

To the authors' knowledge, scarce information of microbiome and metabolome perturbations is available in dogs with inflammatory PLE (iPLE) both before and after treatment. The study of fecal microbiome and metabolome in dogs with iPLE might provide new insights into the magnitude and significance of intestinal dysmetabolism and damage, and potentially guide new therapeutic approaches. Therefore, the aim of this study was to investigate the DI and the fecal concentrations of sterols, long-chain fatty acids and unconjugated bile acids in a population

Abbreviations: BAs, bile acids; CCECAI, chronic canine enteropathy clinical activity index; FAs, total fatty acids; iPLE, inflammatory protein-losing enteropathy; T0, time of the endoscopic procedure; T1, one month after therapy; TPBA, total primary bile acids; TSBA, total secondary bile acids.

of dogs with PLE caused by inflammatory enteropathy, both at diagnosis and short-term follow-up.

2 Materials and methods

2.1 Study design and ethics approval

The experimental protocol was reviewed and approved by the Ethics and Animal Welfare committee of the University of Turin (protocol number 42, 08/01/2021). This was a prospective investigation that involved client-owned dogs, and all owners provided informed consent. All the dogs were referred for a specialist consult to the Unit of Gastroenterology at the Veterinary Teaching Hospital of the University of Turin or to Endovet referral clinics in north-middle Italy between January 2021 and March 2022.

2.2 Cases and control dogs

Thirty-eight privately-owned dogs with a diagnosis of iPLE were enrolled. Inclusion criteria for inflammatory PLE were chronic gastrointestinal signs lasting for more than 3 weeks, hypoalbuminemia of gastrointestinal origin ($\leq$ 2.8 g/dL) and histopathological evidence of benign gastrointestinal inflammation with or without lymphangiectasia on multiple biopsies collected by endoscopy. The histopathologic evaluation was performed according to the standards of the World Small Animal Veterinary Association Gastrointestinal Standardization Group (Day et al., 2008). Fecal flotation and giardia antigen-test, complete blood count, biochemistry, pre- and post-prandial bile acids, urinalysis, urinary protein to creatinine ratio, serum basal cortisol or ACTH stimulation test (if basal cortisol $<$ 2 μg/dl), trypsin-like-immunoreactivity, pancreas specific lipase levels, serum folate and cobalamin concentrations, and abdominal ultrasound examination were required to rule out infectious, parasitic, liver and pancreatic diseases, along with intestinal diseases of other etiology and extraintestinal diseases. Hypoalbuminemic dogs also were required to have no clinically relevant proteinuria (negative urine dipstick test result or urine protein to creatinine ratio $<$ 0.5) and no evidence of clinically relevant hepatic disease (normal pre- and post-prandial bile acid concentrations or normal synthetic liver function and enzyme activity). Exclusion criteria were complete and sustained response to hydrolyzed or limited ingredient diets administered before referral, incomplete diagnostic investigations, and a histopathologic diagnosis of neoplasia. Dogs with iPLE that received antibiotics prior to referral were excluded. Information concerning age, sex, breed, weight, chronic canine enteropathy clinical activity index (CCECAI) score, type of diets and therapeutic treatments prior to referral were registered at admission (Allenspach et al., 2007). The CCECAI was calculated at the time of the consultation, or retrospectively, using the serum albumin concentration, presence or absence of peripheral edema and peritoneal effusion on ultrasound examination and the owner's scores on appetite, activity level, vomiting, fecal consistency and frequency, weight loss and pruritus. All iPLE dogs underwent gastroduodenoscopy. Colonoscopy with ileal intubation was performed when possible, based on the dog's overall risk for prolonged anesthesia due to complications associated with severe hypoalbuminemia. At least 8 endoscopic biopsies from the stomach, duodenum, and when available, ileum and colon, were collected and immediately placed in a tube filled with 10% neutral buffered formalin and submitted for histologic examination. The type and severity of structural and inflammatory lesions in the duodenum, ileum, and colon were recorded based on a 4-point grading scheme (0 = normal, 1 = mild lesions, 2 = moderate lesions, 3 = severe lesions) (Day et al., 2008). Presence or absence of lymphangiectasia was determined based on histopathological evaluation of the diameter of lacteals, with lacteals representing more than 25% of the width of the villous lamina propria were considered dilated and subclassified as mild (25–50% of villous width), moderate (51–75% of villous width), or severe ($>$ 75% of villous width), according to the World Small Animal Veterinary Association guidelines (Day et al., 2008). After the endoscopic procedure and histologic diagnosis (T0), diet and therapy were adjusted on a case basis. All iPLE dogs were prescribed ultra-low fat ($<$ 15g fat/Mcal ME) or hydrolyzed diets in addition to oral prednisolone (0.5–1 mg/kg, q 12–24 h). In some dogs, oral prednisolone was administered with oral chlorambucil (2–4 mg/m2, q24h). Weekly parenteral cobalamin supplementation was given to dogs with hypocobalaminemia or suboptimal serum cobalamin concentrations (serum cobalamin levels within normal range but at the lower limit of the reference range, i.e., $<$ 400 ng/L), as previously described (Berghoff et al., 2013; Kather et al., 2020). Daily oral folate supplementation was given to dogs with hypofolatemia (200 mcg for dogs $<$ 20 kg, and 400 mcg for dogs $\geq$ 20 kg, PO once daily for 4 weeks). Clopidogrel (2 mg/kg, PO once daily) was administered on case-by-case basis. Diet and therapeutic protocols were not changed for the following month. After one month of therapy (T1), all iPLE dogs were re-evaluated by the same clinician. The CCECAI scores were recorded, serum total protein, albumin, cholesterol, and C-reactive protein concentrations were measured. Additional diagnostic investigations were done on a case basis.

Fifty healthy owned-dogs, regularly vaccinated and receiving appropriate ecto-and endo-parasite preventive treatment, belonging to staff at the Veterinary Teaching Hospital of Turin University or that were presented at the same Veterinary Teaching Hospital and referral clinics of the study group for their annual check-up and vaccination, were enrolled as a control group. These dogs were considered healthy based on unremarkable history and physical examination, negative fecal flotation, and absence of any gastrointestinal sign within one year prior to enrollment. In addition, there was no history of antibiotic administration within 3 months prior to enrollment nor ongoing drug administration. Finally, most of the healthy control dogs were fed commercial nutritionally complete and balanced canine diets of different brands.

2.3 Sample collection and storage

Naturally passed feces of iPLE dogs were collected the day before the endoscopic procedure (T0) and after one month of therapy (T1). All owners were instructed to collect and immediately

freeze (−20°C) fecal samples. Feces of healthy control dogs were collected in the same study period of iPLE dogs and immediately frozen at −20°C. Fecal samples, of both iPLE and healthy control dogs, collected at home were frozen at −80°C the day after collection and refrigeration at −20°C. All fecal samples were shipped with priority on dry ice to the Gastrointestinal Laboratory, Department of Small Animal Clinical Sciences, Texas A&M University, USA, for the analyses. The samples' condition was recorded at the destination.

2.4 Fecal dysbiosis index

DNA extraction from 100 mg of each fecal sample was performed using the MoBio Power soil DNA isolation kit (PowerSoil, Mo Bio Laboratories, Carlsbad, CA, USA) according to the manufacturer's instruction (AlShawaqfeh et al., 2017). The qPCR panel consisted of eight bacterial groups: total bacteria, *Faecalibacterium* spp., *Turicibacter* spp., *Escherichia coli*, *Streptococcus* spp., *Blautia* spp., *Fusobacterium* spp., and *Clostridium (Peptacetobacter) hiranonis*. The qPCR assays were performed according to a previously published protocol (AlShawaqfeh et al., 2017). The data obtained were expressed as the log DNA abundance (fg) for each bacterial group/10 ng of total isolated DNA. The abundance of the evaluated bacterial groups was used to calculate the DI according to a mathematical algorithm previously validated (AlShawaqfeh et al., 2017). Dysbiosis was classified as significant (DI > 2), mild to moderate (DI 0–2), minor changes (DI < 2 with individual bacterial groups outside the reference interval), and normal (DI < 2 with no shifts in the overall diversity of the intestinal microbiota).

2.5 Fecal metabolome analysis

A gas chromatography-mass spectrometry (GC-MS) quantitative assay was performed to assess concentrations of the following targeted fecal metabolites: long-chain fatty acids (i.e., palmitic acid, linoleic acid, α-linolenic acid, oleic acid, cis-vaccenic acid, stearic acid, arachidonic acid, gondoic acid, erucic acid, docosanoic acid, and nervonic acid), zoosterols (i.e., cholesterol, coprostanol, cholestanol, and lathosterol), phytosterols (i.e., β-sitosterol, brassicasterol, campesterol, fusosterol, sitostanol, and stigmasterol), and unconjugated bile acids (i.e., cholic acid, chenodeoxycholic acid, lithocholic acid, deoxycholic acid, and ursodeoxycholic acid). A previously described protocol was used (Galler et al., 2022b; Honneffer, 2017; Batta et al., 2002). Briefly, a lyophilized fecal sample weighing 10–14 mg was aliquoted into a glass centrifuge tube. Deuterated internal standards including d7-sitostanol, d6-cholesterol, d4-stearic acid, d4-cholestane, d4-cholic acid, and d4-lithocholic acid were added to each sample. After the addition of concentrated HCl, the samples were incubated at 65°C for 4 h. The samples were then dried under nitrogen gas, followed by a silylation reaction by adding Sylon HTP (Sigma-Aldrich, St. Louis, MO, USA) and 30 minutes incubation at 65°C. After incubation, samples were dried with nitrogen gas again, then hexane was added. After the mixtures were centrifuged, the supernatants were injected individually into Agilent 8890 GC coupled with a 5977B GC/MSD (Agilent Technologies, Santa Clara, California, USA). The mass spectrometer was operated in selected ion monitoring mode for quantitative analysis, and Agilent ChemStation (Agilent Technologies, Santa Clara, California, USA) was used for peak integration and concentration calculations (Galler et al., 2022b; Honneffer, 2017; Batta et al., 2002).

These data were exported and the recorded weight of lyophilized feces for each sample was used to calculate concentrations in micrograms or nanograms per milligram of lyophilized feces. Data for the assessment of bile acids were reported as total amounts in nanograms per milligram of lyophilized fecal content and as percent of total bile acids measured. Total primary bile acids (TPBA) comprise the sum of cholic acid and chenodeoxycholic acid; total secondary bile acids (TSBA) comprise the sum of lithocholic acid, deoxycholic acid, and ursodeoxycholic acid. Total bile acids represent the sum of all measured bile acids. The percentage of TPBA% and TSBA%, which referred to the sum of CA and CDCA divided by the total measured BAs and the sum of LCA, DCA, and UDCA divided by the total measured BAs, were also calculated. Total measured phytosterols comprise the sum of β-sitosterol, brassicasterol, fusosterol, campesterol, sitostanol, and stigmasterol. Total measured zoosterols comprise the sum of cholesterol, coprostanol, cholestenol, and lathosterol. Total measured sterols comprise the sum of phyto- and zoosterols. Total measured fatty acid concentrations (FAs) comprise the sum of all measured long-chain fatty acids. Data for the assessment of sterols and FAs were reported as micrograms per milligram lyophilized feces.

The quality control and positive control used in this study were described earlier (Honneffer, 2017). In brief, quality control was implemented using a series of five samples: a preparation blank (PB), a zero blank (ZB), a sterol continuing calibration verification (S-CCV), a fatty acid continuing calibration verification (F-CCV), and a laboratory control sample (LCS). The PB contained only butanol and hydrochloric acid and ZB, similar to the PB but with the addition of internal standards were served to monitor contamination throughout preparation and analysis. The S-CCV and F-CCV were mixtures of stock solutions with known concentrations of sterols and fatty acids, respectively, to confirm accuracy. The LCS consisted of pooled and lyophilized fecal samples, ground and stored frozen to ensure consistency in analytical procedures.

2.6 Statistical analysis

All data were analyzed with the software GraphPad Prism 9 (Dotmatics). Data were tested for normal distribution using Shapiro-Wilk test. Comparisons of sex and breed between iPLE and healthy control dogs were evaluated using Fisher's exact tests. Comparisons of quantitative clinicopathological variables, qPCR bacterial abundance, and fecal metabolite concentration between iPLE and healthy control dogs were analyzed using the Student's *t*-test for normally distributed data and the Mann-Whitney *U*-test for non-normally distributed data. The same statistical tests were used whenever quantitative variables needed to be compared between two groups, depending on their distribution. Comparisons of quantitative clinicopathological variables, qPCR

bacterial abundance, and fecal metabolite concentrations in iPLE dogs between T0 and T1 were performed using a paired *t*-test or Wilcoxon matched-pairs signed rank test, depending on their distribution. Furthermore, fold changes between T0 and T1 for each fecal metabolite studied, DI and each single bacterial taxa, have been calculated. Fold change was determined as the ratio of T1 to T0 fecal content, with a fold change greater than 1 indicating an increase in metabolite abundance and a fold change less than 1 indicating a decrease in metabolite abundance. Fold changes greater than 2 or less than 0.5 were considered biologically relevant. The One-Way ANOVA or Kruskal-Wallis test was used, based on variable distribution, for comparisons of quantitative variables in cases of groups ≥ 3. All fecal metabolites studied were compared between the various diet groups consumed prior to inclusion at T0 and they were also compared between the diet groups prescribed between T0 and T1. Spearman or Pearson rank tests were used to test correlations between the abundance of bacterial taxa and fecal concentrations of all the fecal metabolites studied. Spearman's test was applied when the variables were not normally distributed (r_p = Pearson's correlation coefficient), while Pearson's test was used for variables that followed a normal distribution (r_s = Spearman's correlation coefficient). Correlations between clinicopathological variables and bacterial abundance or targeted metabolites were also tested with the same approach.

Significance was set at $p < 0.05$. The *p*-values were adjusted with Bonferroni correction to account for multiple comparisons.

Principal coordinate analysis and hierarchical clustering heatmaps were generated using Metaboanalyst 5.0 based on the log-transformed with Pareto scaling data. To generate the PCA plot, the MetaboAnalyst software used the PERMANOVA test (Permutational Multivariate Analysis of Variance).

3 Results

3.1 Animals

Five out of fifty healthy control dogs had an increased DI (> 2), and at re-check with the owner it was discovered that 3 of them showed sporadic gastrointestinal symptoms, and all 3 dogs were therefore excluded from analysis.

The final study population consisted of 47 healthy control dogs and 38 dogs with iPLE. Eight dogs of the iPLE group were mixed breed (21.1%) and 30 dogs were purebred (78.9%), represented as follows: German Shepherd (6 dogs), Border Collie (3 dogs), Rottweiler, Belgian Shepherd, Chihuahua, Golden Retriever (2 dogs each breed), Cavalier King Charles, Dachshund, American Staffordshire Terrier, Australian Shepherd, English Setter, Maltese, Pitbull, French Bulldog, Podenco, Labrador Retriever, Yorkshire Terrier, Spanish Greyhound, Cesky Terrier (1 dog each breed). The control group included 19 mixed breed dogs (40%) and 28 pure breed dogs (represented by seventeen different breeds). Age, sex, and body weight did not significantly differ between healthy control and iPLE dogs.

At T0, the iPLE dogs showed the following median (range) values: CCECAI score 8 (3–17), total protein 4.1 g/dL (2–7.4), albumin 1.8 g/dL (0.9–2.7), cholesterol 116 mg/dL (63–327), and C-reactive protein 64.6 mg/L (0–48.4). Cobalamin and folate were measured in 24 out of 38 dogs with iPLE. Twelve iPLE dogs (50%) out of 24 had serum cobalamin concentrations lower than the reference interval, 6 (25%) had suboptimal serum cobalamin levels (normal but < 400 ng/L), and the remaining 6 dogs (25%) had values within the mid to high reference range (> 400 ng/L). Eleven iPLE dogs (45.8%) out of 24 had serum folate concentrations lower than the reference interval. Canine pancreatic lipase was measured in 21 iPLE dogs (55.2%) and it was increased in 4 of them (19%). All dogs with iPLE included in the study had gastrointestinal duodenoscopy performed. Twenty-six iPLE dogs (68.4%) had concurrent lower GI endoscopy in which the ileum was successfully intubated in 9 cases (23.7%). On histopathology, a predominantly lymphoplasmacytic infiltration of the intestinal mucosa was found in all iPLE dogs. With regard to the severity of lymphoplasmacytic infiltrate, mild (grade 1) duodenal, ileal and colonic histologic lesions were found in 0, 0, and 2 dogs, respectively; moderate (grade 2) duodenal, ileal and colonic histologic lesions were found in 18, 7, and 24 dogs, respectively; marked (grade 3) duodenal, ileal, and colonic histologic lesions were found in 20, 2, and 7 dogs, respectively. Dilated crypts with proteinaceous material and cellular debris (crypt abscesses) were identified in 9 iPLE dogs (23.7%). Lymphangiectasia was identified in 30 iPLE dogs (78.9%) and it was further classified as mild (n = 13, 43.3%), moderate (n = 15, 50%), and severe (n = 2, 6.7%). On endoscopy, pinpoint to coalescing white spots were found in 17 (56.6%) out of 30 iPLE dogs in which lymphangiectasia was detected histologically.

Prior to the admission 12 dogs with iPLE (31.6%) received highly digestible gastrointestinal diets, 2 dogs (5.2%) low fat diets, 12 dogs (31.6%) commercial limited ingredient diets, 4 dogs (10.6%) home-cooked selected protein diets, and 6 dogs (15.8%) hydrolyzed diets. Two dogs (5.2%) were fed different diet types. After T0, ultra-low fat and hydrolyzed diets were prescribed to 23 (60.5%) and 15 (39.5%) dogs, respectively. All iPLE dogs received oral prednisolone at the dose of 0.5 mg/kg twice daily. In addition, oral chlorambucil (2–4 mg/m2) was prescribed to 2 dogs (5.2%). Eighteen iPLE dogs received weekly parenteral cobalamin supplementation, 11 dogs received daily oral folate supplementation. Sixteen dogs received oral clopidogrel. Two dogs (5.2%) died for causes related to the iPLE between T0 and T1. Table 1 shows the selected clinicopathological variables of both populations at T0.

At T1, the iPLE dogs showed the following median (range) values: CCECAI score 4 (0–13), total protein 5.1 g/dL (2.8–7.5), albumin 2.2 g/dL (1.3–3.1), cholesterol 138 mg/dL (66–237), and C-reactive protein 2.1 mg/L (0–31.4). Median CCECAI score was significantly decreased compared to that recorded at T0 (p = 0.001), while total protein and albumin were significantly increased ($p < 0.0001$). Cholesterol and C-reactive protein did not significantly change at T1.

Information regarding individual iPLE dogs is provided in Supplementary Table 1.

3.2 Dysbiosis Index (DI) and fecal metabolomics

The median DI was significantly higher in dogs with iPLE compared to healthy control dogs ($p < 0.0001$). The abundances

TABLE 1 Selected clinicopathological characteristics of healthy control dogs and dogs with iPLE at the time of the endoscopic procedure (T0).

Parameter	*N*	Median value	Min-max
iPLE dogs			
Age (months)	38	95.5	(19–171)
Body weight (Kg)	38	18	(3.5–42)
Sex (F/M) spayed/neutered	38 (19/19) 13/1	– –	–
CCECAI	38	8	(3–17)
Clinical disease severity groups (Allenspach et al., 2007)			
• Mild	5		
• Moderate	16		
• Severe	8		
• Very Severe	9		
TP (g/dL)	38	4.1	(2–7.4)
Albumin (g/dL)	38	1.8	(0.9–2.7)
Cholesterol (mg/dL)	36	116	(63–327)
CRP (mg/l)	34	4.6	(0–48.4)
Folate (ng/mL)	24	8.1	(2–24)
Cobalamin (pg/dL)	24	253	(62–1000)
Healthy dogs			
Age (months)	47	72	(18–204)
Weight (Kg)	47	18	(3.5–42)
Sex (F/M) spayed/neutered	47 (25/22) 22/13	– –	

N, Number of observations; CCECAI, canine chronic enteropathy clinical activity index; CRP, C-reactive protein; F, female; iPLE, inflammatory protein-losing-enteropathy; M, male; TP, total protein. Value, Data expressed as median (min-max).

of *E. coli* ($p = 0.001$) and *Blautia* ($p = 0.004$) were significantly higher in dogs with iPLE compared to healthy control dogs. The abundances of *C. hiranonis* ($p = 0.041$) and *Turicibacter* ($p < 0.0001$) were significantly lower in dogs with iPLE compared to healthy control dogs. All results are summarized in Figure 1 and Table 2.

Of the iPLE dogs, 11 (29%) had DI values > 2, indicating a severe shift in the microbiome. In 9 iPLE dogs (23.7%) the DI was mildly to moderately increased (0–2). Five iPLE dogs (13.1%) had normal DI values (< 2), but the abundance of individual bacteria was outside the respective reference ranges, indicating minor shift in the microbiome. DI values were normal without individual bacterial abundance changes in 13 iPLE dogs (34.2%). Of the healthy control dogs, 29 (62%) had normal DI values, while 18 (38%) had abnormal DI values with 7 dogs (15%) having a DI > 0 with 2 of these (4%) with a DI > 2 and one of them showed low *C. hiranonis* abundance; 11 healthy control dogs (23%) exhibited minor changes in the microbiome. No significant correlations were found between the DI and the following variables at T0: age, gender, body weight, CCECAI, serum concentrations of total protein, albumin, cholesterol, C-reactive protein, cobalamin, and folate.

Sixteen fecal samples were available for DI analysis at T1. The median DI value at T1 did not significantly differ from that at T0. The abundance of *Turicibacter* was significantly increased compared to that of T0 ($p = 0.026$). These results are shown in Figure 2. The classification of iPLE and healthy control dogs based on DI values at T0 and T1 is reported in Table 3. Nine out of 16 iPLE dogs exhibited a fold change indicating more than twofold decrease in the DI, with a fold change value less than 0.5. Only 1 iPLE dog showed a threefold increase in DI at T1 compared to T0.

3.2.1 Fecal unconjugated bile acids concentrations

At T0, fecal concentrations of TPBA and their percentage (TPBA%) did not differ between healthy control and iPLE dogs. Similarly, TSBA and their percentage (TSBA%) did not significantly differ between healthy control and iPLE dogs. However, a subset of iPLE dogs ($n = 12$; 31.5%) showed increased fecal TPBA and decreased fecal TSBA, and 8 of them showed concurrent *C. hiranonis* reduction. Significant moderate negative correlations between the abundance of *C. hiranonis* and both TPBA and TPBA% ($r_s = -0.48$, $p < 0.0001$; $r_s = -0.44$, $p < 0.0001$) were found. Significant weak to moderate positive correlations between the abundance of *C. hiranonis* and both TSBA and TSBA% ($r_s = 0.22$, $p = 0.043$; $r_s = 0.44$, $p < 0.0001$) were found. Significant moderate negative correlations between DI and both TSBA and TSBA% ($r_s = -0.54$, $p = 0.001$; $r_s = -0.50$, $p = 0.001$) were found. Specifically, a moderate negative correlation was found between DI and lithocholic acid and deoxycholic acid ($r_s = -0.55$, $p = 0.001$; $r_s = -0.53$, $p = 0.001$). No significant correlation was found between each single unconjugated bile acid and the CCECAI score, serum albumin and serum cholesterol. The concentrations of both primary and secondary bile acids did not significantly differ among groups of dogs classified based on different types of diet fed prior to the admission.

No significant differences in fecal bile acids content were found at T1, compared to T0 in iPLE dogs. No significant differences were found in fecal primary and secondary bile acids content comparing dogs that were prescribed ultra-low fat diets and those that were prescribed hydrolyzed diets after T0.

Summary statistics of fecal bile acid concentrations at T0 and T1 are shown in Figure 3 and Table 4.

3.2.2 Fecal long-chain fatty acids concentrations

At T0, FAs and the concentration of each long-chain fatty acids measured, except α-linolenic acid, were significantly higher in dogs with iPLE compared to healthy control group (all $p < 0.0001$). The median α-linolenic acid concentration was lower in iPLE dogs compared to healthy control dogs, but this difference was not statistically significant. Summary statistics of FAs at T0 are shown in Figure 4 and Table 4.

FAs did not significantly differ between dogs with and without lymphangiectasia, nor between dogs with mild and moderate to severe lymphangiectasia. A significant weak to moderate negative correlation between total FAs and both serum total protein and albumin concentrations ($r_p = -0.34$, $p = 0.036$; $r_p = -0.57$, $p = 0.001$) was found; a significant moderate positive correlation with fecal cholesterol concentration ($r_s = 0.55$, $p = 0.001$) was found. Significant weak to moderate negative correlations between

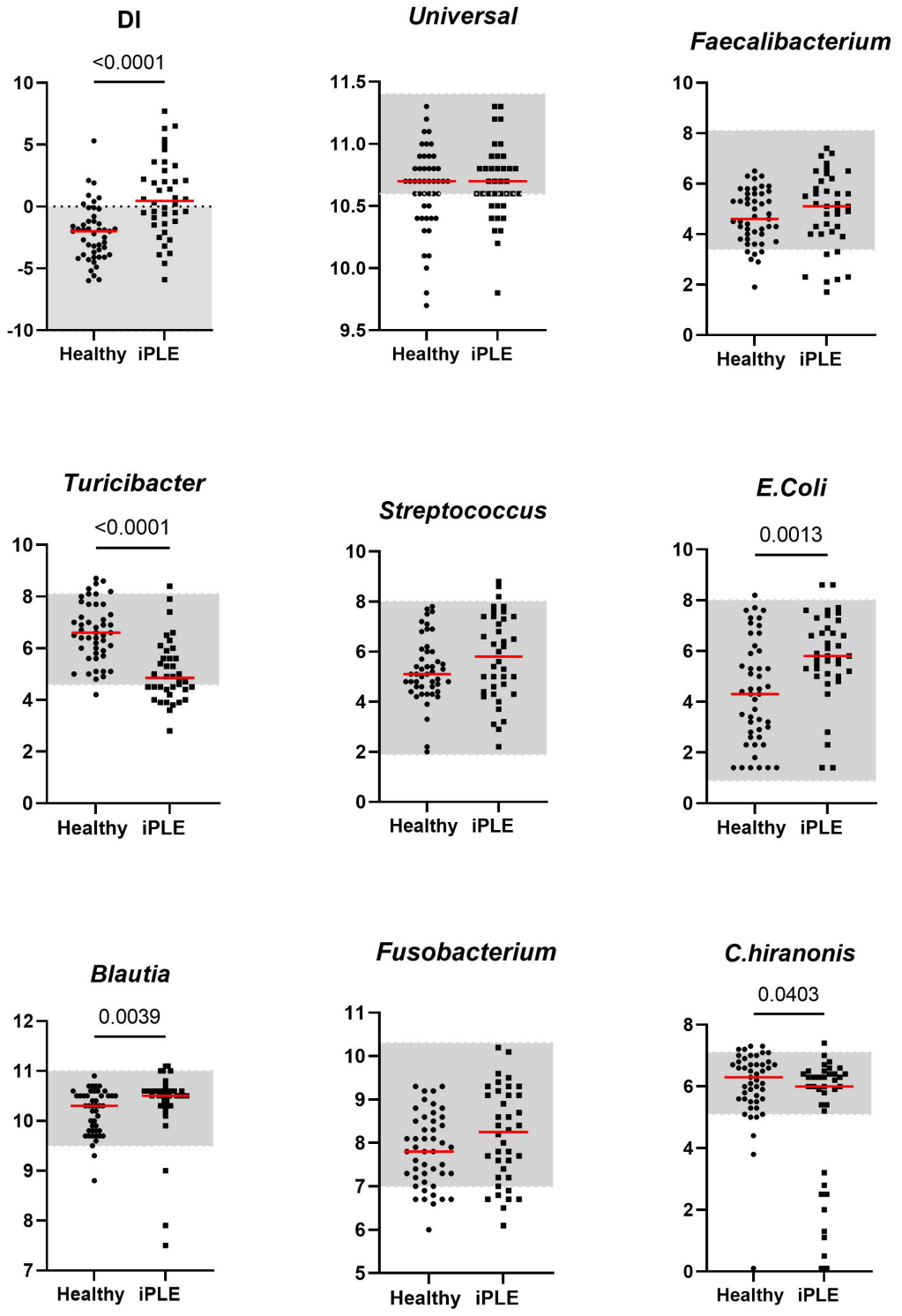

FIGURE 1
Comparison of Dysbiosis index (DI) and each taxa abundance between healthy control dogs and iPLE dogs at T0. Bacterial abundance is expressed as log DNA. The gray area represents the reference interval. Horizontal red lines represent medians. Only the significant *p*-values are shown in the graph.

nervonic, cis-vaccenic, stearic, oleic, gondoic, myristic, palmitic acid and serum albumin (r_p = −0.37, p = 0.022; r_p = −0.57, p = 0.001; r_p = −0.46, p = 0.003; r_p = −0.53, p = 0.001; r_p = −0.48, p = 0.002; r_p = −0.58, p = 0.001; r_p = −0.36, p = 0.024) were found.

Significant weak to moderate positive correlations between the CCECAI score and FAs (r_s = 0.32, p = 0.049), and concentrations of myristic acid (r_s = 0.34, p = 0.034), oleic acid (r_s = 0.43, p = 0.006), cis-vaccenic acid (r_s = 0.35, p = 0.031) and gondoic acid (r_s = 0.42, p = 0.008) were found. No significant correlation was found

10.3389/fmicb.2024.1433175

TABLE 2 Summary statistic of the abundance of bacterial groups assessed for the calculation of the DI in healthy dogs and iPLE dogs.

	Healthy dogs median (range)	iPLE dogs median (range)	*p*-value	adjusted *p*-value
	n = 47	*n* = 38		
DI	−2.0 (−6.0–5.3)	0.4 (−5.9–7.7)	< 0.0001*	0.001*
Universal	10.7 (9.7–11.3)	10.6 (9.8–11.3)	0.468	4.21
Faecalibacterium spp.	4.6 (1.9–6.5)	5.1 (1.7–7.4)	0.388	3.49
Turicibacter spp.	6.6 (4.2–8.7)	4.8 (2.8–8.4)	< 0.0001*	0.001*
Streptococcus spp.	5.1 (2.0–7.8)	5.8 (2.2–8.8)	0.177	1.59
E. coli	4.3 (1.4–8.2)	5.8 (1.4–8.6)	0.001*	0.005*
Blautia spp.	10.3 (8.8–10.9)	10.5 (7.5–11.1)	0.004*	0.04*
Fusobacterium spp.	7.8 (6–9.3)	8.2 (6.1–10.2)	0.102	0.91
C. hiranonis	6.3 (0.1–7.3)	6.0 (0.1–7.4)	0.040*	0.36

Data are expressed as median (minimum−maximum) logDNA/gram of feces. *P*-value and adjusted *p*-value are set at 0.05 (95% confidence interval); *statistically significant. DI, dysbiosis index; iPLE, inflammatory protein-losing enteropathy; *N*, numbers of observations.

between FAs and DI values, nor between DI and each long-chain fatty acid measured. Few correlations were found between long-chain fatty acids measured and single bacterial taxa. Specifically, a mild and positive correlation was found between nervonic, myristic, gondoic acid and *E. coli* (r_s = 0.35, p = 0.027; r_s = 0.38, p = 0.017; r_s = 0.34, p = 0.033), and a weak negative correlation was found between arachidonate and *Streptococcus* (r_s = −0.36, p = 0.026). FAs (p = 0.011), stearic acid (p = 0.022), palmitic acid (p = 0.040), linoleic acid (p = 0.010) and arachidonic acid (p = 0.039) were significantly higher in dogs that were fed hydrolyzed diets prior to the admission compared to dogs that received other diets (Figure 5).

At T1, the concentrations of oleic acid (p = 0.044), stearic acid (p = 0.013), erucic acid (p = 0.018) and nervonic acid (p = 0.002) significantly decreased (Figure 6 and Table 4). At fold change analysis some metabolites exhibited fold changes that were biologically meaningful. However, the analysis did not clearly identify a distinct subset of iPLE dogs that responds in a consistent manner to the treatment based on fecal metabolite changes. The results of the fold change analysis are presented in Supplementary Table 2. No significant differences in fatty acids (FAs) or individual long-chain fatty acids between dogs prescribed an ultra-low fat diet and those prescribed a hydrolyzed diet were found.

3.2.3 Fecal sterols concentrations

At T0, the concentration of total sterols was significantly higher in dogs with iPLE compared to that of healthy control dogs (p < 0.0001). The concentration of total zoosterols were significantly higher in dogs with iPLE compared to those of healthy control dogs (p < 0.0001), while total phytosterols were lower in iPLE than in healthy dogs (p = 0.001). Among the zoosterols, the concentration of cholesterol (p < 0.0001), and lathosterol (p < 0.0001) were significantly higher in dogs with iPLE, compared to healthy control dogs. In contrast, the concentration of coprostanol (p = 0.024) was significantly lower in iPLE dogs. The fecal concentration of cholestanol didn't differ between iPLE dogs and healthy control dogs. The concentration of each measured phytosterol was significantly lower in dogs with iPLE compared to healthy control dogs, except for brassicasterol, which did not differ significantly. Summary statistics of sterols at T0 are shown in Figure 7 and Table 4.

No significant differences for the concentrations of both total phytosterols and zoosterols were found between dogs with and without lymphangiectasia, nor between dogs with mild and moderate to severe lymphangiectasia. No significant correlations were found between CCECAI sore and fecal concentrations of all measured sterols. No significant correlation was identified between DI values and the fecal concentrations of all measured sterols, except for a moderate negative correlation between coprostanol and DI (r_s = −0.40, p = 0.012). However, when correlating fecal concentrations of coprostanol with individual bacterial taxa, no significant correlations were found. A weak and positive correlation was found between total phytosterols and *Streptococcus* (r_p = 0.32, p = 0.049). No significant correlations between each sterol measured and serum total protein, albumin, and cholesterol were found. The concentrations of phytosterols and zoosterols did not significantly differ among groups of dogs classified based on different types of diet fed prior to the admission.

At T1, neither total sterols, nor total phytosterols and total zoosterols differed significantly compared to T0. Individual sterols measured also did not differ between T0 and T1. At fold change analysis, some sterols exhibited fold changes that were biologically meaningful. However, the analysis did not clearly identify a distinct subset of iPLE dogs that responds in a consistent manner to the treatment. No significant difference was found in fecal phytosterols and zoosterols content comparing dogs that were prescribed ultra-low fat diets after T0 and dogs that were prescribed hydrolyzed diet.

3.2.4 Fecal metabolites content

Figures 8, 9 show the comprehensive analysis of the differences in the targeted fecal metabolites content among healthy control dogs and dogs with iPLE.

4 Discussion

This prospective study aimed to evaluate intestinal dysbiosis and changes in fecal targeted metabolites in dogs with iPLE

10.3389/fmicb.2024.1433175

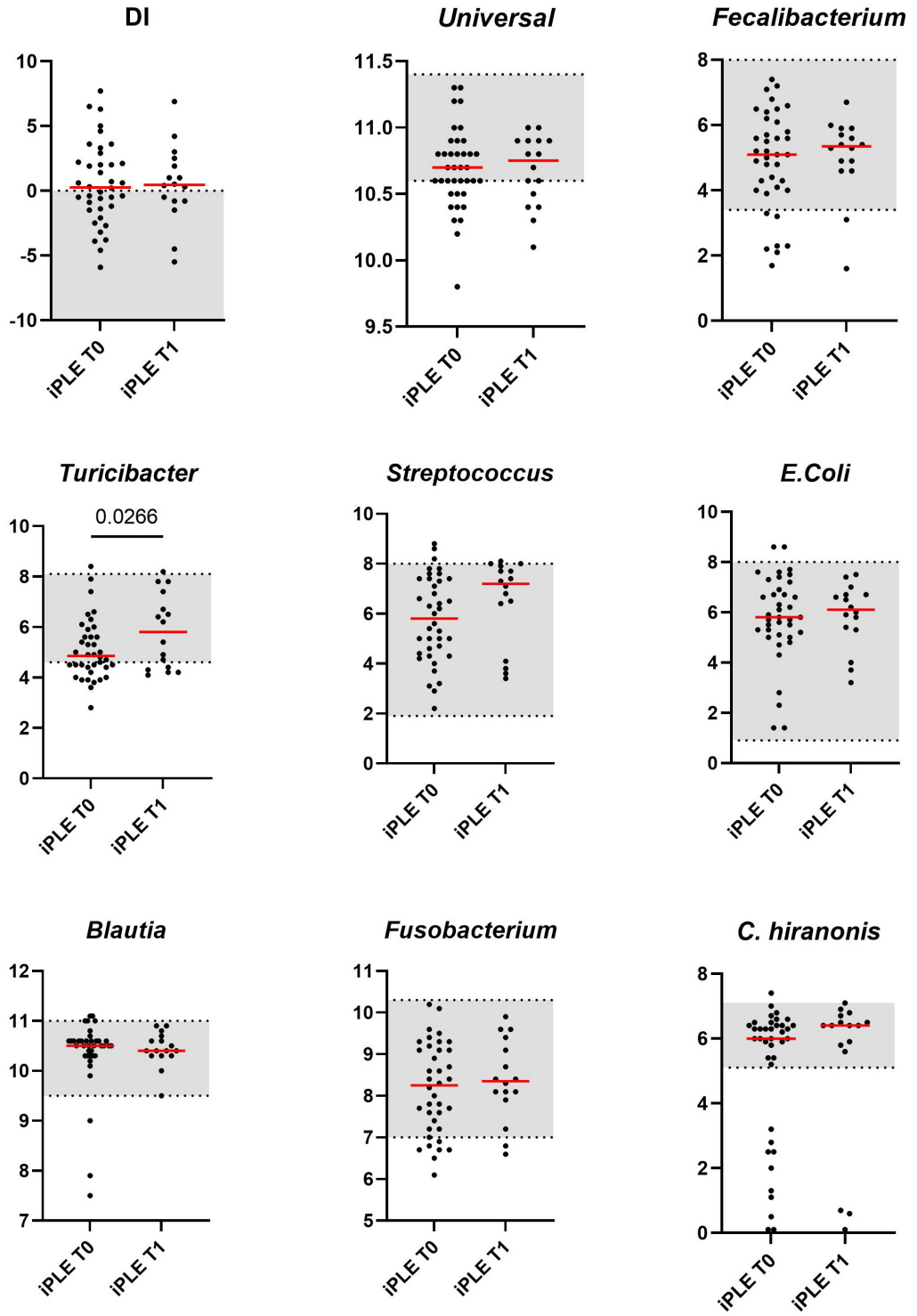

FIGURE 2
Comparison of Dysbiosis index (DI) and each taxa abundance of iPLE dogs between T0 and T1. Bacterial abundance is expressed as log DNA. The gray area represents the reference interval. Horizontal red lines represent medians. Only the significant *p*-values are shown in the graph.

compared to healthy control dogs, and to investigate the impact of treatment on both the microbiome and the fecal metabolome in dogs with iPLE.

Several studies report a reduction of intestinal bacterial richness and diversity in a subset of dogs with gastrointestinal diseases, describing intestinal dysbiosis as a frequent finding in dogs with chronic enteropathy (Pilla and Suchodolski, 2020; AlShawaqfeh et al., 2017; Honneffer, 2017; Honneffer, 2014). Presence and severity of intestinal dysbiosis are not enough to differentiate the heterogeneous group of canine chronic enteropathies; however, the evaluation of both fecal microbiome and metabolome could reveal

TABLE 3 Classification of intestinal dysbiosis severity in healthy dogs and iPLE dogs based on DI values at diagnosis (T0) and after 1 month of therapy (T1).

	Healthy dogs (*N* = 47)	iPLE dogs at T0 (*N* = 38)	iPLE dogs at T1 (*N* = 16)
Significant dysbiosis	2	11	4
Mild to moderate changes	5	9	6
Minor changes	11	5	1
Normal	29	13	5

Significant Dysbiosis (DI > 2); mild to moderate changes (DI 0−2); minor changes (DI < 2, with individual bacterial groups outside the reference interval); normal (DI < 2, with no shifts in the overall diversity of the intestinal microbiota). iPLE, protein losing enteropathy; *n*, number of observations; T0 = diagnosis; T1, after 1 month of therapy.

pathophysiologic mechanisms and potentially lead to new treatment strategies.

In this study, a qPCR-based index (DI) was employed to evaluate intestinal dysbiosis in dogs with iPLE. This quantitative assay is characterized by several advantages compared to sequencing techniques, including higher reproducibility, shorter analysis times, lower cost, and accessibility (AlShawaqfeh et al., 2017; Sung et al., 2023a; Sung et al., 2023b).

As expected, the median DI value was higher in dogs with iPLE compared to healthy dogs. However, 34.2% of dogs with iPLE had a normal DI value. This result might suggest that dysbiosis is a component of a more intricate pathogenetic process, but it is not a consistent finding in dogs with chronic intestinal inflammation, as also found elsewhere (AlShawaqfeh et al., 2017; Galler et al., 2022b). On the contrary, 29% of dogs with iPLE showed DI values > 2, that are indicative of severe dysbiosis and major shifts in the intestinal microbiome. This degree of dysbiosis is frequently observed both in case of severe gastrointestinal dysfunction and mucosal damage, and following antibiotic administration (Pilla and Suchodolski, 2020; Suchodolski et al., 2009; Pilla et al., 2020). Moreover, the effects of antibiotics on the microbiome last for several weeks and slowly decrease in the absence of chronic and persistent gastrointestinal disease in a subset of dogs (Stavroulaki et al., 2023). In this study, severe dysbiosis is presumed to be a consequence of the gastrointestinal mucosal damage and dysfunction, since iPLE dogs that received antibiotics in the 3 months prior to the admission were not enrolled. As expected, *C. hiranonis* abundance was significantly decreased in dogs with iPLE (AlShawaqfeh et al., 2017; Blake et al., 2019; Galler et al., 2022b) compared to the control group, and 26% of dogs with iPLE showed *C. hiranonis* abundance below the lower reference interval. *C. hiranonis* plays a key role in the conversion of primary to secondary bile acids and its decrease in fecal abundance leads to abnormal conversion of primary to secondary bile acid (AlShawaqfeh et al., 2017; Blake et al., 2019; Galler et al., 2022b; Manchester et al., 2019). In previous studies, it was shown that dysbiosis in dogs with chronic enteropathies, including some dogs with PLE, is often associated with shifts in the microbiome and reductions in some taxa such as *Faecalibacterium, Turicibacter*, and *C. hiranonis* (AlShawaqfeh et al., 2017; Sung et al., 2023a; Galler et al., 2022b). However, these changes are not consistent across all iPLE dogs, as there is a subset of iPLE dogs with clear shifts in the microbiome, and a subset of iPLE dogs that overlaps with healthy dogs both on 16S rRNA gene sequencing, DNA shotgun sequencing, and qPCR based assays (Sung et al., 2023a). This suggests some differences in the pathophysiology between these subsets that need to be further explored. Although the microbiome studies in dogs with PLE are still rare, it is evident that the similar subsets exist in dogs with PLE. In this study the DI was normal in a subset of dogs with iPLE, and in current (yet unpublished) dataset based on DNA shotgun sequencing the same results was evident that a subset of iPLE dogs clustered with the healthy controls. Therefore, future studies need to further explore the differences in underlying pathology between these subsets.

It is also interesting to note that some healthy control dogs, asymptomatic and not having a recent antibiotic history, were found to be dysbiotic (from mild to severe microbial shifts). These results suggest that microbial alterations are also present in dogs without gastrointestinal signs. However, only 2 healthy control dogs (4%) had a DI > 2. Nevertheless, subclinical intestinal inflammation of healthy control dogs was not ruled out with histopathologic examination of intestinal biopsies. In contrast to some previous studies (AlShawaqfeh et al., 2017; Galler et al., 2022a), a positive correlation between the CCECAI score and the DI value was not found here. This lack of correlation may be explained by the high CCECAI scores in all dogs with iPLE, with little inter-individual CCECAI variability.

Lastly, the results regarding serum cobalamin levels were available for 24 dogs with iPLE. The 50% of these dogs showed hypocobalaminemia and 25% showed suboptimal levels of cobalamin. All iPLE dogs with hypocobalaminemia and suboptimal levels of cobalamin were supplemented with parenteral or enteral cyanocobalamin. No significant correlation was found between the DI value and serum cobalamin concentrations. A recent study comparing the intestinal microbiome of dogs with and without hypocobalaminemia speculated that decreased serum cobalamin concentrations likely reflect the severity related to the underlying pathophysiology (Toresson et al., 2023). In light of this finding and considering that in this study only 29% of dogs with iPLE exhibited severe dysbiosis, the lack of correlation between hypocobalaminemia and dysbiosis might suggest that both low serum cobalamin concentrations and dysbiosis reflect the severity of mucosal damage and the disease, but they are not dependent variables.

Dogs with iPLE did not have any significant differences in fecal bile acid content compared to healthy control dogs. However, a subset of 31.5% of iPLE dogs had a concurrent increase in TPBA and a decrease in fecal TSBA content, suggesting reduced bile acid conversion in this subset of dogs with iPLE. These findings likely arose from bile acid malabsorption and intestinal dysbiosis. Bile acids are the main catabolic product of cholesterol metabolism with the important role of facilitating lipid digestion and absorption (Russell and Setchell, 1992). About 5–10% of primary bile acids are not reabsorbed in the ileum via the apical sodium-dependent bile acid transporter (Giaretta, 2018; Giaretta et al., 2018) and undergo conversion into secondary bile acids by the large intestinal microbiota. In dogs, *C. hiranonis* represents the main bile acid converter bacteria, having significant 7α-dehydroxylating activity (Blake et al., 2019; Manchester et al., 2019). Moreover, increased fecal primary bile acids could also be the consequence of decreased

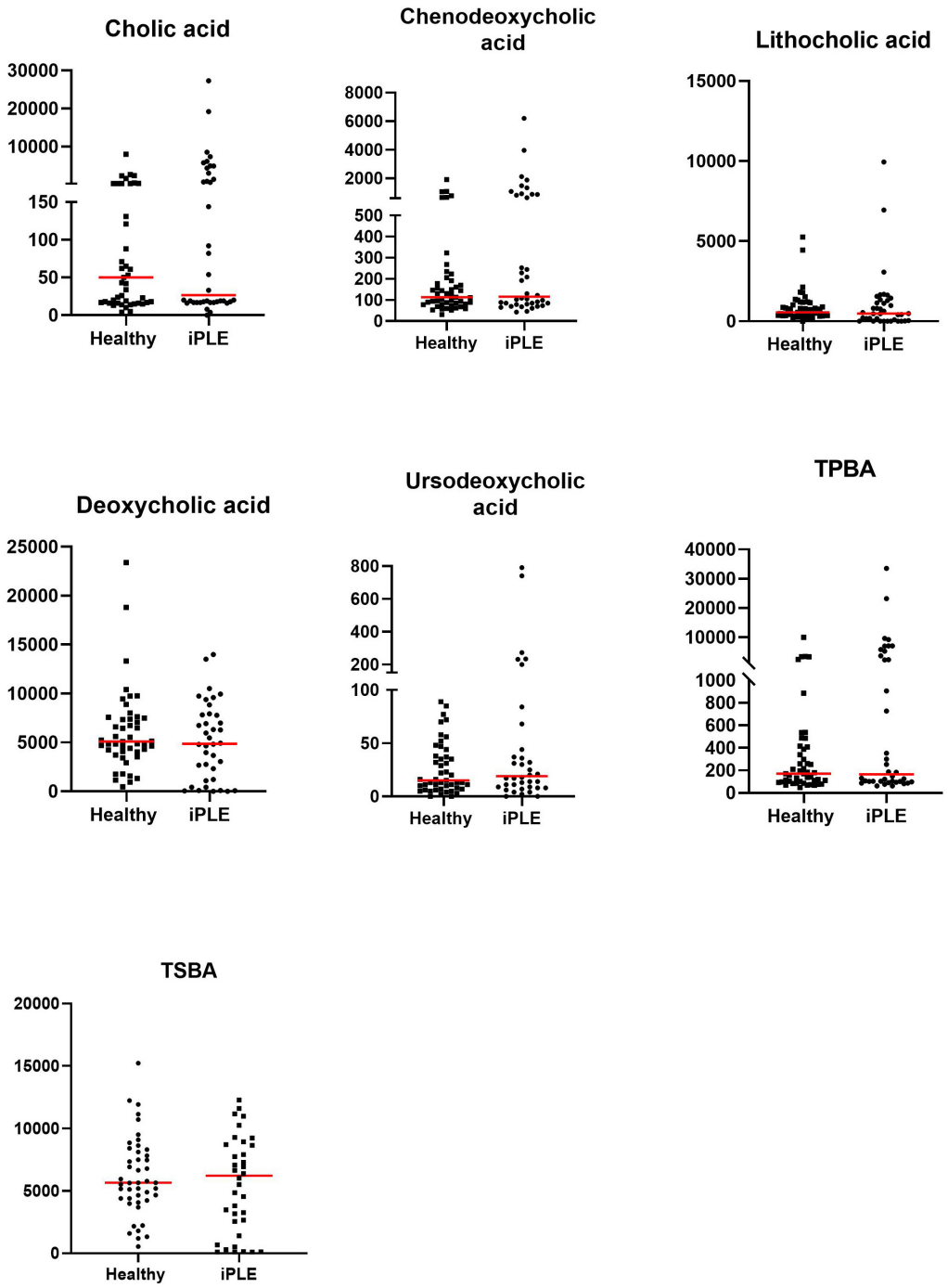

FIGURE 3
Fecal concentrations of unconjugated bile acids (ng/mg) in healthy control dogs and iPLE dogs. Red lines represent median value. Only the significant *p*-values are shown in the graph.

sodium-dependent bile acids transporter expression in the ileum and/or increased intestinal transit time (Giaretta et al., 2018). In contrast to the beneficial effects of secondary fecal bile acids, primary bile acids are implicated in the dysregulation of the local immune and inflammatory response (Fiorucci et al., 2021; Gérard, 2013; Vítek, 2015). In this study *C. hiranonis* correlated negatively with primary bile acids and positively with secondary bile acids and its abundance was decreased in 8 out of 12 dogs that showed an increase in TPBA and a decrease in TSBA. These results support the role of *C. hiranonis* in the bile acid conversion and highlight the impact of intestinal dysbiosis in bile acid metabolism. A recent case report describe the successful use of bile acid sequestrants in dogs with chronic enteropathy that are non-responders to conventional therapeutic protocols (Toresson et al., 2021), suggesting bile acid malabsorption diarrhea as described in humans (Walters and Pattni, 2010; Camilleri, 2015). Therefore, the short-term use of bile acid sequestrants in some dogs with iPLE and bile acid dysmetabolism

10.3389/fmicb.2024.1433175

TABLE 4 Summary statistics of fecal unconjugated bile acids, sterols and fatty acids concentrations in healthy control dogs and dogs with iPLE at diagnosis (T0) and after 1 month of therapy (T1).

Fecal unconjugated bile acids, sterols and fatty acids of healthy dogs and iPLE dogs at T0 (n = 38)				
	Healthy dogs median (range)	iPLE dogs median (range)	p-value	adjusted p-value
Unconjugated bile acids				
Cholic acid (ng/mg)	50 (4–7985)	26.5 (0–27271)	0.416	1.000
Chenodeoxycholic acid (ng/mg)	113 (31–1910)	116 (43–6213)	0.230	1.000
Lithocolic acid (ng/mg)	558 (9–5252)	475 (5–9946)	0.274	1.000
Deoxycholic acid (ng/mg)	5104 (477–23381)	4871 (8–13988)	0.376	1.000
Ursodeoxycholic acid (ng/mg)	15 (0–89)	19 (0–791)	0.320	1.000
TPBA (ng/mg)	171 (48–9895)	166 (62–33485)	0.347	1.000
TSBA (ng/mg)	5649 (533–27901)	6201 (90–23979)	0.450	1.000
TPBA (%)	3 (1–95)	4.5 (1–98)	0.219	1.000
TSBA (%)	97 (5–99)	95.5 (2–99)	0.219	1.000
Sterols				
Coprostanol (μg/mg)	0.05 (0.01–0.34)	0.02 (0.01–20.10)	0.024*	0.840
Cholesterol (μg/mg)	2.28 (0.95–26.10)	7.34 (1.03–20.40)	<0.0001*	0.003*
Cholestanol (μg/mg)	0.30 (0.05–1.06)	0.18 (0.02–1.55)	0.060	1.000
Lathosterol (μg/mg)	0.01 (0.01–0.11)	0.06 (0.01–0.16)	<0.0001*	0.003*
Brassicasterol (μg/mg)	0.02 (0.01–0.07)	0.02 (0.01–0.23)	0.058	1.000
Campesterol (μg/mg)	0.31 (0.11–1.37)	0.25 (0.03–1.45)	0.032*	1.000
Stigmasterol (μg/mg)	0.17 (0.05–0.63)	0.14 (0.02–0.67)	0.021*	0.735
Fusosterol (μg/mg)	0.07 (0.02–0.28)	0.05 (0.01–0.30)	0.014*	0.490
Beta–sitosterol (μg/mg)	1.16 (0.33–4.08)	0.59 (0.02–4.30)	0.001*	0.035*
Sitostanol (μg/mg)	0.27 (0.03–1.49)	0.08 (0.01–1.26)	0.002*	0.070
Total measured sterols (μg/mg)	5.16 (2.49–27.80)	11.30 (3.04–26.40)	<0.0001*	0.003*
Total measured zoosterols (μg/mg)	2.71 (1.10–26.70)	9.35 (1.14–26.20)	<0.0001*	0.003*
Total measured phytosterols (μg/mg)	2.25 (0.64–7.78)	1.21 (0.13–7.82)	0.001*	0.035*
Fatty acids				
Myristic acid (μg/mg)	0.62 (0.26–2.60)	1.98 (0.41–8.12)	<0.0001*	0.003*
Palmitic acid (μg/mg)	4.81 (1.61–15.30)	16.90 (2.09–22.20)	<0.0001*	0.003*
Linoleic acid (μg/mg)	4.09 (1.42–20.10)	7.49 (2.25–28.90)	<0.0001*	0.003*
α-linolenic acid (μg/mg)	0.35 (0.08–5.23)	0.20 (0.05–2.65)	0.072	1.000
Oleic acid (μg/mg)	3.84 (1.35–20.20)	10.40 (3.41–22.20)	<0.0001*	0.003*
Cis-vaccenic acid (μg/mg)	0.93 (0.06–4.87)	7.07 (0.29–26.00)	<0.0001*	0.003*
Stearic acid (μg/mg)	2.19 (0.52–19.90)	8.35 (0.76–41.40)	<0.0001*	0.003*
Arachidonic acid (μg/mg)	1.65 (0.48–4.26)	3.75 (0.62–10.30)	<0.0001*	0.003*
Gondoic acid (μg/mg)	0.21 (0.09–0.76)	0.84 (0.19–5.52)	<0.0001*	0.003*
Docosonoic acid (μg/mg)	0.27 (0.12–1.26)	0.84 (0.21–5.08)	<0.0001*	0.003*
Erucic acid (μg/mg)	0.12 (0.04–0.66)	0.40 (0.10–8.64)	<0.0001*	0.003*
Nervonic acid (μg/mg)	0.32 (0.10–1.40)	1.21 (0.18–4.85)	<0.0001*	0.003*
Total measured fatty acids (μg/mg)	19.70 (6.99–64.8)	61.80 (12.90–136.00)	<0.0001*	0.003*

(Continued)

10.3389/fmicb.2024.1433175

TABLE 4 (Continued)

Fecal unconjugated bile acids, sterols and fatty acids of iPLE dogs at T0 and T1 (n = 16)				
	iPLE dogs T0 median (range)	iPLE dogs T1 median (range)	p-value	adjusted p-value
Unconjugated bile acids				
Cholic acid (ng/mg)	19 (4–19179)	128.5 (15–32721)	0.192	1.000
Chenodeoxycholic acid (ng/mg)	94 (43–3969)	256 (61–5794)	0.390	1.000
Lithocolic acid (ng/mg)	475 (6–1628)	774 (2–2905)	0.234	1.000
Deoxycholic acid (ng/mg)	4377 (14–9955)	5863 (6–11166)	0.211	1.000
Ursodeoxycholic acid (ng/mg)	19 (2–272)	31.5 (3–390)	0.291	1.000
TPBA (ng/mg)	106 (62–23148)	490 (78.00–38515)	0.524	1.000
TSBA (ng/mg)	5015 (101–11594)	7424 (55–13401)	0.211	1.000
TPBA (%)	3 (1–97)	8 (1.00–99)	0.329	1.000
TSBA (%)	97 (3–99)	92 (1–99)	0.329	1.000
Sterols				
Coprostanol (μg/mg)	0.02 (0.01–20.14)	0.02 (0.01–15.79)	0.106	1.000
Cholesterol (μg/mg)	6.21 (2.88–14.30)	4.38 (1.88–9.00)	0.055	1.000
Cholestanol (μg/mg)	0.21 (0.08–0.76)	0.22 (0.07–0.74)	0.695	1.000
Lathosterol (μg/mg)	0.06 (0.01–0.16)	0.03 (0.01–0.84)	0.064	1.000
Brassicasterol (μg/mg)	0.02 (0.01–0.07)	0.02 (0.01–0.06)	0.687	1.000
Campesterol (μg/mg)	0.23 (0.04–0.50)	0.28 (0.07–0.83)	0.252	1.000
Stigmasterol (μg/mg)	0.13 (0.02–0.40)	0.17 (0.05–0.74)	0.257	1.000
Fusosterol (μg/mg)	0.03 (0.01–0.28)	0.06 (0.01–0.24)	0.277	1.000
Beta-sitosterol (μg/mg)	0.44 (0.05–1.93)	1.17 (0.14–3.21)	0.223	1.000
Sitostanol (μg/mg)	0.07 (0.01–0.68)	0.12 (0.02–1.28)	0.182	1.000
Total measured sterols (μg/mg)	10.96 (5.38–26.44)	8.78 (4.20–20.10)	0.129	1.000
Total measured zoosterols (μg/mg)	9.75 (3.06–26.22)	6.17 (2.03–19.78)	0.104	1.000
Total measured phytosterols (μg/mg)	0.89 (0.21–3.32)	1.67 (0.3–5.94)	0.182	1.000
Fatty acids				
Myristic acid (μg/mg)	1.57 (0.41–5.62)	0.80 (0.45–4.81)	0.073	1.000
Palmitic acid (μg/mg)	15.08 (3.47–19.63)	11.47 (4.33–19.44)	0.231	1.000
Linoleic acid (μg/mg)	6.77 (3.01–10.16)	5.36 (2.81–34.02)	0.348	1.000
α-linolenic acid (μg/mg)	0.14 (0.07–1.92)	0.45 (0.09–2.12)	0.487	1.000
Oleic acid (μg/mg)	7.90 (3.47–18.37)	5.34 (2.76–19.44)	0.044*	1.000
Cis-Vaccenic acid (μg/mg)	6.72 (1.49–15.85)	2.63 (0.99–14.90)	0.104	1.000
Stearic acid (μg/mg)	8.16 (2.97–18.16)	5.70 (2.14–18.36)	0.013*	0.455
Arachidonic acid (μg/mg)	4.30 (1.37–10.25)	2.29 (0.95–5.29)	0.051	1.000
Gondoic acid (μg/mg)	0.67 (0.19–2.49)	0.42 (0.18–1.66)	0.140	1.000
Docosonoic acid (μg/mg)	0.93 (0.24–5.08)	0.69 (0.27–2.18)	0.226	1.000
Erucic acid (μg/mg)	0.39 (0.10–1.19)	0.24 (0.06–0.57)	0.018*	0.630
Nervonic acid (μg/mg)	1.18 (0.18–2.49)	0.67 (0.23–1.85)	0.002*	0.070
Total measured fatty acids (μg/mg)	53.36 (24.17–94.01)	39.86 (17.60–92.13)	0.083	1.000

H, healthy; iPLE, inflammatory protein-losing enteropathy; T0, diagnosis; T1, after 1 month of therapy; TPBA, total primary bile acids; TSBA, total secondary bile acids; *statistically significant.

that are non-responsive to conventional therapy could be useful and deserves further investigation.

Marked perturbations in fecal long-chain fatty acid and sterol content of dogs with iPLE were found, indicating lipid malabsorption and dysmetabolism as previously described for dogs with chronic enteropathy and humans with inflammatory bowel disease (Piotrowska et al., 2021; Ma et al., 2019; Galler et al., 2022a; Honneffer, 2017). Increased fecal lipid content might be the result

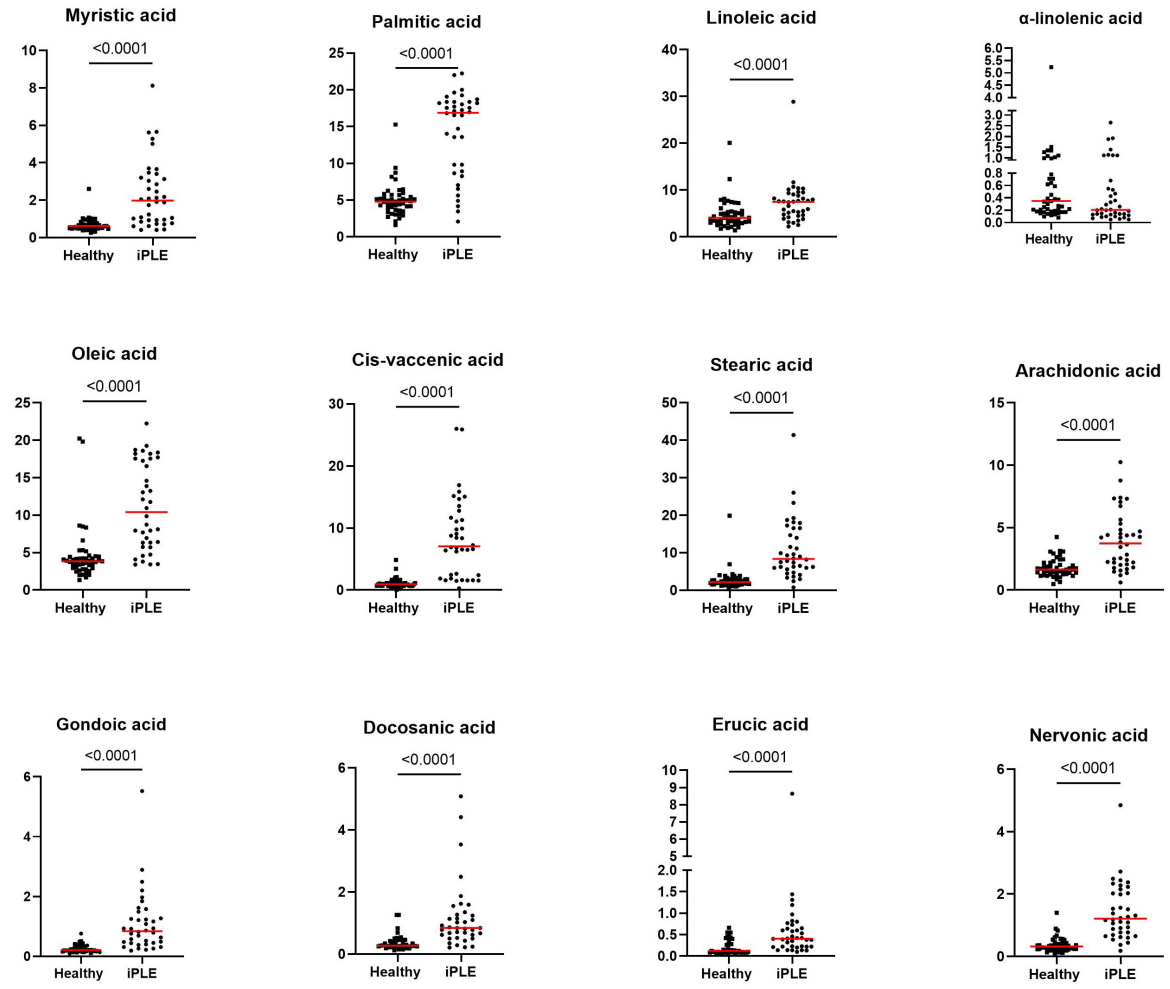

FIGURE 4
Fecal concentrations of long-chain fatty acids (μg/mg) in healthy control dogs and iPLE dogs. Red lines represent median value. The *p*-values expressed are unadjusted (adjusted *p*-value are reported in Table 4).

of different concurrent mechanisms, including altered epithelial transport as a result of damaged intestinal mucosa, reduced intestinal absorptive area and/or accelerated intestinal transit time. Long-chain fatty acids play an important role in maintaining the intestinal homeostasis, serving as antioxidants, and acting by various mechanisms that interfere with pro- and anti-inflammatory mediators (Wang et al., 2013). Moreover, their excesses in the gut lumen increase colonic motility and lead to osmotic diarrhea (Zhao et al., 2018). Arachidonic acid and its parent compound, linoleic acid, are omega-6 fatty acids that provide stability and fluidity to cell membranes. However, during periods of injury and inflammation, metabolism of arachidonic acid leads to the production of pro-inflammatory eicosanoids such as prostaglandin E2 thromboxane A2, and leukotriene B4 (Piotrowska et al., 2021). The increase in linolenic and arachidonic acid fecal content might suggest damage to the lipid bilayer of the intestinal epithelium and the presence of an active gastrointestinal inflammatory response in dogs with PLE. Palmitic acid affects intestinal epithelial and barrier integrity and permeability in in vitro studies (Gori et al., 2020), while nervonic acid could reflect depth and severity of the intestinal damage. Indeed, nervonic acid is an abundant component of the myelin sheath of nerves, and the muscularis and submucosal plexus are connected to the epithelium in the mucosa by enteric nerves and glial cells (Li et al., 2019). Moreover, nerves and glial cells that contain nervonic acid are also found in the mucosal layer (Ten Hove et al., 2021). A negative correlation between fecal content of nervonic acid and serum albumin concentration was found, further supporting the role of this fatty acid as a surrogate marker of intestinal damage. Nervonic acid is not commonly found within dietary components, making it unlikely that diet influences fecal nervonic acid content (Li et al., 2019). Even though the difference was not statistically significant, α-linolenic acid was the only long-chain fatty acid that was decreased in iPLE dogs. The α-linolenic acid is an omega-3 fatty acid with anti-inflammatory properties, acting as a competitive substrate for the enzymes and products of omega-6 polyunsaturated fatty-acid metabolism (Piotrowska et al., 2021). The omega-3/omega-6 imbalance possibly results in a disruption of the host's immunity and overproduction of pro-inflammatory cytokines, perpetuating the inflammatory stimulus at intestinal level, similar to previous observations (Ma et al., 2019). A positive correlation between the CCECAI score and total FAs, along with some of the long-chain fatty acids measured was found,

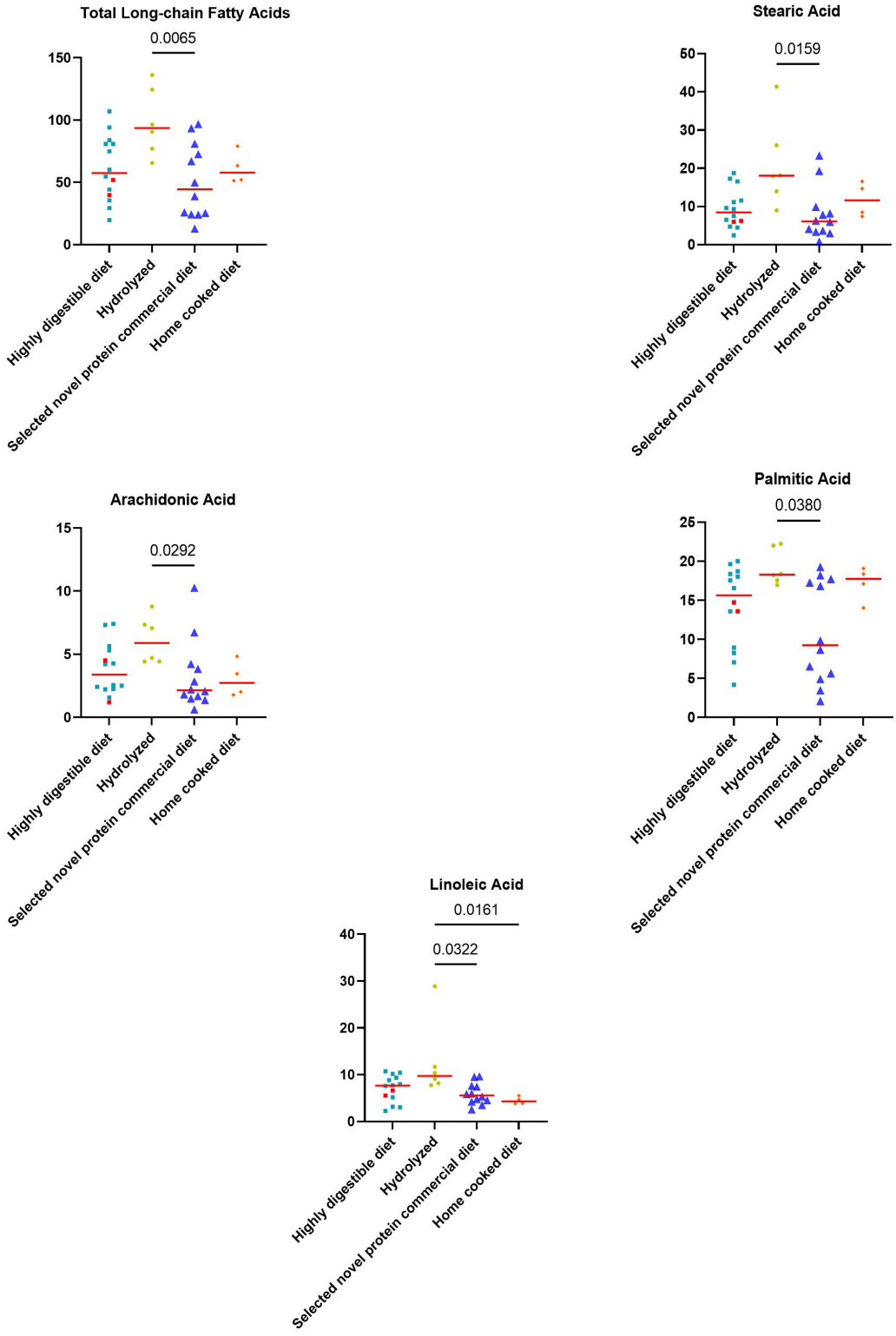

FIGURE 5
Fecal concentrations of metabolites that differed significantly between diet groups prior to the inclusion. The two iPLE dogs that were fed with highly digestible gastrointestinal low-fat diets are highlighted in red. Red lines represent median values. Significant *p*-values from the post-hoc analysis for multiple comparisons following the Kruskal-Wallis test are displayed.

suggesting that the clinical severity may be associated with the severity of the intestinal damage. To the contrary, no significant correlation was found between FAs and DI values, but few weak correlations were found between *E. coli* and nervonic, gondoic and myristic acids, and between *Streptococcus* and arachidonic acid. These results suggest that dysbiosis does not influence the fecal

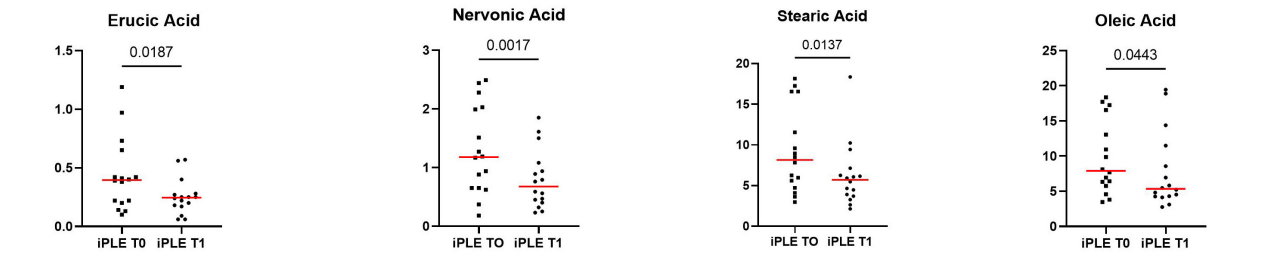

FIGURE 6
Fecal concentrations of selected metabolites that significantly improved at T1 in dogs with iPLE. Red lines represent median value. The *p*-values expressed are unadjusted (adjusted *p*-value are reported in Table 4).

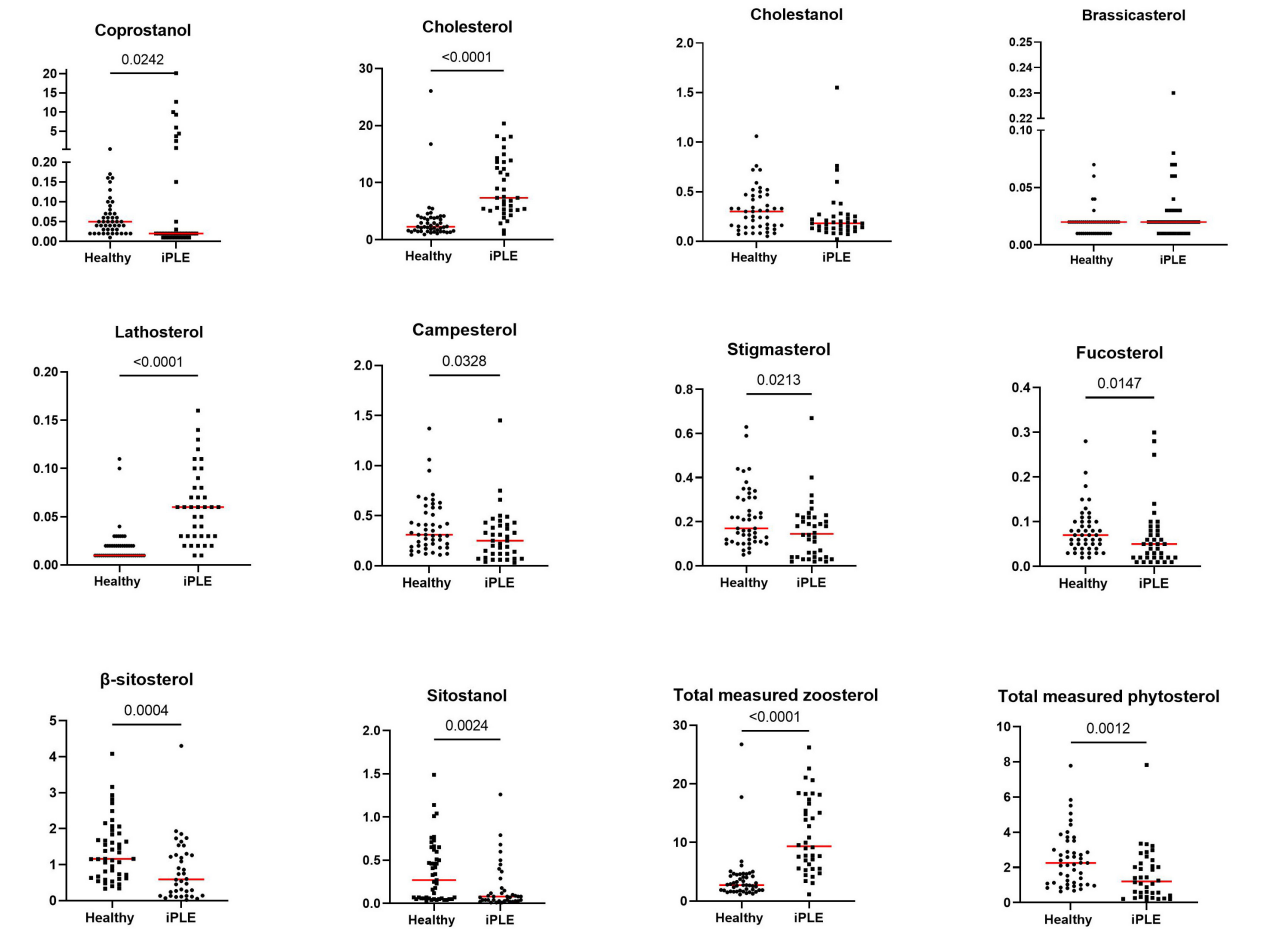

FIGURE 7
Fecal concentrations of sterols (μg/mg) in healthy control dogs and iPLE dogs. Red lines represent median value. The *p*-values expressed are unadjusted (adjusted *p*-value are reported in Table 4).

content of long-chain fatty acids, and the few weak correlations found are insufficient to establish a clear role of dysbiosis in the observed metabolomic alterations. The relationship between *E. coli* and long-chain fatty acids is multifaceted and not well described (Mitchell and Ellermann, 2022); *E. coli* use long-chain fatty acids as an energy source and for membrane biosynthesis. At the same time, long-chain fatty acids can act as signaling molecules that influence *E. coli* virulence, particularly in pathogenic strains (Mitchell and Ellermann, 2022). However, further studies are needed to investigate the potential relationship between bacteria and metabolites.

At T1, a decrease in some long-chain fatty acids, including nervonic acid, was observed, although the values were still elevated compared to healthy dogs. This result might reflect the decrease in intestinal inflammatory stimulus and partial mucosal healing after treatment.

Sterols are a subclass of lipids embedded in cell membranes. They can be classified into two major groups: zoosterols, sterols of

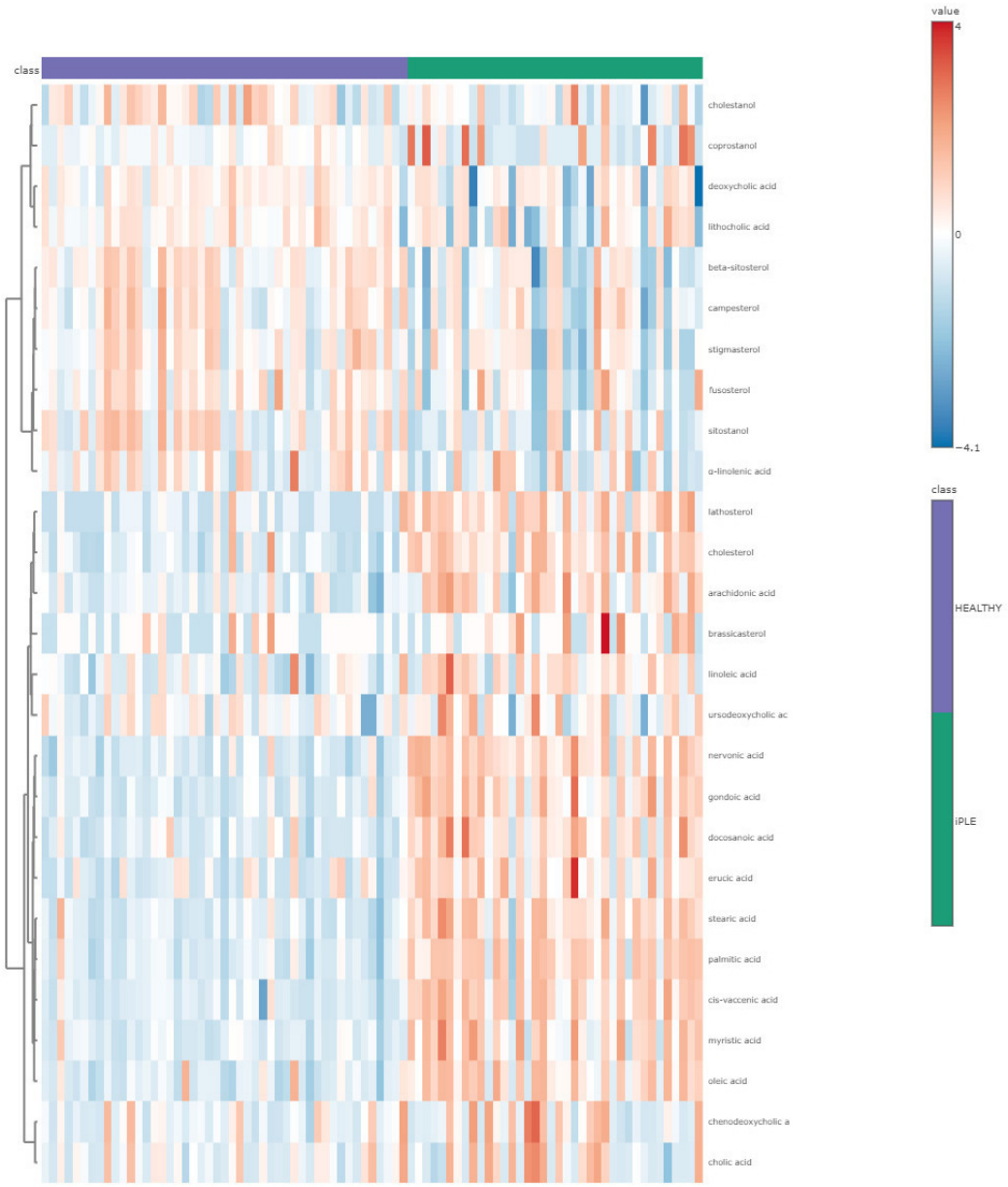

FIGURE 8
The heatmap provides intuitive visualization of the targeted fecal metabolites content differences among healthy control dogs and dogs with iPLE at T0. Each colored cell on the map corresponds to a concentration value, with samples in columns and metabolites in rows. The *t*-test was used by the software for the statistical analysis.

animal origin, and phytosterols, sterols of plant origin. In this study, dogs with iPLE showed a significant increase in fecal zoosterols and a significant decrease in phytosterols compared to healthy dogs. Similarly, recent analyses report decreased phytosterols in both dogs and cats with chronic enteropathy (Sung et al., 2023b; Honneffer, 2017). Phytosterols have anti-inflammatory properties, they can reduce cholesterol absorption in the gastrointestinal tract and they cannot be synthesized endogenously (Aldini et al., 2014; De Jong et al., 2003). Because of this, their fecal concentration is the end result of dietary ingestion and absorption. Therefore, malabsorption could be a reason for their increased fecal concentration. Moreover, unabsorbed phytosterols reach the colon and undergo bacterial metabolization; so it is reasonable to consider that dysbiosis may also play a role in phytosterol fecal content (Cuevas-Tena et al., 2018). However, in this study, we did not find a significant difference in phytosterol fecal content between dysbiotic and eubiotic dogs, and no correlation between fecal content of phytosterols and bacterial tax were found. Cholesterol is a key-role zoosterol, and it derives mainly from liver synthesis. Therefore, there is no absolute need for dietary intake, but regulation of the latter helps maintain a stable pool of cholesterol (Lecerf and de Lorgeril, 2011). In this study, fecal concentrations of cholesterol and lathosterol were significantly higher in iPLE dogs, contrary to coprostanol that was significantly decreased. Coprostanol is the non-absorbable end product of bacterial cholesterol metabolism (Kriaa et al., 2019). In this study, a significant negative and

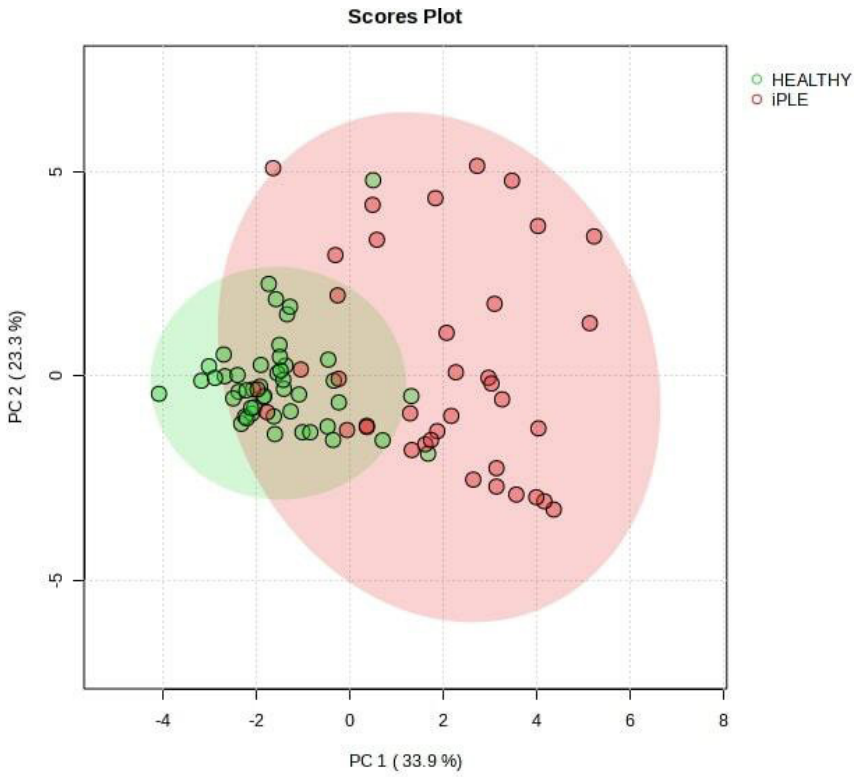

FIGURE 9
Principal Component Analysis (PCA) score plots of the targeted fecal metabolites for healthy control dogs and dogs with iPLE. The statistical significances of the group patterns are evaluated using PERMANOVA test (Permutational Multivariate Analysis of Variance). The figure shows healthy dogs cluster from iPLE dogs. PC1 = first principal component. PC2 = second principal component.

moderate correlation between the DI value and the coprostanol fecal content was found. Dogs with iPLE and normal DI values had higher fecal concentrations of coprostanol, compared to iPLE dogs with dysbiosis. This result could suggest reduced microbial conversion of cholesterol secondary to microbiota shift. Currently, human studies report *Eubacterium* and *Bacteroides* as main bacteria genera involved in cholesterol-to-coprostanol conversion, but other bacteria could exhibit similar properties (Gérard, 2013; Kriaa et al., 2019). The increase in fecal cholesterol concentration can result from various mechanisms acting simultaneously in dogs with iPLE. Firstly, it might increase due to the bile acid dysmetabolism. Secondly, enterocyte shedding from severe mucosal damage leads to an increased cholesterol concentration in the intestinal lumen, as it is a primary component of enterocyte membranes. Thirdly, cholesterol circulates esterified with fatty acids as lipoproteins in lymph vessels. In PLE disorders, intestinal inflammation leads to impaired drainage and altered permeability at the lacteal level, resulting in lacteal engorgement and rupture, with loss of proteins and lipids (cholesterol and fatty acids) into the intestinal lumen. Lastly, fecal cholesterol concentrations depend on animal diet sources, but we did not find any significant difference among different diet groups, nor at T0 or T1. In this study, no significant differences were found in the fecal concentrations of cholesterol between iPLE dogs with and without lymphangiectasia. These results, however, are not surprising since different factors can act simultaneously causing an increase in fecal cholesterol concentration, and because diet has a less important role on cholesterol compared to endogenous synthesis, as explained before. At T1, no significant changes were observed in fecal sterol content, in contrast to certain fatty acids, which decreased between T0 and T1. These fatty acids, however, did not return to levels comparable to healthy control dogs. This result possibly reflects a limited improvement in the aforementioned mechanisms with therapy, although one month of treatment may be too short to fully restore severe intestinal mucosal inflammation and damage.

In this study, the therapeutic and dietary protocols were not standardized, as the severity and chronicity of the disease, along with the alimentary history, dictated the choice of the therapeutic approach. For this reason, the changes in fecal lipid metabolism observed at T1 cannot be attributed to either dietary choices, use of anti-inflammatory/immunosuppressive medications, or a combination of both. Based on recent studies, dietary management with low fat or ultra-low fat diets seems to be the cornerstone of PLE treatment (Tolbert et al., 2022; Myers et al., 2023). Indeed, fat-restricted diets could break the cycle of intestinal protein and lipid leakage, decreasing lymphatic flow and lacteal distension. On the other hand, since some dogs with PLE have severe inflammation, pursuit of a hydrolyzed diet might be a valid therapeutic option (Green and Kathrani, 2022). In this study, fecal FA content (specifically, stearic acid, palmitic acid, linoleic acid, and arachidonic acid) was significantly higher in iPLE dogs that were fed a hydrolyzed diet prior to admission compared to dogs of other diet groups. Some hydrolyzed diets are soy-based, and soybeans have high content of stearic and linoleic acid.

Considering the overall results obtained in this study, it's interesting to note that within the same population of dogs affected by the same gastrointestinal disease and with comparable clinical severity, there are subsets of iPLE dogs characterized by different microbiomic, metabolomic, and clinicopathological features. It's possible to speculate that it's not the disease itself that determines these alterations, but rather the severity of the intestinal mucosa damage. Dysbiosis, as well as hypocobalaminemia, are markers of underlying gastrointestinal damage, but they do not necessarily correlate with clinical disease activity. Conversely, certain fecal metabolomic perturbations (i.e., arachidonic acid, nervonic acid, and cholesterol) could serve as markers of disease activity and mucosal damage. However, this remains speculative at time, and further studies focused on this topic are needed.

This study is not without limitations. Firstly, due to ethical concerns, healthy control dogs did not undergo endoscopy to rule out the presence of asymptomatic gastrointestinal inflammation and lymphangiectasia. Secondly, follow-up fecal samples were not available for all iPLE dogs and only at 1 month after the histologic diagnosis. To ensure clinical relevance, it might be necessary to include more dogs at follow-up and consider a longer interval after the diagnosis. Last but not least, the dietetic and therapeutic approaches were not standardized, mainly due to different chronicity and severity of the disease among iPLE dogs, as explained above.

In summary, this study showed changes in the fecal microbiome and metabolome of dogs with iPLE. Notably, dysbiosis, bile acid, fatty acid, and sterol dysmetabolism were observed. Different therapeutic protocols lead to an improvement of some metabolome perturbations at short-term follow-up. Considering the important role of these compounds in inflammation and gastrointestinal tract functionalities, a comprehensive profile with long-chain fatty acids, sterols, and bile acids might help to better understand intestinal dysfunction in dogs with iPLE and possibly guide new therapeutic options in the future.

Data availability statement

The original contributions presented in the study are included in the article/Supplementary material, further inquiries can be directed to the corresponding author.

Ethics statement

The animal studies were approved by the Ethics and Animal Welfare committee of the University of Turin (protocol number 42, 08/01/2021). The studies were conducted in accordance with the local legislation and institutional requirements. Written informed consent was obtained from the owners for the participation of their animals in this study.

Author contributions

FC: Data curation, Formal analysis, Investigation, Writing – original draft, Writing – review and editing. JS: Conceptualization, Funding acquisition, Resources, Supervision, Writing – review and editing. AB: Investigation, Writing – review and editing. FB: Investigation, Writing – review and editing. EB: Investigation, Writing – review and editing. ElB: Investigation, Writing – review and editing. RF: Investigation, Writing – review and editing. MT: Supervision, Writing – review and editing. C-CC: Formal analysis, Writing – review and editing. PRG: Supervision, Writing – review and editing. PG: Conceptualization, Investigation, Writing – original draft, Writing – review and editing.

Funding

The author(s) declare financial support was received for the research, authorship, and/or publication of this article. This research was partially funded (shipping of samples and Open Access Publishing) as part of the project "Research funded by the University (ex-60%)." The microbiome and metabolome analyses were performed at the GI laboratory at the Texas A&M University, USA, at the laboratory's own costs.

Acknowledgments

We thank the staff of the Veterinary Teaching Hospital of Turin University and the Associazione Professionale Endovet for the precious support in finalizing the study. Parts of this manuscript were presented as an oral communication at the EuroGut 2023 in Edinburgh, UK, and as an oral abstract at the ECVIM Congress 2023 in Barcelona, Spain.

Conflict of interest

JS, MT, C-CC, and PRG are employed by the Gastrointestinal Laboratory at Texas A&M University, which provides assays for intestinal function and microbiota analysis on a fee-for-service basis.

The remaining authors declare that the research was conducted in the absence of any commercial or financial relationships that could be construed as a potential conflict of interest.

Publisher's note

Supplementary material

The Supplementary Material for this article can be found online at: https://www.frontiersin.org/articles/10.3389/fmicb.2024.1433175/full#supplementary-material

References

Aldini, R., Micucci, M., Cevenini, M., Fato, R., Bergamini, C., Nanni, C., et al. (2014). Antiinflammatory effect of phytosterols in experimental murine colitis model: Prevention, induction, remission study. *PLoS One* 9:e108112. doi: 10.1371/journal.pone.0108112

Allenspach, K., and Iennarella-Servantez, C. (2021). Canine protein losing enteropathies and systemic complications. *Vet. Clin. North Am. Small Anim. Pract.* 51, 111–122. doi: 10.1016/j.cvsm.2020.09.010

Allenspach, K., Wieland, B., Gröne, A., and Gaschen, F. (2007). Chronic enteropathies in dogs: Evaluation of risk factors for negative outcome. *J. Vet. Intern. Med.* 21, 700–708. doi: 10.1111/j.1939-1676.2007.tb03011.x

AlShawaqfeh, M., Wajid, B., Minamoto, Y., Markel, M., Lidbury, J., Steiner, J., et al. (2017). A dysbiosis index to assess microbial changes in fecal samples of dogs with chronic inflammatory enteropathy. *FEMS Microbiol. Ecol.* 93:11. doi: 10.1093/femsec/fix136

Batta, A., Salen, G., Batta, P., Stephen Tint, G., Alberts, D., and Earnest, D. (2002). Simultaneous quantitation of fatty acids, sterols and bile acids in human stool by capillary gas–liquid chromatography. *J. Chromatogr. B* 775, 153–161. doi: 10.1016/S1570-0232(02)00289-1

Bauset, C., Gisbert-Ferrándiz, L., and Cosín-Roger, J. (2021). Metabolomics as a promising resource identifying potential biomarkers for inflammatory bowel disease. *J. Clin. Med.* 10:622. doi: 10.3390/jcm10040622

Berghoff, N., Parnell, N., Hill, S., Suchodolski, J., and Steiner, J. (2013). Serum cobalamin and methylmalonic acid concentrations in dogs with chronic gastrointestinal disease. *Am. J. Vet. Res.* 74, 84–89. doi: 10.2460/ajvr.74.1.84

Blake, A., Guard, B., Honneffer, J., Lidbury, J., Steiner, J., and Suchodolski, J. (2019). Altered microbiota, fecal lactate, and fecal bile acids in dogs with gastrointestinal disease. *PLoS One* 14:e0224454. doi: 10.1371/journal.pone.0224454

Camilleri, M. (2015). Bile acid diarrhea: Prevalence, pathogenesis, and therapy. *Gut Liver* 9, 332–339. doi: 10.5009/gnl14397

Craven, M., and Washabau, R. (2019). Comparative pathophysiology and management of protein-losing enteropathy. *J. Vet. Intern. Med.* 33, 383–402. doi: 10.1111/jvim.15406

Cuevas-Tena, M., Alegría, A., and Lagarda, M. J. (2018). Relationship between dietary sterols and gut microbiota: A review. *Eur. J. Lipid Sci. Technol.* 120:1800054. doi: 10.1002/ejlt.201800054

Day, M., Bilzer, T., Mansell, J., Wilcock, B., Hall, E., Jergens, A., et al. (2008). Histopathological standards for the diagnosis of gastrointestinal inflammation in endoscopic biopsy samples from the dog and cat: A report from the world small animal veterinary association gastrointestinal standardization group. *J. Comp. Pathol.* 138, S1–S43. doi: 10.1016/j.jcpa.2008.01.001

De Jong, A., Plat, J., and Mensink, R. (2003). Metabolic effects of plant sterols and stanols (Review). *J. Nutr. Biochem.* 14, 362–369. doi: 10.1016/S0955-2863(03)00002-0

Fiorucci, S., Carino, A., Baldoni, M., Santucci, L., Costanzi, E., Graziosi, L., et al. (2021). Bile acid signaling in inflammatory bowel diseases. *Dig. Dis. Sci.* 66, 674–693. doi: 10.1007/s10620-020-06715-3

Galler, A., Klavins, K., and Burgener, I. A. A. (2022a). Preliminary metabolomic study of yorkshire terrier enteropathy. *Metabolites* 12:264. doi: 10.3390/metabo12030264

Galler, A., Suchodolski, J., Steiner, J., Sung, C., Hittmair, K., Richter, B., et al. (2022b). Microbial dysbiosis and fecal metabolomic perturbations in Yorkshire Terriers with chronic enteropathy. *Sci. Rep.* 12:12977. doi: 10.1038/s41598-022-17244-6

Gérard, P. (2013). Metabolism of cholesterol and bile acids by the gut microbiota. *Pathogens* 3, 14–24. doi: 10.3390/pathogens3010014

Giaretta, P. (2018). Distribution of bile acid receptor TGR5 in the gastrointestinal tract of dogs. *Histol. Histopathol.* 34, 69–79. doi: 10.14670/HH-18-025

Giaretta, P., Rech, R., Guard, B., Blake, A., Blick, A., Steiner, J., et al. (2018). Comparison of intestinal expression of the apical sodium-dependent bile acid transporter between dogs with and without chronic inflammatory enteropathy. *J. Vet. Intern. Med.* 32, 1918–1926. doi: 10.1111/jvim.15332

Gori, M., Altomare, A., Cocca, S., Solida, E., Ribolsi, M., Carotti, S., et al. (2020). Palmitic acid affects intestinal epithelial barrier integrity and permeability in vitro. *Antioxidants* 9:417. doi: 10.3390/antiox9050417

Green, J., and Kathrani, A. (2022). Incidence of relapse of inflammatory protein-losing enteropathy in dogs and associated risk factors. *J. Vet. Intern. Med.* 36, 1981–1988. doi: 10.1111/jvim.16561

Honneffer, J. (2014). Microbiota alterations in acute and chronic gastrointestinal inflammation of cats and dogs. *World J. Gastroenterol.* 20:16489. doi: 10.3748/wjg.v20.i44.16489

Honneffer, J. (2017). *Microbiota and metabolomic changes across various canine gastrointestinal diseases*. [Ph.D. thesis]. College Station, TX: Texas A & M University.

Jergens, A., and Heilmann, R. (2022). Canine chronic enteropathy-Current state-of-the-art and emerging concepts. *Front. Vet. Sci.* 9:923013. doi: 10.3389/fvets.2022.923013

Kang, J., Myers, C., Harris, S., Kakiyama, G., Lee, I., Yun, B., et al. (2019). Bile acid 7α-dehydroxylating gut bacteria secrete antibiotics that inhibit clostridium difficile: Role of secondary bile acids. *Cell Chem. Biol.* 26:27–34.e4. doi: 10.1016/j.chembiol.2018.10.003

Kather, S., Grützner, N., Kook, P., Dengler, F., and Heilmann, R. (2020). Review of cobalamin status and disorders of cobalamin metabolism in dogs. *J. Vet. Intern. Med.* 34, 13–28. doi: 10.1111/jvim.15638

Kriaa, A., Bourgin, M., Mkaouar, H., Jablaoui, A., Akermi, N., Soussou, S., et al. (2019). Microbial reduction of cholesterol to coprostanol: An old concept and new insights. *Catalysts* 9:167. doi: 10.3390/catal9020167

Lecerf, J., and de Lorgeril, M. (2011). Dietary cholesterol: From physiology to cardiovascular risk. *Br. J. Nutr.* 106, 6–14. doi: 10.1017/S0007114511000237

Li, Q., Chen, J., Yu, X., and Gao, J.-M. (2019). A mini review of nervonic acid: Source, production, and biological functions. *Food Chem.* 301:125286. doi: 10.1016/j.foodchem.2019.125286

Ma, C., Vasu, R., and Zhang, H. (2019). The role of long-chain fatty acids in inflammatory bowel disease. *Mediat. Inflamm.* 2019, 1–10. doi: 10.1155/2019/8495913

Manchester, A., Webb, C., Blake, A., Sarwar, F., Lidbury, J., Steiner, J., et al. (2019). Long-term impact of tylosin on fecal microbiota and fecal bile acids of healthy dogs. *J. Vet. Intern. Med.* 33, 2605–2617. doi: 10.1111/jvim.15635

Marsilio, S., Chow, B., Hill, S., Ackermann, M., Estep, J., Sarawichitr, B., et al. (2021). Untargeted metabolomic analysis in cats with naturally occurring inflammatory bowel disease and alimentary small cell lymphoma. *Sci. Rep.* 11: 9198. doi: 10.1038/s41598-021-88707-5

Minamoto, Y., Otoni, C., Steelman, S., Büyükleblebici, O., Steiner, J., Jergens, A., et al. (2015). Alteration of the fecal microbiota and serum metabolite profiles in dogs with idiopathic inflammatory bowel disease. *Gut Microbes* 6, 33–47. doi: 10.1080/19490976.2014.997612

Mitchell, M. K., and Ellermann, M. (2022). Long chain fatty acids and virulence repression in intestinal bacterial pathogens. *Front. Cell. Infect. Microbiol.* 12:928503. doi: 10.3389/fcimb.2022.928503

Myers, M., Martinez, S., Shiroma, J., Watson, A., and Hostutler, R. (2023). Prospective evaluation of low-fat diet monotherapy in dogs with presumptive protein-losing enteropathy. *J. Am. Anim. Hosp. Assoc.* 59, 74–84. doi: 10.5326/JAAHA-MS-7248

Pilla, R., and Suchodolski, J. (2020). The role of the canine gut microbiome and metabolome in health and gastrointestinal disease. *Front. Vet. Sci.* 6:498. doi: 10.3389/fvets.2019.00498

Pilla, R., Gaschen, F., Barr, J., Olson, E., Honneffer, J., Guard, B., et al. (2020). Effects of metronidazole on the fecal microbiome and metabolome in healthy dogs. *J. Vet. Intern. Med.* 34, 1853–1866. doi: 10.1111/jvim.15871

Pilla, R., Guard, B., Blake, A., Ackermann, M., Webb, C., Hill, S., et al. (2021). Long-term recovery of the fecal microbiome and metabolome of dogs with steroid-responsive enteropathy. *Animals* 11:2498. doi: 10.3390/ani11092498

Piotrowska, M., Binienda, A., and Fichna, J. (2021). The role of fatty acids in Crohn's disease pathophysiology – An overview. *Mol. Cell Endocrinol.* 538:111448. doi: 10.1016/j.mce.2021.111448

Russell, D., and Setchell, K. (1992). Bile acid biosynthesis. *Biochemistry* 31, 4737–4749. doi: 10.1021/bi00135a001

Stavroulaki, E., Suchodolski, J., and Xenoulis, P. (2023). Effects of antimicrobials on the gastrointestinal microbiota of dogs and cats. *Vet. J.* 291:105929. doi: 10.1016/j.tvjl.2022.105929

Suchodolski, J., Dowd, S., Westermarck, E., Steiner, J., Wolcott, R., Spillmann, T., et al. (2009). The effect of the macrolide antibiotic tylosin on microbial diversity in the canine small intestine as demonstrated by massive parallel 16S rRNA gene sequencing. *BMC Microbiol.* 9:210. doi: 10.1186/1471-2180-9-210

Sung, C., Pilla, R., Chen, C., Ishii, P., Toresson, L., Allenspach-Jorn, K., et al. (2023a). Correlation between targeted qPCR assays and untargeted DNA shotgun metagenomic sequencing for assessing the fecal microbiota in dogs. *Animals* 13:2597. doi: 10.3390/ani13162597

Sung, C., Pilla, R., Marsilio, S., Chow, B., Zornow, K., Slovak, J., et al. (2023b). Fecal concentrations of long-chain fatty acids, sterols, and unconjugated bile acids in cats with chronic enteropathy. *Animals* 13:2753. doi: 10.3390/ani13172753

Ten Hove, A., Seppen, J., and De Jonge, W. (2021). Neuronal innervation of the intestinal crypt. *Am. J. Physiol. Gastrointest. Liver Physiol.* 320, G193–G205. doi: 10.1152/ajpgi.00239.2020

Tizard, I., and Jones, S. (2018). The microbiota regulates immunity and immunologic diseases in dogs and cats. *Vet. Clin. North Am. Small Anim. Pract.* 48, 307–322. doi: 10.1016/j.cvsm.2017.10.008

Tolbert, M., Murphy, M., Gaylord, L., and Witzel-Rollins, A. (2022). Dietary management of chronic enteropathy in dogs. *J. Small Anim. Pract.* 63, 425–434. doi: 10.1111/jsap.13471

Toresson, L., Steiner, J., and Suchodolski, J. (2021). Cholestyramine treatment in two dogs with presumptive bile acid diarrhoea: A case report. *Canine Med. Genet.* 8:1. doi: 10.1186/s40575-021-00099-x

Toresson, L., Suchodolski, J., Spillmann, T., Lopes, B., Shih, J., Steiner, J., et al. (2023). The Intestinal microbiome in dogs with chronic enteropathies and cobalamin deficiency or normocobalaminemia–a comparative study. *Animals* 13:1378. doi: 10.3390/ani13081378

Vítek, L. (2015). Bile acid malabsorption in inflammatory bowel disease. *Inflamm. Bowel Dis.* 21, 476–483. doi: 10.1097/MIB.0000000000000193

Walters, J., and Pattni, S. (2010). Managing bile acid diarrhoea. *Ther. Adv. Gastroenterol.* 3, 349–357. doi: 10.1177/1756283X10377126

Wang, T., Liu, M., Portincasa, P., and Wang, D. (2013). New insights into the molecular mechanism of intestinal fatty acid absorption. *Eur. J. Clin. Invest.* 43, 1203–1223. doi: 10.1111/eci.12161

Ward, J., Lajczak, N., Kelly, O., O'Dwyer, A., Giddam, A., Ní Gabhann, J., et al. (2017). Ursodeoxycholic acid and lithocholic acid exert anti-inflammatory actions in the colon. *Am. J. Physiol. Gastrointest. Liver Physiol.* 312, G550–G558. doi: 10.1152/ajpgi.00256.2016

Weng, Y., Gan, H., Li, X., Huang, Y., Li, Z., Deng, H., et al. (2019). Correlation of diet, microbiota and metabolite networks in inflammatory bowel disease. *J. Dig. Dis.* 20, 447–459. doi: 10.1111/1751-2980.12795

Xu, J., Verbrugghe, A., Lourenço, M., Janssens, G., Liu, D., Van De Wiele, T., et al. (2016). Does canine inflammatory bowel disease influence gut microbial profile and host metabolism? *BMC Vet. Res.* 12:114. doi: 10.1186/s12917-016-0736-2

Zhao, L., Huang, Y., Lu, L., Yang, W., Huang, T., Lin, Z., et al. (2018). Saturated long-chain fatty acid-producing bacteria contribute to enhanced colonic motility in rats. *Microbiome* 6:107. doi: 10.1186/s40168-018-0492-6

Ziese, A., and Suchodolski, J. (2021). Impact of changes in gastrointestinal microbiota in canine and feline digestive diseases. *Vet. Clin. North Am. Small Anim. Pract.* 51, 155–169. doi: 10.1016/j.cvsm.2020.09.004

frontiers | Frontiers in Microbiology

TYPE Original Research
PUBLISHED 21 October 2024
DOI 10.3389/fmicb.2024.1458090

OPEN ACCESS

EDITED BY
Xu Wang,
Auburn University, United States

REVIEWED BY
Stephanie Skinner,
Friendship Hospital for Animals, United States
Lynn Weber,
University of Saskatchewan, Canada

*CORRESPONDENCE
Jenessa A. Winston
✉ winston.210@osu.edu

RECEIVED 01 July 2024
ACCEPTED 16 September 2024
PUBLISHED 21 October 2024

CITATION
Rowe JC, Summers SC, Quimby JM and Winston JA (2024) Fecal bile acid dysmetabolism and reduced ursodeoxycholic acid correlate with novel microbial signatures in feline chronic kidney disease.
Front. Microbiol. 15:1458090.
doi: 10.3389/fmicb.2024.1458090

Fecal bile acid dysmetabolism and reduced ursodeoxycholic acid correlate with novel microbial signatures in feline chronic kidney disease

John C. Rowe[1,2], Stacie C. Summers[3], Jessica M. Quimby[1,2] and Jenessa A. Winston[1,2]*

[1]Department of Veterinary Clinical Sciences, The Ohio State University College of Veterinary Medicine, Columbus, OH, United States, [2]Comparative Hepatobiliary Intestinal Research Program (CHIRP), The Ohio State University College of Veterinary Medicine, Columbus, OH, United States, [3]Department of Clinical Sciences, Oregon State University Carlson College of Veterinary Medicine, Corvallis, OR, United States

Background: Microbial-derived secondary bile acids (SBAs) are reabsorbed and sensed via host receptors modulating cellular inflammation and fibrosis. Feline chronic kidney disease (CKD) occurs with progressive renal inflammation and fibrosis, mirroring the disease pathophysiology of human CKD patients.

Methods: Prospective cross-sectional study compared healthy cats ($n = 6$) with CKD (IRIS Stage 2 $n = 17$, Stage 3 or 4 $n = 11$). Single timepoint fecal samples from all cats underwent targeted bile acid metabolomics. 16S rRNA gene amplicon sequencing using DADA2 with SILVA taxonomy characterized the fecal microbiota.

Results: CKD cats had significantly reduced fecal concentrations (median 12.8 ng/mg, Mann–Whitney $p = 0.0127$) of the SBA ursodeoxycholic acid (UDCA) compared to healthy cats (median 39.4 ng/mg). Bile acid dysmetabolism characterized by <50% SBAs was present in 8/28 CKD and 0/6 healthy cats. Beta diversity significantly differed between cats with <50% SBAs and >50% SBAs (PERMANOVA $p < 0.0001$). Twenty-six amplicon sequence variants (ASVs) with >97% nucleotide identity to *Peptacetobacter hiranonis* were identified. *P. hiranonis* combined relative abundance was significantly reduced (median 2.1%) in CKD cats with <50% SBAs compared to CKD cats with >50% SBAs (median 13.9%, adjusted $p = 0.0002$) and healthy cats with >50% SBAs (median 15.5%, adjusted $p = 0.0112$). *P. hiranonis* combined relative abundance was significantly positively correlated with the SBAs deoxycholic acid (Spearman $r = 0.5218$, adjusted $p = 0.0407$) and lithocholic acid (Spearman $r = 0.5615$, adjusted $p = 0.0156$). Three *Oscillospirales* ASVs and a *Roseburia* ASV were also identified as significantly correlated with fecal SBAs.

Clinical and translational importance: The gut-kidney axis mediated through microbial-derived SBAs appears relevant to the spontaneous animal CKD model of domestic cats. This includes reduced fecal concentrations of the microbial-derived SBA UDCA, known to regulate inflammation and fibrosis and be reno-protective. Microbes correlated with fecal SBAs include *bai* operon containing *P. hiranonis*, as well as members of *Oscillospirales*, which also harbor a functional *bai* operon. Ultimately, CKD cats represent a translational opportunity to study the role of SBAs in the gut-kidney axis, including the potential to identify novel

microbial-directed therapeutics to mitigate CKD pathogenesis in veterinary patients and humans alike.

KEYWORDS

bile acid inducible (*bai*) operon, chronic kidney disease (CKD), 7α-dehydroxylation, *Peptacetobacter hiranonis*, *Oscillospirales*, ursodeoxycholic acid, gut microbiota, dysbiosis

1 Introduction

Primary bile acids (PBAs) classically are lipid molecules produced and secreted by the liver into the intestinal tract to aid in digestion and absorption of nutrients such as fats (Ciaula et al., 2018). Beyond digestion, upon reabsorption bile acids also act as signaling molecules to orchestrate host physiology through bile acid activated receptors, including the nuclear farnesoid X receptor (FXR) and Takeda G protein-coupled 5 Receptor (TGR5) (Perino and Schoonjans, 2022). The composition of the bile acid pool available for intestinal reabsorption is dictated by the microbial community in the gut, or microbiota (Collins et al., 2023). The microbiota perform biotransformations of PBAs into microbial-derived secondary bile acids (SBAs) through enzymatic reactions that vastly expand the host-derived bile acid pool (Winston and Theriot, 2020). Microbial biotransformation potential is a product of the genes harbored by the gut microbiota, with only select microbes capable of performing important gatekeeping reactions to bile acid pool diversification (Collins et al., 2023; Winston and Theriot, 2020). For example, deconjugation of PBAs by gut microbes possessing bile salt hydrolase (BSH) makes unconjugated PBAs available for further biotransformation (Foley et al., 2019). Subsequent 7α-dehydroxylation performed by gut microbes containing the bile acid inducible (*bai*) operon allows for the conversion of the PBAs cholic acid (CA) and chenodeoxycholic acid (CDCA) into the SBAs deoxycholic acid (DCA) and lithocholic acid (LCA), respectively (Collins et al., 2023; Winston and Theriot, 2020; Funabashi et al., 2020). A limited number of culturable microbes are known to perform this function: *Clostridium scindens* (Kitahara et al., 2000), *Clostridium hylemonae* (Ridlon et al., 2010), *Peptacetobacter hiranonis* (formerly *Clostridium hiranonis*) (Kitahara et al., 2001), and *Extibacter muris* (in mice) (Streidl et al., 2021). However, recent metagenomic evidence suggests that currently unculturable members of the human gut microbiota within the order *Oscillospirales* may also harbor a functional *bai* operon (Vital et al., 2019; Kim et al., 2022). Separate reactions performed by microbes with hydroxysteroid dehydrogenases (HSDHs) allow for the generation of additional SBAs, such as ursodeoxycholic acid (UDCA) from CDCA (Collins et al., 2023; Winston and Theriot, 2020). As a result of microbial generation of SBAs, in healthy humans greater than 90% of fecal bile acids are SBAs (Ridlon et al., 2006). This composition is less clearly defined in healthy cats with most studies presenting healthy cat populations with a predominance of SBAs (Rowe and Winston, 2024), though isolated publications have included individuals with <50% SBAs within presumptively healthy cat populations (Sung et al., 2023).

Deviation of the gut microbiota from normal, known as dysbiosis, can alter microbial community function such that bile acid transformation is also impacted, creating a bile acid dysmetabolism. Bile acid dysmetabolism has been connected to multiple disease states in humans including *Clostridioides difficile* infection (Winston and Theriot, 2016), inflammatory bowel disease (Lloyd-Price et al., 2019), neurologic disease (McMillin and DeMorrow, 2016), cardiovascular disease (Rodríguez-Morató and Matthan, 2020), obesity, type 2 diabetes, dyslipidemia, and nonalcoholic fatty liver disease (Chávez-Talavera et al., 2017), as well as chronic kidney disease (CKD) (Chen et al., 2019; Wang et al., 2016; Li et al., 2019). Though less investigated, bile acid dysmetabolism is also recognized in various disease states of dogs and cats (Rowe and Winston, 2024).

Cats represent a spontaneous translational disease model of CKD, as development of CKD is reported to occur in up to 80% of cats 15 years or older (Bartges, 2012; Marino et al., 2014). CKD pathogenesis includes progressive tubulointerstitial inflammation and fibrosis (Jepson, 2016; McLeland et al., 2015). Given that the host bile acid activated receptors FXR and TGR5 are expressed in the kidney and have the potential to modulate host inflammatory and fibrotic responses, investigation of a bile acid dysmetabolism that may contribute to or mitigate CKD progression is warranted. Indeed, rodent models have demonstrated these mechanisms to be reno-protective in kidney injury induced via cisplatin (Yang et al., 2020) and gentamicin (Abd-Elhamid et al., 2018). To date, dysbiosis resulting in bile acid dysmetabolism in cats has been minimally explored (Rowe and Winston, 2024). Still, reduced alpha diversity in the gut microbial community has been shown in cats with CKD (Summers et al., 2019), and a single report investigating fecal metabolome in cats with CKD ($n = 10$) did not document a bile acid dysmetabolism (Hall et al., 2020). Further characterization of potential dysbiosis and resulting bile acid dysmetabolism in cats may provide insight into microbial directed therapeutic interventions for cats with CKD and microbial mechanisms that are conserved across species, including humans with CKD.

The aims of this study were (1) to determine if fecal bile acid dysmetabolism exists in cats with CKD, and (2) characterize gut microbiota features associated with the bile acid dysmetabolism in the context of feline CKD using targeted fecal bile acid quantification and 16S rRNA gene sequencing of fecal samples collected from cats with and without CKD.

2 Materials and methods

2.1 Study population and design

The present study utilized fecal samples collected from a prior study (Summers et al., 2019) and applied a post-hoc evaluation of

fecal bile acid concentrations. Cats presenting to the Colorado State University Veterinary Teaching Hospital (CSU-VTH) were prospectively enrolled into a cross-sectional study approved by the CSU-VTH Institutional Animal Care and Use Committee (IACUC) as previously described (Summers et al., 2019). Briefly, enrollment was performed from August 2016 to August 2017 and yielded a population of cats with CKD ($n = 28$) and a healthy older control population ($n = 6$). All cats with CKD met inclusion following evaluation of client history, physical examination, medical record review, complete blood count, serum chemistry (including creatinine >1.6 mg/dL), urinalysis (including urine specific gravity (USG) < 1.035), serum total thyroxine concentration, blood pressure, fecal flotation, and urine protein to creatinine ratio (if 1+ protein or greater determined by urinalysis) (Summers et al., 2019). Cats with CKD were staged according to the International Renal Interest Society (IRIS) Guidelines (Stage 2 $n = 17$, Stage 3 or 4 $n = 11$) (IRIS Kidney, 2023). All healthy older control cats were owned by employees, veterinary students, or staff at CSU-VTH, were at least 8 years old, and underwent the same laboratory screening. Health status was determined by a veterinary board-certified internist based on clinical history, physical examination, available prior medical record review, and normal laboratory screening tests including serum creatinine <1.6 mg/dL and USG > 1.035 (Summers et al., 2019). Exclusion criteria included the administration of antimicrobials, antacids, or probiotics within 6 weeks of enrollment. Cats with uncontrolled hyperthyroidism as well as suspicion or confirmation of gastrointestinal disease, including gastrointestinal parasitism and food responsive enteropathy, were also excluded from the population (Summers et al., 2019). Diet information was collected from all owners; however, no dietary exclusion criteria were utilized. Basic demographic information is shown in Supplementary Table S1.

In the present study, healthy cats were required to have an ideal body condition score (BCS) of 4 or 5 out of 9 and did not include any cats with a BCS of 6 or greater, given that the gut microbiota and microbial-derived metabolites can be impacted by obesity status in both cats and people (Cline et al., 2021; Kieler et al., 2016; Rowe et al., 2024; Pinart et al., 2022). This restriction accounts for four less healthy older control cats compared to the prior study (Summers et al., 2019). A single CKD cat with an obese BCS (8/9) was also removed from the present analysis due to the possible confounding influence of comorbid obesity on the gut microbiota. CKD cats with overweight BCS (6 or 7 out of 9) were retained in the analysis as current guidelines recommend maintaining weight in CKD cats with these BCSs (Cline et al., 2021), thus capturing a realistic client-owned CKD cat population.

A fresh naturally voided fecal sample frozen within 24 h was used for microbiome and bile acid analyses. All fecal samples were collected by owners and placed on ice until being frozen at −80°C for further analysis. The prior study first utilized fecal samples for microbiota analysis (Summers et al., 2019). Targeted bile acid metabolomics were performed on remaining stored samples with sufficient fecal material. A single healthy cat and a single CKD cat from the prior study did not have sufficient sample for targeted bile acid metabolomics.

Within CKD cats, a subpopulation of 8/28 cats with <50% fecal SBAs were also analyzed in comparison to the healthy cats ($n = 6$) as well as CKD cats with >50% fecal SBAs ($n = 20$).

2.2 Quantification of fecal bile acid concentrations

Frozen fecal samples were shipped to and then analyzed by a fee for service laboratory (Metabolon Inc.) using liquid chromatography and tandem mass spectrometry (LC–MS/MS) to obtain fecal bile acid concentrations. This targeted metabolomic approach evaluated 15 fecal bile acids. The unconjugated bile acids assessed were cholic acid (CA), chenodeoxycholic acid (CDCA), deoxycholic acid (DCA), lithocholic acid (LCA), and ursodeoxycholic acid (UDCA). The taurine and glycine conjugated forms of all five unconjugated bile acids were also assessed. Briefly, calibration of all measured bile acids was performed with eight different known concentrations spiked into an acidified methanol solution. Quality control samples, calibration samples, and study samples were all also spiked with a labeled internal standard and subjected to protein precipitation with an organic solvent (acidified methanol). After centrifugation, organic supernatant was dried using a stream of nitrogen. Dried extracts were then reconstituted and injected onto an Agilent 1,290 Infinity/Sciex QTRAP 6500 LC–MS/MS system equipped with a C18 reverse phase ultra-high performance liquid chromatography (UHPLC) column. The mass spectrometer was operated in negative mode using electrospray ionization. Quantitation was performed using a weighted linear least squares regression generated from fortified calibration standards prepared immediately prior to each sample run. Raw data were collected and processed using AB SCIEX software Analyst (v1.6.3). Fecal bile acid concentrations are reported as nanogram per milligram of feces.

2.3 Fecal microbiota analysis

Publicly available forward-end read 16S rRNA gene amplicon sequencing data were obtained from the National Institutes of Health Sequence Read Archive from accession number SRP 117611, which were generated as previously described (Summers et al., 2019). Paired-end sequences were unavailable for evaluation; therefore, the publicly available forward-end reads were utilized. Python (v3.7.16) was used to obtain sequences using fasterq-dump (SRA Toolkit v3.0.5) (GitHub, 2023) and then forward primer sequence (5'-GTGCCAGCMGCCGCGGTAA-3′) was removed from all reads using cutadapt (v1.18) (Martin, 2011).

Sequence analysis of the V4 region of 16S rRNA gene amplicons was then performed through R Studio (v2023.03.1 + 446) (R Core Team, 2013). Further sequence trimming, filtering, and chimera removal was performed, including truncation of sequence length to 240 base pairs, and amplicon sequence variants (ASVs) generated using the DADA2 pipeline (v1.18.0) (Callahan et al., 2016). Taxonomy was then assigned to ASVs using the SILVA 16S rRNA sequence database (v138.1) (Quast et al., 2013). Subsequent taxonomy table creation was performed with the phyloseq package (v1.42.0) in R Studio (McMurdie and Holmes, 2013).

Evaluation of microbial community alpha and beta diversity measures utilized both phyloseq (v1.42.0) and vegan (v2.6–4) packages in R Studio (McMurdie and Holmes, 2013; Oksanen et al., 2022). Alpha diversity metrics that were evaluated included total number of observed ASVs, Shannon Diversity Index, and Inverse

Simpson Diversity Index. Further visualization of alpha diversity metrics was generated using GraphPad Prism (Prism 10 v10.1.0 for macOS, GraphPad Software LLC, La Jolla, CA, USA). Beta diversity was assessed using Bray–Curtis dissimilarity distances and visualized via non-metric multidimensional scaling (NMDS) with a stress threshold of <0.2 considered acceptable and plots were generated using ggplot2 (v3.4.0) (Clarke, 1993).

Further evaluation of 16S rRNA gene amplicon sequence taxonomy was performed using National Center for Biotechnology Information (NCBI) Basic Local Alignment Search Tool (BLAST) (Altschul et al., 1990) as well as the NCBI Multiple Sequence Alignment Viewer (v1.25.0).

2.4 Statistical analysis

Within GraphPad Prism, data were assessed for normality with the Shapiro–Wilk test and determined to be non-normally distributed for both relative abundance and fecal bile acid concentration data. The non-parametric two-tailed Mann–Whitney and Kruskal-Wallis tests were applied as appropriate and significance determined following adjustment for false discovery rate (FDR). All FDR tests performed throughout this study used the Benjamini, Krieger, and Yekutieli method (Benjamini et al., 2006).

The alpha diversity metric of total observed ASVs were normally distributed, passing the Shapiro–Wilk test, and thus a parametric one-way ANOVA was applied for multiple comparisons. Differences in microbial community beta diversity were assessed by permutational multivariate analysis of variance (PERMANOVA) using the phyloseq (v1.42.0) and vegan (v2.6–4) packages in R Studio.

Differentially abundant taxa were identified using the DESeq2 package (v1.30.0) in R Studio (Love et al., 2014). Parameters of the test were set to Test = Wald, FitType = Parametric, Cook's Cutoff = FALSE, independentFiltering = FALSE (i.e., not applied to the dataset), and Benjamini-Hochberg post-hoc correction was applied to generate false discovery rate adjusted p values similar to previously described (Nealon et al., 2023). Comparisons were made on a log2 fold change (log2FC) basis and were visualized using the package EnhancedVolcano (v1.16.0) in R Studio.

MetaboAnalyst (v5.0) was used to analyze fecal bile acid concentration data. No additional transformation, scaling, or normalization was performed on concentration data prior to analysis. Analyses performed within MetaboAnalyst included principal component analysis (prcomp package and R script chemometrics.R) and Random Forest machine learning algorithm (randomForest package). All package versions were contained within MetaboAnalyst v5.0 using R (v4.2.2). Additional fecal bile acid concentration heatmap generation was performed in R Studio with the heatmap.2 function from the gplots package (v3.1.3) and hierarchical clustering performed with the hclust function.

Two-tailed Spearman rank correlation using GraphPad Prism and R Studio was used to assess correlations between the relative abundances of taxa and concentration of bile acids detected in fecal samples. Within R Studio, the psych (v2.2.9) package was utilized to first perform Spearman correlation analysis with the corr.test function, then the corrplot package (v0.92) was utilized to visualize the Spearman correlation matrices with the corrplot function.

3 Results

3.1 Fecal ursodeoxycholic acid is reduced in CKD cats

The profiles of fecal bile acid concentrations from healthy cats and cats with CKD were largely similar and demonstrated considerable overlap via principal component analysis (PCA) (Figure 1A). A Random Forest machine learning algorithm was used to assess which fecal bile acid concentrations may be able to best discriminate between healthy cats and cats with CKD (Figure 1B). Of the 15 fecal bile acids, TUDCA and UDCA best discriminated between healthy cats and cats with CKD. UDCA was in significantly greater concentration in feces of healthy cats (median 39.4 ng/mg) than cats with CKD (median 12.8 ng/mg, Mann–Whitney $p = 0.0127$) (Figure 1C). When subdivided by IRIS stage and compared to healthy cats, cats with IRIS Stage 2 CKD had reduced fecal UDCA (median 14.1 ng/mg, FDR adjusted $p = 0.0699$) and cats with IRIS Stage 3 or 4 CKD had significantly reduced fecal UDCA (median 6.2 ng/mg, FDR adj. $p = 0.0092$) (Figure 1D). There were no significant differences when TUDCA was assessed, though TUDCA was only detected in feces from one healthy cat (Figure 1E). In cats with CKD there was a trend of increasing fecal TUDCA concentration with IRIS stage 2 cats (median 0.115 ng/mg, FDR adj. $p = 0.1621$) and cats with IRIS Stage 3 or 4 (median 0.0279 ng/mg, FDR adj. $p = 0.1621$) compared to healthy cats (Figure 1F).

3.2 Gut microbiota members correlate with reduced fecal UDCA in CKD cats

Alpha diversity was significantly reduced in cats with CKD characterized by a reduced number of total observed ASVs in cats with CKD (median 240 ASVs, Mann–Whitney $p = 0.0029$) compared to healthy cats (median 312 ASVs) (Figure 2A). When IRIS stage was considered, both IRIS Stage 2 cats (median 267 ASVs, FDR adjusted $p = 0.0105$) and IRIS Stage 3 or 4 cats (median 229 ASVs, FDR adjusted $p = 0.0001$) had significantly fewer ASVs compared to healthy cats (Figure 2B). Moreover, IRIS Stage 3 or 4 cats had significantly fewer ASVs than cats with IRIS Stage 2 (FDR adjusted $p = 0.0105$) (Figure 2B). The beta diversity assessed by Bray-Curtis distances were not different between healthy cats and cats with CKD (PERMANOVA $p = 0.2205$) (Figure 2C). These findings are in agreement with the original analysis of this publicly available 16S rRNA gene amplicon sequencing data set, which utilized a different bioinformatics pipeline and taxonomy assignment database (Summers et al., 2019).

Differentially abundant ASVs were determined by log2 fold change (log2FC) with DESeq2 when all cats with CKD were compared to healthy cats (Figure 2D). An ASV belonging to the enteropathogen genus *Campylobacter* (ASV 161) was significantly enriched in cats with CKD (log2FC = 21.8, FDR adj. $p < 0.0001$). Separately, a *Peptoclostridium* sp. (ASV 248) was significantly reduced

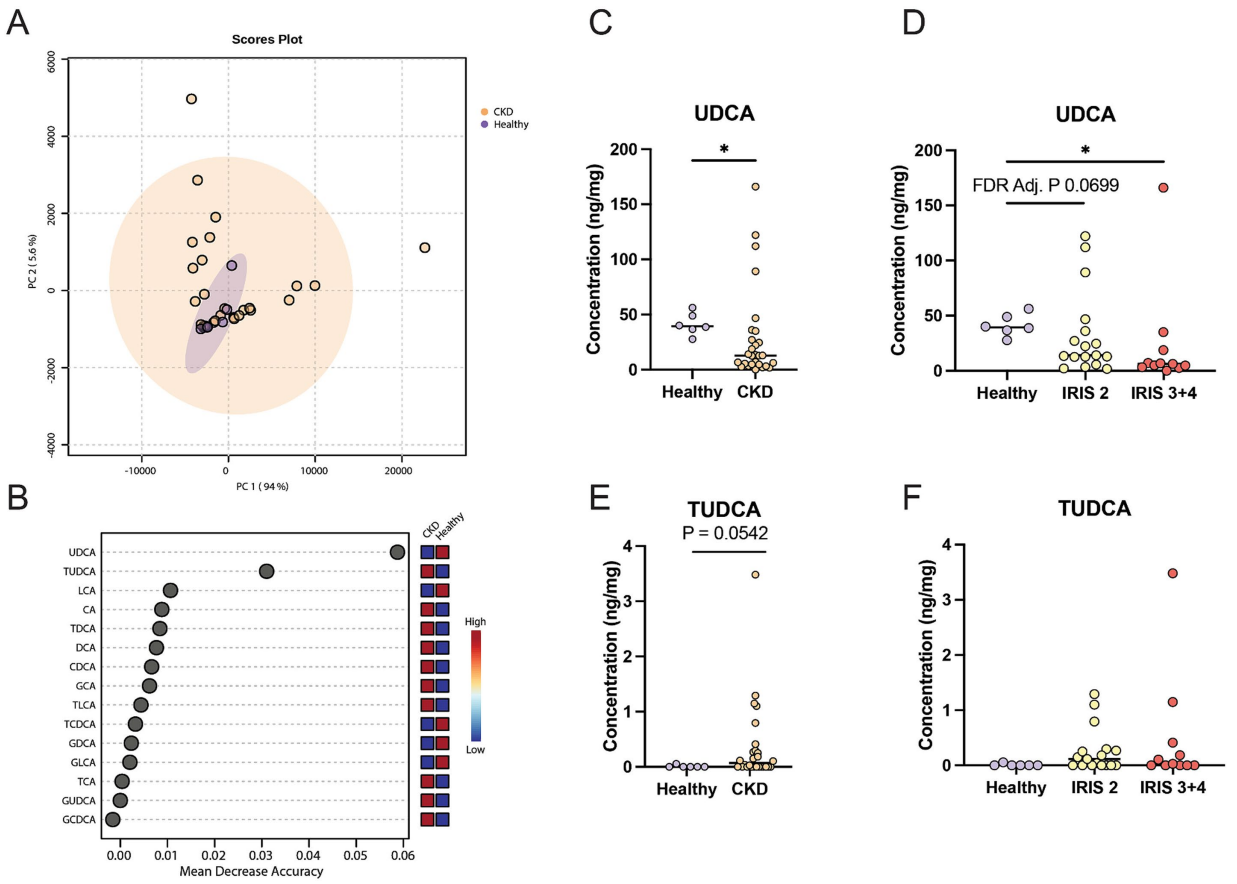

FIGURE 1
Fecal bile acid concentrations in cats with chronic kidney disease. **(A)** Principal component analysis of fecal bile acid concentrations in healthy cats (individual samples represented by purple points) and cats with CKD (individual samples represented by orange points) and a 95% confidence interval clouds for the clustering of each group. Variance explained by each principal component is listed on the corresponding axis. **(B)** Random Forest machine learning algorithm with dots corresponding to a fecal bile acid along the left-hand y-axis and the listed mean decrease in accuracy along the x-axis. Boxes along the right-hand y-axis demonstrate whether the fecal bile acid is high (red) or low (blue) in healthy and CKD cat groups. **(C)** Fecal concentration of UDCA in healthy cats and cats with CKD, significance determined via Mann–Whitney; * $p < 0.05$. **(D)** Fecal concentration of UDCA in healthy cats, cats with IRIS CKD Stage 2, and cats with IRIS CKD Stage 3 or 4, significance determined via Kruskal-Wallis with FDR adjustment; significant discoveries noted by *. **(E)** Fecal concentration of TUDCA in healthy cats and cats with CKD, significance determined via Mann–Whitney. **(F)** Fecal concentration of UDCA in healthy cats, cats with IRIS CKD Stage 2, and cats with IRIS CKD Stage 3 or 4 cats, significance determined via Kruskal-Wallis with FDR adjustment.

in abundance in cats with CKD (log2FC = −25.8, FDR adj. $p < 0.0001$). This ASV was further investigated with NCBI Blast and found to have 99.58% sequence identity with the 16S rRNA gene DNA sequence of *Peptacetobacter hiranonis* (Table 1).

ASVs differentially abundant in only cats with IRIS Stage 3 or 4 CKD compared to healthy cats were also explored to capture microbial alterations that may exist with CKD progression (Figure 2E). Again, the same *Campylobacter* sp. (ASV 161) was enriched in cats with IRIS Stage 3 or 4 CKD (log2FC = 23.3, FDA adj. $p < 0.0001$). Similarly, the same *Peptoclostridium* sp. (ASV 248) was significantly reduced in abundance in cats with IRIS Stage 3 or 4 CKD (log2FC = −30.2, FDR adj. $p < 0.0001$). A microbe identified to the family level as *Lachnospiraceae* (ASV 286) was also significantly reduced in cats with IRIS Stage 3 or 4 CKD (log2FC = −22.8, FDR adj. $p < 0.0001$).

Lachnospiraceae (ASV 286) had a significant moderate positive correlation with fecal UDCA concentration (Spearman $\rho = 0.4478$, $p = 0.0079$) (Figure 3A). *Lachnospiraceae* (ASV 286) was detected in 3/6 healthy cats (median relative abundance = 0.0005%; range = 0–0.37%) and 7/28 CKD cats (median relative abundance = 0%; range = 0–0.20%) (Figure 3B). An uncultured *Clostridia UCG-014* (ASV 151) not identified in the DESeq2 analysis had a stronger significant moderate positive correlation with fecal UDCA concentration (Spearman $\rho = 0.5076$, $p = 0.0022$) (Figure 3C). This *Clostridia UCG-014* (ASV 151) was detected in all healthy cats at a significantly greater relative abundance (median relative abundance = 0.16%; range = 0.04–0.53%) than in cats with CKD where it was detected in 22/28 cats (median relative abundance = 0.004%; range = 0–0.51%; Mann–Whitney $p = 0.0010$) (Figure 3D). *Campylobacter* (ASV 161) had a significant moderate negative correlation with fecal UDCA concentration (Spearman $\rho = -0.3806$, $p = 0.0264$) (Figure 3E). *Campylobacter* (ASV 161) was not detected in any of the healthy cats but was detected in 13/28 of cats with CKD (median relative abundance = 0%; range = 0–0.62%; Mann–Whitney $p = 0.0663$) (Figure 3F).

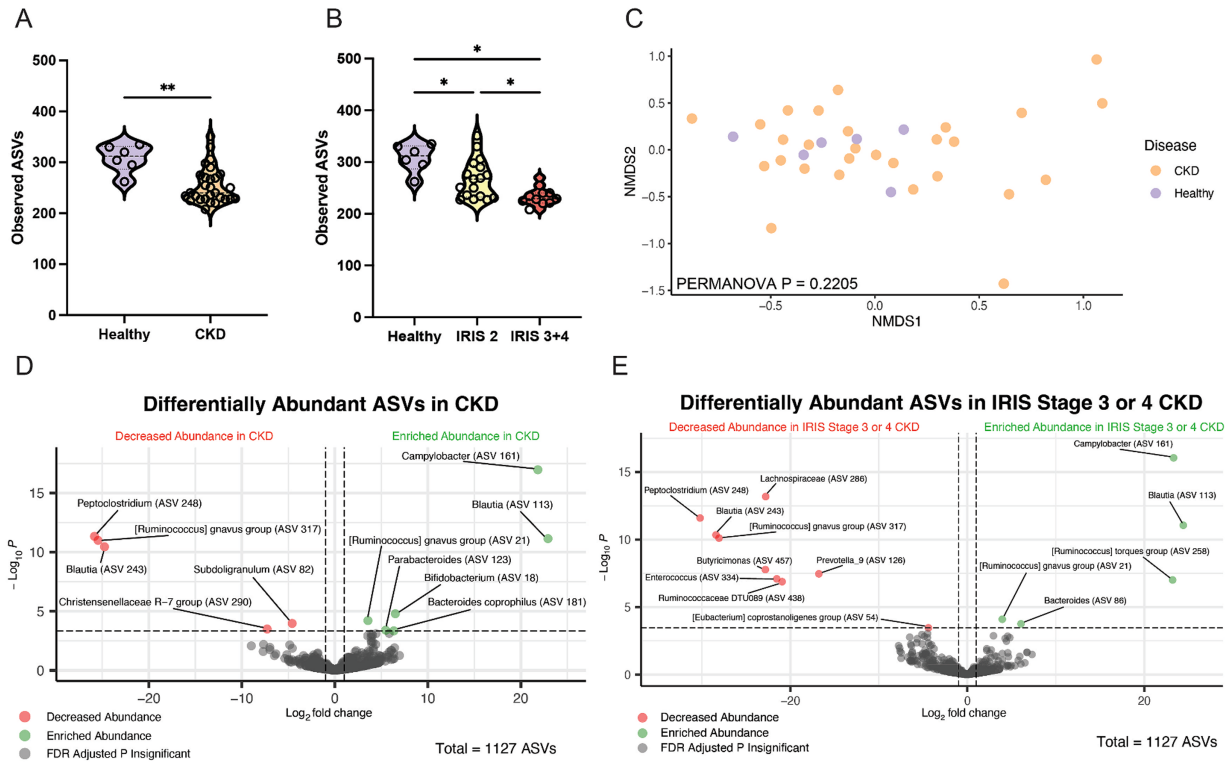

FIGURE 2
Fecal microbiota of cats with chronic kidney disease. **(A)** Alpha diversity in healthy cats and cats with CKD represented by violin plots of total observed ASVs and significance determined via Mann–Whitney; ** $p < 0.01$. **(B)** Alpha diversity in healthy cats, cats with IRIS CKD Stage 2, and cats with IRIS CKD Stage 3 or 4 cats represented by violin plots of total observed ASVs and significance determined via parametric one-way ANOVA with FDR adjustment; significant discoveries noted by *. **(C)** Beta diversity determined with Bray–Curtis dissimilarity distances depicted with non-metric multi-dimensional scaling (NMDS) plot with individual samples represented by points for healthy cats (purple) and cats with CKD (orange) and significance determined with PERMANOVA. **(D)** Volcano plot displaying differentially abundant ASVs determined with DESeq2 that are either reduced in abundance (red) or enriched in abundance (green) in cats with CKD compared to healthy cats. Points maintaining significance following FDR adjustment ($p < 0.05$) and having a log2FC of at least magnitude 2 are plotted and colored. All gray points do not meet these criteria. **(E)** Volcano plot displaying differentially abundant ASVs determined with DESeq2 that are either reduced in abundance (red) or enriched in abundance (green) in cats with IRIS CKD Stage 3 or 4 s compared to healthy. Points maintaining significance following FDR adjustment ($p < 0.05$) and having a log2FC of at least magnitude 2 are plotted and colored. All gray points do not meet these criteria.

3.3 A subpopulation of CKD cats experience fecal bile acid dysmetabolism with <50% secondary bile acids

Within cats with CKD, 29% (8/28) had a fecal bile acid dysmetabolism characterized by the total bile acid composition of <50% SBAs detected (Figure 4A). By contrast, no healthy cats had a composition of fecal bile acids with <50% SBAs. To further investigate this difference, the subpopulation of CKD cats with fecal bile acid dysmetabolism (<50% SBAs) ($n = 8$) were compared to healthy and CKD cats with normal bile acid metabolism (>50% SBAs) ($n = 26$) (Figure 4B). Using Random Forest machine learning algorithm, fecal concentrations of the host derived PBAs CA and CDCA were best able to discriminate between cats with normal bile acid metabolism (defined as >50% SBAs) and those with a bile acid dysmetabolism (<50% SBAs) (Figure 4C). Based on principal component analysis, distinct clustering of the cats with normal bile acid metabolism (>50% SBAs) and those CKD cats with bile acid dysmetabolism (<50% SBAs) is demonstrated (Figure 4D). The relationship of reduced fecal concentration of UDCA in CKD cats was reexamined by comparing healthy cats to CKD cats with normal bile acid metabolism (>50% SBAs) and CKD cats with bile acid dysmetabolism (<50% SBAs). The fecal UDCA concentrations remained significantly reduced in the population of CKD cats with normal bile acid metabolism (>50% SBAs) (median 9.8 ng/mg; FDR adj. $p = 0.0092$) compared to healthy cats (median 39.4 ng/mg) (Figure 4E). However, the fecal concentration of UDCA in CKD cats with bile acid dysmetabolism (<50% SBAs) was not significantly different from healthy cats (median 31.05 ng/mg, FDR adj. $p = 0.2303$) (Figure 4E). In total, using unsupervised hierarchical clustering, the total composition of fecal bile acids clustered by SBA percentage as opposed to disease status (Figure 4F).

3.4 CKD cats with bile acid dysmetabolism (<50% SBAs) have a distinct gut microbial community structure

The microbial community structure of CKD cats with bile acid dysmetabolism (<50% SBAs) was compared to cats with normal bile acid metabolism (>50% SBAs) including healthy and a subset of CKD cats (Figure 5A). Alpha diversity assessed by total ASVs, Shannon Diversity Index, and Inverse Simpson Diversity Index were all

TABLE 1 ASVs identified in cats with at least 97% sequence identity with *P. hiranonis* of the sequenced V4 region of the 16S rRNA gene.

ASV ID	Range % Relative Abundance	V4 region of 16S rRNA gene amplicon sequence 5′-3′	Silva taxonomy (v138.1)	NCBI BLAST Result(s)	Nucleotide Identity (%)
1	0.20–31.33%	TACGTAGGGGGCTAGCGTTATCCGGATTTACTGGGCGTAAAGGGTGCGTAGGCGGTCTTTCAAGTCAGGAGTTAAAGGCTACGGCTCAACCGT AGTAAGCTCCTGATACTGTCTGACTTGAGTGCAG GAGAGGAAAGCGGAATTCCCAGTGTAGCGGTGAAA TGCGTAGATATTGGGAGGAACACCAGTAGCGAAGGCGGCTTTCTGGACTGTAACTGACGCTGAGGCACGAAAGCGTGG	Genus: *Peptoclostridium*	*P. hiranonis*	100%
74	0–4.05%	TACGTAGGGGGCTAGCGTTATCCGGATTTACTGGGCGTAAAGGG TGCGTAGGCGGTCTTTCAAGTCAGGAGTTAAAGGCTACGGCTCAA CCGTAGTAAGCTCCTGATACTGTCTGACTTGAGTGCAGGAGAGGAA AGCGGAATTCCCAGTGTAGCGGTGAAATGCGTAGATATTGGGAGGAA CATCAGTAGCGAAGGCGGCTTTCTGGACTGTAACTGACGCTGAGGCACGAAAGCGTGG	Genus: *Peptoclostridium*	Uncultured *P. hiranonis*	100% 99.58%
94	0–3.11%	TACGTAGGGGGCTAGCGTTATCCGGATTTACTGGGCGTAAAGGGTGCGTAGGCGGTCTTTCAAGTCAGGAGTTAAAGGCTACGGCTCAA CCGTAGTAAGCTCCTGATACTGTCTGACTTGAGTGCAGGAGAGGAAAGTGGAATTCCCAGTGTAGCGGTGAAATGCGTAGATATTGGGAGGAACA CCAGTAGCGAAGGCGGCTTTCTGGACTGTAACTGACGCTGAGGCACGAAAGCGTGG	Genus: *Peptoclostridium*	*C. hiranonis* *P. hiranonis*	100% 99.58%
115	0–1.59%	TACGTAGGGGGCTAGCGTTATCCGGATTTACTGGGCGTAAAGGGTGCGTAGGTGGTCTTTCAAGTCAGGAGTTAAAGGCTACGGCTCAACCGTAGTA AGCTCCTGATACTGTCTGACTTGAGTGCAGGAGAGGAAAGCGGAATTCCCAGTGTAGCGGTGAAATGCGTAGATATTGGGAGGAACACCAGTAG CGAAGGCGGCTTTCTGGACTGTAACTGACGCTGAGGCACGAAAGCGTGG	Genus: *Peptoclostridium*	*P. hiranonis*	99.58%
137	0–4.12%	TACGTAGGGGGCTAGCGTTATCCGGATTTACTGGGCGTAAAGGGTGC GTAGGCGGTCTTTCAAGTCAGGAGTTAAAGGCTACGGCTCAACCGTAG TAAGCTCCTGATACTATCTGACTTGAGTGCAGGAGAGGAAAGCGGAATTCCCAGTGTAGCGGTGAAATGCGTAGATATTGGGAGGAACACCAG TAGCGAAGGCGGCTTTCTGGACTGTAACTGACGCTGAGGCACGAAAGCGTGG	Genus: *Peptoclostridium*	*P. hiranonis*	99.58%
165	0–2.71%	TACGTAGGGGGTTAGCGTTATCCGGATTTACTGGGCGTAAAGGGTGCGTAGGCGGTCTTTCAAGTCAGGAGTTAAAGGCTACGGCTCAACCGTAGTA AGCTCCTGATACTGTCTGACTTGAGTGCAGGAGAGGAAAGCGGAATTCCCAGTGTAGCGGTGAAATGCGTAGATATTGGGAGGAACACCA GTAGCGAAGGCGGCTTTCTGGACTGTAACTGACGCTGAGGCACGAAAGCGTGG	Genus: *Peptoclostridium*	*P. hiranonis*	99.58%
176	0–1.70%	TACGTAGGGGGCTAGCGTTATCCGGATTTACTGGGCGTAAAGGGTGCGT AGGCGGTCTTTCAAGTCAGGAGTTAAAGGCTACGGCTCAACCGT AGTAAG CTCCTGATACTGTCTGACTTGAGTGCAGGAGAGGAAAGCGGAATTCCCAG TGTAGCGGTGAAATGCGTAGATATTGGGAGGAACAC CAGTAGCGAAGGCGGTTTTCTGGACTGTAACTGACGCTGAGGCACGAAAGCGTGG	Genus: *Peptoclostridium*	*P. hiranonis*	99.58%
226	0–1.51%	TACGTAGGGGGCTAGCGTTATCCGGATTTACTGGGCGTAAAGGGTGCGTA GGCGGTCTTTCAAGTCAGGAGTTAAAGGCTACGGCTCAACCGTA GTAAGC TCCTGATACTGTCTGACTTGAGTGCAGGAGAGGAAAGCGGAATTCCCAGT GTAGTGGTGAAATGCGTAGATATTGGGAGGAACACCAGTAGC GAAGGCGGCTTTCTGGACTGTAACTGACGCTGAGGCACGAAAGCGTGG	Genus: *Peptoclostridium*	Uncultured *P. hiranonis*	100% 99.58%
236	0–1.34%	TACGTAGGGGGCTAGCGTTATCCGGATTTACTGGGCGTAAAGGGTGCGTA GGCAGTCTTTCAAGTCAGGAGTTAAAGGCTACGGCTCAAC CGTAGTAAGC TCCTGATACTGTCTGACTTGAGTGCAGGAGAGGAAAGCGGAATTCCCAGT GTAGCGGTGAAATGCGTAGATATTGGGAGGAACACCA GTAGCGAAGGCGGCTTTCTGGACTGTAACTGACGCTGAGGCACGAAAGCGTGG	Genus: *Peptoclostridium*	*P. hiranonis*	99.58%
248	0–0.67%	TACGTAGGGGGCTAGCGTTATCCGGATTTACTGGGCGTAAAGGGTGCGT AGGCGGTCTTTCAAGTCAGGAGTTAAAGGCTACGGCTCAAC CGTAGTAAG CTCCTGATACTGTCTGACTTGAGTGTAGGAGAGGAAAGCGGAATTCCCAG TGTAGCGGTGAAATGCGTAGATATTGGGAGGAACACC AGTAGCGAAGGCGGCTTTCTGGACTGTAACTGACGCTGAGGCACGAAAGCGTGG	Genus: *Peptoclostridium*	*P. hiranonis*	99.58%
256	0–1.15%	TACGTAGGGGGCTAGCGTTATCCGGATTTACTGGGCGTAAAGGGTGCGTA GGTGGTCTTTCAAGTCAGGAGTTAAAGGCTACGGCTCA ACCGTAGTAAGC TCCTGATACTGTCTGACTTGAGTGCAGGAGAGGAAAGCGGAATTCCCAGT GTAGTGGTGAAATGCGTAGATATTGGGAGG AACACCAGTAGCGAAGGCGGCTTTCTGGACTGTAACTGACGCTGAGGCACGAAAGCGTGG	Genus: *Peptoclostridium*	Uncultured *P. hiranonis*	99.58% 99.17%

(Continued)

10.3389/fmicb.2024.1458090

TABLE 1 (Continued)

ASV ID	Range % Relative Abundance	V4 region of 16S rRNA gene amplicon sequence 5′-3′	Silva taxonomy (v138.1)	NCBI BLAST Result(s)	Nucleotide Identity (%)
265	0–1.06%	TACGTAGGGGGCTAGCGTTATCCGGATTTACTGGGCGTAAAGGGTGCGTA GGCGGTCTCTCAAGTCAGGAGTTAAAGGCTACGGCTCAACCGTAGT AAGC TCCTGATACTGTCTGACTTGAGTGCAGGAGAGGAAAGCGGAATTCCCAGT GTAGCGGTGAAATGCGTAGATATTGGGAGGAACACCAGTAGC GAAGGCGGCTTTCTGGACTGTAACTGACGCTGAGGCACGAAAGCGTGG	Genus: *Peptoclostridium*	*P. hiranonis*	99.58%
297	0–0.77%	TACGTAGGGGGCTAGCGTTATCCGGATTTACTGGGCGTAAAGGGTGCGTA GGCGGTCTTTCAAGTCAGGAGTTAAAGACTACGGCTCAACCGTAGTA AGCTCCTGATACTGTCTGACTTGAGTGCAGGAGAGGAAAGCGGAATTCCCAGT GTAGCGGTGAAATGCGTAGATATTGGGAGGAACACCAGT AGCGAAGGCGGCTTTCTGGACTGTAACTGACGCTGAGGCACGAAAGCGTGG	Genus: *Peptoclostridium*	Uncultured *P. hiranonis*	100% 99.58%
308	0–0.43%	TACGTAGGGGGCTAGCGTTATCCGGATTTACTGGGCGTAAAGGGTGCGTAGGCGGTCTTTCAAGTCAGGAGTTAAAGGCTACGGCTCAACTGTAGTAAG CTCCTGATACTGTCTGACTTGAGTGCAGGAGAGGAAAGCGGAATTCCCAGTGTAGCGGTGAAATGCGTAGATATTGGGAGGAACACCAGTAGCGAAGGCG GCTTTCTGGACTGTAACTGACGCTGAGGCACGAAAGCGTGG	Genus: *Peptoclostridium*	Uncultured *P. hiranonis*	100% 99.58%
323	0–0.62%	TACGTAGGGGGCTAGCGTTATCCGGATTTACTGGGCGTAAAGGGTGCGTAGGCGGTCTTTCAAGTCAGGAGTTAAAGGCTACGGCTCAACCGTAGTAA GCTCCTGGTACTGTCTGACTTGAGTGCAGGAGAGGAAAGCGGAATTCCCAGTGTAGCGGTGAAATGCGTAGATATTGGGAGGAACACCAGTAGCAAA GGCGGCTTTCTGGACTGTAACTGACGCTGAGGCACGAAAGCGTGG	Genus: *Peptoclostridium*	*P. hiranonis*	99.17%
325	0–0.61%	TACGTAGGGGGCTAGCGTTATCCGGATTTACTGGGCGTAAAGGGTGCGTAGGCGGTCTTTCAAGTCAGGAGTTAAAGGCTACGGCTCAACCGT AGTAAGCTCCTGATACTGTCTGACTTGAGTGCAGGAGAGGAAAACGGAATTCCCAGTGTAGCGGTGAAATGCGTAGATATTGGGAGGAACACC AGTAGCGAAGGCGGCTTTCTGGACTGTAACTGACGCTGAGGCACGAAAGCGTGG	Genus: *Peptoclostridium*	Uncultured *P. hiranonis*	100% 99.58%
342	0–0.56%	TACGTAGGGGGCTAGCGTTATCCGGATTTACTGGGCGTAAAGGGTGCGTAGGCGGTCTTTCAAGTCAGGAGTTAAAGGCTACGGCTCAACC GTAGTAAGCTCCTGATACTGTCTGACTTGAGTGCAGGAGAGGAAAGCGGAATTCCCAGTGTAGCGGTGAAATGCGTAGATATTGGGAGGAACAC CAGTAGCGAAGGCGGCTTTCTGGACTGTGACTGACGCTGAGGCACGAAAGCGTGG	Genus: *Peptoclostridium*	*P. hiranonis*	99.58%
374	0–0.49%	TACGTAGGGGGCTAGCGTTATCCGGATTTACTGGGCGTAAAGGGTGCGTAGGCGGTCTTTCAAGTCAGGAGTTAAAGGCTACGGCTCAACCGT AGTAAGCTCCTGATACTGTCTGACTTGAGTGCAGGAGAGGAAAGCGGAATTCCCAGTGTAGCGGTGAAATGCGTAGATATTGGGAGGAACACT AGTAGCGAAGGCGGCTTTCTGGACTGTAACTGACGCTGAGGCACGAAAGCGTGG	Genus: *Peptoclostridium*	Uncultured *P. hiranonis*	100% 99.58%
392	0–0.43%	TACGTAGGGGGCTAGCGTTATCCGGATTTACTGGGCGTAAAGGGTGCGTAGGCGGTCTTTCAAGTCAGGAGTTAAAGGCTACGGCTTAA CCGTAGTAAGCTCCTGATACTGTCTGACTTGAGTGCAGGAGAGGAAAGCGGAATTCCCAGTGTAGCGGTGAAATGCGTAGATATTGGGAGGA ACACCAGTAGCGAAGGCGGCTTTCTGGACTGTAACTGACGCTGAGGCACGAAAGCGTGG	Genus: *Peptoclostridium*	Uncultured *P. hiranonis*	100% 99.58%
393	0–0.43%	TACGTAGGGGGCTAGCGTTATCCGGATTTACTGGGCGTAAAGGGTGCGTAGGCGGTCTTTCAAGTCAGGAGTTAAAGGCTACGGCTCA ACCGTAGTAAGCTCCTGATACTGTCTGACTTGAGTTCAGGAGAGGAAAGCGGAATTCCCAGTGTAGCGGTGAAATGCGTAGATAT TGGGAGGAACACCAGTAGCGAAGGCGGCTTTCTGGACTGTAACTGACGCTGAGGCACGAAAGCGTGG	Genus: *Peptoclostridium*	*P. hiranonis*	99.58%
408	0–0.40%	TACGTAGGGGGCTAGCGTTATCCGGATTTACTGGGCGTAAAGGGTGCGTAGGCGGTCTTTCAAGTCAGGAGTTAAAGGCTACGGCTCAACC GTAGTAAGCTCCTGATACTGTCTGACTTGAGTGCAGGAGAGGAAAGCGGAATTCCCAGTGTAGCGGTGAAATGCGTAGATATTGGGAGGAATACC AGTAGCGAAGGCGGCTTTCTGGACTGTAACTGACGCTGAGGCACGAAAGCGTGG	Genus: *Peptoclostridium*	Uncultured *P. hiranonis*	100% 99.58%
442	0–0.04%	TACGTAGGGGGCTAGCGTTATCCGGATTTACTGGGCGTAAAGGGTGCGTAGGCGGTCTTTCAAGTCAGGAGTTAAAGGCTACGGCTCAA CCGTAGTAAGCTCCTGATACTGTCTGACTTGAGTGCAGGAGAGGAAAGCGGAATTCCCAGTGTAGCGGTGAAATGCGTAGATATTGGGAG GAACACCAGTAGCGAAGGCGGCTTTCTGGACTGTAACTGACGCTGAGGCACGAAAGCTGGG	Genus: *Peptoclostridium*	*P. hiranonis*	99.58%
461	0–0.29%	TACGTAGGGGGCTAGCGTTATCCGGATTTACTGGGCGTAAAGGGTGCGTAGGCGGTCTTTCAAGTCAGGAGTTAAAGGCTACA GCTCAACCGTAGTAAGCTCCTGATACTGTCTGACTTGAGTGCAGGAGAGGAAAGCGGAATTCCCAGTGTAGCGGTGAAATGCGTAGATATTGGGA GGAACACCAGTAGCGAAGGCGGCTTTCTGGACTGTAACTGACGCTGAGGCACGAAAGCGTGG	Genus: *Peptoclostridium*	*P. hiranonis*	99.58%

(Continued)

10.3389/fmicb.2024.1458090

TABLE 1 (Continued)

ASV ID	Range % Relative Abundance	V4 region of 16S rRNA gene amplicon sequence 5′-3′	Silva taxonomy (v138.1)	NCBI BLAST Result(s)	Nucleotide Identity (%)
495	0–0.25%	TACGTAGGGGGCTAGCGTTATCCGGATTTACTGGGCGTAAAGGGTGCGTAGGCGGTCTTTCAAGTCAAGAGTTAAAGGCTACGGCT CAACCGTAGTAAGCTCCTGATACTGTCTGACTTGAGTGCAGGAGAGGAAAGCGGAATTCCCAGTGTAGCGGTGAAATGCGTAGATATTGGG AGGAACACCAGTAGCGAAGGCGGCTTTCTGGACTGTAACTGACGCTGAGGCACGAAAGCGTGG	Genus: *Peptoclostridium*	*P. hiranonis*	99.58%
531	0–0.22%	TACGTAGGGGGCTAGCGTTATCCGGATTTACTGGGCGTAAAGGGTGCGTAGGCGGTCTTTCAAGTCAGGAGTTAAAGGCTACGGCTC AACCGTAGTAAGCTCCTGATACTGTTTGACTTGAGTGCAGGAGAGGAAAGTGGAATTCCCAGTGTAGCGGTGAAATGCGTAGATATTG GGAGGAACACCAGTAGCGAAGGCGGCTTTCTGGACTGTAACTGACGCTGAGGCACGAAAGCGTGG	Genus: *Peptoclostridium*	*C. hiranonis* *P. hiranonis*	99.58% 99.17%
558	0–0.06%	TACGTAGGGGGCTAGCGTTATCCGGATTTACTGGGCGTAAAGGGTGCGTAGGCGGTCTTTCAAGTCAGGAGTTTAAAGGCTACGGCT CAACCGTAGTAAGCTCCTGATACTGTCTGACTTGAGTGCAGGAGAAAGCGGAATTCCCAGTGTAGCGGTGAAATGCGTAGATATTAG GAGGAACATCAGTGGCGAAGGCGGCTTACTGGACTGAAACTGACACTGAGGCACGAAAGCGTGG	Family: Peptostreptococcaceae	Uncultured *P. hiranonis*	97.92% 97.50%
589	0–0.16%	TACGTAGGGGGCTAGCGTTATCCGGATTTACTGGGCGTAAAGGGTGCGTAGGCGGTCTTTCAAGTCAGGAGTTTAAAGGCTACGGCTC AACCGTAGTAAGCTCCTGATACTGTCTGACTTGAGTGCAGGAGAAAGCGGAATTCCCAGTGTAGCGGTGAAATGCGTAGATATTGGGAG GAACACCAGTGGCGAAGGCGGCTTTCTGGACTGTAACTGACGCTGAGGCACGAAAGCGTGG	Genus: *Peptoclostridium*	Uncultured *P. hiranonis*	100% 99.58%
707	0–0.08%	TACGTAGGGGGCTAGCGTTATCCGGATTTACTGGGCGTAAAGGGTGCGTAGGTGGTCTTTCAAGTCAGGAGTTTAAAGGCTACGGCTC AACCGTAGTAAGCTCCTGATACTGTCTGACTTGAGTGCAGGAGAGGAAAGTGGAATTCCCAGTGTAGCGGTGAAATGCGTAGATATTGGG AGGAACACCAGTAGCGAAGGCGGCTTTCTGGACTGTAACTGACGCTGAGGCACGAAAGCGTGG	Genus: *Peptoclostridium*	*C. hiranonis* *P. hiranonis*	99.58% 99.17%

significantly reduced in cats with CKD with bile acid dysmetabolism (<50% SBAs) when compared to both healthy cats (FDR adj. $p = 0.006$, 0.009, and 0.0096, respectively) and CKD cats with normal bile acid metabolism (>50% SBAs) (FDR adj. $p = 0.0427$, 0.0017, and 0.0438, respectively) (Figures 5B–D). Beta diversity assessed with Bray–Curtis dissimilarity distances was significantly different in CKD cats with bile acid dysmetabolism (<50% SBAs) when compared to both healthy cats and CKD cats with normal bile acid metabolism (>50% SBAs) (PERMANOVA $p < 0.001$) (Figure 5A). Differentially abundant ASVs were determined with DESeq2 when CKD cats with bile acid dysmetabolism (<50% SBAs) were compared to healthy and CKD cats with normal bile acid metabolism (>50% SBAs). *Lachnospiraceae* (ASV 305) was significantly reduced in CKD cats with bile acid dysmetabolism (<50% SBAs) (log2FC = −21.6, FDR adj. $p < 0.0001$). Sorted by FDR adjusted *p*-value, the next three ASVs also found to be significantly reduced were *Roseburia* sp. (ASV 66) (log2FC = −4.8, FDR adj. $p = 0.0013$), *Oscillibacter* sp. (ASV 152) (log2FC = −3.4, FDR adj. $p = 0.0016$), and *Desulfovibrio* sp. (ASV 56) (log2FC = −5.2, FDR adj. p = 0.0016) (Figure 5E). The top three ASVs enriched in CKD cats with bile acid dysmetabolism (<50% SBAs) were *Blautia* sp. (ASV 192) (log2FC = 26.4, FDR adj. $p < 0.0001$), *Olsenella* sp. (ASV 7) (log2FC = 6.9, FDR adj. p < 0.0001), and *Peptoclostridium* sp. (ASV 308) (log2FC = 24.3, FDR adj. $p < 0.0001$) (Figure 5E). The *Peptoclostridium* sp. (ASV 308) was also investigated for sequence similarity to *P. hiranonis* with NCBI Blast and found to have 99.58% sequence identity (Table 1).

Given that *P. hiranonis* produces SBAs via the *bai* operon, it was unexpected for an ASV with sequence similarity to this organism to have increased relative abundance in cats with reduced SBAs; thus, all ASVs with a family level taxonomic assignment of *Peptostreptococcaceae* ($n = 65$ ASVs) were screened with NCBI Blast for sequence similarity to *P. hiranonis* (Table 1). A total of 26 ASVs with at least 97% sequence identity to the *P. hiranonis* complete genome isolate in NCBI were identified. Multiple sequence alignment using ASV 1 (identified as with *P. hiranonis*) as the consensus sequence was performed to visualize locations of nucleotide variation with sequences from the V4 region of the 16S rRNA gene amongst the 26 ASVs consistent with *P. hiranonis* (Figure 6A). Additionally, the proportion of which ASVs made up the composition of total ASVs with at least 97% sequence identity to *P. hiranonis* within a single fecal sample were also visualized, with ASV 1 contributing at minimum 73% of all *P. hiranonis* relative abundance to all fecal samples (Figure 6B).

3.5 Reduced relative abundance of *Peptacetobacter hiranonis*, *Roseburia*, and *Oscillospirales* ASVs in CKD cats with bile acid dysmetabolism (<50% SBAs) correlate with fecal bile acid composition

All ASVs identified as differentially abundant in CKD cats with bile acid dysmetabolism (<50% SBAs) were assessed for significant correlations with the fecal bile acid composition (Figure 7). Of those, *Roseburia* (ASV 66) was significantly positively correlated with the SBA LCA (Spearman $\rho = 0.6442$, FDR adj. $p = 0.0150$). *Roseburia* sp. (ASV 66) amplicon sequence had 98.75% sequence identity to *Roseburia intestinalis* when compared to the reference 16S rRNA gene sequence with NCBI Blast. Additionally, *Oscillibacter* sp. (ASV 152) was significantly negatively correlated with the PBAs CA (Spearman

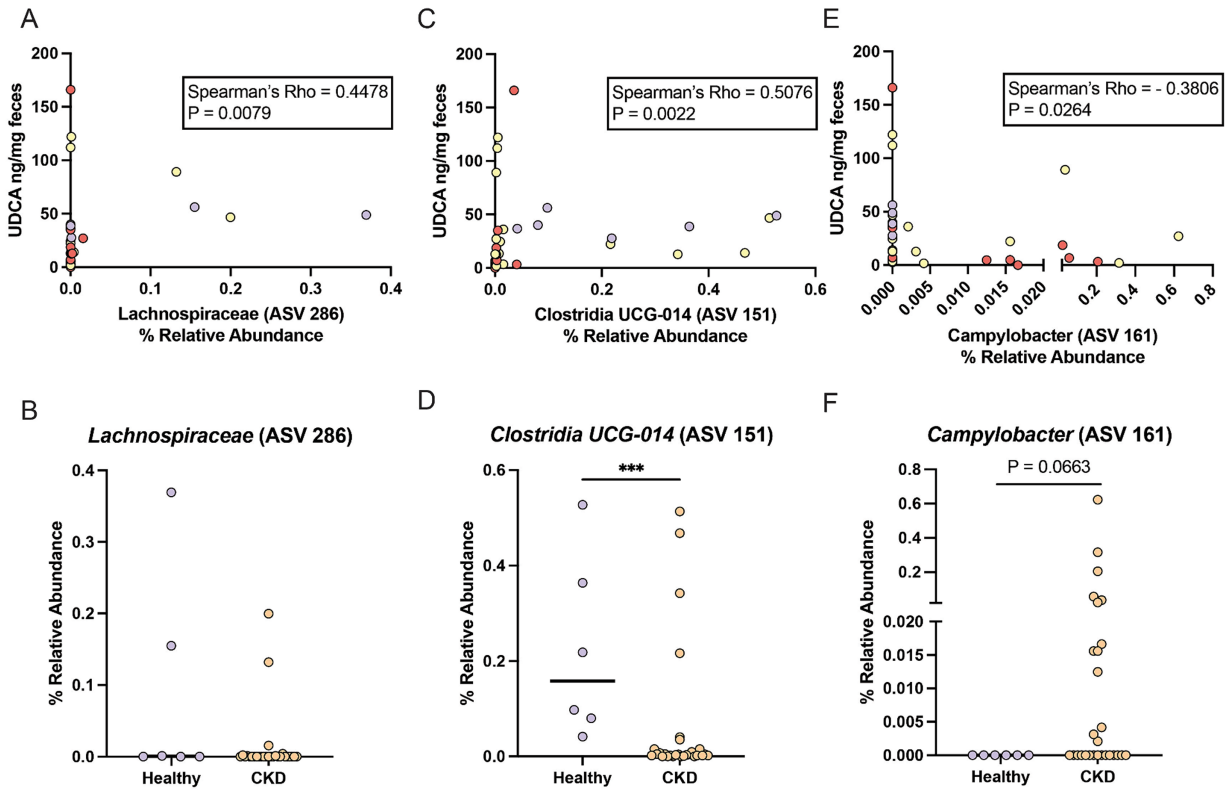

FIGURE 3
ASVs that correlate with reduced fecal UDCA concentrations in cats with CKD and healthy cats. **(A)** Spearman correlation of the relative abundance of *Lachnospiraceae* (ASV 286) and fecal UDCA concentration. Points are colored by healthy cats (purple), cats with IRIS CKD Stage 2 (yellow) and cats with IRIS CKD Stage 3 or 4 (red). **(B)** Relative abundance of *Lachnospiraceae* (ASV 286) in healthy cats (purple) and cats with CKD (orange) with significance determined by Mann–Whitney. **(C)** Spearman correlation of the relative abundance of *Clostridia UCG-014* (ASV 151) and fecal UDCA concentration. Points are colored by healthy cats (purple), cats with IRIS CKD Stage 2 (yellow) and cats with IRIS CKD Stage 3 or 4 (red). **(D)** Relative abundance of *Clostridia UCG-014* (ASV 151) in healthy cats (purple) and cats with CKD (orange) with significance determined by Mann–Whitney; *** $p < 0.001$. **(E)** Spearman correlation of the relative abundance of *Campylobacter* (ASV 161) and fecal UDCA concentration. Points are colored by healthy cats (purple), cats with IRIS CKD Stage 2 (yellow) and cats with IRIS CKD Stage 3 or 4 (red). **(F)** Relative abundance of *Campylobacter* (ASV 161) in healthy cats (purple) and cats with CKD (orange) with significance determined by Mann–Whitney.

ρ = −0.7551, FDR adj. $p = 0.0003$) and GCA (Spearman $\rho = -0.6443$, FDR adj. $p = 0.0150$) and the SBA TUDCA (Spearman $\rho = -0.6229$, FDR adj. $p = 0.0238$).

Given that *Oscillibacter* taxonomically is within the order *Oscillospirales* and family *Oscillospiraceae*, which have metagenomically been described to contain the *bai* operon and possibly contribute to SBA production (Vital et al., 2019; Kim et al., 2022), the dataset was further screened for taxonomically similar organisms with similar correlation pattern to the fecal bile acid composition as *Oscillibacter*. This screening produced two additional ASVs within the order *Oscillospirales* (Table 2), one uncultured *UBA1819* genus within the *Ruminococcaceae* family (ASV 157) and one *Colidextribacter* sp. (ASV 186).

These two ASVs, along with the previously identified *Oscillibacter* sp. (ASV 152) and *Roseburia* sp. (ASV 66), as well as the total relative abundance of the 26 ASVs with at least 97% sequence identity to *P. hiranonis* were all assessed for correlation with the fecal bile acid composition (Figure 8A). The total relative abundance of the 26 *P. hiranonis* ASVs had significant positive correlation with the SBAs DCA (Spearman $\rho = 0.5218$, FDR adj. $p = 0.0407$) and LCA (Spearman ρ = 0.5615, FDR adj. $p = 0.0156$). The relative abundance of *P. hiranonis* ASVs was significantly reduced in CKD cats with bile acid dysmetabolism (<50% SBAs) (median relative abundance = 2.1%; range = 0.21–5.67%) compared to CKD cats with normal bile acid metabolism (>50% SBAs) (median relative abundance = 13.9%; range = 2.92–42.02%; FDR adj. $p = 0.0002$) and healthy cats (median relative abundance = 9.7%; range = 3.27–31.38%; FDR adj. $p = 0.0112$) (Figure 8B).

Roseburia sp. (ASV 66) relative abundance had a significant negative correlation with the PBA CA (Spearman $\rho = -0.5841$, FDR adj. $p = 0.0105$) and significant positive correlation with the SBA LCA (Spearman $\rho = 0.6442$, FDR adj. $p = 0.0023$) (Figure 8A). The relative abundance of *Roseburia* sp. (ASV 66) in CKD cats with bile acid dysmetabolism (<50% SBAs) (median relative abundance = 0.011%; range = 0.0031–0.036%) was not statistically significantly reduced compared to CKD cats with normal bile acid metabolism (>50% SBA) (median relative abundance = 0.22%; range = 0–2.66%; FDR adj. $p = 0.0674$) or healthy cats (median relative abundance = 0.20%; range = 0.019–1.72%; FDR adj. $p = 0.0600$) (Figure 8C).

Oscillibacter sp. (ASV 152) relative abundance had a significant negative correlation with the PBAs CA (Spearman $\rho = -0.7551$, FDR adj. $p < 0.0001$), CDCA (Spearman $\rho = -0.5719$, FDR adj. $p = 0.0126$), and GCA (Spearman $\rho = -0.6443$, FDR adj. $p = 0.0023$) as well as the SBA TUDCA (Spearman $\rho = -0.6229$, FDR adj. $p = 0.0038$)

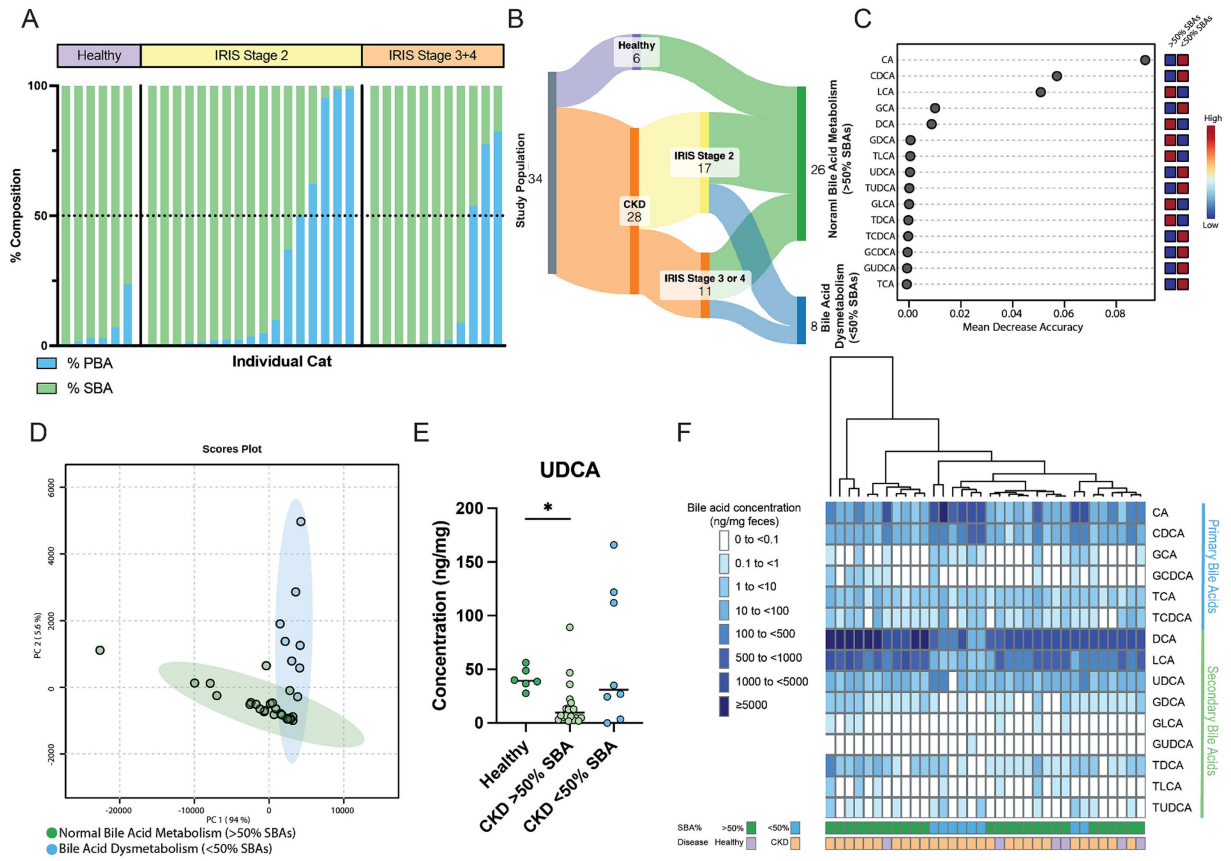

FIGURE 4
Distinct fecal bile acid pool composition in CKD cats with bile acid dysmetabolism characterized by <50% SBAs. **(A)** Stacked bar chart demonstrating the composition of PBAs (blue) and SBAs (green) in the feline fecal bile acid pool. A horizontal dotted line demarcates 50% composition. Each bar along the x-axis represents an individual cat, with individuals grouped by healthy or IRIS CKD Stage. **(B)** Sankey diagram demonstrating cats within normal bile acid metabolism (>50% SBAs) and bile acid dysmetabolism (<50% SBAs) groups. **(C)** Random Forest machine learning algorithm with dots corresponding to a fecal bile acid along the left-hand y-axis and the listed mean decrease in accuracy along the x-axis. Boxes along the right-hand y-axis demonstrate whether the fecal bile acid is high (red) or low (blue) in normal bile acid metabolism (>50% SBAs) and bile acid dysmetabolism (<50% SBAs) groups. **(D)** Principal component analysis of fecal bile acid concentrations in CKD cats with normal bile acid metabolism (>50% SBAs) (individual samples represented by green points) and CKD cats with bile acid dysmetabolism (<50% SBAs) (individual samples represented by blue points) and a 95% confidence interval clouds for the clustering of each group. Variance explained by each principal component is listed on the corresponding axis. **(E)** Fecal concentration of UDCA in healthy cats, CKD cats with normal bile acid metabolism (>50% SBAs), and CKD cats with bile acid dysmetabolism (<50% SBAs); significance determined via Kruskal-Wallis with FDR adjustment, significant discoveries noted by *. **(F)** Unsupervised hierarchical clustering of fecal bile acid composition. Individual samples are in columns and are colored along the bottom x-axis by both percentage of SBA and disease status. Each row represents a single bile acid listed along the right-hand y-axis. Shade of blue within a square corresponds to the concentration (ng/mg of feces) of each bile acid, with breakpoint concentrations by color shown at the left-hand side of the figure mat. Dendrogram at the top represents relative sample similarity determined by hclust in R Studio.

(Figure 8A). The relative abundance of *Oscillibacter* sp. (ASV 152) was significantly reduced in CKD cats with bile acid dysmetabolism (<50% SBAs) (median relative abundance = 0.0057%; range = 0–0.024%) compared to CKD cats with normal bile acid metabolism (>50% SBAs) (median relative abundance = 0.059%; range = 0.0052–0.34%; FDR adj. $p = 0.0008$) and healthy cats (median relative abundance = 0.096%; range = 0.034–0.18%; FDR adj. $p = 0.0009$) (Figure 8D).

Ruminococcaceae UBA1819 sp. (ASV 157) relative abundance had a significant negative correlation with the PBAs CA (Spearman $\rho = -0.8176$, FDR adj. $p < 0.0001$), CDCA (Spearman $\rho = -0.6475$, FDR adj. $p = 0.0023$), and GCA (Spearman $\rho = -0.5143$, FDR adj. $p = 0.0428$) as well as the SBA TUDCA (Spearman $\rho = -0.6071$, FDR adj. $p = 0.0058$) (Figure 8A). The relative abundance of *Ruminococcaceae UBA1819* sp. (ASV 157) was significantly reduced in CKD cats with bile acid dysmetabolism (<50% SBAs) (median relative abundance = 0.0016%; range = 0–0.20%) compared to CKD cats with normal bile acid metabolism (>50% SBAs) (median relative abundance = 0.024%; range = 0–1.26%; FDR adj. $p = 0.0011$) and healthy cats (median relative abundance = 0.069%; range = 0.0083–0.14%; FDR adj. $p = 0.0011$) (Figure 8E).

Colidextribacter sp. (ASV 186) relative abundance had a significant negative correlation with the PBAs CA (Spearman $\rho = -0.7560$, FDR adj. $p < 0.0001$), CDCA (Spearman $\rho = -0.5188$, FDR adj. $p = 0.0409$), and GCA (Spearman $\rho = -0.5809$, FDR adj. $p = 0.0105$) as well as a significant positive correlation with the SBA LCA (Spearman $\rho = 0.6417$, FDR adj. $p = 0.0023$) (Figure 8A). The relative abundance of *Colidextribacter* sp. (ASV 186) was significantly reduced in CKD cats with bile acid dysmetabolism (<50% SBAs) (median relative abundance = 0.0026%; range = 0–0.038%; range = 0–0.26%) compared

10.3389/fmicb.2024.1458090

TABLE 2 ASVs from the order *Oscillospirales* with significant correlations to fecal bile acid composition in cats.

ASV ID	Range % Relative Abundance	V4 region of 16S rRNA Gene Amplicon Sequence 5′-3′	Silva Taxonomy (v138.1)	NCBI BLAST Result(s)	Nucleotide Identity (%)
152	0–0.34%	TACGTAGGTGGCAAGCGTTGTCCGGATTTACTGGGTGTAAAGGGCGTGCAGCCGGCCGGCA AGTCAGATGTGAAATCTGGAGGCTTAACCTCCAAACTGCATTTGAAACTGTAGGTCTTGAGT ACCGGAGAGGTTATCGGAATTCCTTGTGTAGCGGTGAAATGCGTAGATATAAGGAAGAACAC CAGTGGCGAAGGCGGATAACTGGACGGCAACTGACGGTGAGGCGCGAAAGCGTG	Order: Oscillospirales Family: Oscillospiraceae Genus: *Oscillibacter*	*Oscillibacter* sp. PEA192 DNA, complete genome Dysosmobacter welbionis strain J115 chromosome, complete genome	100% 100%
157	0–1.26%	AACGTAGGGTGCAAGCGTTGTCCGGAATTACTGGGTGTAAAGGGAGCGCAGGCGGATTGGCAA GTTGGGAGTGAAATCTATGGCTCAACCCATAAATTGCTTTCAAACTGTCAGTCTTGAGTGGT GTAGAGGTAGGCGGAATTCCCGGTGTAGCGGTGGAATGCGTAGATATCGGGAGGAACACCAGTGG CGAAGGCGGCCTACTGGGCACTAACTGACGCTGAGGCTCGAAAGCATG	Order: Oscillospirales Family: Ruminococcaceae Genus: UBA1819	*Ruthenibacterium lactatiformans* isolate	100%
186	0–0.33%	TACGTAGGTGGCAAGCGTTATCCGGATTTACTGGGTGTAAAGGGCGTGTAGGCGGGATCGCAAGT CAGATGTGAAAACTGGAGGCTCAACCTCCAGCCTGCATTTGAAACTGTGGTTCTTGAGTACTGG AGAGGCAGACGGAATTCCTAGTGTAGCGGTGAAATGCGTAGATATTAGGAGGAACACCAGTGGCGA AGGCGGTCTGCTGGACAGCAACTGACGCTGAGGCGCGAAAGCGTG	Order: Oscillospirales Family: Ruminococcaceae Genus: *Colidextribacter*	*Clostridiales bacterium* CCNA10 DNA, complete genome *Flintibacter butyricus* partial 16S rRNA gene	100% 100%

to CKD cats with normal bile acid metabolism (>50% SBAs) (median relative abundance = 0.0052%, FDR adj. $p = 0.0022$) and healthy cats (median relative abundance = 0.075%; range = 0.0094–0.33%; FDR adj. $p = 0.0014$) (Figure 8F).

4 Discussion

Here, it is reported that cats with CKD have an altered fecal bile acid profile compared to apparently clinically healthy cats. The altered fecal bile acid profile is characterized by a reduced concentration of the microbial-derived SBA UDCA. Even when a subpopulation of CKD cats with bile acid dysmetabolism (<50% SBAs) was separated, the presence of reduced fecal UDCA concentrations in CKD cats with normal bile acid metabolism (>50% SBAs) compared to healthy cats remained. The reduction in UDCA is associated with differentially abundant microbes, notably reduced relative abundance of a *Lachnospiraceae* sp. (ASV 286) and an uncultured *Clostridia* sp. (ASV 151). Other members within these taxonomic classifications are known to perform both the deconjugation function via BSH (Foley et al., 2019; Lucas et al., 2021) as well as utilize HSDH enzymes to generate SBAs from PBAs (Lucas et al., 2021; Sutherland and Williams, 1985; Coleman et al., 1994; Lou et al., 2016). Both of those biotransformations are crucial for the microbial production of the SBA UDCA. While not possible with the 16S rRNA gene amplicon sequencing performed in this study, future analysis employing metagenomics could profile genetic capacities to provide mechanistic insight into functional potential of the feline gut microbiome in CKD cats and potentially causative support for the correlative findings described herein. Additionally, it is also described here that the enteropathogen *Campylobacter* is detected within feces of cats with CKD and its increasing relative abundance negatively correlates with fecal UDCA concentration. The clinical significance of these findings are unknown and require further investigation, though it is noted that *Campylobacter* is also described as enriched in abundance from a metagenomic characterization of the gut microbiota of obese cats (Ma et al., 2022).

Reduced fecal concentrations of UDCA in cats with CKD is notable given the signaling activity profile of UDCA to host cells. UDCA can be directly sensed by the host as agonist for the cell surface expressed bile acid activated receptor TGR5 as well as an antagonist of the nuclear receptor FXR (Ticho et al., 2019). While expression is yet to be described in cats, both TGR5 and FXR are known to be expressed in the kidneys of humans and rodents (Herman-Edelstein et al., 2018). UDCA can act to modulate and mitigate inflammation in both acute and chronic settings through multiple mechanisms (Poupon, 2012). This had led to exploring its adjunctive use as an anti-inflammatory to treat human patients with SARS-CoV-2 infection (Brevini et al., 2023) and colitis (Ward et al., 2017) in addition to its original purpose as a therapy for primary biliary cirrhosis (Goulis et al., 1999). The anti-fibrotic properties of UDCA have recently been linked to inhibition of cellular autophagy *in vitro* in a liver fibrosis model (Ye et al., 2020). Given the chronic inflammatory and fibrosing pathophysiology of CKD, it is important to determine if reduced microbial production of UDCA can exacerbate CKD. It has been reported that other TGR5 agonists both inhibit development of kidney disease in murine models of obesity and diabetes (Wang et al., 2016), and more recently that a TGR5

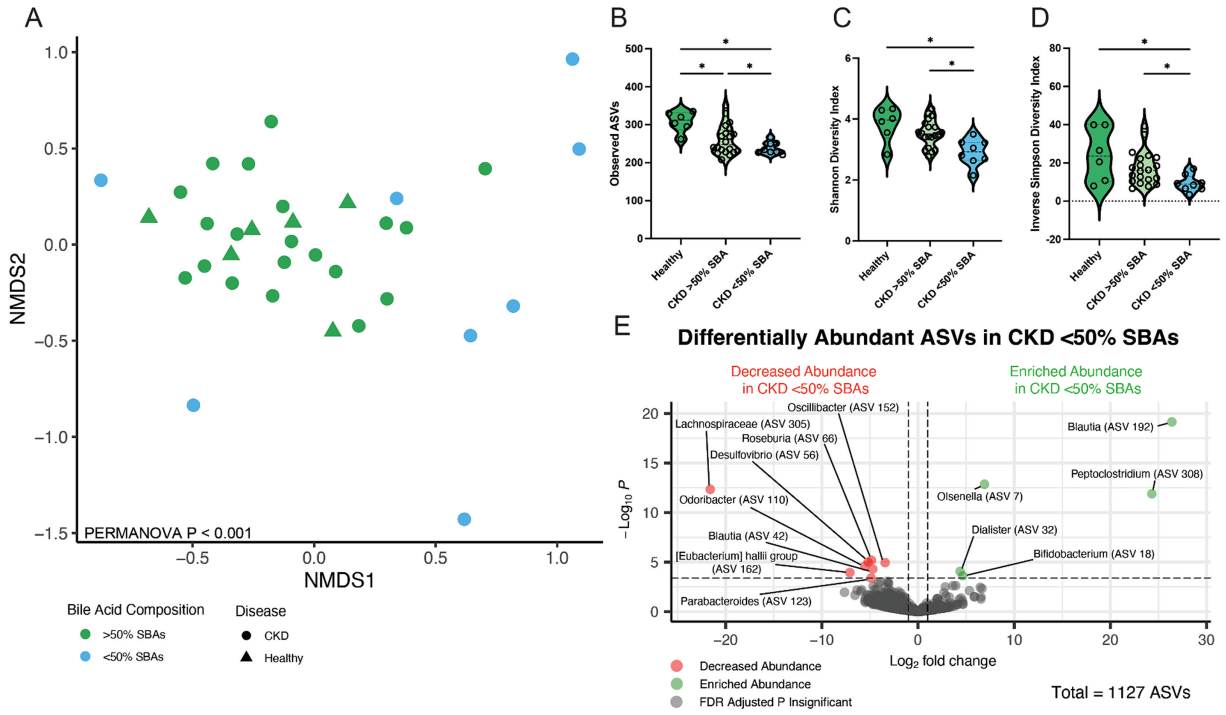

FIGURE 5
Fecal microbial population from CKD cats with bile acid dysmetabolism (<50% SBAs) is distinct from healthy cats and CKD cats with normal bile acid metabolism (>50% SBAs). **(A)** Beta diversity determined with Bray–Curtis dissimilarity distances depicted with non-metric multi-dimensional scaling (NMDS) plot with individual samples represented by points for cats with normal bile acid metabolism (>50% SBAs; green) and bile acid dysmetabolism (<50% SBAs; blue) and significance determined with PERMANOVA. **(B)** Alpha diversity in healthy cats, CKD cats with normal bile acid metabolism (>50% SBAs), and CKD cats with bile acid dysmetabolism (<50% SBAs) represented by violin plots of total observed ASVs and significance determined via parametric one-way ANOVA with FDR adjustment; significant discoveries noted by *. **(C)** Alpha diversity in healthy cats, CKD cats with normal bile acid metabolism (>50% SBAs), and CKD cats with bile acid dysmetabolism (<50% SBAs) represented by violin plots of Shannon Diversity Index and significance determined via parametric one-way ANOVA with FDR adjustment; significant discoveries noted by *. **(D)** Alpha diversity in healthy cats, CKD cats with normal bile acid metabolism (>50% SBAs), and CKD cats with bile acid dysmetabolism (<50% SBAs) represented by violin plots of Inverse Simpson Diversity Index and significance determined via parametric one-way ANOVA with FDR adjustment; significant discoveries noted by *. **(E)** Volcano plot displaying differentially abundant ASVs determined with DESeq2 that are either reduced in abundance (red) or enriched in abundance (green) in CKD cats with bile acid dysmetabolism (<50% SBAs) compared to healthy cats and CKD cats with normal bile acid metabolism (>50% SBAs). Points maintaining significance following FDR adjustment ($p < 0.05$) and having a log2FC of at least magnitude 2 are plotted and colored. All gray points do not meet these criteria.

agonist produced by the gut microbe *Bacteroides fragilis* can ameliorate renal fibrosis in both unilateral ureteral obstruction and adenine-induced CKD murine models (Zhou et al., 2022). In a mouse model of cisplatin induced acute kidney injury, UDCA protects the murine kidney from developing kidney injury by limiting oxidative damage and preserving mitochondrial function (Yang et al., 2020). UDCA is similarly protective in a gentamicin-induced rodent nephrotoxicity model by modulating NF-κB mediated inflammation (Abd-Elhamid et al., 2018). UDCA is commercially available as Ursodiol and is a widely utilized therapeutic in both human and veterinary medicine (Poupon et al., 1991; Otte et al., 2013), making UDCA a potentially beneficial adjunctive therapy for CKD treatment from a cytoprotective, anti-fibrotic, and anti-inflammatory perspective. The data presented here suggest that cats with CKD may represent a spontaneous translational disease model where the therapeutic potential of modulation of bile acid metabolism can be further explored. Importantly, to determine whether a reduced fecal concentration of UDCA in cats with CKD is biologically relevant in CKD pathophysiology, additional information characterizing circulating serum concentrations of UDCA, uptake of UDCA by the host kidney, and UDCA's ability to interact with bile acid activated receptors in the kidney is required.

It is also reported here that a subpopulation of cats with CKD experience a fecal bile acid dysmetabolism characterized by fecal bile acid profile with <50% SBAs. In people (Ridlon et al., 2006) and in dogs (Rowe and Winston, 2024), the fecal bile acid pool is typically composed of >80–90% microbial-derived SBAs in states of health. Fecal bile acid profiles have been minimally characterized in cats (Rowe and Winston, 2024), with three studies performed in the context of dietary impact on fecal bile acid profiles (Anantharaman-Barr et al., 1994; Jackson et al., 2020; Ephraim and Jewell, 2021), three studies in the context of antimicrobial impact (Whittemore et al., 2018; Whittemore et al., 2019; Stavroulaki et al., 2022), and a single study investigating CKD and dietary impact (Hall et al., 2020). From these studies, the primary association leading to a bile acid dysmetabolism and decreased microbial-derived SBAs is the administration of antimicrobials, which causes reduced microbiota diversity and can persist for at least 6 weeks based on one study of cats administered clindamycin (Whittemore et al., 2019). In the present study, cats were excluded if they received antimicrobials within 6

10.3389/fmicb.2024.1458090

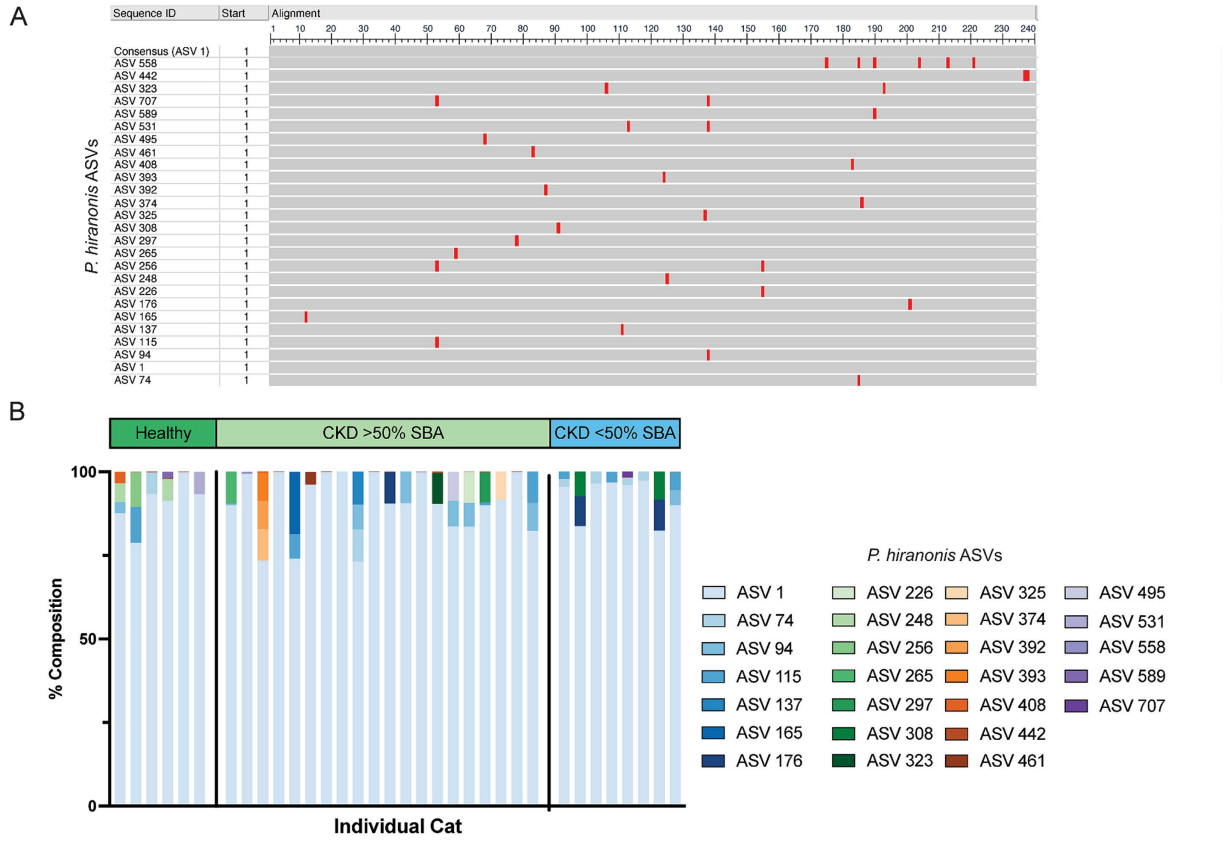

FIGURE 6
26 ASVs with at least 97% nucleotide identity to *P. hiranonis* are identified in the fecal microbiota of cats. **(A)** Multiple sequence alignment of the 26 ASVs with at least 97% sequence identity to *P. hiranonis*. ASV 1 was used as the consensus sequence. Red bars indicate the location in the 240 base pair sequence of amplicons that nucleotide variation from the consensus sequence occurs within the V4 region of the 16S rRNA gene. **(B)** Stacked bar plot representing the relative composition of all 26 ASVs identified with at least 97% sequence identity to *P. hiranonis* in individual cat fecal samples.

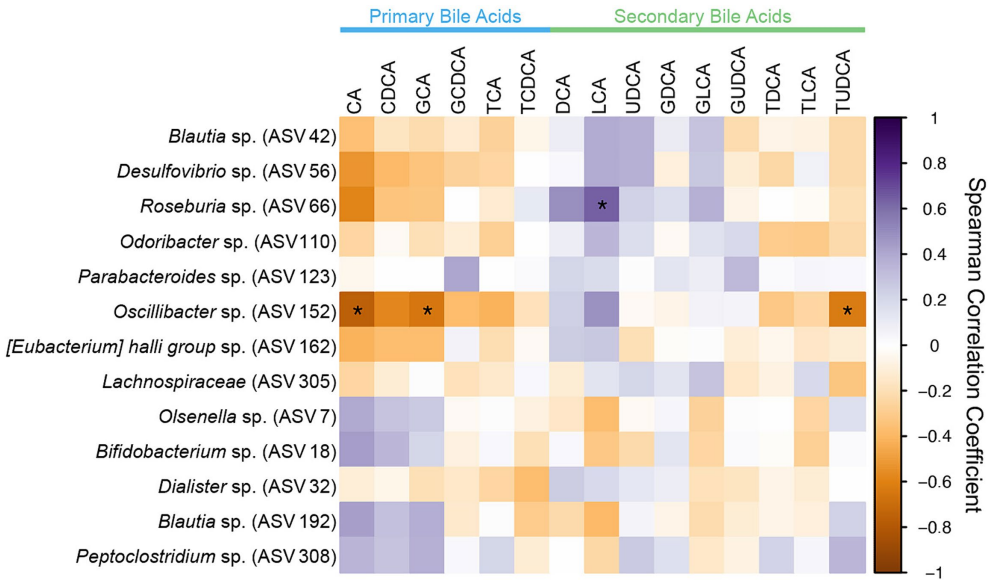

FIGURE 7
Spearman correlation matrix of fecal bile acid concentrations for individual bile acids and differentially abundant ASVs identified in CKD cats with bile acid dysmetabolism (<50% SBAs) using DESeq2. Spearman ρ for each pair of fecal bile acid concentration and each ASV relative abundance denoted by color of the square at the corresponding intersection. Squares denoting positive correlations are purple, with darker shades indicating stronger positive correlations. Squares denoting negative correlations are orange, with darker shades indicating stronger negative correlations. * denotes FDR adjusted $p < 0.05$.

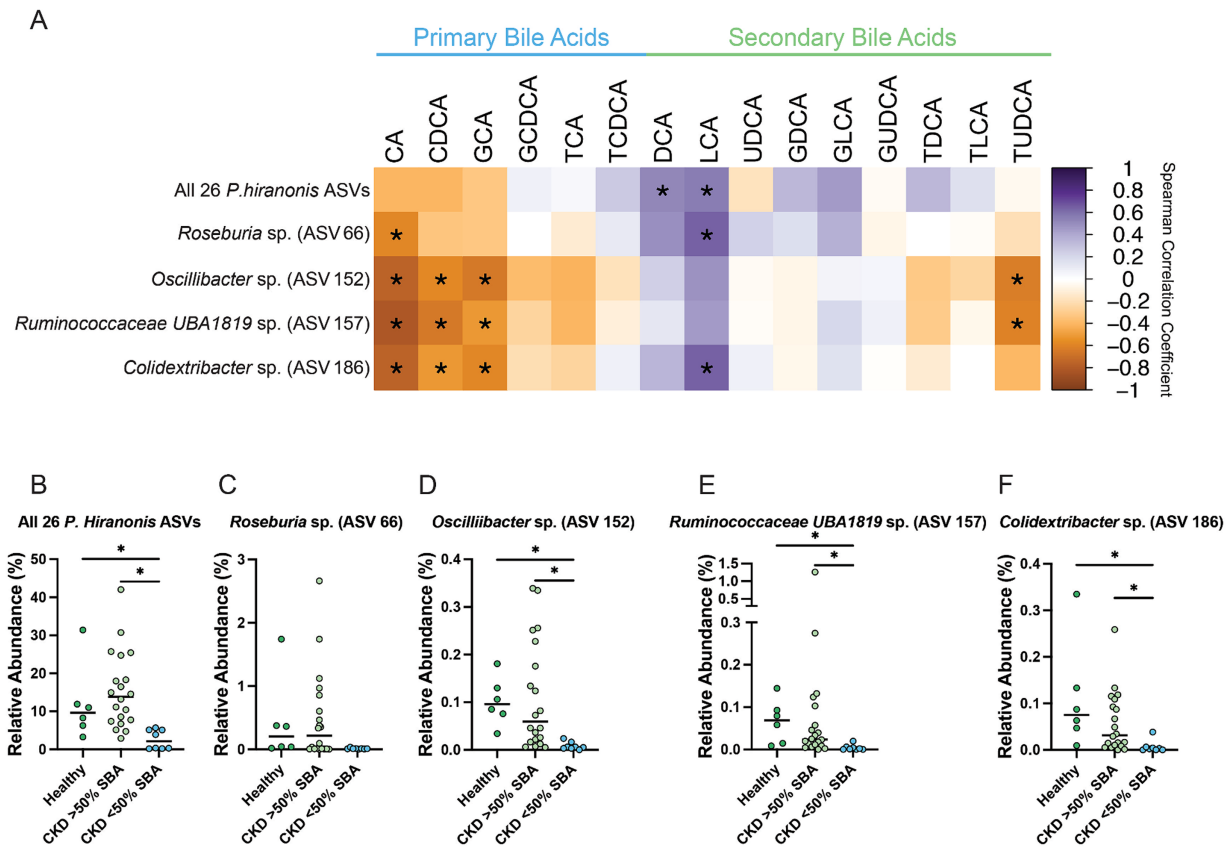

FIGURE 8
Fecal bile acid composition correlates with differentially abundant *P. hiranonis*, *Roseburia* sp., and *Oscillospirales* ASVs. **(A)** Spearman correlation matrix of fecal bile acid concentrations for individual bile acids with the relative abundance of 26 combined *P. hiranonis* ASVs, *Roseburia* sp. (ASV 66), *Oscillibacter* sp. (ASV 152), *Ruminococcaceae UBA1819* (ASV 157), and *Colidextribacter* sp. (ASV 186). Spearman ρ for each pair of fecal bile acid concentration and ASV relative abundance denoted by color of the square at the corresponding intersection. Squares denoting positive correlations are purple, with darker shades indicating stronger positive correlations. Squares denoting negative correlations are orange, with darker shades indicating stronger negative correlations. * denotes FDR adjusted $p < 0.05$. Relative abundance in healthy cats, CKD cats with normal bile acid metabolism (>50% SBAs), and CKD cats with bile acid dysmetabolism (<50% SBAs) for **(B)** All 26 *P. hiranonis* ASVs, **(C)** *Roseburia* sp. (ASV 66), **(D)** *Oscillibacter* sp. (ASV 152), **(E)** *Ruminococcaceae UBA1819* (ASV 157), and **(F)** *Colidextribacter* sp. (ASV 186). Significance determined via Kruskal-Wallis with FDR adjustment; significant discoveries noted by *.

weeks of enrollment. However, it is possible that antimicrobial administration prior to 6 weeks before enrollment could create a persistent dysbiosis longer than 6 weeks. Current longitudinal data of healthy research cats demonstrates persistent changes in microbial diversity following clindamycin can persist for 630 days, even though the SBA DCA normalizes by that same time (Whittemore et al., 2018). Diet is also a major driver of gut microbiota composition (Pilla and Suchodolski, 2021), so it is possible that lack of dietary controls in the present study is contributing to the heterogeneity of fecal bile acid profiles seen in both apparently clinically healthy cats and cats with CKD. Moreover, it is recently reported that cats with underlying gastrointestinal disease can have fecal bile acid dysmetabolism characterized by <50% SBAs (Sung et al., 2023). So, while effort was made to exclude cats in the present study with primary gastrointestinal disease, it is possible that unidentified primary gastrointestinal disease could also have been a contributing factor, especially with the known difficulty of clinical signs alone to exclude the presence of underlying gastrointestinal pathology in cats (Marsilio et al., 2019). Ultimately, it is not possible from the data presented here to determine a singular driver leading to the subpopulation of CKD cats with bile acid dysmetabolism (<50% SBAs) but this could indicate distinct populations of CKD cats.

Still, it is important to explore the gut microbial community structure alterations corresponding with the subpopulation of CKD cats with bile acid dysmetabolism (<50% SBAs) as they may represent a clinically important and relevant disease state. The largest driver for conversion of host PBAs into microbial-derived SBAs is the 7α-dehydroxylation (Funabashi et al., 2020). This process conferred through the *bai* operon is known to be present in only a select few culturable microbes: *Clostridium scindens* (Kitahara et al., 2000), *Clostridium hylemonae* (Ridlon et al., 2010), *Peptacetobacter hiranonis* (formerly *Clostrdium hiranonis*) (Kitahara et al., 2001), and *Extibacter muris* (in mice) (Streidl et al., 2021). Recently, *Roseburia intestinalis* has been suggested to contain only a portion of the *bai* operon and provide a minor contribution of 7α-dehydroxylation activity when cultured *in vitro* with CA (Lucas et al., 2021). From the present study, a single *Roseburia* sp. (ASV 66) with 98.75% sequence identity to *Roseburia intestinalis* to the V4 region of 16S rRNA gene negatively correlated with CA and positively correlated with the SBA LCA. Of known full *bai* operon-containing organisms, only *P. hiranonis* has

been identified in cats, and is currently used in a validated assay to assess dysbiosis in cats with chronic enteropathy (Sung et al., 2022). Here, 26 ASVs were identified as having 97% nucleotide identity or greater with the V4 region of 16S rRNA gene of *P. hiranonis* when assessed against the full genome in the NCBI database. Of those ASVs, some were identified in relative abundances as high as 30%, while others were found in relative abundances of less than 1% (Figure 6B). When all 26 *P. hiranonis* ASVs are combined and assessed for correlation with fecal bile acid composition, the total *P. hiranonis* ASVs were significantly positively correlated with the concentrations of SBAs DCA and LCA. There was also significantly reduced relative abundance of these *P. hiranonis* ASVs in CKD cats with bile acid dysmetabolism (<50% SBAs). Taken together, it appears that *P. hiranonis* is likely an important producer of SBAs in cats, and this function can be lost in states of dysbiosis leading to fecal bile acid dysmetabolism.

Here it is also identified that three ASVs belonging to the order *Oscillospirales* also either significantly negatively correlated with PBA concentration or are significantly positively correlated with SBA concentration. This correlation pattern is similar to the pattern demonstrated by the known 7α-dehydroxylation performing *P. hiranonis*. The relative abundances of all three *Oscillospirales* ASVs were significantly reduced in CKD cats with a fecal bile acid dysmetabolism characterized by a PBA predominant fecal bile acid profile. Recently, human gut metagenome assembled genome (MAG) data, describes unculturable members of *Oscillospirales* that harbor the *bai* operon and contribute to 7α-dehydroxylation (Vital et al., 2019; Kim et al., 2022). These microbes also contain the genetic potential to generate secondary *allo*-bile acids via a direct pathway without the involvement of other microbial transformations (Lee et al., 2022; Ridlon et al., 2023). These recent findings highlight members of the family *Oscillospirales* as novel microbes to perform bile acid biotransformation within the human gut microbiota. Further, in human inflammatory bowel disease patients two ASVs identified via 16S rRNA gene amplicon sequencing as uncultured *Oscillospiraceae* positively correlated in relative abundance with fecal concentrations of the SBAs DCA and LCA (Lavelle et al., 2022). The presence and/or function of *Oscillospirales* as possible novel bile acid converting organisms in other species besides humans is currently not described in the literature. The data presented here are not causative but suggest similar or the same microbes identified by metagenomics of human gut microbes are also present within the gut microbiota of cats and thus may contribute to PBA conversion into SBAs in some capacity. Further investigation of bile acid dysmetabolism in cats via paired metagenomic sequencing and targeted metabolomics will allow for interrogation of the correlative data presented here that suggest a relationship may exist between *Oscillospirales* and microbial bile acid metabolism in cats.

Notably, when fecal UDCA concentrations are considered in CKD cats with <50% SBAs, a heterogeneity of concentrations is observed. UDCA production is mechanistically not tied to 7α-dehydroxylation directly, but rather can be achieved through a variety of reactions including hydroxysteroid dehydrogenase (HSDH) enzymes that act at the 7th carbon position. This enzymatic activity is provided by many members of the gut microbiota (Rowe and Winston, 2024). It is possible that a heterogenous spread of fecal UDCA concentrations are present in CKD cats with <50% SBAs given the greater availability of PBAs to undergo modification via non 7α-dehydroxylation methods, including through HSDH enzymes. Further exploration of this phenomenon may be better explained by incorporation of metagenomic sequencing to identify gut microbiota members with bile acid biotransformation genes and thorough evaluation of the fecal bile acid pool beyond the 15 BAs assessed in the present study. Leveraging a multi-omics approach may reveal other SBAs that have proportionally different representation when there is diminished 7α-dehydroxylation capability by the gut microbiota.

The overall sample size represents a limitation that can be commonly encountered in clinical veterinary studies. Still, the sample size presented here represents an expansion on the previous investigation of fecal bile acid concentrations in CKD cats (Hall et al., 2020) and is one of only a few investigations to employ multi-omics by pairing assessment of the gut microbiome and targeted fecal bile acid composition in cats (Rowe and Winston, 2024). As previously discussed, the lack of strict dietary controls is also limiting along with the propensity of cats to develop histopathologic evidence of significant gastrointestinal disease in the absence of clinical signs (Marsilio et al., 2019). However, it is important to note that these limitations also represent a realistic feline population that would be encountered in clinical practice. Additionally, the availability of only forward reads from SRA is an inherent limitation of the *post-hoc* analysis presented here compared to the increased certainty of sequenced nucleotides from paired-end sequencing. However, as previously mentioned microbiome results from the previous publication (Summers et al., 2019) were replicated with the updated amplicon sequencing pipelined used herein.

Overall, the finding of reduced fecal concentrations of the SBA UDCA in cats with CKD is significant given the known ability of UDCA to modulate inflammation and fibrosis, including in rodent models of kidney injury (Yang et al., 2020; Abd-Elhamid et al., 2018; Brevini et al., 2023). Translational investigation of this finding warrants further exploration of fecal bile acids in people with CKD. Given these results, we postulate that commercially available and FDA-approved in people Ursodiol (ursodeoxycholic acid) could be considered for study as a component of multimodal treatment in human and veterinary patients with CKD. Separate from UDCA, fecal bile acid dysmetabolism characterized by <50% SBAs also occurs in a subpopulation of cats with CKD. The dysmetabolism is partially explained by reduced abundance of *P. hiranonis*, which to date is the only described member of the feline gut microbiota with the capability to perform 7α-dehydroxylation. Members of the order *Oscillospirales* displayed a similar pattern in correlation of abundance of SBAs within the bile acid pool. Metagenomic characterization of *Oscillospirales* have only recently suggested a role in bile acid metabolism, including the genetic potential to perform 7α-dehydroxylation in the human gut microbiota (Vital et al., 2019; Kim et al., 2022), making application of metagenomics an important next step to better characterize the phenomenon first described here in cats. If these microbial community members are shown to have the same genetic potential as described in the human gut microbes, it strengthens the use of cats with CKD as a potential translational spontaneously occurring disease model to explore the role of bile acid metabolism in the gut-kidney axis.

Data availability statement

The datasets presented in this study can be found in online repositories. The names of the repository/repositories and accession number(s) can be found at: https://www.ncbi.nlm.nih.gov/, SRP117611.

Ethics statement

The animal studies were approved by Colorado State University Veterinary Teaching Hospital Institutional Animal Care and Use Committee. The studies were conducted in accordance with the local legislation and institutional requirements. Written informed consent was obtained from the owners for the participation of their animals in this study.

Author contributions

JR: Writing – review & editing, Writing – original draft, Visualization, Methodology, Investigation, Formal analysis, Data curation. SS: Writing – review & editing, Writing – original draft, Resources, Project administration, Funding acquisition, Data curation, Conceptualization. JQ: Writing – review & editing, Writing – original draft, Supervision, Project administration, Funding acquisition, Data curation, Conceptualization. JW: Writing – review & editing, Writing – original draft, Visualization, Supervision, Resources, Methodology, Formal analysis, Data curation, Conceptualization.

Funding

The author(s) declare that financial support was received for the research, authorship, and/or publication of this article. Buttons Fund for Feline Chronic Kidney Disease Research; University of Colorado Cancer Center Shared Resource Support Grant, Grant/Award Number: P30CA046934. J.A.W. is funded by a NIH National Institute of Allergy and Infectious Diseases Mentored Clinical Scientist Development Award (5K08AI153550).

Acknowledgments

Sankey diagram created in Figure 4 utilized SankeyMATIC.com.

Conflict of interest

S.C.S. is a research consultant for IDEXX Laboratories, Inc. and has previous work funded by Nestle Purina and IDEXX Laboratories, Inc. She has received a speaker honorarium from Royal Canin, IDEXX Laboratories, Inc., and Boehringer-Ingelheim. Preliminary results from this analysis were presented in abstract form at the 2020 Annual Forum of American College of Veterinary Internal Medicine, (Abstract NU26: Fecal primary and secondary bile acids in cats with chronic kidney disease.). J.Q's work has been funded by EveryCat Health Foundation, Morris Animal Foundation, Nestle Purina, Trivium Vet, Zoetis. She has received compensation as a member of the scientific advisory board of Nestle Purina, Elanco, Zoetis. She also has consulted or served as a key opinion leader for Boehringer Ingelheim, Dechra, Elanco, Gallant, Heska, Hill's, IDEXX, Nestle Purina, Royal Canin, SN Biomedical, Vetoquinol, Zoetis and received compensation. J.A.W's laboratory has been funded by EveryCat Health Foundation, Morris Animal Foundation, American Kennel Club's Canine Health Foundation, Nestle Purina, FDA, and National Institutes of Health. She has received speaker honorariums from Royal Canin, Nestle Purina, and DVM360.

The remaining author declares that the research was conducted in the absence of any commercial or financial relationships that could be construed as a potential conflict of interest.

Publisher's note

Supplementary material

The Supplementary material for this article can be found online at: https://www.frontiersin.org/articles/10.3389/fmicb.2024.1458090/full#supplementary-material

References

Abd-Elhamid, T. H., Elgamal, D. A., Ali, S. S., Ali, F. E. M., Hassanein, E. H. M., El-Shoura, E. A. M., et al. (2018). Reno-protective effects of ursodeoxycholic acid against gentamicin-induced nephrotoxicity through modulation of NF-κB, eNOS and caspase-3 expressions. *Cell Tissue Res.* 374, 367–387. doi: 10.1007/s00441-018-2886-y

Altschul, S. F., Gish, W., Miller, W., Myers, E. W., and Lipman, D. J. (1990). Basic local alignment search tool. *J. Mol. Biol.* 215, 403–410. doi: 10.1016/S0022-2836(05)80360-2

Anantharaman-Barr, G., Ballèvre, O., Gicquello, P., Bracco-Hammer, I., Vuichoud, J., Montigon, F., et al. (1994). Fecal bile acid excretion and taurine status in cats fed canned and dry diets. *J. Nutr.* 124, 2546S–2551S.

Bartges, J. W. (2012). Chronic kidney disease in dogs and cats. *Vet. Clin.* 42, 669–92, vi. doi: 10.1016/j.cvsm.2012.04.008

Benjamini, Y., Krieger, A. M., and Yekutieli, D. (2006). Adaptive linear step-up procedures that control the false discovery rate. *Biometrika* 93, 491–507. doi: 10.1093/biomet/93.3.491

Brevini, T., Maes, M., Webb, G. J., John, B. V., Fuchs, C. D., Buescher, G., et al. (2023). FXR inhibition may protect from SARS-CoV-2 infection by reducing ACE2. *Nature* 615, 134–142. doi: 10.1038/s41586-022-05594-0

Callahan, B. J., McMurdie, P. J., Rosen, M. J., Han, A. W., Johnson, A. J. A., and Holmes, S. P. (2016). DADA2: high-resolution sample inference from Illumina amplicon data. *Nat. Methods* 13, 581–583. doi: 10.1038/nmeth.3869

Chávez-Talavera, O., Tailleux, A., Lefebvre, P., and Staels, B. (2017). Bile acid control of metabolism and inflammation in obesity, type 2 diabetes, dyslipidemia, and

nonalcoholic fatty liver disease. *Gastroenterology* 152, 1679–1694.e3. doi: 10.1053/j.gastro.2017.01.055

Chen, Y. Y., Chen, D. Q., Chen, L., Liu, J. R., Vaziri, N. D., Guo, Y., et al. (2019). Microbiome–metabolome reveals the contribution of gut–kidney axis on kidney disease. *J. Transl. Med.* 17:5. doi: 10.1186/s12967-018-1756-4

Ciaula, A. D., Garruti, G., Baccetto, R. L., Molina-Molina, E., Bonfrate, L., Portincasa, P., et al. (2018). Bile acid physiology. *Ann. Hepatol.* 16, 4–14. doi: 10.5604/01.3001.0010.5493

Clarke, K. R. (1993). Non-parametric multivariate analyses of changes in community structure. *Aust. J. Ecol.* 18, 117–143. doi: 10.1111/j.1442-9993.1993.tb00438.x

Cline, M. G., Burns, K. M., Coe, J. B., Downing, R., Durzi, T., Murphy, M., et al. (2021). 2021 AAHA nutrition and weight management guidelines for dogs and cats*. *J. Am. Anim. Hosp. Assoc.* 57, 153–178. doi: 10.5326/JAAHA-MS-7232

Coleman, J. P., Hudson, L. L., and Adams, M. J. (1994). Characterization and regulation of the NADP-linked 7 alpha-hydroxysteroid dehydrogenase gene from *Clostridium sordellii*. *J. Bacteriol.* 176, 4865–4874. doi: 10.1128/jb.176.16.4865-4874.1994

Collins, S. L., Stine, J. G., Bisanz, J. E., Okafor, C. D., and Patterson, A. D. (2023). Bile acids and the gut microbiota: metabolic interactions and impacts on disease. *Nat. Rev. Microbiol.* 21, 236–247. doi: 10.1038/s41579-022-00805-x

Ephraim, E., and Jewell, D. E. (2021). Effect of nutrition on age-related metabolic markers and the gut microbiota in cats. *Microorganisms* 9:2430. doi: 10.3390/microorganisms9122430

Foley, M. H., O'Flaherty, S., Barrangou, R., and Theriot, C. M. (2019). Bile salt hydrolases: gatekeepers of bile acid metabolism and host-microbiome crosstalk in the gastrointestinal tract. *PLoS Pathog.* 15:e1007581. doi: 10.1371/journal.ppat.1007581

Funabashi, M., Grove, T. L., Wang, M., Varma, Y., McFadden, M. E., Brown, L. C., et al. (2020). A metabolic pathway for bile acid dehydroxylation by the gut microbiome. *Nature* 582, 566–570. doi: 10.1038/s41586-020-2396-4

GitHub (2023) Downloading SRA toolkit. Available at: https://github.com/ncbi/sra-tools/wiki/01.-Downloading-SRA-Toolkit (Accessed November 5, 2023).

Goulis, J., Leandro, G., and Burroughs, A. K. (1999). Randomised controlled trials of ursodeoxycholic-acid therapy for primary biliary cirrhosis: a meta-analysis. *Lancet* 354, 1053–1060. doi: 10.1016/S0140-6736(98)11293-X

Hall, J. A., Jewell, D. E., and Ephraim, E. (2020). Changes in the fecal metabolome are associated with feeding Fiber not health status in cats with chronic kidney disease. *Meta* 10:281. doi: 10.3390/metabo10070281

Herman-Edelstein, M., Weinstein, T., and Levi, M. (2018). Bile acid receptors and the kidney. *Curr. Opin. Nephrol. Hypertens.* 27, 56–62. doi: 10.1097/MNH.0000000000000374

IRIS Kidney (2023) Guidelines - IRIS Staging of CKD [Internet]. Available at: http://www.iris-kidney.com/guidelines/staging.html (Accessed November 5, 2023).

Jackson, M. I., Waldy, C., and Jewell, D. E. (2020). Dietary resistant starch preserved through mild extrusion of grain alters fecal microbiome metabolism of dietary macronutrients while increasing immunoglobulin a in the cat. *PLoS One* 15:e0241037. doi: 10.1371/journal.pone.0241037

Jepson, R. E. (2016). Current understanding of the pathogenesis of progressive chronic kidney disease in cats. *Vet. Clin. N. Am. Small Anim. Pract.* 46, 1015–1048. doi: 10.1016/j.cvsm.2016.06.002

Kieler, I. N., Mølbak, L., Hansen, L. L.Hermann-Bank ML, and Bjornvad, C. R. (2016). Overweight and the feline gut microbiome – a pilot study. *J. Anim. Physiol. Anim. Nutr.* 100, 478–484. doi: 10.1111/jpn.12409

Kim, K. H., Park, D., Jia, B., Baek, J. H., Hahn, Y., and Jeon, C. O. (2022). Identification and characterization of major bile acid 7α-Dehydroxylating Bacteria in the human gut. *mSystems.* 7, e00455–e00422. doi: 10.1128/msystems.00455-22

Kitahara, M., Takamine, F., Imamura, T., and Benno, Y. (2000). VPI 12708 and related strains with high bile acid 7alpha-dehydroxylating activity to Clostridium scindens and proposal of *Clostridium hylemonae* sp. nov., isolated from human faeces. *Int. J. Syst. Evol. Microbiol.* 50, 971–978. doi: 10.1099/00207713-50-3-971

Kitahara, M., Takamine, F., Imamura, T., and Benno, Y. (2001). *Clostridium hiranonis* sp. nov., a human intestinal bacterium with bile acid 7alpha-dehydroxylating activity. *Int. J. Syst. Evol. Microbiol.* 51, 39–44. doi: 10.1099/00207713-51-1-39

Lavelle, A., Nancey, S., Reimund, J. M., Laharie, D., Marteau, P., Treton, X., et al. (2022). Fecal microbiota and bile acids in IBD patients undergoing screening for colorectal cancer. *Gut Microbes* 14:2078620. doi: 10.1080/19490976.2022.2078620

Lee, J. W., Cowley, E. S., Wolf, P. G., Doden, H. L., Murai, T., Caicedo, K. Y. O., et al. (2022). Formation of secondary Allo-bile acids by novel enzymes from gut Firmicutes. *Gut Microbes* 14:2132903. doi: 10.1080/19490976.2022.2132903

Li, R., Zeng, L., Xie, S., Chen, J., Yu, Y., and Zhong, L. (2019). Targeted metabolomics study of serum bile acid profile in patients with end-stage renal disease undergoing hemodialysis. *PeerJ.* 7:e7145. doi: 10.7717/peerj.8265

Lloyd-Price, J., Arze, C., Ananthakrishnan, A. N., Schirmer, M., Avila-Pacheco, J., Poon, T. W., et al. (2019). Multi-omics of the gut microbial ecosystem in inflammatory bowel diseases. *Nature* 569, 655–662. doi: 10.1038/s41586-019-1237-9

Lou, D., Wang, B., Tan, J., Zhu, L., Cen, X., Ji, Q., et al. (2016). The three-dimensional structure of *Clostridium absonum* 7α-hydroxysteroid dehydrogenase: new insights into the conserved arginines for NADP(H) recognition. *Sci. Rep.* 6:22885. doi: 10.1038/srep22885

Love, M. I., Huber, W., and Anders, S. (2014). Moderated estimation of fold change and dispersion for RNA-seq data with DESeq2. *Genome Biol.* 15:550. doi: 10.1186/s13059-014-0550-8

Lucas, L. N., Barrett, K., Kerby, R. L., Zhang, Q., Cattaneo, L. E., Stevenson, D., et al. (2021). Dominant bacterial Phyla from the human gut show widespread ability to transform and conjugate bile acids. *mSystems.* 6:21. doi: 10.1128/msystems.00805-21

Ma, X., Brinker, E., Graff, E. C., Cao, W., Gross, A. L., Johnson, A. K., et al. (2022). Whole-genome shotgun metagenomic sequencing reveals distinct gut microbiome signatures of obese cats. *Microbiol. Spectr.* 10, e00837–e00822. doi: 10.1128/spectrum.00837-22

Marino, C. L., Lascelles, B. D. X., Vaden, S. L., Gruen, M. E., and Marks, S. L. (2014). Prevalence and classification of chronic kidney disease in cats randomly selected from four age groups and in cats recruited for degenerative joint disease studies. *J. Feline Med. Surg.* 16, 465–472. doi: 10.1177/1098612X13511446

Marsilio, S., Ackermann, M. R., Lidbury, J. A., Suchodolski, J. S., and Steiner, J. M. (2019). Results of histopathology, immunohistochemistry, and molecular clonality testing of small intestinal biopsy specimens from clinically healthy client-owned cats. *J. Vet. Intern. Med.* 33, 551–558. doi: 10.1111/jvim.15455

Martin, M. (2011). Cutadapt removes adapter sequences from high-throughput sequencing reads. *EMBnet. J.* 17, 10–12. doi: 10.14806/ej.17.1.200

McLeland, S. M., Cianciolo, R. E., Duncan, C. G., and Quimby, J. M. (2015). A comparison of biochemical and histopathologic staging in cats with chronic kidney disease. *Vet. Pathol.* 52, 524–534. doi: 10.1177/0300985814561095

McMillin, M., and DeMorrow, S. (2016). Effects of bile acids on neurological function and disease. *FASEB J.* 30, 3658–3668. doi: 10.1096/fj.201600275R

McMurdie, P. J., and Holmes, S. (2013). Phyloseq: an R package for reproducible interactive analysis and graphics of microbiome census data. *PLoS One* 8:e61217. doi: 10.1371/journal.pone.0061217

Nealon, N. J., Wood, A., Rudinsky, A. J., Klein, H., Salerno, M., Parker, V. J., et al. (2023). Fecal identification markers impact the feline fecal microbiota. *Front Vet Sci.* 10:1039931. doi: 10.3389/fvets.2023.1039931

Oksanen, J., Simpson, G. L., Blanchet, F. G., Kindt, R., Legendre, P., Minchin, P. R., et al. (2022) Vegan: community ecology package [internet]. Available at: https://CRAN.R-project.org/package=vegan (Accessed April 3, 2023).

Otte, C. M. A., Penning, L. C., Rothuizen, J., and Favier, R. P. (2013). Retrospective comparison of prednisolone and ursodeoxycholic acid for the treatment of feline lymphocytic cholangitis. *Vet. J.* 195, 205–209. doi: 10.1016/j.tvjl.2012.06.020

Perino, A., and Schoonjans, K. (2022). Metabolic messengers: bile acids. *Nat. Metab.* 4, 416–423. doi: 10.1038/s42255-022-00559-z

Pilla, R., and Suchodolski, J. S. (2021). The gut microbiome of dogs and cats, and the influence of diet. *Vet. Clin.* 51, 605–621. doi: 10.1016/j.cvsm.2021.01.002

Pinart, M., Dötsch, A., Schlicht, K., Laudes, M., Bouwman, J., Forslund, S. K., et al. (2022). Gut microbiome composition in obese and non-obese persons: a systematic review and Meta-analysis. *Nutrients* 14:12. doi: 10.3390/nu14010012

Poupon, R. (2012). Ursodeoxycholic acid and bile-acid mimetics as therapeutic agents for cholestatic liver diseases: an overview of their mechanisms of action. *Clin. Res. Hepatol. Gastroenterol.* 36, S3–S12. doi: 10.1016/S2210-7401(12)70015-3

Poupon, R. E., Balkau, B., Eschwège, E., and Poupon, R. (1991). A multicenter, controlled trial of Ursodiol for the treatment of primary biliary cirrhosis. *N. Engl. J. Med.* 324, 1548–1554. doi: 10.1056/NEJM199105303242204

Quast, C., Pruesse, E., Yilmaz, P., Gerken, J., Schweer, T., Yarza, P., et al. (2013). The SILVA ribosomal RNA gene database project: improved data processing and web-based tools. *Nucleic Acids Res.* 41, D590–D596. doi: 10.1093/nar/gks1219

R Core Team (2013). R: A language and environment for statistical Computing. Vienna: R Core Team.

Ridlon, J. M., Daniel, S. L., and Gaskins, H. R. (2023). The Hylemon-Björkhem pathway of bile acid 7-dehydroxylation: history, biochemistry, and microbiology. *J. Lipid Res.* 64:100392. doi: 10.1016/j.jlr.2023.100392

Ridlon, J. M., Kang, D. J., and Hylemon, P. B. (2006). Bile salt biotransformations by human intestinal bacteria. *J. Lipid Res.* 47, 241–259. doi: 10.1194/jlr.R500013-JLR200

Ridlon, J. M., Kang, D. J., and Hylemon, P. B. (2010). Isolation and characterization of a bile acid inducible 7α-dehydroxylating operon in *Clostridium hylemonae* TN271. *Anaerobe* 16, 137–146. doi: 10.1016/j.anaerobe.2009.05.004

Rodríguez-Morató, J., and Matthan, N. R. (2020). Nutrition and gastrointestinal microbiota, microbial-derived secondary bile acids, and cardiovascular disease. *Curr. Atheroscler. Rep.* 22:47. doi: 10.1007/s11883-020-00863-7

Rowe, J. C., and Winston, J. A. (2024). Collaborative metabolism: gut microbes play a key role in canine and feline bile acid metabolism. *Vet. Sci.* 11:94. doi: 10.3390/vetsci11020094

Rowe, J. C., Winston, J. A., Parker, V. J., McCool, K. E., Suchodolski, J. S., Lopes, R., et al. (2024). Gut microbiota promoting propionic acid production accompanies caloric restriction-induced intentional weight loss in cats. *Sci. Rep.* 14:11901. doi: 10.1038/s41598-024-62243-4

Summers, S. C., Quimby, J. M., Isaiah, A., Suchodolski, J. S., Lunghofer, P. J., and Gustafson, D. L. (2019). The fecal microbiome and serum concentrations of indoxyl sulfate and p-cresol sulfate in cats with chronic kidney disease. *J. Vet. Intern. Med.* 33, 662–669. doi: 10.1111/jvim.15389

Stavroulaki, E. M., Suchodolski, J. S., Pilla, R., Fosgate, G. T., Sung, C. H., Lidbury, J., et al. (2022). The serum and fecal Metabolomic profiles of growing kittens treated with amoxicillin/clavulanic acid or doxycycline. *Animals* 12:330. doi: 10.3390/ani12030330

Streidl, T., Karkossa, I., Segura Muñoz, R. R., Eberl, C., Zaufel, A., Plagge, J., et al. (2021). The gut bacterium Extibacter muris produces secondary bile acids and influences liver physiology in gnotobiotic mice. *Gut Microbes* 13:1854008. doi: 10.1080/19490976.2020.1854008

Sung, C. H., Marsilio, S., Chow, B., Zornow, K. A., Slovak, J. E., Pilla, R., et al. (2022). Dysbiosis index to evaluate the fecal microbiota in healthy cats and cats with chronic enteropathies. *J. Feline Med. Surg.* 24, e1–e12. doi: 10.1177/1098612X221077876

Sung, C. H., Pilla, R., Marsilio, S., Chow, B., Zornow, K. A., Slovak, J. E., et al. (2023). Fecal concentrations of long-chain fatty acids, sterols, and unconjugated bile acids in cats with chronic enteropathy. *Animals* 13:2753. doi: 10.3390/ani13172753

Sutherland, J. D., and Williams, C. N. (1985). Bile acid induction of 7 alpha- and 7 beta-hydroxysteroid dehydrogenases in *Clostridium limosum*. *J. Lipid Res.* 26, 344–350. doi: 10.1016/S0022-2275(20)34377-7

Ticho, A. L., Malhotra, P., Dudeja, P. K., Gill, R. K., and Alrefai, W. A. (2019). Bile acid receptors and gastrointestinal functions. *Liver Res.* 3, 31–39. doi: 10.1016/j.livres.2019.01.001

Vital, M., Rud, T., Rath, S., Pieper, D. H., and Schlüter, D. (2019). Diversity of Bacteria exhibiting bile acid-inducible 7α-dehydroxylation genes in the human gut. *Comput. Struct. Biotechnol. J.* 17, 1016–1019. doi: 10.1016/j.csbj.2019.07.012

Wang, X. X., Edelstein, M. H., Gafter, U., Qiu, L., Luo, Y., Dobrinskikh, E., et al. (2016). G protein-coupled bile acid receptor TGR5 activation inhibits kidney disease in obesity and diabetes. *J. Am. Soc. Nephrol.* 27, 1362–1378. doi: 10.1681/ASN.2014121271

Ward, J. B. J., Lajczak, N. K., Kelly, O. B., O'Dwyer, A. M., Giddam, A. K., Ní Gabhann, J., et al. (2017). Ursodeoxycholic acid and lithocholic acid exert anti-inflammatory actions in the colon. American journal of physiology-gastrointestinal and liver. *Physiology* 312, G550–G558. doi: 10.1152/ajpgi.00256.2016

Whittemore, J. C., Stokes, J. E., Laia, N. L., Price, J. M., and Suchodolski, J. S. (2018). Short and long-term effects of a synbiotic on clinical signs, the fecal microbiome, and metabolomic profiles in healthy research cats receiving clindamycin: a randomized, controlled trial. *PeerJ.* 6:e5130. doi: 10.7717/peerj.5130

Whittemore, J. C., Stokes, J. E., Price, J. M., and Suchodolski, J. S. (2019). Effects of a synbiotic on the fecal microbiome and metabolomic profiles of healthy research cats administered clindamycin: a randomized, controlled trial. *Gut Microbes* 10, 521–539. doi: 10.1080/19490976.2018.1560754

Winston, J. A., and Theriot, C. M. (2016). Impact of microbial derived secondary bile acids on colonization resistance against *Clostridium difficile* in the gastrointestinal tract. *Anaerobe* 41, 44–50. doi: 10.1016/j.anaerobe.2016.05.003

Winston, J. A., and Theriot, C. M. (2020). Diversification of host bile acids by members of the gut microbiota. *Gut Microbes* 11, 158–171. doi: 10.1080/19490976.2019.1674124

Yang, Y., Liu, S., Gao, H., Wang, P., Zhang, Y., Zhang, A., et al. (2020). Ursodeoxycholic acid protects against cisplatin-induced acute kidney injury and mitochondrial dysfunction through acting on ALDH1L2. *Free Radic. Biol. Med.* 152, 821–837. doi: 10.1016/j.freeradbiomed.2020.01.182

Ye, H. L., Zhang, J. W., Chen, X. Z., Wu, P. B., Chen, L., and Zhang, G. (2020). Ursodeoxycholic acid alleviates experimental liver fibrosis involving inhibition of autophagy. *Life Sci.* 242:117175. doi: 10.1016/j.lfs.2019.117175

Zhou, W., Wu, W. H., Si, Z. L., Liu, H. L., Wang, H., Jiang, H., et al. (2022). The gut microbe *Bacteroides fragilis* ameliorates renal fibrosis in mice. *Nat. Commun.* 13:6081. doi: 10.1038/s41467-022-35690-8

frontiers | Frontiers in Microbiology

TYPE Original Research
PUBLISHED 29 January 2025
DOI 10.3389/fmicb.2025.1515865

OPEN ACCESS

EDITED BY
Rachel Pilla,
University of Milan, Italy

REVIEWED BY
Elena Dalle Vedove,
CIAM S.r.l, Italy
Chi-Hsuan Sung,
Texas A and M University, United States

*CORRESPONDENCE
Xiaoqiong Li
✉ 0707lianlan@163.com

†These authors have contributed equally to this work

RECEIVED 23 October 2024
ACCEPTED 10 January 2025
PUBLISHED 29 January 2025

CITATION
Ren Q, Li Y, Duan M, Li J, Shi F, Zhou Y, Hu W, Mao J and Li X (2025) *In vitro* modeling of feline gut fermentation: a comprehensive analysis of fecal microbiota and metabolic activity.
Front. Microbiol. 16:1515865.
doi: 10.3389/fmicb.2025.1515865

In vitro modeling of feline gut fermentation: a comprehensive analysis of fecal microbiota and metabolic activity

Qianle Ren[1,2†], Yuling Li[1†], Mingmei Duan[1], Jinjun Li[1], Fangshu Shi[1], Yun Zhou[3], Wanjing Hu[3], Junfu Mao[4] and Xiaoqiong Li[1*]

[1]State Key Laboratory for Managing Biotic and Chemical Threats to the Quality and Safety of Agro-products & Food Sciences Institute, Zhejiang Academy of Agricultural Sciences, Hangzhou, China, [2]College of Veterinary Medicine, Jilin University, Changchun, China, [3]Guangzhou MYBAO Biotechnology Co., Ltd, Guangzhou, China, [4]New Ruipeng Pet Group Inc., Beijing, China

The gut microbiota (GM) is a large and diverse microbial community that plays essential roles in host health. The *in vitro* fermentation model of the fecal GM serves as a valuable complement to food and health research in both humans and animals. Despite advancements in standardized protocols for culturing human GM, research concerning animals—particularly companion animals—remains limited. This study aims to identify the optimal *in vitro* fermentation method for cat gut microbiota by comprehensively analyzing fecal microbiota and fermentation characteristics. We evaluated seven culture media previously used to simulate the gut microenvironment in humans, dogs, and cats: anaerobic medium base (AMB), Minimum medium (MM), Pet medium (PM), VI medium (VI), VL medium (VL), Yeast culture medium (JM), and yeast casitone fatty acid agar medium (YCFA). Fresh fecal samples were fermented in these media for 48 h, followed by 16S rRNA sequencing to assess bacterial community composition and targeted metabolite monitoring during fermentation. The results revealed that the substrate composition in the medium differentially impacts bacterial community structure and fermentation characteristics. High levels of carbon and nitrogen sources can substantially increase gas production, particularly CO_2, while also significantly enhancing the production of short-chain fatty acids (SCFAs). Additionally, substrates with a high carbon-to-nitrogen ratio promote the production of more SCFAs and biogenic amines, and enrich the *Bacteroidaceae* family, even when the total substrate amount is lower. Comprehensive analysis of gut microbiota and metabolites reveals that PM medium effectively simulates a nutrient-deficient microenvironment in the cat gut during *in vitro* fermentation. This simulation maintains bacterial community stability and results in lower metabolite levels. Therefore, using PM medium to culture cat gut microbiota for 48 h, without focusing on specific bacterial genera, represents the most suitable *in vitro* model.

This finding contributes to understanding the optimal conditions for simulate cat gut microbiota and may provide a new approach for investigating the food pharmaceuticals on the cat gut microbiota and related health.

KEYWORDS

cat, gut microbiota, *in vitro* fermentation, targeted metabolites, SCFAs

1 Introduction

Cats are among the most popular companion animals, and their health has become an increasing concern for pet owners (Wu et al., 2024). The GM, a complex microbial community involved in barrier protection, nutrition, metabolism, and immunity, is integral to host health (Li et al., 2024). It maintains gut and host homeostasis by defending against intestinal pathogens, providing nutrients, promoting nutrient digestion and absorption, enhancing barrier function, stimulating intestinal development, and regulating the immune system (Paone and Cani, 2020; Hill and Round, 2021; de Vos et al., 2022). Like those in the human microbiome, the key phyla in the microbiota of cats and dogs include *Firmicutes*, *Bacteroidetes*, *Proteobacteria*, *Actinobacteria*, and *Fusobacteria*. These microbes ferment dietary fiber and unabsorbed carbohydrates to produce lactic acid and short-chain fatty acids (SCFAs) while also generating gases such as carbon dioxide and hydrogen (Swanson et al., 2011; Vázquez-Baeza et al., 2016; Coelho et al., 2018). SCFAs, primarily acetate, propionate, and butyrate, serve as energy substrates for colonic epithelial cells, maintain epithelial barrier integrity, regulate energy metabolism, and exhibit anti-inflammatory effects, thereby contributing to gut and host health (Arpaia et al., 2013; Koh et al., 2016; Zhang et al., 2021). Conversely, bacterial fermentation of proteins through amino acid decarboxylation produces various biogenic amines (BAs), such as serotonin, putrescine, cadaverine, histamine, and tyramine, which pose significant toxicological risks (Lau et al., 2022).

Animal experiments are commonly used to study changes in and functions of the GM. For example, animal models have been established to investigate the effects of high-fructose corn syrup on skeletal health and the GM in male mice (Han et al., 2022), explore whether resveratrol alleviates type II diabetes by modulating the GM (Hou et al., 2023), and evaluate the antiaging effects of the dietary dye morin (Shenghua et al., 2020). However, conducting animal experiments is expensive and ethically controversial. Thus, *in vitro* fermentation has been utilized as an effective tool for assessing drug effects and conducting health-related research (Zhou et al., 2018; Yousi et al., 2019; Van den Abbeele et al., 2020).

Limitations in studying human and animal GM include difficulties in accessing the gut, complexity in microbial analysis, and ethical concerns. *In vitro* fermentation can address these challenges and provide an alternative research method (Wan et al., 2021). Establishing a stable *in vitro* cultivation method that maintains the bacterial community structure during drug experiments is crucial. Previous research has shown that MM medium, a peptone-containing oligotrophic fermentation medium, serves as a static batch fermentation model for human fecal samples and has been used to study the effects of single foods or nutrients on the composition and function of the GM (Pérez-Burillo et al., 2021). YCFA medium was used to culture chicken cecal contents, selectively enriching Desulfovibrionaceae (Crhanova et al., 2019). JM was used as an *in vitro* colonic model for dogs and cats to evaluate the effects of different yeast-derived formulations on the GM composition and metabolites (Van den Abbeele et al., 2020). Lei et al. (2012) used VL and VI media to cultivate human and chicken GM, respectively, analyzed differences in microbial composition and fermentation metabolites, and investigated the relationship between GM composition and function. AMB medium was identified as suitable for cultivating human GM *in vitro* (Wan et al., 2021). Like JM, PM has been used for *in vitro* fermentation experiments in dogs and cats to study the impact of different dietary fiber sources on microbial fermentation activity (Sunvold et al., 1995).

Studies indicate that approximately 50 to 90% of the GM can be cultured *in vitro* under suitable nutritional conditions. The addition of specific nutritional components or pharmaceutical ingredients can selectively culture certain bacterial taxa (Browne et al., 2016; Lau et al., 2016). *In vitro* gut models are categorized into simple static single-chamber models and more complex dynamic multichamber models. The thermostatic batch culture system, a widely used simple colon model, offers advantages such as ease of operation, no need for nutrient replenishment, and the ability to culture microbial communities in large batches (Deschamps et al., 2022). However, it is constrained by substrate availability, which limits the culture duration. In contrast, continuous fermentation dynamic models can consist of either single or multiple connected chambers. These models allow for the monitoring of parameters such as temperature, pH, and transit time in various gut regions, including the colon, while continuously replenishing substrates to sustain the GM over extended periods (from several weeks to months) (Fehlbaum et al., 2015). Despite these benefits, continuous fermentation models are more susceptible to contamination and are more challenging to use. Various media are used as *in vitro* alternatives for humans and animals, but comprehensive evaluations of the effectiveness of these media in simulating the gut environment are lacking. In this study, we inoculated fecal samples from healthy pet cats into the aforementioned seven culture media and analyzed the GM structure, SCFAs, and targeted metabolite levels after 48 h of fermentation. By comprehensively analyzing the GM and metabolites during cultivation, we determined the optimal *in vitro* fermentation medium for cat GM. Hence, an optimal fermentation medium should accurately simulate the growth environment of a cat's GM while preserving its original community structure. The findings of this study could serve as a

valuable reference for conducting *in vitro* cultivation experiments on cat fecal GM.

2 Material and methods

2.1 Reagents and materials

The SCFA standard solutions, including butyric acid, acetic acid, propionic acid, butanoic acid, isobutyric acid, valeric acid, and isovaleric acid, were obtained from Shanghai Aladdin Bio-Chem Technology Co., Ltd (Shanghai, China). Standards for eight BAs or their hydrochlorides—serotonin, phenylethylamine, spermine, agmatine, cadaverine, putrescine, octopamine, tyramine, and histamine—were purchased from Sangon Biotech (Shanghai, China). YCFA broth was acquired from Qingdao Haibo Biotechnology Co., Ltd (Shandong, China). Anaerobic medium base (AMB), minimum medium (MM), pet medium (PM), VI medium (VI), VL medium (VL), and yeast culture medium (JM) were prepared in house on the basis of prior research conducted in our laboratory. All other reagents used were of analytical grade.

2.2 *In vitro* culturing of the intestinal microbiota

Seven types of culture media—MM, VL, VI, PM, YCFA, JM, and AMB—were selected to simulate the intestinal environment. The compositions of these media are detailed in Supplementary Table 1. The constituents of the seven culture media were classified into eight distinct categories: sugars, nitrogen sources, vitamins, inorganic salts, minerals, and mucin. The visualization of bubble sizes corresponded to the concentration of each nutrient category (g/L), thereby enabling a detailed analysis of the effects and interactions of various nutrients on the bacterial community (Tramontano et al., 2018; Yousi et al., 2019). Data visualization was conducted utilizing ChiPlot. Media were prepared following published methods with minor modifications (Sunvold et al., 1995; Lei et al., 2012; Crhanova et al., 2019; Van den Abbeele et al., 2020; Wan et al., 2021). Each broth sample was added to a shaking tube.

Fecal samples were collected from nine healthy pet cats, with the uncultured original fecal group denoted the OR group. Information about the cats is provided in Supplementary Table 2, and this study was conducted with the consent of the cat owners. Approximately 2 g of each sample was placed in 20 mL of sterile physiological saline (0.9%, w/v), sealed with liquid paraffin, and transported on dry ice, with experiments conducted within 3 h. Subsequent experiments were performed in an anaerobic workstation (HYQX-III-Z, Shanghai YOKE Medical Instrument Co., Ltd., Shanghai, China) with an anaerobic gas mixture of 5% H_2, 5% CO_2, and 90% N_2. After the samples were allowed to stand under anaerobic conditions for a few minutes, 1 mL of the supernatant was collected from beneath the liquid paraffin layer and added to a shaking tube containing 10 mL of broth. The culture media were connected to anaerobic gas through shaking tubes. Each broth was replicated three times, with unvaccinated broth serving as a control. All shaking tubes were cultured under anaerobic conditions at 37°C for 96 h with shaking at 100 rpm.

2.3 Sample collection

At 0, 24, and 48 h of fermentation, three sets of cultures were collected, rapidly frozen in liquid nitrogen, and stored at −80°C for subsequent analyses. For each time point, nine sample tubes were collected for gas production analysis, BA determination, pH measurement, ammonia analysis, SCFA analysis, and 16S rRNA sequencing.

2.4 Gas production analysis

After 48 h of fermentation, gas production and the levels of H_2, CO_2, CH_4, and H_2S were determined via a gas analyzer (HL-QT01, Hangzhou Hailu Medical Technology Co., Ltd.). The detection chamber was adjusted to a specific vacuum level via a vacuum generator, and the gases in the sample container were monitored by the 315 sensor in the detection chamber. The software (Multi-Gas Analyzer.exe) was used with a nonfecal medium as the zero gas to calculate the gas content and composition.

2.5 Determination of BAs

The assessment method for BAs in fermentation liquid samples was adapted from Sang et al. (2020) with modifications. Specifically, 100 μL of 2 mol/L sodium hydroxide solution, 300 μL of saturated sodium bicarbonate solution, and 2 mL of dansyl chloride derivatization reagent were sequentially added to 1 mL of pretreated samples. The mixture was incubated at 40°C in the dark for 45 min, after which 100 μL of concentrated ammonia was added to terminate the reaction. After standing for 30 min, the mixture was adjusted to volume with acetonitrile. The supernatant was filtered through a 0.22 μm organic phase membrane. For untreated fecal samples, PBS was used for dissolution. After centrifugation at 3,000 × *g* for 5 min at 4°C, the supernatant was processed as described for fermentation. BA quantification was performed via a Shimadzu high-performance liquid chromatography system with two elution solutions: A (ultrapure water, 0.1% acetic acid) and B (acetonitrile, 0.1% acetic acid). An automatic sampler passed through a ChromCore C18 column (4.6 × 250 mm, 5 μm) at a flow rate of 0.80 mL/min and a column temperature of 30°C, with ultraviolet detection at 254 nm; the injection volume was 10 μL. The gradient elution program was as follows: 0–2 min, 45% A; 2–20 min, 45–18% A; 20–27 min, 18–5% A; 27–30 min, 5% A; 30–32 min, 5–45% A; and 32–42 min, 45% A. Calibration curves were generated by analyzing a standard BA mixed solution for quantifying each BA.

2.6 Determination of pH value

At 0, 24, and 48 h of fermentation, 0.5 mL samples of fermentation broth were collected, and fermentation was stopped by immersing the samples in an ice–water bath for 10 min. The pH values of the fermentation broth were subsequently measured via a pH-5S meter (Shanghai Sansi Instrument Factory, Shanghai, China).

2.7 Ammonia and SCFA analysis

A fully automatic biochemical analyzer (HB-21, Suzhou Hailu Biotechnology Co., Ltd., China) was used to analyze fermentation liquid samples collected 48 h postfermentation with an ammonia detection reagent kit (enzyme method) from Zhejiang Ningbo Meikang Biotechnology Co., Ltd., China.

Five hundred microliters of fermentation broth was mixed with 100 microliters of butyric acid solution at a 1:5 ratio for acidification for 24 h, followed by storage at −80°C. Prior to SCFA determination, the samples were thawed and centrifuged at 14,000 rpm for 5 min, after which the supernatant was filtered through a 0.22 μm membrane. A gas chromatograph (GC-2010 Plus; equipped with a DB-FFAP column from Agilent Technologies, Inc., Santa Clara, CA, USA) was used for sample analysis.

2.8 DNA extraction, 16S rDNA amplicon library preparation and HiSeq sequencing

Bacterial DNA was extracted from the fecal samples via a fecal DNA kit (Omega Biotek, Norcross, GA, USA). The DNA concentration and purity were quantified with a NanoDrop 2000 UV-Visible spectrophotometer (Thermo Scientific, Wilmington, USA). DNA integrity was assessed by 1% agarose gel electrophoresis. The V3-V4 hypervariable region of the 16S rRNA gene was amplified via the gene-specific primers 338F (5′-ACTCCTACGGGAGGCAGAG-3′) and 806R (5′-GGACTACCVGGGTATCTAAT-3′). The PCR mixture included 10 μL of template DNA, 2 μL of ddH_2O, 3 μL of primers, and 15 μL of Phusion High-Fidelity PCR Master Mix (New England Biolabs).

The PCR products were extracted from a 2% agarose gel and purified via the AxyPrep DNA Gel Extraction Kit (Axygen Biosciences, Union City, CA, USA). The purified DNA was quantified via a QuantiFluor-ST fluorometer (Promega, USA). Sequencing of the amplicons with equimolar and paired-end libraries was performed on the HiSeq 2500 platform (Illumina, CA, USA) following standard protocols provided by Shanghai Majorbio Pharmaceutical Technology Co., Ltd.

The raw paired-end sequencing data were quality controlled via fastp software[1] (version 0.19.6). FLASH software was employed to assemble the cleaned sequences. The optimized sequences resulting from quality control and assembly were denoised via the DADA2 plugin in QIIME 2 with default parameters. We excluded sequences corresponding to chloroplast and mitochondrial origins, as well as those with a relative abundance of less than 0.5% across all sequences, from our analysis. Furthermore, we conducted rarefaction analysis on each sample, normalizing the sequence counts to the minimum observed, with all samples standardized to a uniform count of 16,666 sequences per sample. Taxonomic classification of amplicon sequence variants (ASVs) was performed via the naive Bayes classifier in QIIME 2. The Shannon diversity and Chao indices were computed via mothur v.1.30. Principal coordinate analysis (PCoA) based on the Bray-Curtis distance metric was employed to visualize the distance matrix of microbiota across different culture media at the ASV level.

1 https://github.com/opengene/fastp

2.9 Statistical analysis

Using IBM SPSS Statistics 27 for statistical analysis, the Shapiro–Wilk test and Levene's test were employed to assess data normality and homogeneity of variances, respectively. For normally distributed data with equal variances (pH changes during the 0–48 h fermentation process in JM, YCFA, MM, and PM groups), one-way analysis of variance (ANOVA) followed by Bonferroni *post hoc* tests was conducted. For normally distributed data with unequal variances (ammonia, total gas production and H_2 production after 48 h of fermentation), Welch's test and Games-Howell *post hoc* tests were applied. For non-normally distributed data (BAs, CO_2, H_2S, and CH_4 production, as well as gut microbiota α-diversity after 48 h of fermentation), the Kruskal-Wallis test with multiple pairwise comparisons was used. Bonferroni correction was applied to adjust significance thresholds for multiple comparisons. A p-value of < 0.05 was considered statistically significant.

3 Results

3.1 Comparison of media composition

In this study, we employed seven culture media—MM, AMB, VL, VI, YCFA, PM, and JM—to cultivate the GM of cats. All media were composed of commercially available ingredients (Figure 1). MM lacks sugars and has the fewest nutritional components. The JM medium contains the highest contents of mucin, inorganic salts, and minerals. PM is the only medium supplemented with SCFAs as an energy source. VI and VL contain the highest amounts of sugars and relatively more nitrogen sources, inorganic salts, and minerals. The nutritional compositions of AMB and YCFA are similar; however, AMB has a lower nitrogen content and higher vitamin content than YCFA does.

3.2 Effects of microbial metabolic activity in terms of BAs, ammonia and gas production

Figure 2A shows the production of BAs from the seven culture media and the original fecal samples after 48 h of fermentation. BA production in the MM and VL groups was significantly greater than that in the control group OR ($p < 0.001$), whereas that in the JM, AMB, and PM groups was similar to that in group OR. We further evaluated the ammonia concentration in the fermentation broth of the seven culture media. As illustrated in Figure 2B, the ammonia concentration ranked from highest to lowest as follows: AMB > MM > PM > JM > YCFA > VI > VL, with significant intergroup differences ($p < 0.05$).

Additionally, Figure 2C shows the proportions of CO_2, H_2S, CH_4, and H_2 in each group. The VI group presented the

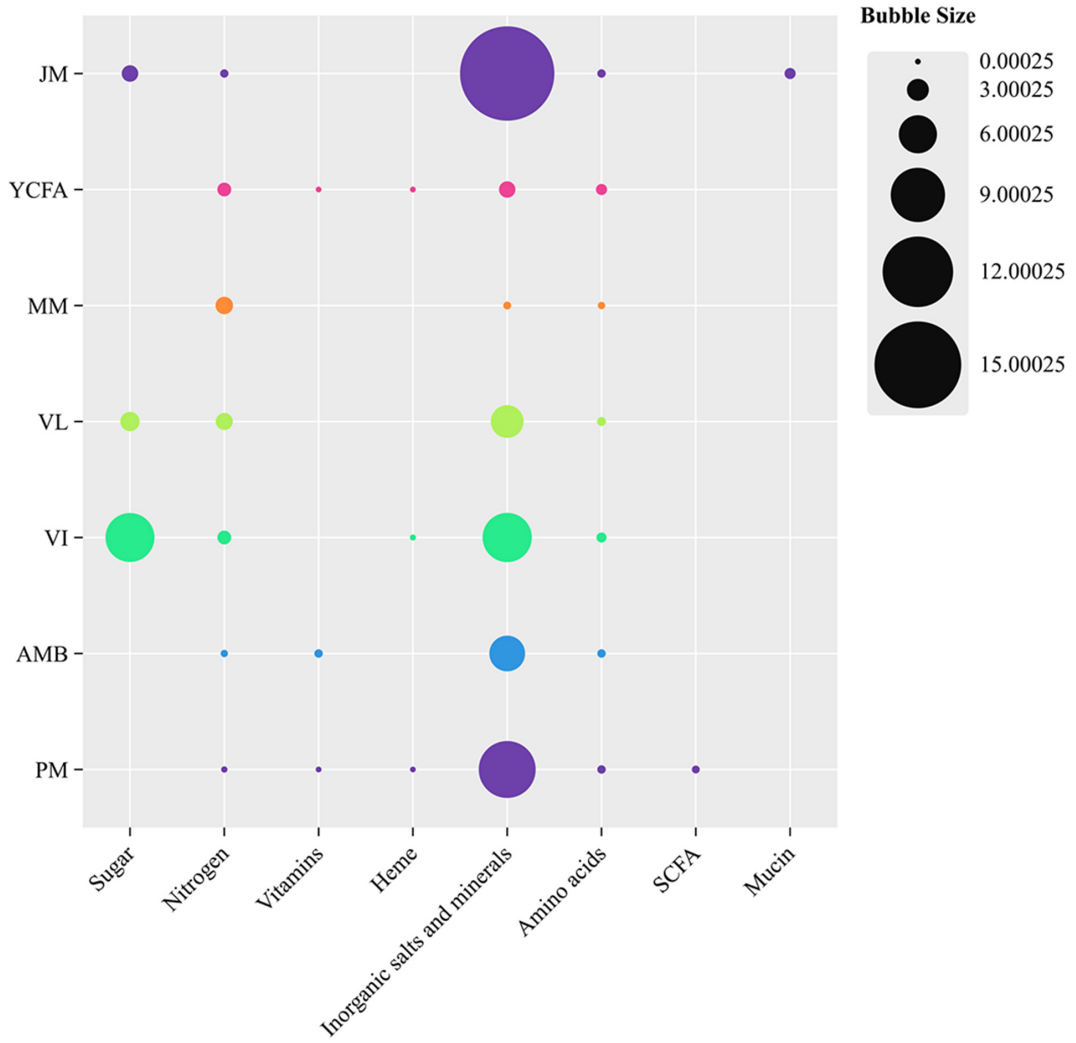

FIGURE 1
Comparison of different nutritional components in seven culture media: MM, AMB, VL, VI, YCFA, PM, and JM. The size of the bubbles is linearly related to the concentration of each nutritional category (g/L). ChiPlot was used for data visualization.

highest proportion of CO_2, whereas the PM group presented the lowest proportion, with significant differences between the groups ($p < 0.05$). The YCFA group had the highest proportion of H_2S, while the VL group had the lowest, with significant differences ($p < 0.05$). The VI group presented the highest proportion of CH_4, whereas the YCFA group presented the lowest proportion, with significant differences ($p < 0.05$). The VI group also had the highest proportion of H_2, while the PM group had the lowest, with significant differences ($p < 0.05$). The total gas production after 48 h of fermentation ranked as follows: VI > VL > JM > YCFA > MM > AMB > PM, with significant differences among the groups ($p < 0.05$) (Figure 2D).

3.3 Overall microbial metabolic activity in terms of pH and SCFA production

Changes in pH can indicate the production of specific metabolites, primarily a decrease in pH due to acidic metabolites (e.g., SCFAs) and an increase in pH due to protein hydrolysis fermentation metabolites (e.g., BAs) (Van den Abbeele et al., 2020). During the simulation of the feline GM, with the exception of YCFAs, the pH values of the other media significantly decreased throughout the fermentation process compared with those before fermentation (0 h) (Figure 3A). The major decline occurred between 24 and 48 h, suggesting increased bacterial metabolic activity and the production of acidic metabolites.

SCFAs are crucial metabolic byproducts in the fermentation process and are primarily generated through the fermentation of indigestible carbohydrates (Ma et al., 2024). We detected the levels of SCFAs in the seven different culture media during the 48-h fermentation process (0, 24, and 48 h). As shown in Figure 3B, total SCFA production increased with prolonged fermentation time, reflecting changes in pH values. The VL and VI groups presented the highest total SCFA production at 48 h (28.3 ± 0.42 mmol), followed by the MM group, whereas the PM group presented the lowest SCFA production (6.57 ± 0.76 mmol). These findings indicate that the composition of the culture media significantly

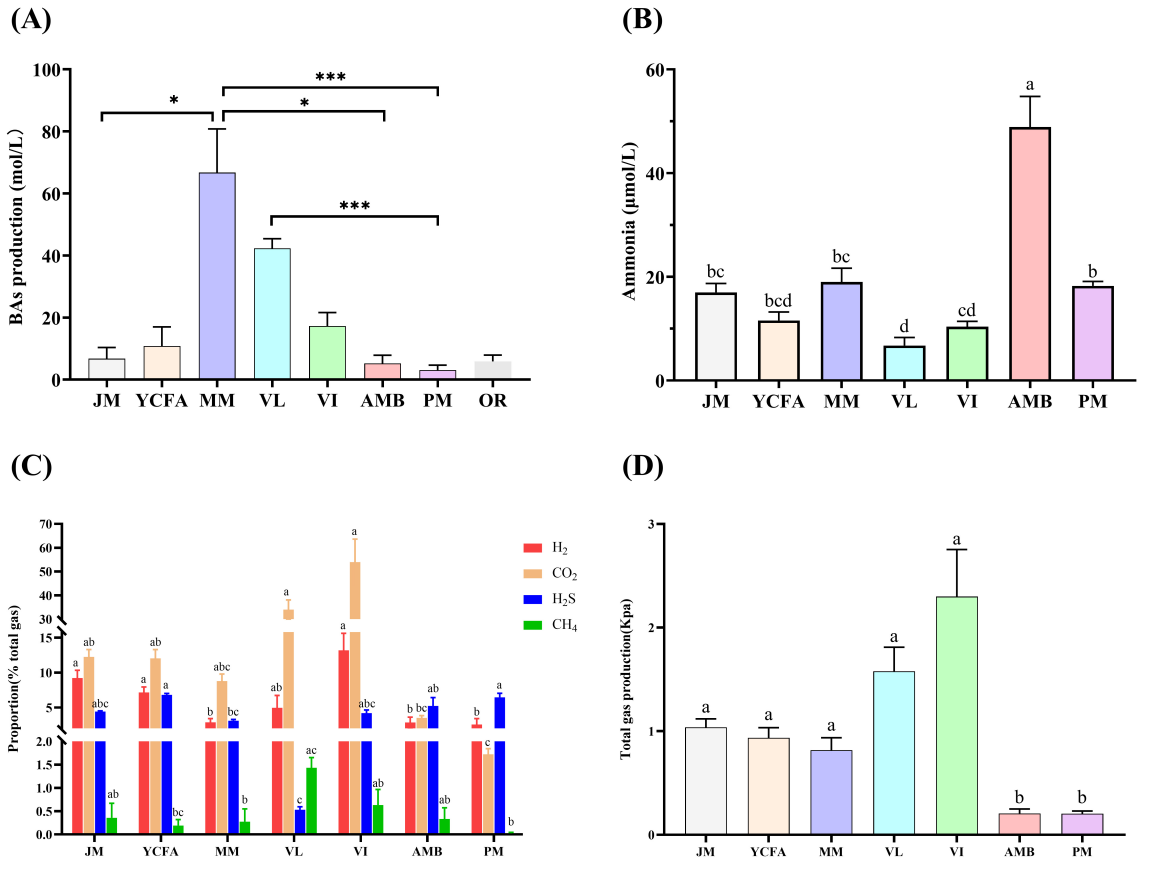

FIGURE 2
The production of BAs, ammonia and gas in different media after 48 h of fermentation. **(A)** BA production; compared with original feces OR, * indicates $p < 0.05$, *** indicates $p < 0.001$, no mark indicates that the difference was not significant. **(B)** Ammonia production; **(C)** proportions of H_2, CO_2, H_2S and CH_4 produced; **(D)** total gas production. Different letters indicate significant differences ($p < 0.05$), and the same letters indicate no significant difference ($p > 0.05$). The data are expressed as the means ± SEMs ($n = 9$).

influences SCFA production. Nutrient-rich media with high carbon and nitrogen sources promote the rapid growth of SCFA-producing bacteria, resulting in increased SCFA levels. Conversely, nutrient-deficient media (PM and AMB) slow bacterial growth, leading to lower SCFA levels.

3.4 Effects of various cultivation media on the GM community

Cat fecal samples were inoculated with the seven tested media and fermented *in vitro* for 48 h. Sequencing was performed via the Illumina MiSeq platform, and the results were compared with those of OR to assess the effect of each medium on the gut flora. Alpha diversity, reflected by the Ace, Chao, Shannon, and Simpson indices, estimates microbial community diversity and abundance (Le Chatelier et al., 2013). Figures 4A–D show that the Chao and Ace indices of the VI group were significantly lower ($p < 0.05$) than those of the original cat feces M group. The Chao and Ace indices of the PM and AMB groups significantly increased, both of which were greater than those of the VI group ($p < 0.05$). The Simpson index was lowest in the PM group and highest in the MM group. The Shannon index was highest for the PM group and lowest for the MM group, but these differences were not significant.

To clearly present the PCoA results, we divided the analysis into two separate figures to compare the seven treatment groups with group OR. On the basis of nutritional components, different culture media were categorized into carbohydrate groups (VI, VL, JM) and nitrogen source groups (AMB, PM, YCFA, MM). PCoA describes the diversity of the GM among groups and compares it with that of OR. The PCoA results revealed that in the carbohydrate groups, the VI group exhibited a relatively large dispersion, indicating significant intragroup differences. The JM, VI, and VL groups were distinctly separated from the OR group, suggesting differences in community composition (Figure 4E). In the nitrogen source groups, there was no significant difference between the PM, YCFA, and MM groups and the OR group except for the AMB group, indicating a similarity in community composition. These data explain 35.26 and 14.77% of the variance in the PCoA model for PC1 and PC2, respectively (Figure 4F), suggesting the reliability of these profiles. Additionally, we employed Weighted UPGMA clustering analysis to observe the differences and similarities among various groups (Supplementary Figure 1). The results indicated that the PM group exhibited a high degree of similarity with the OR group, followed by the VI group. The remaining groups, however, showed significant differences from the OR group.

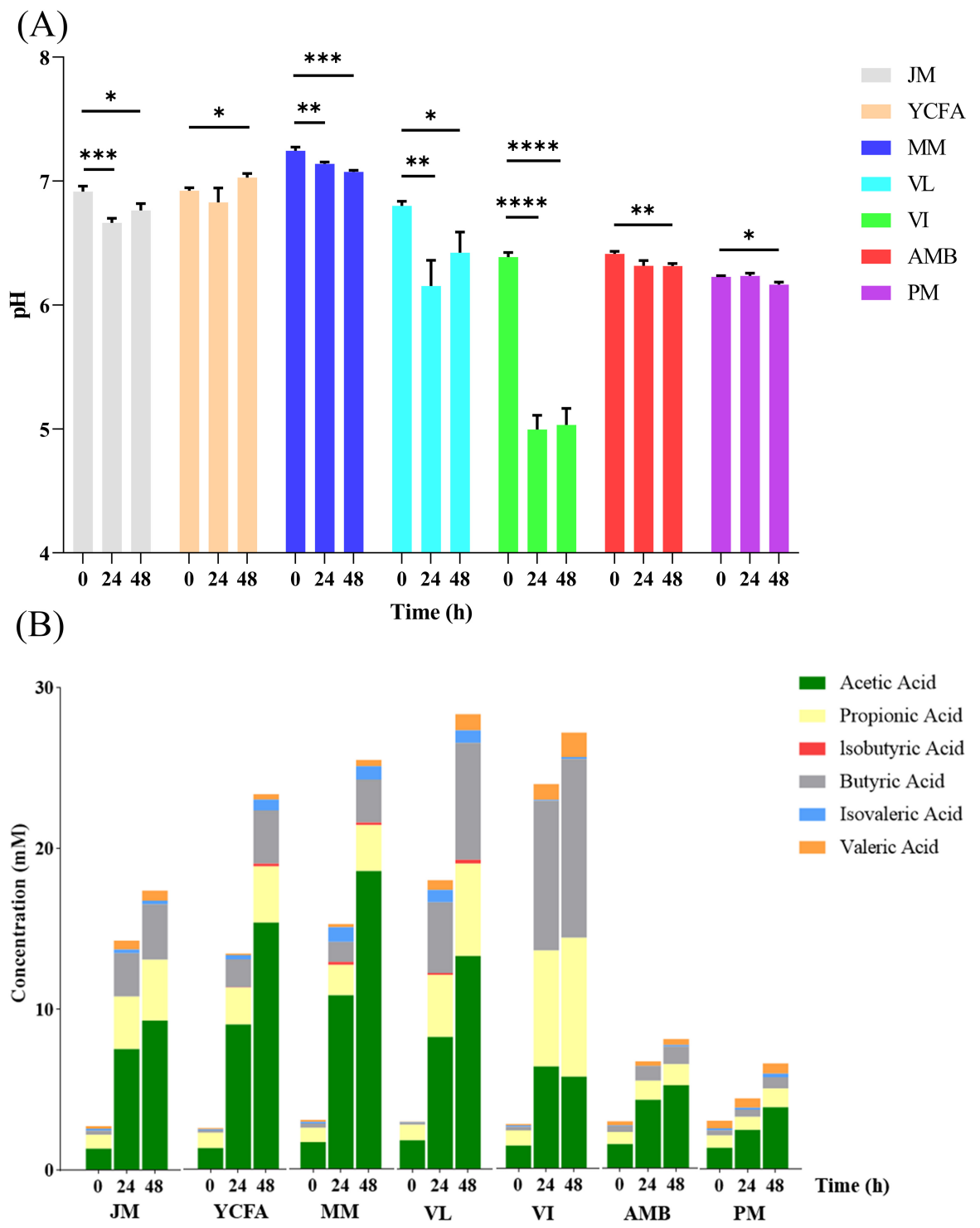

FIGURE 3
(A) Changes in pH in different media and times during *in vitro* culture; * indicates $p < 0.05$; ** indicates $p < 0.01$; *** indicates $p < 0.001$; **** indicates $p < 0.0001$. The data are expressed as the means ± SEMs ($n = 9$). **(B)** SCFA levels in different media and at different times during *in vitro* culture. The data are expressed as the means ($n = 9$).

3.5 Composition of the GM

We used seven pairwise Venn diagrams to illustrate the retention of ASVs (Amplicon Sequence Variants) by the seven media compared to OR (Figures 5A–G). The results showed that PM medium shared 383 ASVs with OR, the highest among all groups. Additionally, PM uniquely retained 250 ASVs, while OR had 301 unique ASVs. The second-highest retention was observed in AMB medium, which shared 337 ASVs with OR. The other media exhibited relatively poorer retention performance.

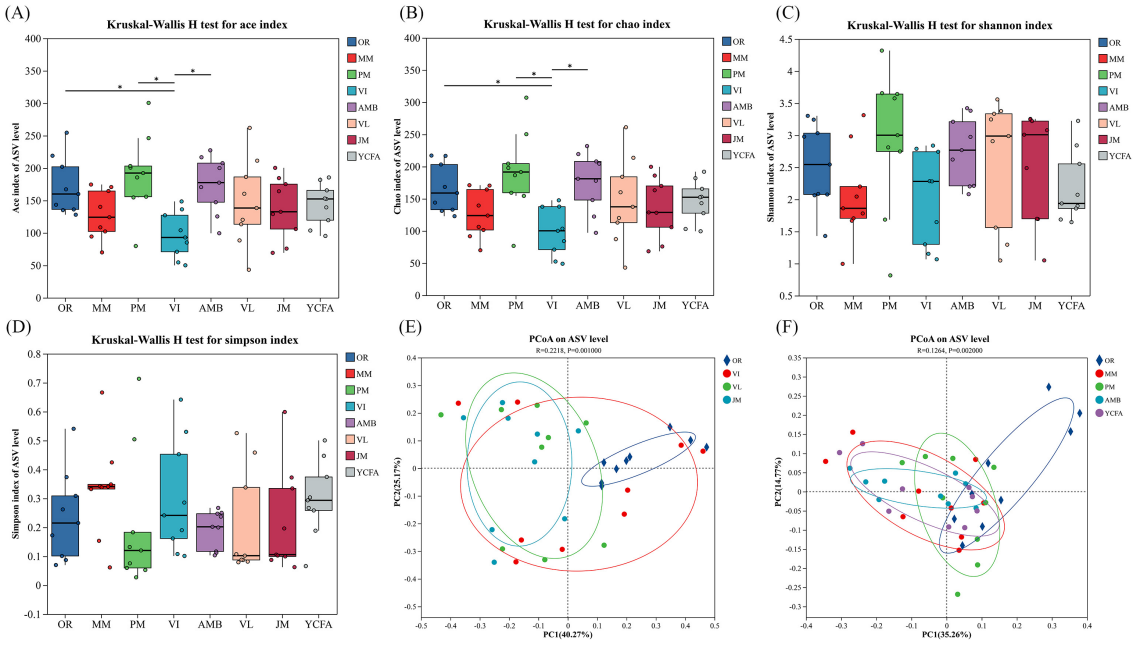

FIGURE 4
(A–D) Community diversity as measured by the Ace index **(A)**, Chao index **(B)**, Shannon index **(C)** and Simpson index **(D)** of the MM, AMB, JM, PM, VI, VL, YCFA, and OR groups after 48 h of fermentation. **(E,F)** Principal coordinate analysis (PCoA) between seven different media and the uncultivated group. * indicates $p < 0.05$. The data are expressed as the means ± SEMs ($n = 9$).

To further evaluate the cultivation effects of different media, we conducted an analysis of the microbial community composition and LEfSe differential analysis for the seven media groups and the control group. *Firmicutes*, *Actinobacteria*, *Proteobacteria*, and *Bacteroidota* were the dominant phyla in all groups, whereas *Fusobacteriota* accounted for a relatively small proportion in each group, indicating changes in the relative abundance of the top six phyla across groups (Figure 5H). The heatmap of community composition at the family level (Figure 5I) revealed that only the VI group presented a significant decrease in the content of *Lachnospiraceae* at 48 h compared with the uncultured group M. Groups MM, YCFA, and JM presented little change in the content of *Enterococcaceae* and *Enterobacteriaceae* at 48 h, whereas the content of *Coriobacteriaceae* and *Ruminococcaceae* decreased sharply. *Erysipelotrichaceae* significantly decreased in the MM and JM groups, whereas *Bacteroidaceae* significantly increased in the JM group. In the VL group, the contents of *Bacteroidaceae* and *Tannerellaceae* increased sharply, and *Tannerellaceae* remained relatively stable during incubation, except in the VL group. Microbial families with relatively few observations also showed significant changes, such as *Veillonellaceae, whose abundance* significantly increased in the PM group, and *Selenomonadaceae, whose abundance* significantly increased in the VI group. After 48 h of fermentation, the relative abundance of *Coriobacteriaceae* in six out of the seven culture media, with the exception of VI, was lower than that in the original unfermented fecal samples. This could be attributed to the anaerobic nature of bacteria belonging to the *Ruminococcus* genus, making cultivation challenging. Throughout the cultivation process, the relative abundances of *Enterococcaceae* and *Enterobacteriaceae* remained stable. The analysis of substrate composition revealed that the high carbon-to-nitrogen ratios in JM and VL significantly promoted the growth of *Bacteroidaceae*. Similarly, at the genus level (Figure 5J), comparable results were observed. The dominant and subdominant genera in OR, including *Peptoclostridium*, *Collinsella*, and *Blautia*, were retained in both PM and VL media, where they also remained dominant genera.

LEfSe (linear discriminant analysis effect size) analysis was used to compare the estimated bacterial phylotypes of the seven media at 48 h. Evolutionary maps were plotted via the default parameters ($p < 0.05$, LDA score > 2.0), which revealed differences in abundance between the groups (Supplementary Figure 2). In the OR group, *Clostridia*, *Erysipelotrichaceae*, *Erysipelotrichales*, *Prevotellaceae* and *Holdemanella* were the dominant classes of bacteria. In the PM group, *Lachnospirales*, *Lachnospiraceae*, *Veillonellaceae* and *Megasphaera* were dominant. In the VI group, *Negativicutes*, *Selenomonadaceae* and *Megamonas* were the most dominant. In the AMB group, *Peptostreptococcus*, *Fusobacteriia* and *Fusobacteriales* were dominant. In the VL group, *Tannerellaceae*, *Parabacteroides* and *Alistipes* were the most dominant. In the JM group, *Bacteroidales*, *Bacteroidia* and *Bacteroidaceae* were dominant. In the YCFA group, *Peptostreptococcaceae* and *Peptoclostridium* were the dominant classes of bacteria. The MM group is highly consistent with the YCFA group.

3.6 Functional predictions of the GM communities

For Tax4Fun functional prediction (Figure 6 and Supplementary Figures 3–8), the metabolic pathways of the eight groups were similar, encompassing carbohydrate metabolism,

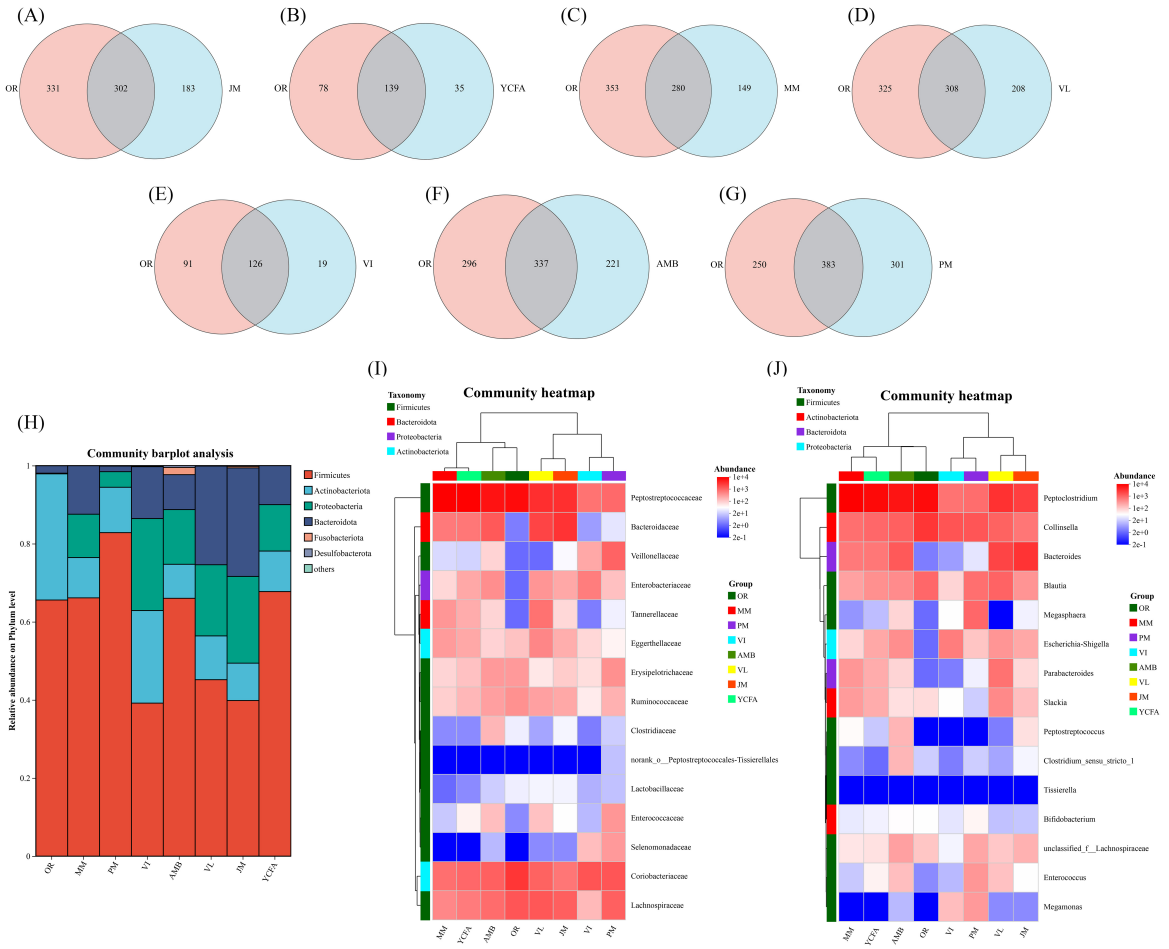

FIGURE 5
(A–G) Venn diagram showing the shared and unique numbers of ASVs between seven culture medium samples and the OR. **(H)** Stacked bar plot showing the average relative abundance at the phylum level. **(I)** Community heatmap showing the average relative abundance at the family level. **(J)** Community heatmap showing the average relative abundance at the genus level.

amino acid metabolism, and energy metabolism. Environmental information processing, genetic information processing, cellular processes, human diseases, and organismal systems are also consistent, with subtle variations in values.

3.7 Correlation analysis between metabolites and the GM

We investigated the correlations among SCFAs, BAs, ammonia, and the GM (Supplementary Figure 9). Species from the *Clostridiaceae* family (*Holdemanella*, *Peptococcus*) were significantly negatively correlated with the production of propionic acid and butyric acid. Conversely, bacteria from the *Bacteroidaceae* family (*Bacteroides*, *Slackia* and *Parabacteroides*) were associated with increased production of acetic acid, propionic acid and butyric acid. The correlation trends between total SCFAs and the GM, as well as between acetic acid-GM and butyric acid-GM, were generally consistent, as acetic and butyric acids are the primary SCFAs. Thus, these data explain the high accumulation rate of SCFAs after 48 h of fermentation in groups enriched with *Bacteroidaceae* and with reduced *Lachnospiraceae*, such as VL, VI, MM, YCFA, and JM. Compared with those in the PM group, the abnormal increase in *Bacteroidaceae* and decrease in *Lachnospiraceae* in these groups disrupted the initial balance of the GM, resulting in increased SCFA production. This significant imbalance impacts the stability and reliability of SCFA content determination in fermentation studies *in vitro*. Additionally, *Enterococcus* was significantly negatively correlated with CO_2 production, *Megasphaera* was significantly positively correlated with H_2S production, and *Enterococcus* and *Holdemanella* were significantly negatively correlated with H_2 production. *Slackia* was negatively correlated with the production of ammonia and BAs, whereas *Escherichia-Shigella* had the opposite effect.

4 Discussion

While research on optimizing *in vitro* fermentation protocols for the human GM is extensive (Van den Abbeele et al., 2018), few studies have focused on the GM of pets, especially cats. The primary objective of this study was to assess the impact of different anaerobic batch culture media on the GM of felines and their associated metabolic products. The ultimate goal was to identify the

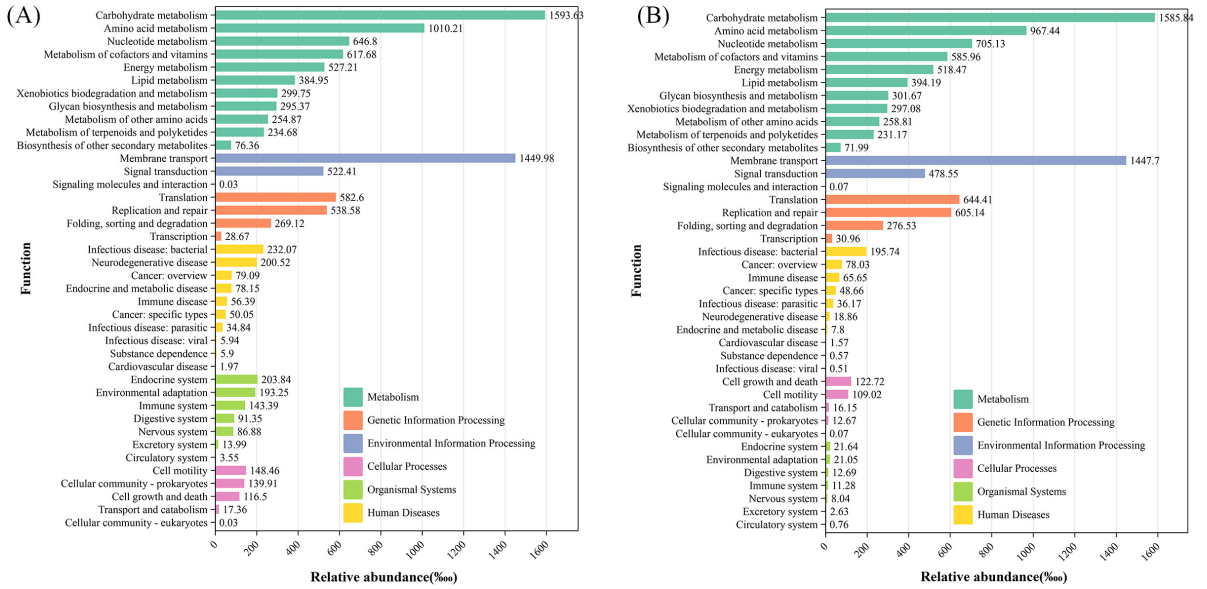

FIGURE 6
Tax4Fun function prediction of the PM-48 h group **(A)** and original feces **(B)** (the composition of the pathways of different components is displayed dynamically; the KEGG pathways of different levels are arranged on the vertical axis; and the length of the column indicates the corresponding functional abundance in the pathway).

most suitable *in vitro* fermentation method for simulating the cat gut microbiome.

Throughout the fermentation process, pH variation serves as an indicator of the overall metabolic activity of the GM, which is influenced by both the composition of the medium and the metabolic characteristics of the microbiota. In this study, among the seven tested media, the MM group presented the highest nitrogen content, whereas the VI group presented the highest carbohydrate content. The GM utilizes nitrogen sources during fermentation, leading to the release of ammonium ions and an increase in pH (Cummings and Macfarlane, 1991; Ma et al., 2017). Conversely, carbohydrate metabolism leads to the generation of organic acids (Laparra and Sanz, 2010), causing a decrease in pH. These factors explained the observed pH values after 48 h of fermentation, with the MM group having the highest pH and the VI group having the lowest pH. During the 48-h fermentation process, the pH exhibited a similar trend across all seven media, suggesting the preliminary feasibility of culturing cat fecal microbiota.

Ammonia in the colon originates primarily from the deamination process of dietary or endogenous proteins. Previous studies have demonstrated that dietary protein supplementation significantly increases the ammonia concentration in the intestines and feces (Geypens et al., 1997). Excessive accumulation of ammonia in the intestines can have adverse effects on overall health, including the disruption of intestinal mucosal repair and an increased risk of colon cancer. In a healthy colon, ammonia levels are typically low (Williams et al., 2001). Conversely, increasing carbohydrate levels, which serve as a source of energy for fermentation and bacterial growth, can reduce intestinal ammonia concentrations (Williams et al., 2001). Consistent with these findings, our study revealed that the VL and VI groups, characterized by high sugar contents, presented the lowest ammonia production. In contrast, the JM, YCFA, MM, and PM groups presented slightly greater ammonia production, whereas the AMB group presented significantly greater ammonia production than did the other groups. Given that cats are obligate carnivores with a diet predominantly composed of nitrogen-rich sources, the use of AMB *in vitro* to study feline dietary health may lead to biased assessments of ammonia production.

BAs are low-molecular-weight organic nitrogen bases that naturally occur as metabolic intermediates and byproducts in living organisms. They play crucial roles in various physiological functions, such as brain activity, gastric acid secretion, and immune responses. However, excessive absorption of BAs can pose health risks (Önal et al., 2013; Butor et al., 2023). BAs can accumulate in food at high concentrations due to the activity of microorganisms with decarboxylase enzymes, and recent outbreaks of foodborne diseases caused by BAs underscore the importance of their detection (Butor et al., 2023).

SCFAs produced by the GM play a vital role in maintaining host health by inhibiting the growth of harmful bacteria through pH reduction (Morrison and Preston, 2016). SCFAs have garnered substantial attention because of their pharmacological and physiological properties and potential impact on host health (Rauf et al., 2022). In *in vitro* fermentation studies investigating the protective effects of probiotics and functional foods, SCFA concentrations are commonly measured. This study revealed that different media compositions resulted in varying microbial community structures and, subsequently, different SCFA levels. When functional foods were studied via *in vitro* experiments, the use of specific media, such as VL, VI, or MM, resulted in higher concentrations of SCFAs than other media. This poses a challenge in attributing the increased SCFA levels solely to the functional food components, as the media itself promotes SCFA production. Therefore, for *in vitro* fermentation studies associated with food

research, media with lower SCFA concentrations, such as PM and AMB, are more appropriate.

Research on the composition of human intestinal gas has identified CO_2, H_2S, CH_4, and H_2 as the predominant gases produced primarily through GM fermentation (Ou et al., 2015). Among these gases, CO_2 is a major byproduct of carbohydrate fermentation. Consistent with previous studies (Zhang et al., 2023), the VI group, which had a high carbohydrate content, presented the highest proportion of CO_2. This suggests that the variations in CO_2 proportions among the groups are largely influenced by the carbohydrate content of the media. The phyla *Firmicutes* and *Bacteroidota* play significant roles in gas production in the intestine, with H_2 production being particularly common due to specific hydrogen-producing GM (Ou et al., 2015; Hylemon et al., 2018; Mutuyemungu et al., 2023). After 48 h of fermentation, the VI group presented the highest proportion of H_2 production among the seven groups, indicating a relatively high abundance of these species. Moreover, H_2 is utilized by other GMs to produce H_2S and CH_4. In this study, the YCFA group had the highest proportion of H_2S production, suggesting a greater abundance of hydrogen sulfide-fermenting bacteria in this group. Additionally, the VL group had the highest proportion of CH_4, although it was the smallest proportion among the seven groups, indicating a relatively lower presence of methane-fermenting microbiota in the feline colon. Under normal circumstances, the production of intestinal gas in the host is minimal. However, an imbalance in the proliferation of gas-producing bacteria can lead to excessive gas production, which can cause abdominal distension and discomfort (Martin-Gallausiaux et al., 2021). Intestinal gas production is closely associated with the pathogenesis of several gastrointestinal diseases and can be considered a biomarker for such conditions (Wang et al., 2021). Compared with the other groups, the PM and AMB groups presented relatively lower gas production, suggesting a more stable fermentation metabolism of the feline intestinal microbiota under these conditions.

After 48 h of cultivation, the microbial communities in the seven groups exhibited distinct changes. Compared with those of the original fecal GM, the Chao and Ace indices of the VI group significantly decreased, with the VL, MM, JM, and YCFA groups also showing slight decreases. In contrast, the Chao and Ace indices of the AMB and PM groups remained high, indicating that these groups effectively maintained community diversity and richness after 48 h of fermentation. PCoA revealed that the microbial community distribution in the original cat feces was similar to that in the PM, YCFA, and MM groups, whereas it significantly differed from that in the VI, VL, and JM groups. We speculate that, owing to differences between *in vivo* and *in vitro* environments and the inability of some bacteria to be cultured outside the body, all seven groups experienced varying degrees of ASV loss after 48 h of cultivation compared with the OR group. Additionally, PM and AMB retained the highest number of ASVs from the original feces, indicating that the PM and AMB effectively preserved the microbial diversity in the original cat fecal microbiota. Fermentation with AMB medium for 48 h effectively maintained the stability of the human intestinal microbial community structure, as reported in previous studies (Wan et al., 2021), which can be attributed to the different compositions of the human and cat intestinal microbial communities (Van den Abbeele et al., 2020). LEfSe analysis revealed differentially abundant taxa among the groups, with the GM community being more diverse in the PM medium, indicating that PM medium is suitable for most anaerobic bacteria. LDA scores revealed that *Lachnospiraceae* and *Tannerellaceae* were the bacterial taxa with significant differences in abundance between the PM and VL groups. Previous studies have shown that *Lachnospiraceae* and *Tannerellaceae* are primarily responsible for SCFA production (Zhao et al., 2022; Ćesić et al., 2023), suggesting a correlation between PM and VL media and high SCFA levels. The community composition results at both the family and genus levels indicated that the AMB and PM medium effectively preserved the dominant and subdominant microbiota from OR, without enriching low-abundance taxa in OR. In addition to AMB and PM, the results for YCFA also showed relatively small deviations from the OR group, and this smaller difference may be related to the poorer nutritional content of these media, resulting in lower modification of the microbiota composition. The observed changes in the gut flora across the groups were due mainly to differences in the media composition, leading to variations in metabolite levels, which is consistent with the SCFA analysis results. Correlation analysis suggested that the high accumulation rate of SCFAs, such as VL, VI, MM, YCFA, and JM, after 24 h of fermentation in groups enriched with *Bacteroidaceae* bacteria and reduced the abundance of *Lachnospiraceae* resulted in a significant imbalance, affecting the stability and reliability of SCFA content determination in *in vitro* fermentation studies.

An ideal *in vitro* gut fermentation model should simulate the *in vivo* conditions of cats. First and foremost, it must maintain a microbial community that is similar in both composition and structure to the selected gut compartment. Specifically, the *in vitro* microbial composition should mirror the inoculum or the simulated intestinal region, effectively preserving both dominant and subdominant genera. Given the vast number of species in feline fecal microbiota that are uncultured *in vitro* and the resolution limitations of 16S rRNA gene sequencing, comparisons are typically conducted at the family and genus levels (Zihler Berner et al., 2013). In our study, at the phylum level, the most abundant *Firmicutes* and the subdominant *Actinobacteriota* in the original feces were well-maintained in the PM medium as well as in other media. At the family level, the dominant *Peptostreptococcaceae*, *Coriobacteriaceae*, and *Lachnospiraceae* in the original feces also showed dominant abundance in the PM medium. Similarly, at the genus level, the dominant genera *Peptoclostridium*, *Collinsella*, and *Blautia* in the original feces and PM were preserved (Figures 5H–J). Although the microbiota structure within the AMB medium exhibited the closest clustering to the OR, the PM medium demonstrated a superior retention of ASVs present in the OR group, with a count of 383 compared to 337 for the AMB medium. This result underscores the PM medium's efficacy in preserving a greater proportion of the microbial diversity inherent in the original cat fecal microbiota (Figures 5A–G). Additionally, the PM group registered the highest α-diversity among the seven experimental groups, as depicted in Figures 4A–C, and showed a closer resemblance to the OR in β-diversity analysis (Figure 4F). Collectively, these observations indicate that the PM medium outperformed the other six culture media in terms of maintaining the fidelity and diversity of the cat fecal microbiota.

Simultaneously, it is imperative to ensure that the metabolic activity of the microbiota in the *in vitro* model closely resembles that observed *in vivo*, particularly regarding the production of

SCFAs, biogenic amine, ammonia, and gases during fermentation. The *in vitro* fermentation process should replicate the production of major SCFAs—namely acetic acid, propionic acid, and butyric acid—in proportions akin to those present in the inoculum (Isenring et al., 2023). Our study revealed that, after 48 h of fermentation, among the seven media tested, only the PM and AMB media generated a modest amount of SCFAs, with acetic acid being the predominant component, followed by propionic and butyric acids, mirroring the SCFA profile in the original feces at the commencement of fermentation (Figure 3B). Both the AMB and PM groups produced comparatively low levels of biogenic amine and gases. However, unlike the PM group, the AMB group yielded the highest amount of ammonia, which is detrimental when simulating colon fermentation conditions. Functional metagenomic prediction is instrumental in assessing the alignment between the metabolic and functional KEGG pathways of microbial communities within the *in vitro* fermentation model and their counterparts in the original microbial communities (Poeker et al., 2019). In our study, the metabolic pathways of the microbial communities across the seven media groups were found to be similar to those of the original fecal group, with only subtle numerical variations observed. Therefore, after a meticulous evaluation of these parameters, we propose that the PM medium is the most appropriate choice for *in vitro* fermentation models.

Furthermore, the chosen *in vitro* model must exhibit reproducibility. Acknowledging the substantial inter-individual variability inherent in gut microbiota, research on *in vitro* model selection should incorporate adequate replication and enhance the interpretability of data by leveraging microbiota from diverse donors. This approach addresses the individual variations within groups and broadens the generalizability of findings (Isenring et al., 2022). In line with this principle, we selected fecal microbiota from nine cats, representing a spectrum of genders, ages, and breeds, to serve as our inocula. This method circumvented the limitations associated with using samples from a single cat or pooling fecal samples for iterative cultivation experiments. Consequently, this strategy had been pivotal in ensuring the reproducibility and reliability of our study's results.

In vitro gut fermentation, uncoupled from the host, offers an optimal system for examining microbial responses to nutritional interventions, as it allows for the measurement of microbial dynamics without the confounding influence of the host (Liu et al., 2020). Both simple static batch fermentation models and complex dynamic models have their respective merits and drawbacks (Deschamps et al., 2022). Batch models, when compared with continuous fermentation models, exhibit certain limitations, including an inability to sustain stable microbial communities derived from the inoculum over prolonged periods, a lack of real-time pH control, and an inefficient removal of metabolic waste (Duysburgh et al., 2020). Consequently, batch and continuous fermentation models demand distinct media requirements. Static batch fermentation is designed to provide short-term energy to the microbial community, without the need for nutritive growth medium renewal until the conclusion of the experiment (Gonza et al., 2024). These methods are therefore constrained by substrate availability over a limited timeframe (24 to 72 h), with parameters such as pH or redox potential remaining unregulated. Therefore, the transition from batch to continuous fermentation models necessitates several considerations. First, a nutritive medium that emulates ileal effluents, comprising a variety of complex carbon and nitrogen sources, electrolytes, BAs, and vitamins, must be continuously supplemented to the bioreactor and refreshed promptly to maintain the balance of microbiota and metabolic products, as well as to accommodate the growth rates of specific microbiota and the production rates of key metabolites (Xie, 2022). Second, the substrate concentration in the medium must be adjusted to fit the continuous supplementation and removal processes inherent to continuous fermentation models (Qin and Zhai, 2024). Thus, when applying our optimally selected PM medium from the batch fermentation model to continuous fermentation, it requires ongoing optimization based on actual microbiota growth conditions. Additionally, beyond controlling temperature and pH, simulating *in vivo* conditions requires careful consideration of retention time, which should be inferred from the digestion rate of food outside the host (Poeker et al., 2019; Qin and Zhai, 2024). Finally, during the post-inoculation stabilization period, fermentation parameters must be adjusted based on observations of fermentation broth color, pH, metabolic products, and 16S rRNA sequencing results, ensuring the preservation of the microbial community from the inoculum (Poeker et al., 2019). It is imperative to emphasize that *in vitro* models for human and animal intestinal microbiota research are merely representations of reality. Inaccurate handling, data analysis, and unsupported correlations with host health and disease treatment can compromise research validity (Isenring et al., 2023). Therefore, the limitations of both batch and continuous *in vitro* models should be meticulously considered.

5 Conclusion

After a 48-h fermentation period in which cat fecal samples were used as inocula, the Pet medium presented the lowest production of total SCFAs, a more stable bacterial community structure, and consistent physicochemical properties. Consequently, the PM effectively preserved the balance of the GM and serves as a suitable *in vitro* model for studying the batch fermentation of potential functional food components via the cat intestinal flora. This approach provides an expedited avenue for investigating the nutritional and health-related value of pet diets.

Data availability statement

The datasets presented in this study can be found in online repositories. The names of the repository/repositories and accession number(s) can be found in this article/Supplementary material.

Ethics statement

The animal studies were approved by the Ethical Committee of the Zhejiang Academy of Agricultural Sciences. The studies were conducted in accordance with the local legislation and institutional requirements. Written informed consent was obtained from the owners for the participation of their animals in this study.

Author contributions

QR: Conceptualization, Data curation, Formal analysis, Investigation, Methodology, Validation, Visualization, Writing – original draft, Writing – review and editing. YL: Conceptualization, Formal analysis, Visualization, Writing – review and editing. MD: Investigation, Methodology, Software, Writing – review and editing. JL: Funding acquisition, Project administration, Resources, Supervision, Writing – review and editing. FS: Data curation, Formal analysis, Investigation, Supervision, Writing – review and editing. YZ: Funding acquisition, Resources, Writing – review and editing. WH: Funding acquisition, Resources, Writing – review and editing. JM: Funding acquisition, Resources, Writing – review and editing. XL: Formal analysis, Funding acquisition, Methodology, Project administration, Resources, Validation, Writing – review and editing.

Funding

The authors declare that financial support was received for the research, authorship, and/or publication of this article. This work was funded by research grants from the Nutrition and Care of Maternal and Child Research Fund Project of the Biostime Institute of Nutrition and Care (Grant No. 2022BINCMCF006) and the State Key Laboratory for Managing Biotic and Chemical Threats to the Quality and Safety of Agro-products (2021DG700024–ZZ202210).

Acknowledgments

We extend our gratitude to our laboratory colleagues and instructors for their continuous support, and we thank Guangzhou Maibao Biotechnology Co., Ltd. for providing experimental materials and assistance.

Conflict of interest

YZ and WH were employed by Guangzhou MYBAO Biotechnology Co., Ltd. JM was employed by New Ruipeng Pet Group Inc.

The remaining authors declare that the research was conducted in the absence of any commercial or financial relationships that could be construed as a potential conflict of interest.

Generative AI statement

The authors declare that no Generative AI was used in the creation of this manuscript.

Publisher's note

Supplementary material

The Supplementary Material for this article can be found online at: https://www.frontiersin.org/articles/10.3389/fmicb.2025.1515865/full#supplementary-material

References

Arpaia, N., Campbell, C., Fan, X., Dikiy, S., van der Veeken, J., deRoos, P., et al. (2013). Metabolites produced by commensal bacteria promote peripheral regulatory T-cell generation. *Nature* 504, 451–455. doi: 10.1038/nature12726

Browne, H. P., Forster, S. C., Anonye, B. O., Kumar, N., Neville, B. A., Stares, M. D., et al. (2016). Culturing of 'unculturable' human microbiota reveals novel taxa and extensive sporulation. *Nature* 533, 543–546. doi: 10.1038/nature17645

Butor, I., Jančová, P., Purevdorj, K., Klementová, L., Kluz, M., Huňová, I., et al. (2023). Effect of selected factors influencing biogenic amines degradation by Bacillus subtilis isolated from food. *Microorganisms* 11:1091. doi: 10.3390/microorganisms11041091

Ćesić, D., Lugović Mihić, L., Ozretić, P., Lojkić, I., Buljan, M., Šitum, M., et al. (2023). Association of gut Lachnospiraceae and chronic spontaneous urticaria. *Life (Basel)* 13:1280. doi: 10.3390/life13061280

Coelho, L. P., Kultima, J. R., Costea, P. I., Fournier, C., Pan, Y., Czarnecki-Maulden, G., et al. (2018). Similarity of the dog and human gut microbiomes in gene content and response to diet. *Microbiome* 6:72. doi: 10.1186/s40168-018-0450-3

Crhanova, M., Karasova, D., Juricova, H., Matiasovicova, J., Jahodarova, E., Kubasova, T., et al. (2019). Systematic culturomics shows that half of chicken caecal microbiota members can be grown in vitro except for two lineages of clostridiales and a single lineage of bacteroidetes. *Microorganisms* 7:496. doi: 10.3390/microorganisms7110496

Cummings, J. H., and Macfarlane, G. T. (1991). The control and consequences of bacterial fermentation in the human colon. *J. Appl. Bacteriol.* 70, 443–459. doi: 10.1111/j.1365-2672.1991.tb02739.x

de Vos, W. M., Tilg, H., Van Hul, M., and Cani, P. D. (2022). Gut microbiome and health: Mechanistic insights. *Gut* 71, 1020–1032. doi: 10.1136/gutjnl-2021-326789

Deschamps, C., Denis, S., Humbert, D., Zentek, J., Priymenko, N., Apper, E., et al. (2022). In vitro models of the canine digestive tract as an alternative to in vivo assays: Advances and current challenges. *Altex* 39, 235–257. doi: 10.14573/altex.2109011

Duysburgh, C., Ossieur, W. P., De Paepe, K., Van den Abbeele, P., Vichez-Vargas, R., Vital, M., et al. (2020). Development and validation of the simulator of the canine intestinal microbial ecosystem (SCIME)1. *J. Anim. Sci.* 98:357. doi: 10.1093/jas/skz357

Fehlbaum, S., Chassard, C., Haug, M. C., Fourmestraux, C., Derrien, M., and Lacroix, C. (2015). Design and investigation of polyferms in vitro continuous fermentation models inoculated with immobilized fecal microbiota mimicking the elderly colon. *PLoS One* 10:e0142793. doi: 10.1371/journal.pone.0142793

Geypens, B., Claus, D., Evenepoel, P., Hiele, M., Maes, B., Peeters, M., et al. (1997). Influence of dietary protein supplements on the formation of bacterial metabolites in the colon. *Gut* 41, 70–76. doi: 10.1136/gut.41.1.70

Gonza, I., Goya-Jorge, E., Douny, C., Boutaleb, S., Taminiau, B., Daube, G., et al. (2024). Food additives impair gut microbiota from healthy individuals and IBD patients in a colonic in vitro fermentation model. *Food Res. Int.* 182:114157. doi: 10.1016/j.foodres.2024.114157

Han, X., Feng, Z., Chen, Y., Zhu, L., Li, X., Wang, X., et al. (2022). Effects of high-fructose corn syrup on bone health and gastrointestinal microbiota in growing male mice. *Front. Nutr.* 9:829396. doi: 10.3389/fnut.2022.829396

Hill, J. H., and Round, J. L. (2021). SnapShot: Microbiota effects on host physiology. *Cell* 184(10), 2796–2796.e2791. doi: 10.1016/j.cell.2021.04.026.

Hou, Q., Huang, J., Zhao, L., Pan, X., Liao, C., Jiang, Q., et al. (2023). Dietary genistein increases microbiota-derived short chain fatty acid levels, modulates homeostasis of the aging gut, and extends healthspan and lifespan. *Pharmacol. Res.* 188:106676. doi: 10.1016/j.phrs.2023.106676

Hylemon, P. B., Harris, S. C., and Ridlon, J. M. (2018). Metabolism of hydrogen gases and bile acids in the gut microbiome. *FEBS Lett.* 592, 2070–2082. doi: 10.1002/1873-3468.13064

Isenring, J., Bircher, L., Geirnaert, A., and Lacroix, C. (2023). In vitro human gut microbiota fermentation models: Opportunities, challenges, and pitfalls. *Microbiome Res. Rep.* 2:2. doi: 10.20517/mrr.2022.15

Isenring, J., Stevens, M. J. A., Jans, C., Lacroix, C., and Geirnaert, A. (2022). Identification of valerate as carrying capacity modulator by analyzing lactiplantibacillus plantarum colonization of colonic microbiota in vitro. *Front. Microbiol.* 13:910609. doi: 10.3389/fmicb.2022.910609

Koh, A., De Vadder, F., Kovatcheva-Datchary, P., and Bäckhed, F. (2016). From dietary fiber to host physiology: Short-Chain fatty acids as key bacterial metabolites. *Cell* 165, 1332–1345. doi: 10.1016/j.cell.2016.05.041

Laparra, J. M., and Sanz, Y. (2010). Interactions of gut microbiota with functional food components and nutraceuticals. *Pharmacol. Res.* 61, 219–225. doi: 10.1016/j.phrs.2009.11.001

Lau, J. T., Whelan, F. J., Herath, I., Lee, C. H., Collins, S. M., Bercik, P., et al. (2016). Capturing the diversity of the human gut microbiota through culture-enriched molecular profiling. *Genome Med.* 8:72. doi: 10.1186/s13073-016-0327-7

Lau, N., Hummel, J., Kramer, E., and Hünerberg, M. (2022). Fermentation of liquid feed with lactic acid bacteria reduces dry matter losses, lysine breakdown, formation of biogenic amines, and phytate-phosphorus. *Transl. Anim. Sci.* 6:txac007. doi: 10.1093/tas/txac007

Le Chatelier, E., Nielsen, T., Qin, J., Prifti, E., Hildebrand, F., Falony, G., et al. (2013). Richness of human gut microbiome correlates with metabolic markers. *Nature* 500, 541–546. doi: 10.1038/nature12506

Lei, F., Yin, Y., Wang, Y., Deng, B., Yu, H. D., Li, L., et al. (2012). Higher-level production of volatile fatty acids in vitro by chicken gut microbiotas than by human gut microbiotas as determined by functional analyses. *Appl. Environ. Microbiol.* 78, 5763–5772. doi: 10.1128/aem.00327-12

Li, K., Xiao, X., Li, Y., Lu, S., Zi, J., Sun, X., et al. (2024). Insights into the interplay between gut microbiota and lipid metabolism in the obesity management of canines and felines. *J. Anim. Sci. Biotechnol.* 15:114. doi: 10.1186/s40104-024-01073-w

Liu, W., Li, X., Zhao, Z., Pi, X., Meng, Y., Fei, D., et al. (2020). Effect of chitooligosaccharides on human gut microbiota and antiglycation. *Carbohydr. Polym.* 242:116413. doi: 10.1016/j.carbpol.2020.116413

Ma, L., Tao, S., Song, T., Lyu, W., Li, Y., Wang, W., et al. (2024). Clostridium butyricum and carbohydrate active enzymes contribute to the reduced fat deposition in pigs. *Imeta* 3:e160. doi: 10.1002/imt2.160

Ma, N., Tian, Y., Wu, Y., and Ma, X. (2017). Contributions of the interaction between dietary protein and gut microbiota to intestinal health. *Curr. Protein Pept. Sci.* 18, 795–808. doi: 10.2174/1389203718666170216153505

Martin-Gallausiaux, C., Marinelli, L., Blottière, H. M., Larraufie, P., and Lapaque, N. (2021). SCFA: Mechanisms and functional importance in the gut. *Proc. Nutr. Soc.* 80, 37–49. doi: 10.1017/s0029665120006916

Morrison, D. J., and Preston, T. (2016). Formation of short chain fatty acids by the gut microbiota and their impact on human metabolism. *Gut Microbes* 7, 189–200. doi: 10.1080/19490976.2015.1134082

Mutuyemungu, E., Singh, M., Liu, S., and Rose, D. J. (2023). Intestinal gas production by the gut microbiota: A review. *J. Functional Foods* 100:105367. doi: 10.1016/j.jff.2022.105367

Önal, A., Tekkeli, S. E., and Önal, C. (2013). A review of the liquid chromatographic methods for the determination of biogenic amines in foods. *Food Chem.* 138, 509–515. doi: 10.1016/j.foodchem.2012.10.056

Ou, J. Z., Yao, C. K., Rotbart, A., Muir, J. G., Gibson, P. R., and Kalantar-zadeh, K. (2015). Human intestinal gas measurement systems: In vitro fermentation and gas capsules. *Trends Biotechnol.* 33, 208–213. doi: 10.1016/j.tibtech.2015.02.002

Paone, P., and Cani, P. D. (2020). Mucus barrier, mucins and gut microbiota: The expected slimy partners? *Gut* 69, 2232–2243. doi: 10.1136/gutjnl-2020-322260

Pérez-Burillo, S., Molino, S., Navajas-Porras, B., Valverde-Moya, ÁJ., Hinojosa-Nogueira, D., López-Maldonado, A., et al. (2021). An in vitro batch fermentation protocol for studying the contribution of food to gut microbiota composition and functionality. *Nat. Protoc.* 16, 3186–3209. doi: 10.1038/s41596-021-00537-x

Poeker, S. A., Lacroix, C., de Wouters, T., Spalinger, M. R., Scharl, M., and Geirnaert, A. (2019). Stepwise development of an in vitro continuous fermentation model for the murine caecal microbiota. *Front. Microbiol.* 10:1166. doi: 10.3389/fmicb.2019.01166

Qin, Y., and Zhai, C. (2024). Global stabilizing control of a continuous ethanol fermentation process starting from batch mode production. *Processes* 12:819. doi: 10.3390/pr12040819

Rauf, A., Khalil, A. A., Rahman, U. U., Khalid, A., Naz, S., Shariati, M. A., et al. (2022). Recent advances in the therapeutic application of short-chain fatty acids (SCFAs): An updated review. *Crit. Rev. Food Sci. Nutr.* 62, 6034–6054. doi: 10.1080/10408398.2021.1895064

Sang, X., Li, K., Zhu, Y., Ma, X., Hao, H., Bi, J., et al. (2020). The impact of microbial diversity on biogenic amines formation in grasshopper sub shrimp paste during the fermentation. *Front. Microbiol.* 11:782. doi: 10.3389/fmicb.2020.00782

Shenghua, P., Ziqin, Z., Shuyu, T., Huixia, Z., Xianglu, R., and Jiao, G. (2020). An integrated fecal microbiome and metabolome in the aged mice reveal anti-aging effects from the intestines and biochemical mechanism of FuFang zhenshu TiaoZhi(FTZ). *Biomed. Pharmacother.* 121:109421. doi: 10.1016/j.biopha.2019.109421

Sunvold, G. D., Fahey, G. C. Jr., Merchen, N. R., and Reinhart, G. A. (1995). In vitro fermentation of selected fibrous substrates by dog and cat fecal inoculum: Influence of diet composition on substrate organic matter disappearance and short-chain fatty acid production. *J. Anim. Sci.* 73, 1110–1122. doi: 10.2527/1995.7341110x

Swanson, K. S., Dowd, S. E., Suchodolski, J. S., Middelbos, I. S., Vester, B. M., Barry, K. A., et al. (2011). Phylogenetic and gene-centric metagenomics of the canine intestinal microbiome reveals similarities with humans and mice. *Isme J.* 5, 639–649. doi: 10.1038/ismej.2010.162

Tramontano, M., Andrejev, S., Pruteanu, M., Klünemann, M., Kuhn, M., Galardini, M., et al. (2018). Nutritional preferences of human gut bacteria reveal their metabolic idiosyncrasies. *Nat. Microbiol.* 3, 514–522. doi: 10.1038/s41564-018-0123-9

Van den Abbeele, P., Moens, F., Pignataro, G., Schnurr, J., Ribecco, C., Gramenzi, A., et al. (2020). Yeast-derived formulations are differentially fermented by the canine and feline microbiome as assessed in a novel in vitro colonic fermentation model. *J. Agric. Food Chem.* 68, 13102–13110. doi: 10.1021/acs.jafc.9b05085

Van den Abbeele, P., Taminiau, B., Pinheiro, I., Duysburgh, C., Jacobs, H., Pijls, L., et al. (2018). Arabinoxylo-oligosaccharides and inulin impact inter-individual variation on microbial metabolism and composition, which immunomodulates human cells. *J. Agric. Food Chem.* 66, 1121–1130. doi: 10.1021/acs.jafc.7b04611

Vázquez-Baeza, Y., Hyde, E. R., Suchodolski, J. S., and Knight, R. (2016). Dog and human inflammatory bowel disease rely on overlapping yet distinct dysbiosis networks. *Nat. Microbiol.* 1:16177. doi: 10.1038/nmicrobiol.2016.177

Wan, C., Wu, K., Lu, X., Fang, F., Li, Y., Zhao, Y., et al. (2021). Integrative analysis of the gut microbiota and metabolome for in vitro human gut fermentation modeling. *J. Agric. Food Chem.* 69, 15414–15424. doi: 10.1021/acs.jafc.1c04259

Wang, X., Li, J., Li, N., Guan, K., Yin, D., Zhang, H., et al. (2021). Evolution of intestinal gases and fecal short-chain fatty acids produced in vitro by preterm infant gut microbiota during the first 4 weeks of life. *Front. Pediatr.* 9:726193. doi: 10.3389/fped.2021.726193

Williams, B. A., Verstegen, M. W., and Tamminga, S. (2001). Fermentation in the large intestine of single-stomached animals and its relationship to animal health. *Nutr. Res. Rev.* 14, 207–228. doi: 10.1079/nrr200127

Wu, W. C., Pan, Y. F., Zhou, W. D., Liao, Y. Q., Peng, M. W., Luo, G. Y., et al. (2024). Meta-transcriptomic analysis of companion animal infectomes reveals their diversity and potential roles in animal and human disease. *mSphere* 9:e0043924. doi: 10.1128/msphere.00439-24

Xie, D. (2022). Continuous biomanufacturing with microbes - Upstream progresses and challenges. *Curr. Opin. Biotechnol.* 78:102793. doi: 10.1016/j.copbio.2022.102793

Yousi, F., Kainan, C., Junnan, Z., Chuanxing, X., Lina, F., Bangzhou, Z., et al. (2019). Evaluation of the effects of four media on human intestinal microbiota culture in vitro. *AMB Express* 9:69. doi: 10.1186/s13568-019-0790-9

Zhang, J., Li, X., Zhao, K., Li, H., Liu, J., Da, S., et al. (2023). In vitro digestion and fermentation combined with microbiomics and metabolomics reveal the mechanism of superfine yak bone powder regulating lipid metabolism by altering human gut microbiota. *Food Chem.* 410:135441. doi: 10.1016/j.foodchem.2023.135441

Zhang, L., Liu, C., Jiang, Q., and Yin, Y. (2021). Butyrate in energy metabolism: There is still more to learn. *Trends Endocrinol. Metab.* 32, 159–169. doi: 10.1016/j.tem.2020.12.003

Zhao, Q., Fu, Y., Zhang, F., Wang, C., Yang, X., Bai, S., et al. (2022). Heat-treated adzuki bean protein hydrolysates reduce obesity in mice fed a high-fat diet via remodeling gut microbiota and improving metabolic function. *Mol. Nutr. Food Res.* 66:e2100907. doi: 10.1002/mnfr.202100907

Zhou, W., Yan, Y., Mi, J., Zhang, H., Lu, L., Luo, Q., et al. (2018). Simulated digestion and fermentation in vitro by human gut microbiota of polysaccharides from bee collected pollen of chinese wolfberry. *J. Agric. Food Chem.* 66, 898–907. doi: 10.1021/acs.jafc.7b05546

Zihler Berner, A., Fuentes, S., Dostal, A., Payne, A. N., Vazquez Gutierrez, P., Chassard, C., et al. (2013). Novel polyfermentor intestinal model (PolyFermS) for controlled ecological studies: Validation and effect of pH. *PLoS One* 8:e77772. doi: 10.1371/journal.pone.0077772

frontiers | Frontiers in Veterinary Science

TYPE Original Research
PUBLISHED 06 February 2025
DOI 10.3389/fvets.2025.1462287

OPEN ACCESS

EDITED BY
Xu Wang,
Auburn University, United States

REVIEWED BY
Ilias Giannenas,
Aristotle University of Thessaloniki, Greece
Jan Kopečný,
Academy of Sciences of the Czech Republic (ASCR), Czechia

*CORRESPONDENCE
Marcio C. Costa
✉ marcio.costa@umontreal.ca

RECEIVED 09 July 2024
ACCEPTED 06 January 2025
PUBLISHED 06 February 2025

CITATION
Arghavani S, Chorfi Y, Segura M, Lesaux AA and Costa MC (2025) Impact of *Saccharomyces cerevisiae* on the intestinal microbiota of dogs with antibiotic-induced dysbiosis.
Front. Vet. Sci. 12:1462287.
doi: 10.3389/fvets.2025.1462287

Impact of *Saccharomyces cerevisiae* on the intestinal microbiota of dogs with antibiotic-induced dysbiosis

Sara Arghavani[1], Younes Chorfi[1], Mariela Segura[2], Achraf Adib Lesaux[3] and Marcio C. Costa[1]*

[1]Department of Veterinary Biomedical Sciences, Faculté de médecine vétérinaire, Université de Montréal, Saint-Hyacinthe, QC, Canada, [2]Department of Pathology and Microbiology, Faculté de médecine vétérinaire, Université de Montréal, Saint-Hyacinthe, QC, Canada, [3]Phileo by Lesaffre, Marcq-en-Barœul, France

Introduction: The gut microbiota plays an important role in the health of dogs, but treatment with antibiotics causes marked dysbiosis. The objectives of this study were to evaluate the impact of yeast probiotic *Saccharomyces cerevisiae* supplementation on the fecal microbiota of dogs and its potential to prevent dysbiosis induced by antibiotics.

Methods: Twenty healthy adult dogs were divided into a control and a yeast probiotic group receiving 1g/kg of *S. cerevisiae* (Actisaf®, Phileo by Lesaffre, Marcq-en-Barœul, France) daily from D0 to D31. Both groups were given oral metronidazole from D11 to D17. Fecal swabs were collected on D0, 3, 11, 17, 20, 24, and 31 for microbiota analysis and blood on D0 and D24 for measurements of cytokines and cortisol.

Results and discussion: At D0, two distinct microbiota profiles comprised of dogs from both groups, control and probiotic, were identified. One profile had higher abundances of species related to stress and inflammation, and the other comprised species associated with good intestinal health. After three days of supplementation with yeast probiotic *S. cerevisiae*, all five dogs from the probiotic group having a stress-related microbiota (membership) shifted to a healthy microbiota. Metronidazole markedly changed the microbiota of both groups (p <0.001). Still, treated dogs had significantly different microbiota on D17 (end of antibiotics treatment). The dysbiosis was resolved in both groups by D24. TNF-α remarkably decreased from D0 to D24 (p = 0.002) in the probiotic group, which also had lower levels than controls on D24 (p = 0.040). There were no significant differences in the other measured cytokines. It was concluded that the use of yeast probiotic *S. cerevisiae* positively shifted the microbiota composition of healthy adult dogs carrying an abnormal microbial profile and that it has the potential to attenuate the dysbiosis caused by oral metronidazole.

KEYWORDS

microbiota manipulation, yeast probiotics, intestinal dysbiosis, gut microbiota, microbiome, antibiotics

1 Introduction

The gastrointestinal tract (GIT) is a complex ecosystem that contains various living microorganisms, including viruses, archaea, fungi, parasites, and bacteria. These microorganisms are collectively known as microbiota (1). The GIT microbiota plays a vital role in maintaining the host's health by modulating the immune system, protecting from pathogens,

10.3389/fvets.2025.1462287

improving intestinal barrier function, and providing essential metabolites (2, 3). It also has a critical role in the metabolism of short-chain fatty acids (SCFAs), bile acids (BA), and indole (4). The importance of the microbiota on the host's health has been better understood after the development of DNA sequencing technologies (5).

Dysbiosis is characterized by an imbalance or a change in the standard microbiota composition. Most dogs with gastrointestinal diseases, such as diarrhea and chronic inflammatory diseases, have concurrent dysbiosis (6, 7) associated with low bacterial diversity, deficient production of metabolites, and an increased abundance of pathogenic or pathobiont species (8). Therefore, restoring normal microbiota composition is important to aid in treating diseases (9). The most used methods to correct dysbiosis are probiotics, prebiotics, fecal microbiota transplantation (FMT), and dietary modulation.

Antibiotics are used in treating gastrointestinal diseases in dogs, but also in treating other infections (e.g., ear, skin, etc.) and have been heavily overused in veterinary medicine (10). Antibiotics are not selective for pathogenic bacteria, affecting beneficial species in the GIT. The use of antibiotics causes compositional changes and a decrease in diversity, a feature of a healthy microbiota (11). However, even though the clinical signs of diarrhea are reduced after the administration of antibiotics, the dysbiosis worsens, and some dogs remain in that abnormal state for an extended period (12–14). In addition to a decreased diversity, compositional changes observed in dogs treated with antibiotics include increased abundance of *Escherichia coli* and decreased beneficial species (e.g., *Clostridium hiranonis* and *Fusobacterium* spp.) (15, 16). Therefore, probiotics have been suggested as an alternative to treating dogs with acute diarrhea (17).

Probiotics are live microorganisms that cause beneficial effects on health when administered in adequate amounts. They have been proposed to restore the microbiota of individuals with dysbiosis (18) and to aid with the prevention of diarrhea in dogs (19). The mechanisms of action of probiotics depend on their strain, some acting on immune modulation, inhibition of pathogens, or improving the intestinal barrier (20). The major bacterial strains used as probiotics in dogs are *Lactobacillus* spp. and *Bifidobacterium* spp. (21, 22). However, the viability of organisms present in commercial veterinary products and the presence of antimicrobial resistance genes have been topics of concern (23, 24). Yeasts are mainly used as food supplementation in dogs, but some species, such as *Saccharomyces* spp., have been used as probiotics (25, 26). The cell wall of *S. cerevisiae* is structured by two fractions: one is the bond of beta-1,3/1,6-glucans and chitin, and the other comprises mannan oligosaccharides (27). Mannan oligosaccharide can act as a prebiotic to increase the population of *Lactobacilli* (28) and *Bifidobacteria* (29), benefiting the host by preserving the integrity of the absorption surface of the GIT (30) and producing SCFA in dogs (31). In rat models, it was also observed that beta-glucan can stimulate the growth of *Lactobacilli* populations (32) and that mannan oligosaccharides increase the number of white blood cells and improve the host's immune response against pathogens (33). The recommended doses for dogs can vary from 250 million to 2 billion CFUs depending on the formulation of the product and the purpose of the use (e.g., treatment of diarrhea or enhancement of immunity).

This study hypothesized that using yeast probiotic *S. cerevisiae* would change the fecal microbiota composition of healthy dogs and would be associated with a more resilient microbiota. The study aimed to evaluate the impact of yeast probiotic *Saccharomyces cerevisiae* supplementation on the fecal microbiota of dogs and its potential to prevent dysbiosis induced by antibiotics.

2 Materials and methods

2.1 Study design

Experimental procedures were performed following the Canadian Council for Animal Care guidelines and were approved by the Animal Care Committee of the Université de Montréal (#21Rech2133).

Twenty healthy adult female intact beagle dogs from a teaching colony were selected for this study. The mean weight of the dogs was 9.6 kg, and the average age was 3.5 years. All dogs were fed a commercial diet (Breed Health Nutrition Beagle Adult Dry Dog Food, Royal Canin) for over 6 months to fulfill their maintenance energy requirements. All dogs had body scores of 4 or 5 out of 9. Dogs from the same pen were released together every morning into a walking area for approximately 1 h. The study took place during the summer. None of the dogs had a history of gastrointestinal disease, nor had they received antimicrobials or other medications during the 3 months before the study. The dogs were housed in the same room in four different stalls (two on each side of the room) with five dogs each.

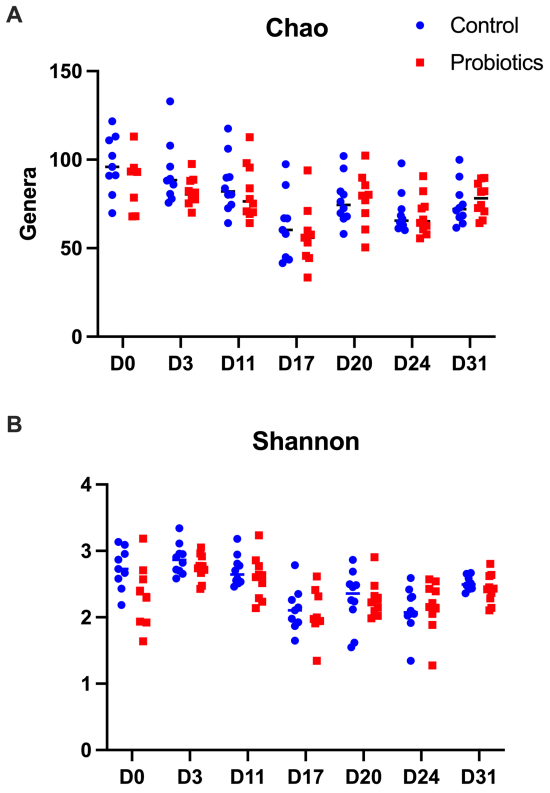

FIGURE 1
Results of the Chao estimator of richness **(A)** and the Shannon indicator of diversity **(B)** found in 20 dogs at baseline (D0) after 3 days of supplementation with yeast probiotic *Saccharomyces cerevisiae* (D3), before the use of antibiotics (D11), after 5 days of treatment with oral metronidazole (D17) and at days 24 and 31 of the trial. CON, controls; PROB, dogs supplemented with *S. cerevisiae* (1 g/kg PO).

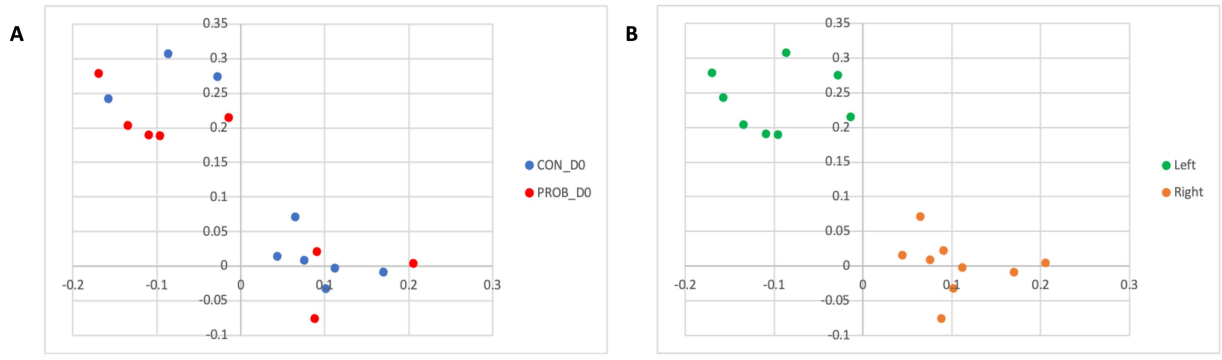

FIGURE 2
Principal coordinate analysis (PCoA) comparing the similarity of the microbiota membership (Jaccard index) obtained from 20 dogs at baseline (D0) according to the treatment group to which they were assigned **(A)** and according to which side of the room they were housed **(B)**. Samples were collected before the beginning of supplemented with the yeast probiotic *Saccharomyces cerevisiae*. PROB, dogs assigned to the supplementation group; CON, dogs assigned to the control group.

Dogs were divided into two groups: a probiotic group, receiving the yeast (Actisaf®, Phileo by Lesaffre, Marcq-en-Barœul, France) from day D0 to D31 (1 g/kg—2.9×10^8 CFU/g per day, orally), and a control group not receiving any supplementation. Each group was represented by one stall on each side of the room (control-left, control-right, probiotic-left, and probiotic-right). All the dogs were treated with oral metronidazole (15 mg/kg every 12 h orally) for 5 days (from D11 to D17). Throughout the study, all dogs remained supervised by the research staff and the veterinarian responsible for the laboratory.

Fecal samples were collected from the dogs using rectal swabs (BD ESwab™ collection and transport system) on D0 (baseline), D3, D11 (before antibiotic treatment), D17 (last day of antibiotic treatment), D20, D24, and D31. The swabs were stored at −80°C until further analysis. Blood samples were collected on D0 and D24 (5–10 mL collected from the jugular vein) using a 10 mL syringe and transferred to a collection tube with no additives. The serum was recovered from the tubes after 4 h at room temperature and stored at −80°C until analysis.

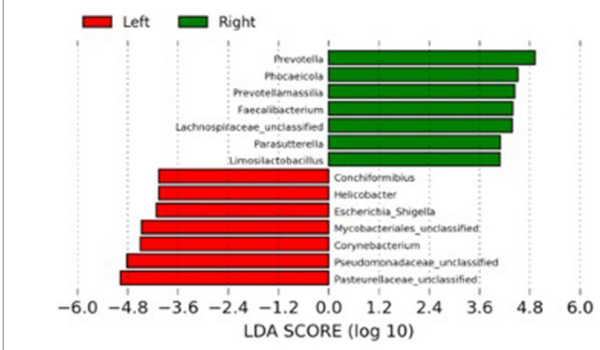

FIGURE 3
Results of the LEfSe analysis indicating the major bacterial taxa (LDA score >3) statistically more abundant in dogs housed on the left or the right side of the room at the baseline of the study (D0).

2.2 Microbiota analysis

Total DNA was extracted from rectal swabs using a commercial kit (DNeasy PowerSoil Kit, QIAGEN) following the manufacturer's instructions. Amplicons were obtained after PCR amplification of the V4 region of the 16S rRNA gene using the primers 515F (GTGCCAGCMGCCGCGGTAA) and 806R (GGACTACHVGGG TWTCTAAT). Sequencing was performed at the Genome Quebec McGill Innovation Centre using an Illumina MiSeq platform for 250 cycles from each end, aiming to overlap the reads fully.

Bioinformatic analysis was performed using the software Mothur (34) following the previously described Standard Operating Procedure (35). Contig assembly was conducted from the original fastq files, excluding sequences longer than 300 bp, containing base pair ambiguities and having polymers longer than 8 bp. The sequences were aligned using the SILVA 16S rRNA reference database and clustered at 97% similarity before chimeras were removed and classified using the Ribosomal Databank Project. Sequences classified as the same genus were clustered (Phylotypes) for further analyses (36).

The Chao and the Shannon index were used to characterize the alpha diversity. Beta diversity (comparison of taxonomic composition between samples) was assessed by the Jaccard index to evaluate community membership (that considers only the presence or absence of each bacterial taxon) and the Bray–Curtis index to evaluate community structure (that also considers how often each taxon appeared in the analysis). A two-dimensional principal coordinate analysis (PCoA) plot was generated to visualize the similarity between samples. The most abundant bacteria (>1%) were visualized by generating bar charts representing the relative abundance of the main phyla and genera found in each sample.

2.3 Cytokine's analysis

The cytokines levels in the serum were analyzed using a ProcartaPlex™ Human, NHP, and Canine Mix & Match Panels kit in a Luminex xMAP (multi-analyte profiling) technology to enable the detection and quantitation of seven cytokines: interferon (IFN)-γ, interleukin (IL)-2, IL-6, IL-8, IL-10, IL-12, and tumor necrosis factor (TNF)-α. Serum samples were diluted before assay, and the procedure

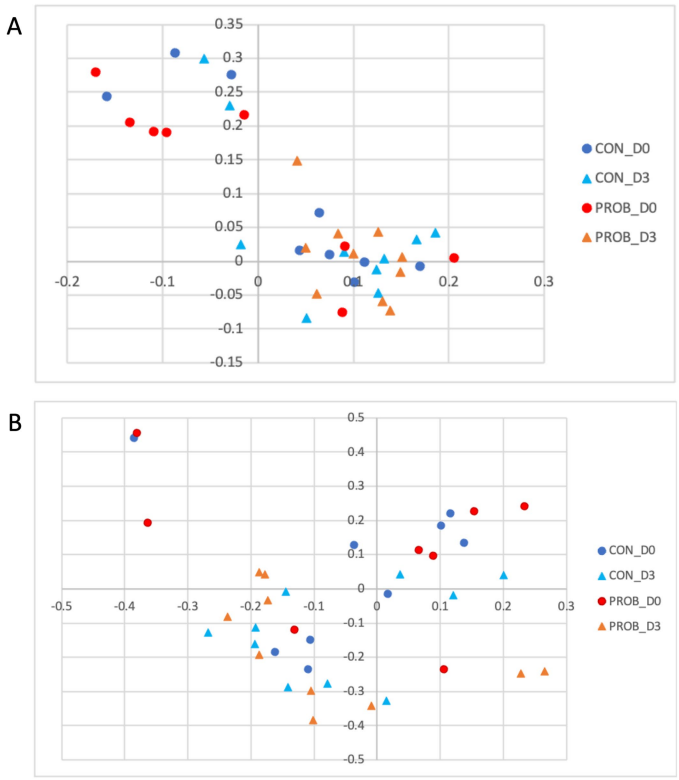

FIGURE 4
Principal coordinate analysis (PCoA) comparing the similarity of the membership **(A)** and structure **(B)** obtained from controls (CON) and dogs supplemented with *Saccharomyces cerevisiae* (PROB) before (D0) and after 3 days of supplementation (D3).

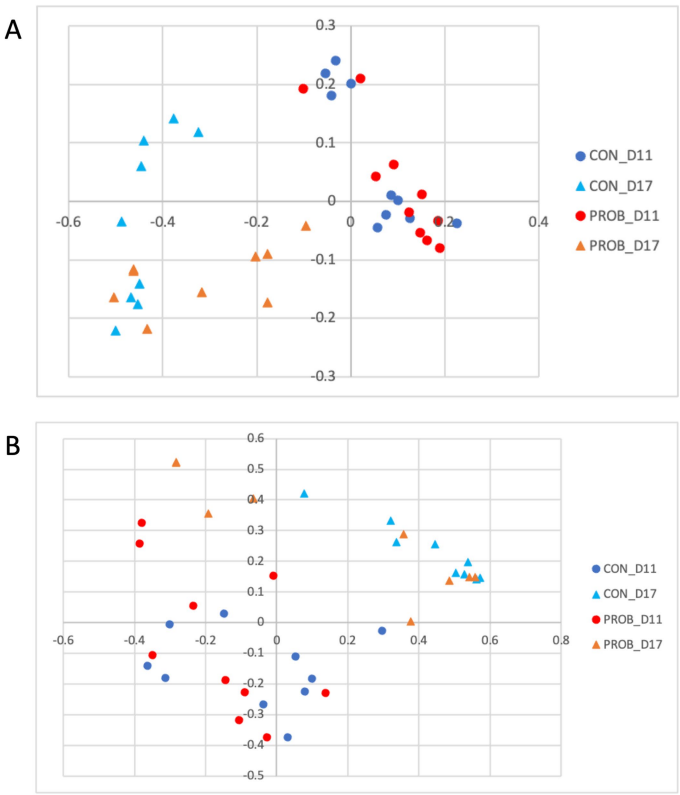

FIGURE 5
Principal coordinate analysis (PCoA) comparing the similarity of the membership **(A)** and structure **(B)** obtained from controls (CON) and dogs supplemented with *Saccharomyces cerevisiae* (PROB) before (D11) and after (D17) treatment with oral metronidazole for 5 days.

10.3389/fvets.2025.1462287

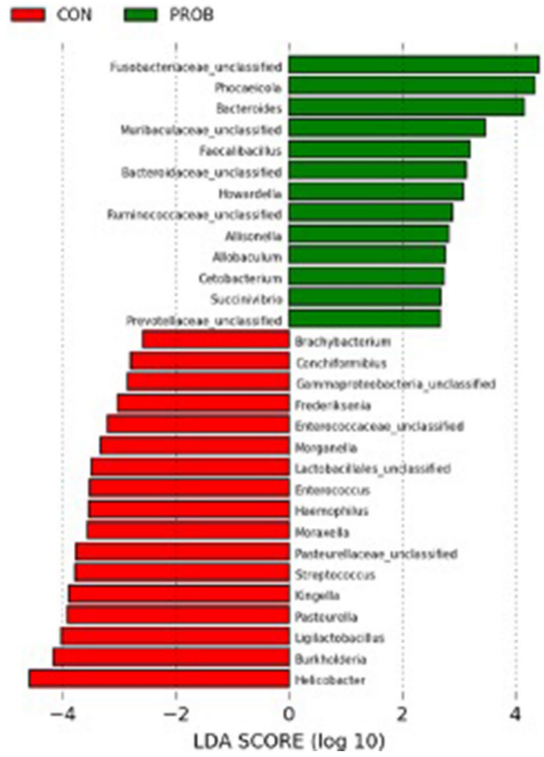

FIGURE 6
Results of the LEfSe analysis indicating the fecal bacteria significantly different (LDA >2) between controls and dogs supplemented with *Saccharomyces cerevisiae* after treatment with oral metronidazole for 5 days (D17).

was performed according to the manufacturer's instructions. The serum matrix solution provided in the kit was used in the sample and standard and control wells as a background. The method was validated with assay controls consisting of recombinant canine cytokines and the intra-assay precision. Luminex technology uses differential dye to capture beads for each target in a multiplex ELISA-like assay. This study used a Bio-Plex device to read and analyze data.

2.4 Statistical analysis

The Chao and Shannon index and cytokines values were compared using a two-way repeated measures analysis of variance (ANOVA) considering the treatment (control and probiotic) and sampling time as variables using the GraphPad Prism Software (37). The PERMANOVA test was applied, considering the same variables to investigate compositional differences in community membership and structure with subsequent pairwise comparisons when appropriate. The analysis of molecular variance (AMOVA) was used for post-hoc comparisons if indicated in the text.

The linear discriminant analysis effect size (LEfSe), which uses a non-parametric factorial Kruskal–Wallis with a subsequent unpaired Wilcoxon test, was applied to detect significant differences in relative abundances associated with the use of probiotics and antibiotics (38).

3 Results

3.1 Microbiota analysis

A total of 4,249,298 reads were obtained from 140 samples, of which 2,987,277 passed all quality filters and were retained. To normalize the number of reads across all samples and decrease the bias of non-uniform sizes, a subsample of 11,015 reads per sample was used for the analysis. In addition to the negative control, four samples were excluded from the analysis due to low reads.

The results of the Chao (richness) and the Shannon (diversity) index are shown in Figure 1. In control dogs, there was a significant decrease in the Chao index after the use of antibiotics (D17) compared to D0, D3 and D11 ($p = 0.005$ and $p = 0.008$, $p = 0.011$, respectively), as well as in D24 compared to D0 ($p = 0.009$). In the PROB group, antibiotics (D17) were associated with lower richness than D0, D11 and D31 ($p = 0.004$, $p = 0.016$, and $p = 0.016$, respectively).

For the Shannon index, samples collected from the CON group on D17, D20 and D24 had a significantly lower diversity than D0 ($p = 0.018$, $p = 0.024$ and $p = 0.026$, respectively). Samples collected on D17, D20, D24 and D31 had lower diversity than samples collected on D3 ($p < 0.010$, $p = 0.020$, $p = 0.001$, and $p = 0.011$, respectively). In addition, there was lower diversity on D17 and D24 compared to D11 ($p = 0.004$ and $p = 0.030$, respectively) but higher diversity on D31 compared to D17 ($p = 0.032$). However, no difference was observed between the control and the probiotic groups.

Regarding beta diversity analysis, which considers the taxonomic information, no significant differences between groups were detected on D0 (p-value = 0.375). However, two distinct clusters of samples comprised of dogs from both groups (CON and PROB) were found in the membership analysis (Figure 2A), which warned for further investigation. It was found that the samples were clustering according to the side of the room where the dogs were housed: left or right (Figure 2B). A post-hoc analysis comparing dogs housed on the left to those on the right side of the room revealed a significant difference in membership (AMOVA test, $p < 0.001$).

The LEfSe analysis was used to characterize the bacterial taxa associated with the different microbiota profiles found on each side of the room at D0. Figure 3 represents differential features with an LDA score >3. Several of the taxa significantly associated with the left side were pathobionts (potentially pathogenic bacteria) generally associated with dysbiosis or inflammation. In contrast, taxa related to dogs on the right side were normal commensals, usually part of a healthy microbiota.

Results of the PERMANOVA test on membership revealed an overall significant impact of treatment with probiotics ($p = 0.002$) and sampling time ($p = 0.001$) but not an interaction between the two variables ($p = 0.125$).

It can be observed that all five dogs in the PROB group that had an inflammation profile on D0 changed their microbiota composition towards a more healthy microbiota after 3 days of supplementation (Figure 4A). The microbiota structure observed in D0 and D3 is presented in Figure 4B. A posthoc analysis (AMOVA) confirmed that the microbiota structure changed significantly from D0 to D3 in the probiotic group (p-value <0.001) but not in the control group (p-value = 0.212).

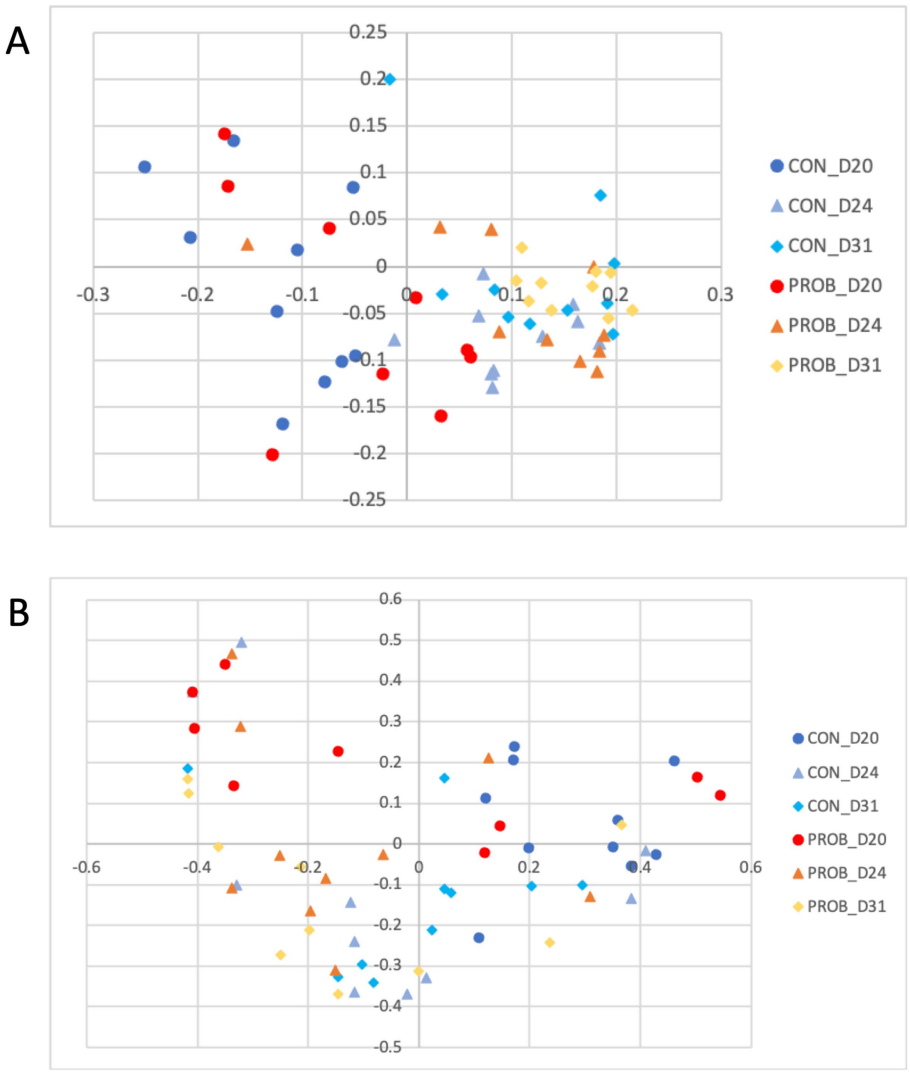

FIGURE 7
Principal coordinate analysis (PCoA) comparing the similarity of the membership **(A)** and structure **(B)** obtained from controls (CON) and dogs supplemented with *Saccharomyces cerevisiae* (PROB) on days 20, 24 and 31 of the study, investigating the long term impact of yeast supplementation.

The microbial structure and membership of both groups significantly changed (AMOVA, p-value <0.001) after antibiotic treatment (D17) (Figure 5).

The comparison between controls and probiotic-supplemented dogs revealed a significant difference in membership (AMOVA, p-value = 0.012) but not structure (AMOVA, p-value = 0.234) on D17. Nevertheless, some bacterial taxa significantly differed between CON and PROB during antibiotic-associated dysbiosis on D17, addressed by the LEfSe analysis (Figure 6).

There was no difference in either membership or structure between D11 and D24 or D31 (all p-values >0.05), suggesting a recovery of the microbiota to its pre-antibiotic state (Figure 7).

3.2 Cytokines and cortisol

TNF-α levels significantly decreased in the probiotic group from D0 to D24 (p-value = 0.03). Still, there was no significant difference in the levels of other cytokines between groups, neither between D0 and D24 (all $p > 0.05$) (Figure 8). In addition, there was no detectable difference in serum cortisol levels.

4 Discussion

The objectives of this study were to evaluate the impact of oral administration of the yeast probiotic *Saccharomyces cerevisiae* on the fecal microbiota of healthy adult dogs and to evaluate *S. cerevisiae*'s potential in preventing dysbiosis induced by antibiotics.

Unexpectedly, the microbial composition of dogs at the beginning of the study (D0) formed two distinct clusters according to the side of the facility in which they were housed. Most bacteria associated with dogs on the left side were inflammation-related species, such as *Escherichia*, *Helicobacter*, *Mycobacteria* and Pseudomonadaceae. Conversely, the bacteria with significantly higher abundances in dogs housed on the right side of the room

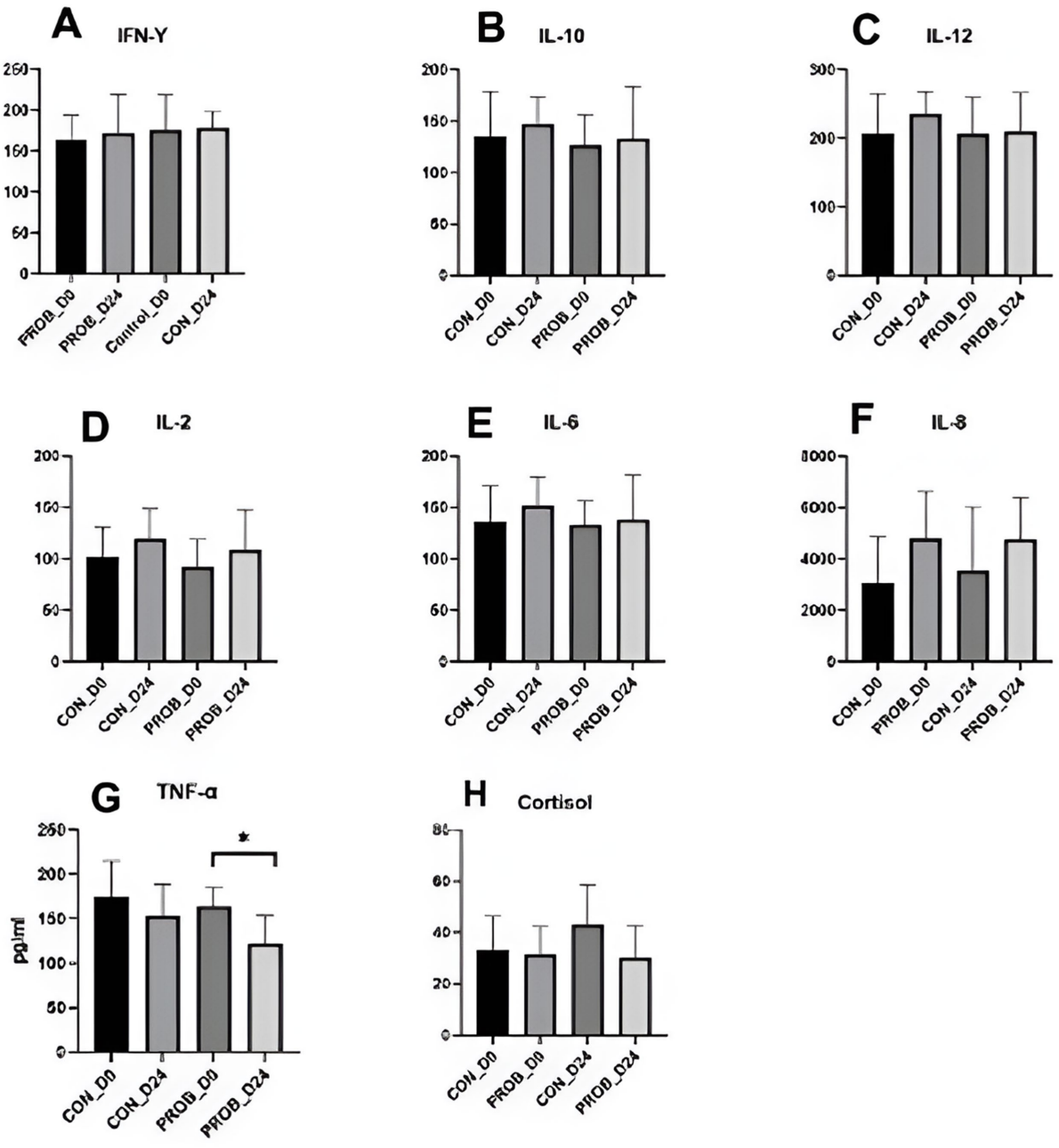

FIGURE 8
Cytokines **(A–F)** and cortisol levels **(G)** in the serum of 20 dogs supplemented with yeast probiotic Saccharomyces cerevisiae (PROB) and a control group (CON) before (D0) and 24 days after yeast supplementation (D24). *Indicates a significant difference between the time points.

were beneficial species such as *Prevotella*, *Faecalibacterium*, and Lachnospiraceae (39). The reasons that could explain such a marked difference are unknown, but interestingly, dogs from the right side were fed first, while the other dogs were continuously barking. Stress has been shown to influence the physiology of the host intestinal cells with consequences in the bacteria present at the mucosal surface and gut lumen (40). Stressor factors such as transportation can also affect the composition and abundance of the fecal microbiota of dogs (41). They could alter the intestinal motility, further contributing to the differences observed at the baseline of the present study. However, there was no difference in cortisol levels when comparing dogs housed at the different sides of the facility. Therefore, further studies employing more specific stress markers or investigating other factors influencing microbiota composition are necessary to explain this finding. Fortunately, this variable was considered during the designing of the study by evenly distributing dogs from both treatment groups (controls and probiotics) across each side of the room. Noteworthy, the teaching dogs have been fed twice daily to minimize the potential stress related to fasting.

Although the altered baseline microbiota composition might have influenced the impact of probiotics over time, after 3 days of supplementation, all five dogs carrying a stress-related profile reverted to a healthier profile. A previous study using a similar supplementation protocol in Beagle dogs showed an increase in the digestibility of fiber that could be associated with increased energy availability in the form of volatile fatty acids, which are a valuable energy source for enterocytes (i.e., butyrate) and have the capacity to modulate the intestinal microbiota composition positively.

As expected, the microbial composition in the control and the probiotic groups changed drastically after 5 days of treatment with metronidazole. Metronidazole can decrease diversity, cause severe changes in the intestinal microbiota of dogs with diarrhea, and induce dysbiosis in healthy dogs (16, 42). In the present study, supplementation with yeast probiotic *S. cerevisiae* was associated with less severe changes in the fecal microbiota of dogs, as animals receiving the probiotic had statistically different microbiota compared with controls on D17. The LEfSe analysis on D17 revealed that several species associated with the use of probiotics were representative of a healthy canine microbiota (i.e., Fusobacteriaceae, *Bacteroides* spp., *Faecalibacillus* spp., Bacterioidaceae, and Ruminococcaceae).

At the end of the study period (D24 and D31), the microbiota of dogs from both groups had recovered from the dysbiosis caused by metronidazole, as the microbial composition was similar to the normal microbiota before antibiotics (D11).

Antimicrobial drugs are typically used to treat gastrointestinal diseases and are known to cause dysbiosis. However, intestinal microbiota dysbiosis has been associated with GIT disorders such as IBD, food allergies, and infections (43–46). The consequences of the disruption of the intestinal microbiota of dogs remain mainly unknown. Still, beneficial bacteria support the digestion of complex nutrients, synthesize essential vitamins, and produce short-chain fatty acids and might even be involved in behavioural aspects (47). A balanced microbiota protects the gut against harmful pathogens through competitive exclusion and modulation of the immune response and is essential to support optimal mucus production and overall gastrointestinal health (3, 48). Thus, dysbiosis might be a causing or predisposing factor associated with diseases such as chronic enteropathies (49, 50).

In this study, antimicrobial treatment did not cause an increase in inflammation markers 7 days after the end of treatment. Still, TNF-α, often increased during gastrointestinal diseases, statistically decreased from D0 to D24 in dogs supplemented with yeast probiotic *S. cerevisiae*. This was possibly caused by the compositional changes from a stress-related microbiota profile of treated dogs from the left side of the room towards a normal microbiota. However, the low number of dogs used in this study precludes significant conclusions, and larger cohorts enrolling stressed or sick dogs are necessary to investigate this supplement's anti-inflammatory properties further. Nevertheless, this study analyzed the microbiota of 140 fecal samples of dogs, bringing novel information related to the bacterial dynamics upon the use of yeast probiotics and antibiotic-related dysbiosis. Further studies, including the analysis of intestinal metabolites such as bile acids and glucans, are necessary to reveal the mechanisms by which yeast supplementation benefits the intestinal microbiota.

In conclusion, it was observed that the use of yeast probiotic *S. cerevisiae* was associated with beneficial changes in the microbial composition of dogs carrying a stress-related profile and had the potential to modulate dysbiosis caused by treatment with oral metronidazole. Further studies are justified to evaluate the benefits of supplementation with yeast probiotic *S. cerevisiae* in dogs with gastrointestinal diseases.

Data availability statement

Raw FASTQ files have been deposited at the NCBI SRA Archive under the accession number PRJNA1211059.

Ethics statement

The animal study was approved by Animal Care Committee of the Université de Montréal. The study was conducted in accordance with the local legislation and institutional requirements. Experimental procedures were performed according to the Canadian Council for Animal Care guidelines and approved by the Animal Care Committee of the Université de Montréal (#21Rech2133).

Author contributions

SA: Formal analysis, Investigation, Methodology, Writing – original draft. YC: Conceptualization, Supervision, Writing – review & editing. MS: Methodology, Resources, Writing – review & editing. AL: Conceptualization, Funding acquisition, Resources, Writing – review & editing. MC: Conceptualization, Data curation, Formal analysis, Funding acquisition, Investigation, Project administration, Resources, Supervision, Writing – original draft, Writing – review & editing.

Funding

The author(s) declare that financial support was received for the research, authorship, and/or publication of this article. Phileo by Lesaffre has partially funded the study's costs. The funder was not involved in the study design, collection, analysis, interpretation of data, the writing of this article, or the decision to submit it for publication.

Conflict of interest

AL works for Phileo by Lesaffre, the manufacturer of the yeast probiotic used in this study.

The remaining authors declare that the research was conducted in the absence of any commercial or financial relationships that could be construed as a potential conflict of interest.

Publisher's note

References

1. Scholtens PA, Oozeer R, Martin R, Amor KB, Knol J. The early settlers: intestinal microbiology in early life. *Annu Rev Food Sci Technol*. (2012) 3:425–47. doi: 10.1146/annurev-food-022811-101120

2. Rowland I, Gibson G, Heinken A, Scott K, Swann J, Thiele I, et al. Gut microbiota functions: metabolism of nutrients and other food components. *Eur J Nutr*. (2018) 57:1–24. doi: 10.1007/s00394-017-1445-8

3. Schmid SM, Tolbert MK. Harnessing the microbiome: probiotics, antibiotics and their role in canine and feline gastrointestinal disease. *Vet Rec*. (2024) 195:13–25. doi: 10.1002/vetr.4915

4. Rowe JC, Winston JA. Collaborative metabolism: gut microbes play a key role in canine and feline bile acid metabolism. *Vet Sci*. (2024) 11:94. doi: 10.3390/vetsci11020094

5. Suchodolski JS, Ruaux CG, Steiner JM, Fetz K, Williams DA. Assessment of the qualitative variation in bacterial microflora among compartments of the intestinal tract of dogs by use of a molecular fingerprinting technique. *Am J Vet Res*. (2005) 66:1556–62. doi: 10.2460/ajvr.2005.66.1556

6. Alshawaqfeh M, Wajid B, Minamoto Y, Markel M, Lidbury J, Steiner J, et al. A dysbiosis index to assess microbial changes in fecal samples of dogs with chronic inflammatory enteropathy. *FEMS Microbiol Ecol*. (2017) 93:fix136. doi: 10.1093/femsec/fix136

7. Ziese A-L, Suchodolski JS. Impact of changes in gastrointestinal microbiota in canine and feline digestive diseases. *Vet Clin North Am Small Anim Pract*. (2021) 51:155–69. doi: 10.1016/j.cvsm.2020.09.004

8. Vázquez-Baeza Y, Hyde ER, Suchodolski JS, Knight R. Dog and human inflammatory bowel disease rely on overlapping yet distinct dysbiosis networks. *Nat Microbiol*. (2016) 1:16177. doi: 10.1038/nmicrobiol.2016.177

9. Milani C, Duranti S, Bottacini F, Casey E, Turroni F, Mahony J, et al. The first microbial colonizers of the human gut: composition, activities, and health implications of the infant gut microbiota. *Microbiol Mol Biol Rev*. (2017) 81:e00036. doi: 10.1128/MMBR.00036-17

10. Hillier A, Lloyd DH, Weese JS, Blondeau JM, Boothe D, Breitschwerdt E, et al. Guidelines for the diagnosis and antimicrobial therapy of canine superficial bacterial folliculitis (Antimicrobial Guidelines Working Group of the International Society for Companion Animal Infectious Diseases). *Vet Dermatol*. (2014) 25:163–e43. doi: 10.1111/vde.12118

11. Modi SR, Collins JJ, Relman DA. Antibiotics and the gut microbiota. *J Clin Invest*. (2014) 124:4212–8. doi: 10.1172/JCI72333

12. Suchodolski JS, Dowd SE, Westermarck E, Steiner JM, Wolcott RD, Spillmann T, et al. The effect of the macrolide antibiotic tylosin on microbial diversity in the canine small intestine as demonstrated by massive parallel 16S rRNA gene sequencing. *BMC Microbiol*. (2009) 9:210–6. doi: 10.1186/1471-2180-9-210

13. Westermarck E, Myllys V, Aho M. Effect of treatment on the jejunal and colonic bacterial flora of dogs with exocrine pancreatic insufficiency. *Pancreas*. (1993) 8:559–62. doi: 10.1097/00006676-199309000-00005

14. Westermarck E, Skrzypczak T, Harmoinen J, Steiner JM, Ruaux CG, Williams DA, et al. Tylosin-responsive chronic diarrhea in dogs. *J Vet Intern Med*. (2005) 19:177–86. doi: 10.1111/j.1939-1676.2005.tb02679.x

15. Chaitman J, Ziese A-L, Pilla R, Minamoto Y, Blake AB, Guard BC, et al. Fecal microbial and metabolic profiles in dogs with acute diarrhea receiving either fecal microbiota transplantation or oral metronidazole. *Front Vet Sci*. (2020) 7:192. doi: 10.3389/fvets.2020.00192

16. Pilla R, Gaschen FP, Barr JW, Olson E, Honneffer J, Guard BC, et al. Effects of metronidazole on the fecal microbiome and metabolome in healthy dogs. *J Vet Intern Med*. (2020) 34:1853–66. doi: 10.1111/jvim.15871

17. Stubing H, Suchodolski JS, Reisinger A, Werner M, Hartmann K, Unterer S, et al. The effect of metronidazole versus a synbiotic on clinical course and core intestinal microbiota in dogs with acute diarrhea. *Vet Sci*. (2024) 11:197. doi: 10.3390/vetsci11050197

18. Bajagai YS, Klieve AV, Dart PJ, Bryden WL. Probiotics in animal nutrition: production, impact and regulation. Rome: FAO (2016).

19. Grześkowiak Ł, Endo A, Beasley S, Salminen S. Microbiota and probiotics in canine and feline welfare. *Anaerobe*. (2015) 34:14–23. doi: 10.1016/j.anaerobe.2015.04.002

20. White R, Atherly T, Guard B, Rossi G, Wang C, Mosher C, et al. Randomized, controlled trial evaluating the effect of multi-strain probiotic on the mucosal microbiota in canine idiopathic inflammatory bowel disease. *Gut Microbes*. (2017) 8:451–66. doi: 10.1080/19490976.2017.1334754

21. Biagi G, Cipollini I, Pompei A, Zaghini G, Matteuzzi D. Effect of a *Lactobacillus animalis* strain on composition and metabolism of the intestinal microflora in adult dogs. *Vet Microbiol*. (2007) 124:160–5. doi: 10.1016/j.vetmic.2007.03.013

22. O'Mahony D, Murphy K, MacSharry J, Boileau T, Sunvold G, Reinhart G, et al. Portrait of a canine probiotic *Bifidobacterium*—from gut to gut. *Vet Microbiol*. (2009) 139:106–12. doi: 10.1016/j.vetmic.2009.05.002

23. Baumgardner RM, Berreta A, Kopper JJ. Evaluation of commercial probiotics for antimicrobial resistance genes. *Can Vet J*. (2021) 62:379–83.

24. Kerek A, Szabo E, Szabo A, Papp M, Banyai K, Kardos G, et al. Investigating antimicrobial resistance genes in probiotic products for companion animals. *Front Vet Sci*. (2024) 11:1464351. doi: 10.3389/fvets.2024.1464351

25. Garrigues Q, Mugnier A, Chastant S, Sicard F, Martin JC, Svilar L, et al. The supplementation of female dogs with live yeast *Saccharomyces cerevisiae* var. *boulardii* CNCM I-1079 acts as gut stabilizer at whelping and modulates immunometabolic phenotype of the puppies. *Front Nutr*. (2024) 11:1366256. doi: 10.3389/fnut.2024.1366256

26. Mcfarland LV, Surawicz CM, Greenberg RN, Fekety R, Elmer GW, Moyer KA, et al. A randomized placebo-controlled trial of *Saccharomyces boulardii* in combination with standard antibiotics for *Clostridium difficile* disease. *JAMA*. (1994) 271:1913–8. doi: 10.1001/jama.1994.03510480037031

27. Middelbos I, Fastinger N, Fahey GC Jr. Evaluation of fermentable oligosaccharides in diets fed to dogs in comparison to fiber standards. *J Anim Sci*. (2007) 85:3033–44. doi: 10.2527/jas.2007-0080

28. Swanson KS, Grieshop CM, Flickinger EA, Bauer LL, Healy H-P, Dawson KA, et al. Supplemental fructooligosaccharides and mannanoligosaccharides influence immune function, ileal and total tract nutrient digestibilities, microbial populations and concentrations of protein catabolites in the large bowel of dogs. *J Nutr*. (2002) 132:980–9. doi: 10.1093/jn/132.5.980

29. Grieshop C, Flickinger E, Bruce K, Patil A, Czarnecki-Maulden G, Fahey GC Jr. Gastrointestinal and immunological responses of senior dogs to chicory and mannan-oligosaccharides. *Arch Anim Nutr*. (2004) 58:483–94. doi: 10.1080/00039420400019977

30. Roberfroid M. Functional food concept and its application to prebiotics. *Dig Liver Dis*. (2002) 34:S105–10. doi: 10.1016/S1590-8658(02)80176-1

31. Musco N, Calabrò S, Roberti F, Grazioli R, Tudisco R, Lombardi P, et al. *In vitro* evaluation of *Saccharomyces cerevisiae* cell wall fermentability using a dog model. *J Anim Physiol Anim Nutr*. (2018) 102:24–30. doi: 10.1111/jpn.12864

32. Snart J, Bibiloni R, Grayson T, Lay C, Zhang H, Allison GE, et al. Supplementation of the diet with high-viscosity beta-glucan results in enrichment for lactobacilli in the rat cecum. *Appl Environ Microbiol*. (2006) 72:1925–31. doi: 10.1128/AEM.72.3.1925-1931.2006

33. Pawar MM, Pattanaik AK, Sinha DK, Goswami TK, Sharma K. Effect of dietary mannanoligosaccharide supplementation on nutrient digestibility, hindgut fermentation, immune response and antioxidant indices in dogs. *J Anim Sci Technol*. (2017) 59:11. doi: 10.1186/s40781-017-0136-6

34. Schloss PD, Westcott SL, Ryabin T, Hall JR, Hartmann M, Hollister EB, et al. Introducing mothur: open-source, platform-independent, community-supported software for describing and comparing microbial communities. *Appl Environ Microbiol*. (2009) 75:7537–41. doi: 10.1128/AEM.01541-09

35. Kozich JJ, Westcott SL, Baxter NT, Highlander SK, Schloss PD. Development of a dual-index sequencing strategy and curation pipeline for analyzing amplicon sequence data on the MiSeq Illumina sequencing platform. *Appl Environ Microbiol*. (2013) 79:5112–20. doi: 10.1128/AEM.01043-13

36. Yang S, Liebner S, Alawi M, Ebenhöh O, Wagner D. Taxonomic database and cut-off value for processing *mcrA* gene 454 pyrosequencing data by MOTHUR. *J Microbiol Methods*. (2014) 103:3–5. doi: 10.1016/j.mimet.2014.05.006

37. Mavrevski R, Traykov M, Trenchev I, Trencheva M. Approaches to modeling of biological experimental data with GraphPad prism software. *WSEAS Trans Syst Control*. (2018) 13:242–7.

38. Segata N, Izard J, Waldron L, Gevers D, Miropolsky L, Garrett WS, et al. Metagenomic biomarker discovery and explanation. *Genome Biol*. (2011) 12:R60. doi: 10.1186/gb-2011-12-6-r60

39. Sung CH, Pilla R, Chen CC, Ishii PE, Toresson L, Allenspach-Jorn K, et al. Correlation between targeted qPCR assays and untargeted DNA shotgun metagenomic sequencing for assessing the fecal microbiota in dogs. *Animals*. (2023) 13:2597. doi: 10.3390/ani13162597

40. Lyte M, Vulchanova L, Brown DR. Stress at the intestinal surface: catecholamines and mucosa–bacteria interactions. *Cell Tissue Res*. (2011) 343:23–32. doi: 10.1007/s00441-010-1050-0

41. Bergeron R, Scott SL, Émond J-P, Mercier F, Cook NJ, Schaefer AL. Physiology and behavior of dogs during air transport. *Can J Vet Res*. (2002) 66:211.

42. Igarashi H, Maeda S, Ohno K, Horigome A, Odamaki T, Tsujimoto H. Effect of oral administration of metronidazole or prednisolone on fecal microbiota in dogs. *PLoS One*. (2014) 9:e107909. doi: 10.1371/journal.pone.0107909

43. Buttó LF, Haller D. Dysbiosis in intestinal inflammation: cause or consequence. *Int J Med Microbiol*. (2016) 306:302–9. doi: 10.1016/j.ijmm.2016.02.010

44. Hill DA, Siracusa MC, Abt MC, Kim BS, Kobuley D, Kubo M, et al. Commensal bacteria-derived signals regulate basophil hematopoiesis and allergic inflammation. *Nat Med*. (2012) 18:538–46. doi: 10.1038/nm.2657

45. Kamada N, Seo S-U, Chen GY, Núñez G. Role of the gut microbiota in immunity and inflammatory disease. *Nat Rev Immunol*. (2013) 13:321–35. doi: 10.1038/nri3430

46. Vaughn BP, Vatanen T, Allegretti JR, Bai A, Xavier RJ, Korzenik J, et al. Increased intestinal microbial diversity following fecal microbiota transplant for active Crohn's disease. *Inflamm Bowel Dis*. (2016) 22:2182–90. doi: 10.1097/MIB.0000000000000893

47. Sacoor C, Marugg JD, Lima NR, Empadinhas N, Montezinho L. Gut-brain axis impact on canine anxiety disorders: new challenges for behavioral veterinary medicine. *Vet Med Int*. (2024) 2024:2856759. doi: 10.1155/2024/2856759

48. Sicard JF, Le Bihan G, Vogeleer P, Jacques M, Harel J. Interactions of intestinal bacteria with components of the intestinal mucus. *Front Cell Infect Microbiol*. (2017) 7:387. doi: 10.3389/fcimb.2017.00387

49. Schmitz SS. Evidence-based use of biotics in the management of gastrointestinal disorders in dogs and cats. *Vet Rec*. (2024) 195:26–32. doi: 10.1002/vetr.4916

50. Toresson L, Spillmann T, Pilla R, Ludvigsson U, Hellgren J, Olmedal G, et al. Clinical effects of faecal microbiota transplantation as adjunctive therapy in dogs with chronic enteropathies-a retrospective case series of 41 dogs. *Vet Sci*. (2023) 10:271. doi: 10.3390/vetsci10040271

frontiers | Frontiers in Veterinary Science

TYPE Original Research
PUBLISHED 26 February 2025
DOI 10.3389/fvets.2025.1520678

OPEN ACCESS

EDITED BY
Xihong Zhou,
Chinese Academy of Sciences (CAS), China

REVIEWED BY
Houqiang Luo,
Wenzhou Vocational College of Science and Technology, China
Sujuan Ding,
Hunan Agricultural University, China
Xiong Jiang,
Hubei Three Gorges Polytechnic, China

*CORRESPONDENCE
Zhigang Liu
✉ liu12024@sina.com

†These authors have contributed equally to this work

RECEIVED 12 November 2024
ACCEPTED 22 January 2025
PUBLISHED 26 February 2025

CITATION
Wu L, Xue L, Ding X, Jiang H, Zhang R, Zheng A, Zu Y, Tan S, Wang X and Liu Z (2025) Integrated microbiome and metabolomics analysis reveals the alleviating effect of *Pediococcus acidilactici* on colitis. *Front. Vet. Sci.* 12:1520678. doi: 10.3389/fvets.2025.1520678

Integrated microbiome and metabolomics analysis reveals the alleviating effect of *Pediococcus acidilactici* on colitis

Lulu Wu[1†], Lixun Xue[1†], Xin Ding[1], Huyan Jiang[2], Ranran Zhang[1], Aifang Zheng[1], Yuan Zu[1], Shuaishuai Tan[1], Xin Wang[1] and Zhigang Liu[1,3,4,5*]

[1]School of Life Sciences, Anqing Normal University, Anqing, China, [2]School of Chemistry and Chemical Engineering, Anqing Normal University, Anqing, China, [3]Engineering Technology Research Center for Aquatic Organism Conservation and Water Ecosystem Restoration in University of Anhui Province, Anqing, China, [4]Key Laboratory of Biodiversity Conservation and Characteristic Resource Utilization in Southwest Anhui, Anqing, China, [5]Anqing Forestry Technology Innovation Research Institute, Anqing, China

Colitis is a complicated disease caused by multiple factors, seriously threatening the host health and the development of animal husbandry. Probiotics have been demonstrate to participate in the active regulation of multiple gastrointestinal disease, gut microbiota and metabolism, but research on the efficacy of *Pediococcus acidilactici* isolated from dogs in alleviating colitis remains scarce. Here, we aimed to investigate the ameliorative effects of *Pediococcus acidilactici* isolated from dogs on colitis induced by LPS and its underlying molecular mechanisms. For this purpose, we collected colon contents from 15 mice for amplicon sequencing and metabolic analysis. Results showed that *Pediococcus acidilactici* could relieve the colon damage and cytokine disorder caused by colitis. Microbiome analysis showed that colitis could cause a significant decrease in the gut microbial diversity and abundance, but *Pediococcus acidilactici* administration could restore the microbial index to the control level. Metabolomics analysis showed that 8 metabolic pathways and 5 (spermine, L-Arginine, 15-Deoxy-Delta12,14-PGJ2, prostaglandin J2, and 15(S)-HETE) metabolites may be involved in the alleviation of colitis by *Pediococcus acidilactici*. In summary, these findings demonstrated that the positive regulation effect of *Pediococcus acidilactici* on gut microbiota and metabolism may be one of its underlying mechanisms to alleviate colitis. Additionally, this study also conveyed a vital message that *Pediococcus acidilactici* isolated from dogs may serve as a promising candidate to ameliorate *Pediococcus acidilactici*.

KEYWORDS

***Pediococcus acidilactici*, colitis, gut microbiota, metabolite, arachidonic acid metabolism**

Introduction

The intestine harbors approximately 10^{14} microbial cells involving over 2,000 distinct species (1–3). These gut-inhabiting microbes, also known as gut microbiota, have been showed to function in host health, metabolism, intestinal homeostasis and intestinal barrier maintenance (4–9). Additionally, the gut microbiota is also essential participant and maintainer of the intestinal mucosal barrier, which play key roles in preventing pathogen invasion and maintaining intestinal homeostasis (6, 7, 10). Gut microbial community, as crucial biochemical converters, can transform the complex chemical space presented by

nutrition and diet into the metabolite environment (11, 12). These metabolites including cholic acid, indole derivatives and short-chain fatty acids (SCFAs) participate in the positive regulation of the host health and intestinal homeostasis by acting on the intestine or other organ systems (13). However, gut microbial homeostats is susceptible to external factors, especially gastrointestinal related diseases (1, 14).

Inflammatory bowel disease (IBD) is a chronic intermittent disease primarily affecting the rectal and colon mucosa (15, 16). It is characterized by intestinal inflammation and damage to the epithelial barrier (17). IBD has gained significant attention in recent years due to its detrimental impact on host health. The prevalence of IBD exceeds 0.3% in developed countries, and its incidence rate is also gradually increasing in newly industrialized countries. Animals, such as dogs, cats, horses, and dairy cows, are also affected by IBD, leading to substantial economic losses and threats to animal welfare (18, 19). IBD is a complex disease influenced by factors such as diet, stress, genetics, and the environment (20). Recent studies have also linked colitis to gut microbial dysbiosis (21–23). Clinically, antibiotics, steroids, and immunosuppressants are commonly used to treat IBD. However, these therapies have drawbacks, including drug dependence, high cost, and antibiotic resistance, particularly for patients requiring long-term medication (24, 25). Therefore, the discovery of healthy and effective management options for IBD is crucial. Emerging research indicates that the regulation of gut microbiota and its metabolites holds great potential in IBD treatment (26–28). Dietary intervention, particularly the probiotics administration, is currently considered one of the most effective methods for regulating gut microbiota and metabolism (29).

Probiotics are microorganisms, such as *Pediococcus acidilactici*, Bifidobacterium, and *Bacillus subtilis*, that provide benefits to the host when consumed in sufficient amounts (30, 31). Previous studies have demonstrated the positive impact of *Pediococcus acidilactici* on host growth performance, digestive enzyme activity, intestinal villus height, and antioxidant capacity (32–34). Furthermore, *Pediococcus acidilactici* has been found to aintain gut microbial homeostasis and improve intestinal barrier function, suggesting their potential in alleviating gastrointestinal diseases (26, 27, 35). The interaction between probiotics, gut microbiota, and the host has become a significant focus in gastrointestinal disease research. Although there is substantial evidence supporting the alleviative effects of probiotics on colitis, there is a lack of studies specifically investigating the dogs source of *Pediococcus acidilactici*. Therefore, our objective is to evaluate whether *Pediococcus acidilactici* derived from dogs can alleviate colitis by modulating gut microbiota and metabolism. Meanwhile, this research will contribute to the expansion of canine probiotics applications and establish a foundation for the prevention and treatment of colitis using probiotics.

Materials and methods

Animals treatment and sample acquisition

In this study, 24 specific pathogen-free (SPF) male Kunming mice (8-week-old, 42–44 g) were randomly divided into three groups following 3 days of adaptive feeding: control group (CON), *Pediococcus acidilactici* treatment group (RSPQ), and the colitis group (DSS). There were 8 mice in each group. The mice were maintained under standard temperature and humidity conditions and provided with a sufficient diet and drinking water. Additionally, from day 1 to day 7, the DSS and RSPQ groups received drinking water supplemented with 3% (w/v) dextran sulfate sodium salt (DSS) to induce colitis. The specific steps of *Pediococcus acidilactici* preparation refer to previous research (36). During days 8–14 of the experiment, the RSPQ group was supplemented with *Pediococcus acidilactici* (0.2 mL, 5×10^9 CFU/mL) that had been prepared in advance, while the DSS and CON groups received an equivalent volume of normal saline. At the conclusion of the experiment on day 15, all mice were euthanized, and colon tissue, colon contents, and serum samples were collected for subsequent analysis.

16S rDNA amplicon sequencing

According to previous studies, the DNA of each samples was extracted using a commercial kit (37). We designed universal primers (338F: ACTCCTACGGGAG GCAGCAG-3 and 806R: GGACTACHVGGGTWTCTAAT) and added sequencing adapters for PCR amplification. Subsequently, the amplified products were purified, quantified, and normalized to form sequencing libraries. The DNA was quantified via utilizing UV–Vis spectrophotometer (NanoDrop 2000, United States) and DNA integrity was assessed by 0.8% agarose gel electrophoresis. Sequencing libraries were constructed using PacBio platform (Biomarker Technologies, China) according to the manufacturer's specifications. The constructed libraries needed to be quality checked (concentration more than 2 nM), and the qualified libraries were sequenced using Illumina Novaseq 6000. The raw image data files were converted into raw sequencing sequences through base calling analysis. Meanwhile, the results were stored in the FASTQ (abbreviated as fq) file format, which contains the sequence information of the sequencing sequences (Reads) and their corresponding sequencing quality information. Moreover, the analysis of gut microbiota included the following operations: (1) Quality control of the original sequencing sequences to remove unqualified data; (2) OTUs clustering and classification based on sequence composition; (3) According to the OTUs results, taxonomic analysis of samples at various taxonomic levels was performed to explore gut microbial composition; (4) Alpha diversity indices were calculated and explore the species diversity within individual sample; (5) Beta diversity analysis was used for comparing gut microbial construction; (6) Statistical analyses were performed using GraphPad Prism (version 9.0c) and R (v3.0.3) software. Differential taxa associated with colitis were identified using Metastats analysis. Data are expressed as mean ± SEM, and statistically significant differences are denoted as $p < 0.05$.

Histological observations and cytokine analysis

In this study, we prepared tissue sections and HE staining according to previous studies (38, 39). Meanwhile, the IL-6, TNF-α, and IL-1β levels were conducted in accordance with the recommendations of the ELISA kits.

Metabolomics analysis

To further investigate the effects of *Pediococcus acidilactici* on the intestinal metabolism, we explored changes in intestinal metabolism using untargeted metabolomics. The metabolomic procedure such as sample preparation, metabolite identification, data processing and metabolic pathway analysis were determined as per previous research (9, 40).

Results

Histopathological and cytokine analysis

In this research, we observed that *Pediococcus acidilactici* administration can restore colitis-induced weight loss in mice (Supplementary Figure S1). Moreover, the histopathological results of each group are presented in Figures 1A–C. Results indicated that the colon in the CON group was clear and no damage was observed. However, the colon of the DSS group exhibited extensive ulceration, a loss of mucosal and intestinal gland architecture, a reduced number of goblet cells, significant hyperplasia and repair of connective tissue (green arrows), and an abundance of newly formed blood vessels (gray arrows). Furthermore, a notable infiltration of lymphocytes was observed in the lamina propria of the colon tissue in the DSS group (blue arrows), alongside a limited presence of eosinophils in the intestinal glands (orange arrows). However, *Pediococcus acidilactici* administration can reduce the range of ulcers and restore colon damage. Serum cytokine analysis revealed that the levels of IL-6, TNF-α, and IL-1β were significantly increased in the DSS group compared with the CON group (Figures 1D–F). However, *Pediococcus acidilactici* administration could significantly reduce the increase in the levels of the above cytokines caused by colitis.

Pediococcus acidilactici restores alterations in gut microbial diversity associated with colitis

In this research, we explored the differences of the gut microbial abundance and diversity by comparing ACE, Chao1, PD_whole_tree and Shannon. There were statistically significant differences in the gut microbial ACE (587.55 ± 40.35 versus 433.04 ± 27.88, $p < 0.05$), Chao1 (583.76 ± 40.46 versus 428.63 ± 28.09, $p < 0.05$), PD_whole_tree (58.05 ± 6.46 versus 40.19 ± 2.27, $p < 0.05$) and Shannon (6.52 ± 0.06 versus 5.63 ± 0.31, $p < 0.05$) indices between DSS and CON groups, whereas the above-mentioned indices were not significantly different between the CON and RSPQ groups (Figures 2A–D). Intergroup analysis intuitively revealed that colitis could significantly decrease gut microbial abundance and diversity, thereby causing gut microbial dysbiosis. However, *Pediococcus acidilactici* administration could restore the gut microbial diversity and abundance to the control level and maintain gut microbial homeostasis. Moreover, PCoA plots generated from the weighted and unweighted UniFrac distances were applied to assess the beta diversity. Results revealed that the individuals in these groups were clustered together, suggesting no significant differences in the gut microbial construction (Figures 2E,F).

Pediococcus acidilactici administration restored gut microbial dysbiosis during colitis

There were 30 phyla and 571 genera identified from acquired samples, varying from 18 to 26 phyla and 131–299 genera per sample. Specifically, the gut microbiota in the CON, DSS and RSPQ groups were predominated by Firmicutes (CON = 40.93%, DSS = 41.71%, RSPQ = 48.23%), Bacteroidota (CON = 54.74%, DSS = 35.32%,

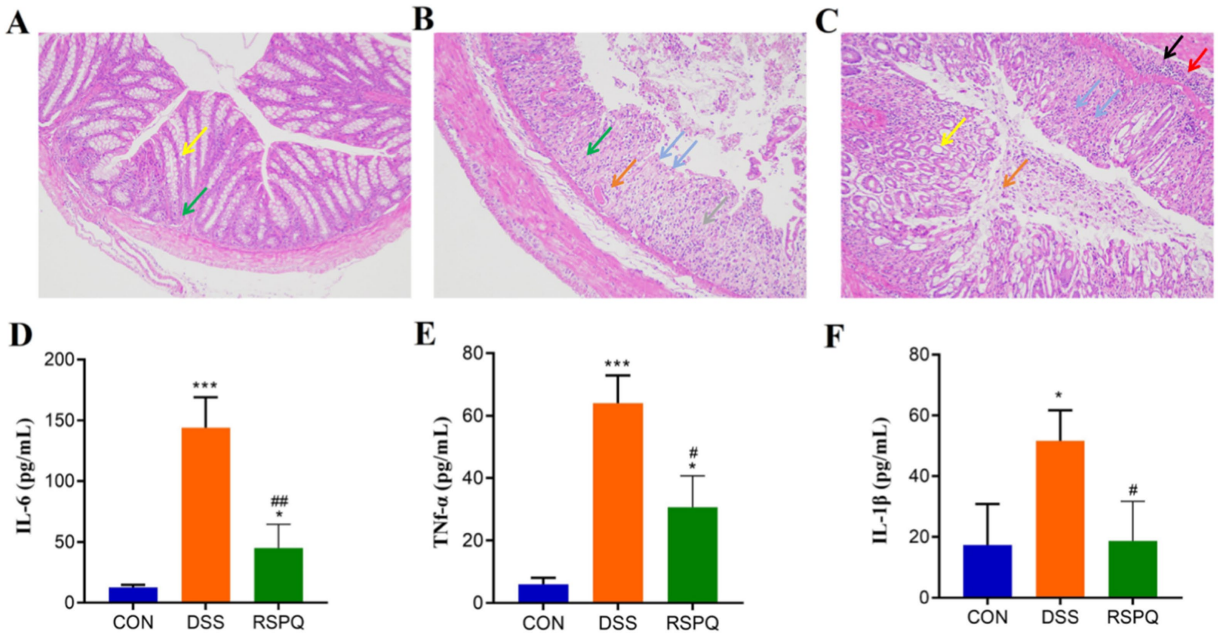

FIGURE 1
Pediococcus acidilactici alleviate intestinal damage and cytokine disorder caused by colitis. **(A–C)** Histopathological observation of colitis in the CON, DSS and RSPQ. **(D–F)** Serum concentrations of IL-6, TNF-α, and IL-1β. $^{*}p < 0.05$ and $^{***}p < 0.001$ vs. the CON, $^{\#}p < 0.05$ and $^{\#\#}p < 0.01$ vs. the DSS.

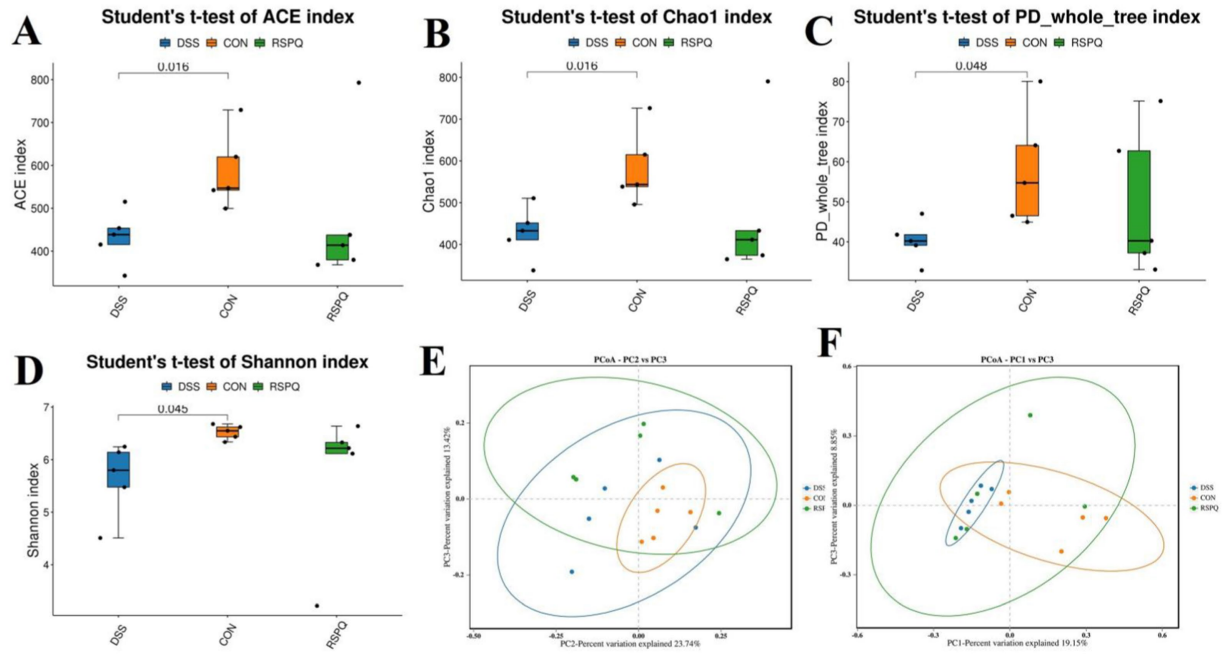

FIGURE 2
Pediococcus acidilactici administration reversed shifts in gut microbial diversity and structure associated with colitis in mice. **(A)** Chao1 index; **(B)** ACE index; **(C)** PD_whole_tree index; **(D)** Shannon index. PCoA plots based on the weighted **(E)** and unweighted **(F)** uniFrac distance. Each point on the graph represents a sample, with distinct colors denoting different groups. The distance between points illustrates the degree of variation among the samples.

RSPQ = 26.50%) and Proteobacteria (CON = 1.12%, DSS = 18.79%, RSPQ = 18.25%) (Figure 3A). Moreover, other phyla such as Campylobacterota (CON = 0.24%, DSS = 0.50%, RSPQ = 0.64%), Verrucomicrobiota (CON = 0.036%, DSS = 0.024%, RSPQ = 1.79%), Actinobacteriota (CON = 0.48%, DSS = 0.35%, RSPQ = 0.42%), Acidobacteriota (CON = 0.37%, DSS = 0.16%, RSPQ = 0.30%) and Cyanobacteria (CON = 0.053%, DSS = 0.10%, RSPQ = 0.68%) in the CON, DSS and RSPQ groups were represented with a lower abundance. Among recognized genera, unclassified_*Muribaculaceae* (19.87%), unclassified_*Lachnospiraceae* (15.04%) and *Lachnospiraceae*_NK4A136_group (13.00%) were the most prevalent bacteria in the CON group, accounting for approximately 47.92 of overall composition (Figure 3B). Additionally, the dominant bacterial genera observed in the DSS group were *Bacteroides* (22.55%), *Escherichia_Shigella* (14.79%) and unclassified_*Lachnospiraceae* (11.38%), whereas *Bacteroides* (16.31%) was the most predominant bacterial genus in the RSPQ groups, followed by *Lachnospiraceae*_NK4A136_group (15.13%) and *Escherichia_Shigella* (12.85%). Furthermore, clustering heatmap also showed the composition and abundance distribution of gut microbiota in the CON, DSS and RSPQ groups and demonstrated the significant effects of colitis on gut microbiota (Figure 3C).

Metastats analysis was used for distinguishing the differential taxa at different classification levels to further explore the effects of *Pediococcus acidilactici* administration on gut microbiota in mice with colitis. At the phylum level, the gut microbiota in the DSS group exhibited significant increase in the relative proportions of Desulfobacterota and Proteobacteria, whereas Bacteroidota, Patescibacteria and Bdellovibrionota decreased dramatically as compared to CON group (Figure 4A). Moreover, 49 bacterial genera were found to be significantly different between CON and DSS groups. Among them, the relative abundances of 15 bacterial genera (unclassified_*Erysipelatoclostridiaceae*, *Bacteroides*, *Akkermansia*, *Turicibacter*, *Erysipelatoclostridium*, unclassified_*env.OPS_17*, *Streptococcus*, unclassified_*Desulfovibrionaceae*, *Bilophila*, *Romboutsia*, *Enterorhabdus*, *Escherichia_Shigella*, *Enterococcus*, uncultured_*Clostridiales_bacterium*, and uncultured_*rumen_bacterium*) significantly increased, whereas the relative richness of 34 bacterial genera (uncultured_*Muribaculaceae_bacterium*, *Prevotellaceae_UCG_001*, unclassified_*Clostridia*, uncultured_*Bacteroidales_bacterium*, unclassified_*Erysipelotrichaceae*, *Alloprevotella*, *ZOR0006*, unclassified_*RF39*, unclassified_*SBR1031*, *A2*, *Alistipes*, *Muribaculum*, *Candidatus_Arthromitus*, *Odoribacter*, *Roseburia*, *Marvinbryantia*, *[Eubacterium]_nodatum_group*, *Prevotellaceae_NK3B31_group*, unclassified_*Rokubacteriales*, unclassified_*Gaiellales*, *Paenibacillus*, unclassified_*Xanthobacteraceae*, *Sphingomonas*, *Mesoplasma*, unclassified_*Muribaculaceae*, uncultured_*soil_bacterium*, unclassified_*Comamonadaceae*, *Candidatus_Saccharimonas*, unclassified_*BIrii41*, unclassified_*Acetobacteraceae*, unclassified_*Isosphaeraceae*, *Rikenellaceae_RC9_gut_group*, *Anaerotruncus*, and unclassified_*TRA3_20*) memorably decreased during colitis (Figure 4B). At the phylum level, the abundances of Patescibacteria and Fusobacteriota was observably more preponderant in RSPQ than in the DSS, whereas the abundances of Proteobacteria was lower (Figure 5A). Moreover, we observed that the relative abundances of six genera (unclassified_*Erysipelatoclostridiaceae*, *Rikenella*, unclassified_*env.OPS_17*, *Erysipelatoclostridium*, *Acetatifactor* and *Aquisphaera*) obviously decreased significantly increased, whereas the relative abundances of

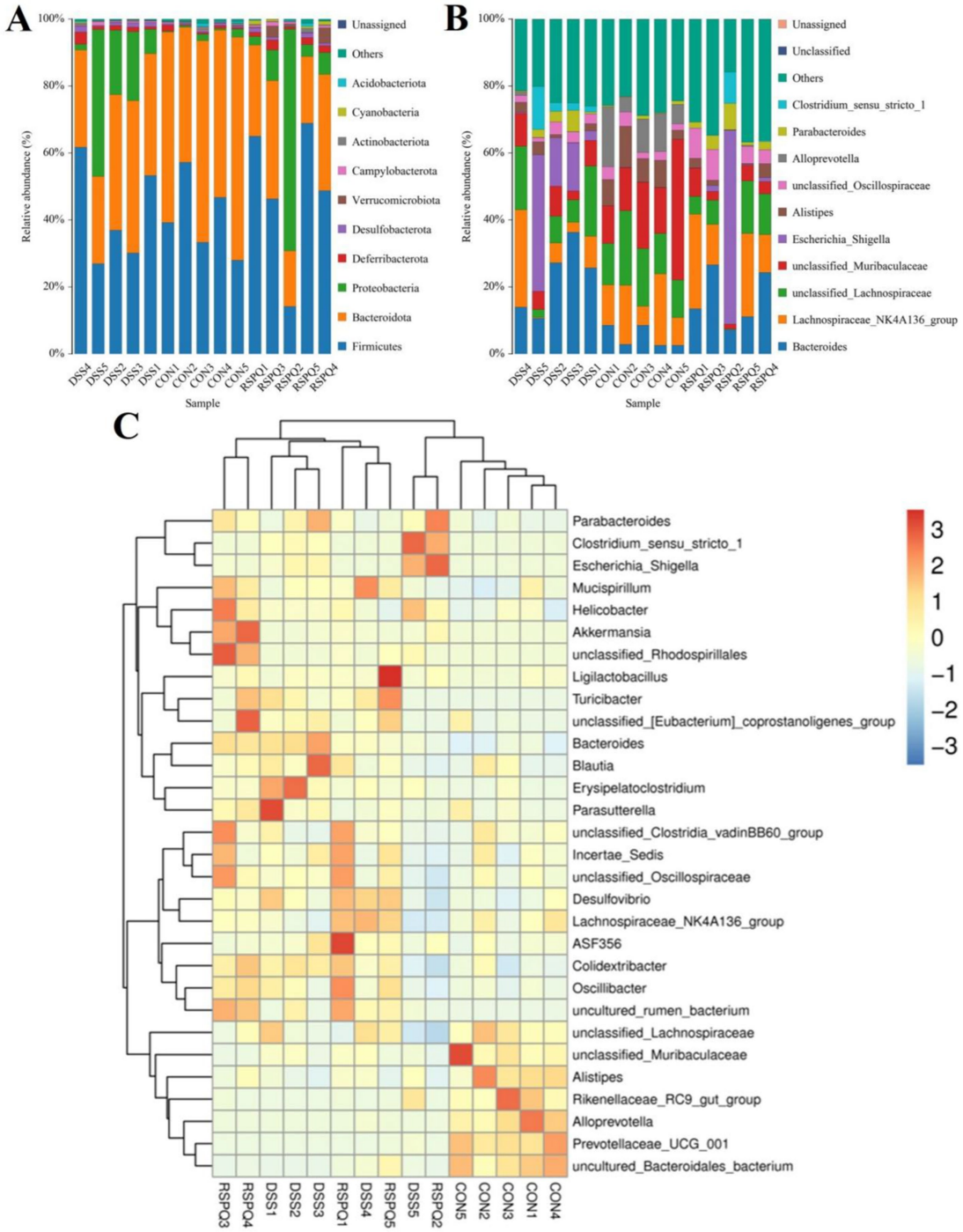

FIGURE 3
Relative abundance distribution of different samples at the phylum **(A)** and genus **(B)** levels. Only the top 10 most abundant bacterial phyla and genera are displayed in each sample. **(C)** Cluster heatmap of different samples at the genus level. The gradient of blue to red represents the alteration of abundance from low to high.

12 genera (*Iunclassified_Clostridia*, unclassified_*Bacilli*, *Robiginitalea*, unclassified_*TRA3_20*, *uncultured_Mollicutes_bacterium*, unclassified_*Anaerolineaceae*, uncultured_*rumen_bacterium*, *Fusobacterium*, *[Eubacterium]_nodatum_group*, *Pediococcus*, *Bdellovibrio* and *Akkermansia*) significantly increased in RSPQ as compared to DSS (Figure 5B).

Pediococcus acidilactici administration ameliorated intestinal metabolism during colitis

The PCA analysis indicated that colitis caused distinct changes in intestinal metabolism, while *Pediococcus acidilactici* administration

10.3389/fvets.2025.1520678

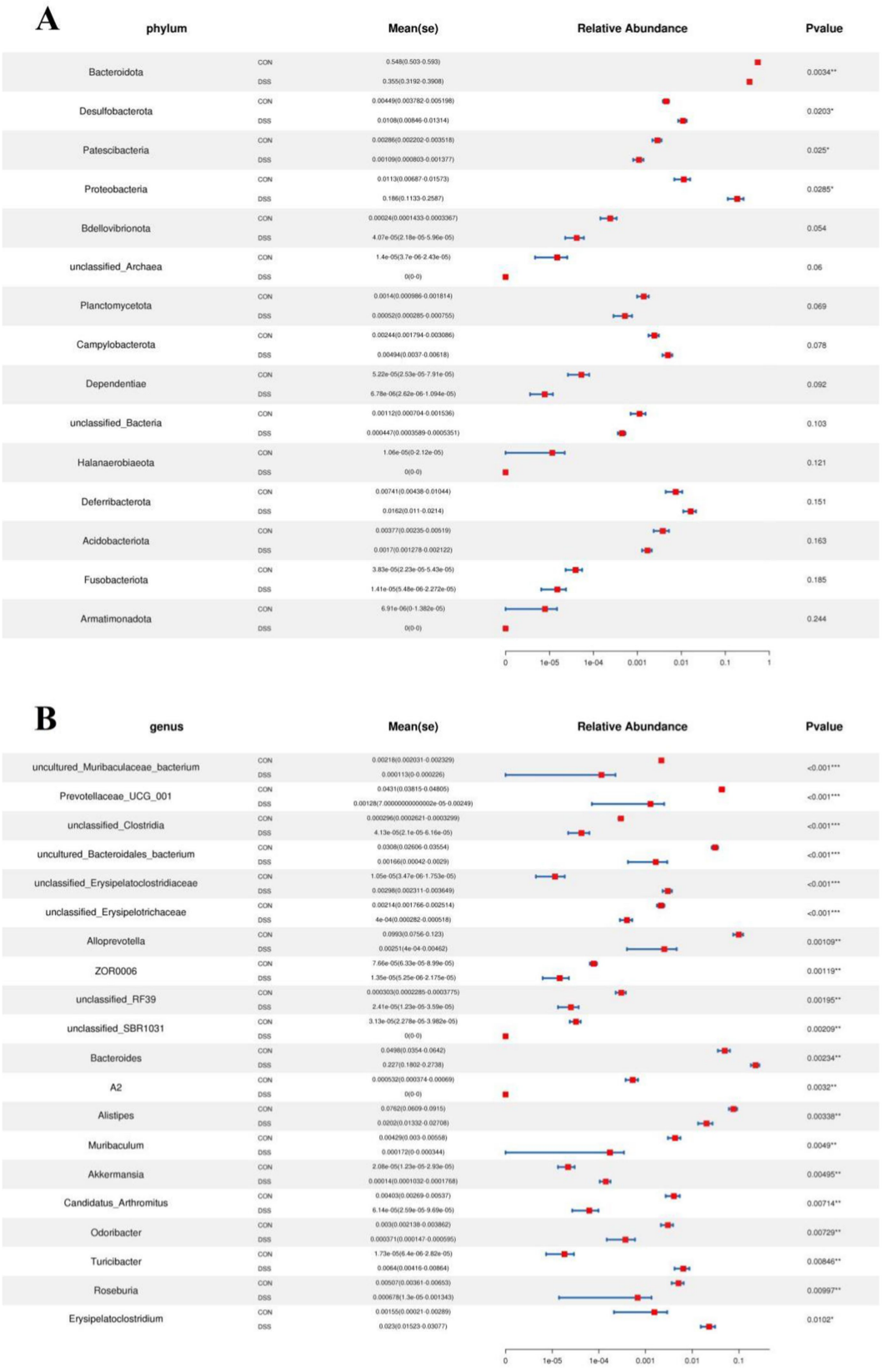

FIGURE 4
Taxa that were significantly different between the CON and DSS groups at the phylum **(A)** and genus **(B)** levels. All of the data represent means ± SD. *$p < 0.05$, **$p < 0.01$, ***$p < 0.001$.

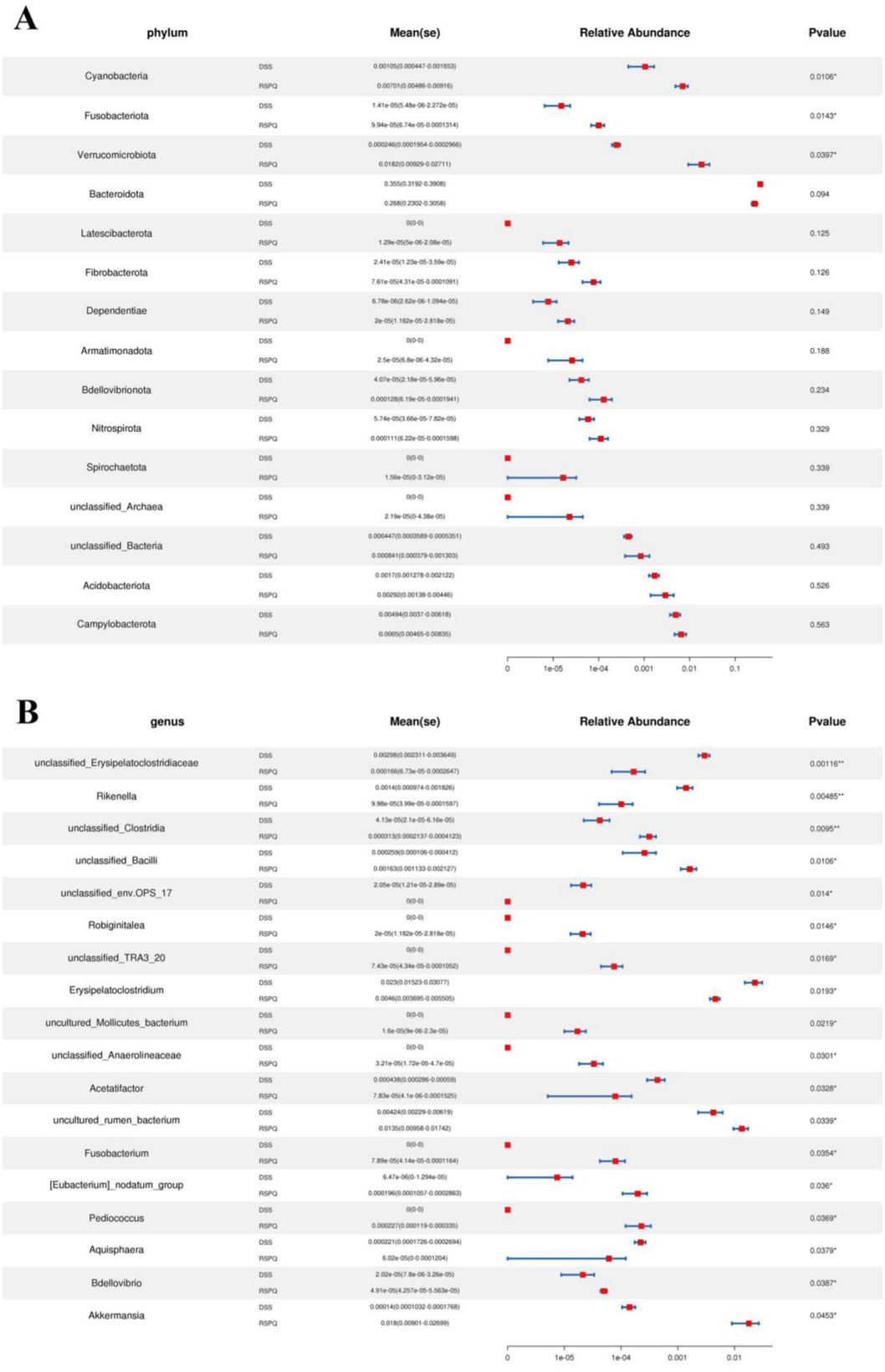

FIGURE 5
Taxa that were significantly different between the RSPQ and DSS groups at the phylum **(A)** and genus **(B)** levels. All of the data represent means ± SD. *$p < 0.05$, **$p < 0.01$.

ameliorated intestinal metabolism in mice with colitis (Figures 6, 7). To further reveal the positive regulation of *Pediococcus acidilactici* on intestinal metabolism, OPLS-DA score plots was applied for pattern discriminant analysis. Results indicated that there was a clear separation among CON, DSS, and RSPQ groups and no fitting occur. There are 957 (455 in positive mode, 502 in negative-ion mode) differential metabolites were detected between CON and DSS groups (Figures 8A,B). Among significantly different metabolites, 740

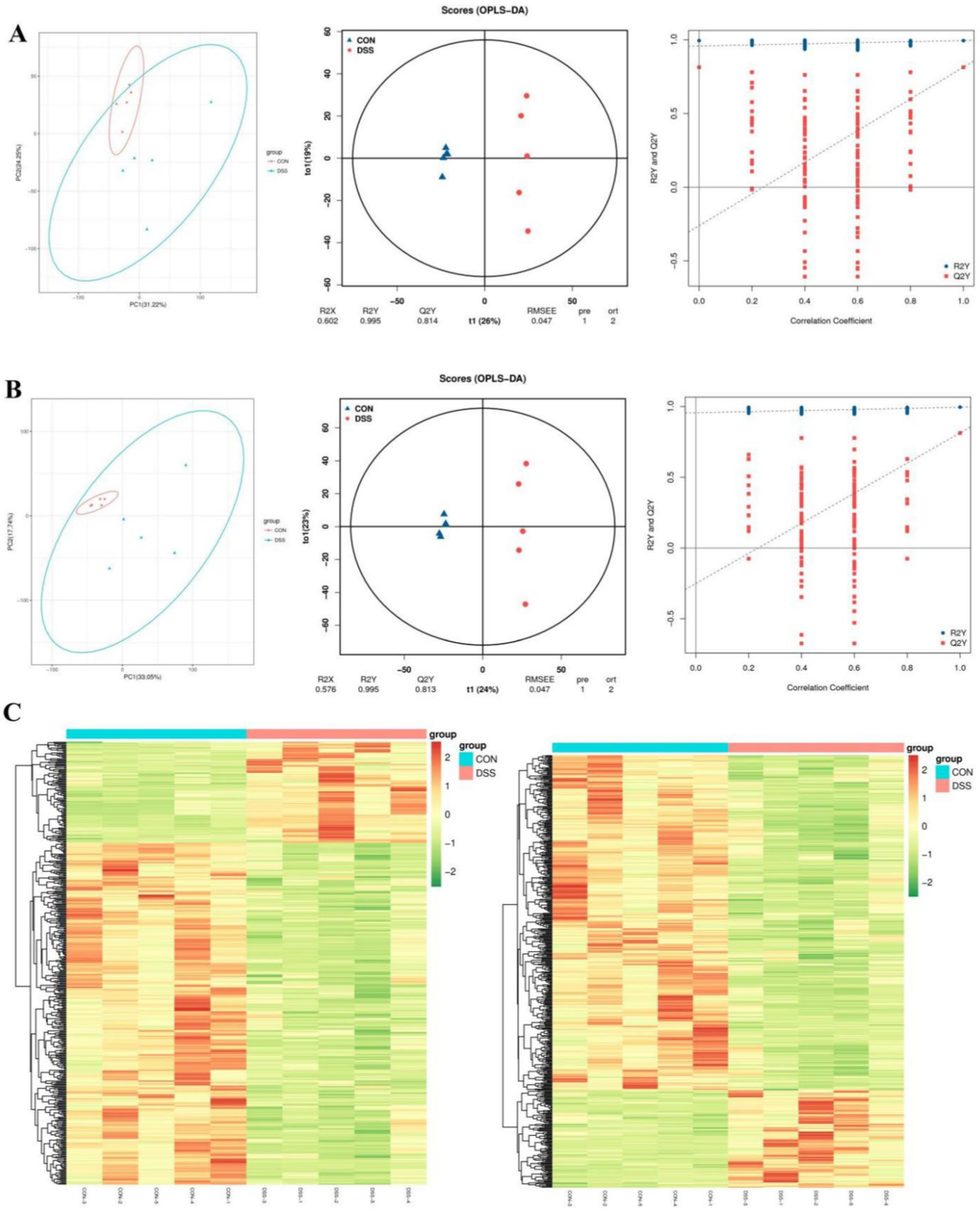

FIGURE 6
Multivariate statistical analysis of intestinal metabolism in CON and DSS groups. **(A,B)** PCA score plots, OPLS-DA score plots and permutation tests of the OPLS-DA in positive-ion and negative-ion modes. **(C)** Cluster heat map of differential metabolites in CON and DSS groups in positive-ion and negative-ion modes.

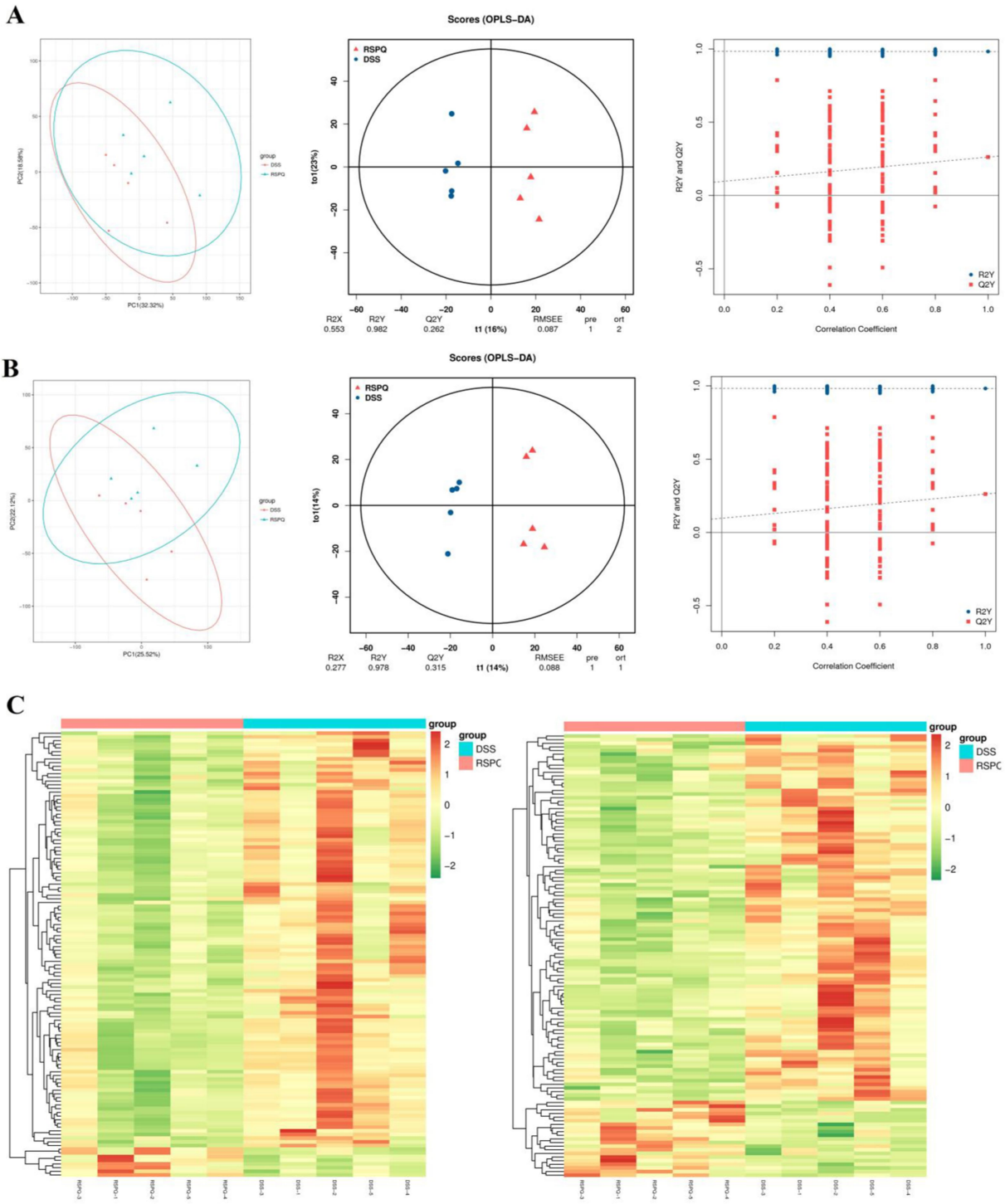

FIGURE 7
Multivariate statistical analysis of intestinal metabolism associated with *Pediococcus acidilactici* and colitis. **(A,B)** PCA score plots, OPLS-DA score plots and permutation tests of the OPLS-DA in positive-ion and negative-ion modes. **(C)** Cluster heat map of differential metabolites in CON and DSS groups in positive-ion and negative-ion modes.

metabolites were down-regulated, whereas 217 metabolites were up-regulated in DSS group. Additionally, we observed that there were 1,018 metabolites exhibiting significant differences between the CON and RSPQ groups (Figures 9A,B). Among these, 208 (89 in positive mode, 119 in negative-ion mode) metabolites were significantly increased, while 810 (403 in positive mode, 407 in negative-ion mode) metabolites were significantly decreased in the RSPQ group compared to the CON group. For the comparison of the DSS and RSPQ groups, 243 metabolites (121 in positive mode, 122 in negative-ion mode) were totally identified, while the richness of 28 metabolites increased dramatically, whereas 215 metabolites showed the opposite trend.

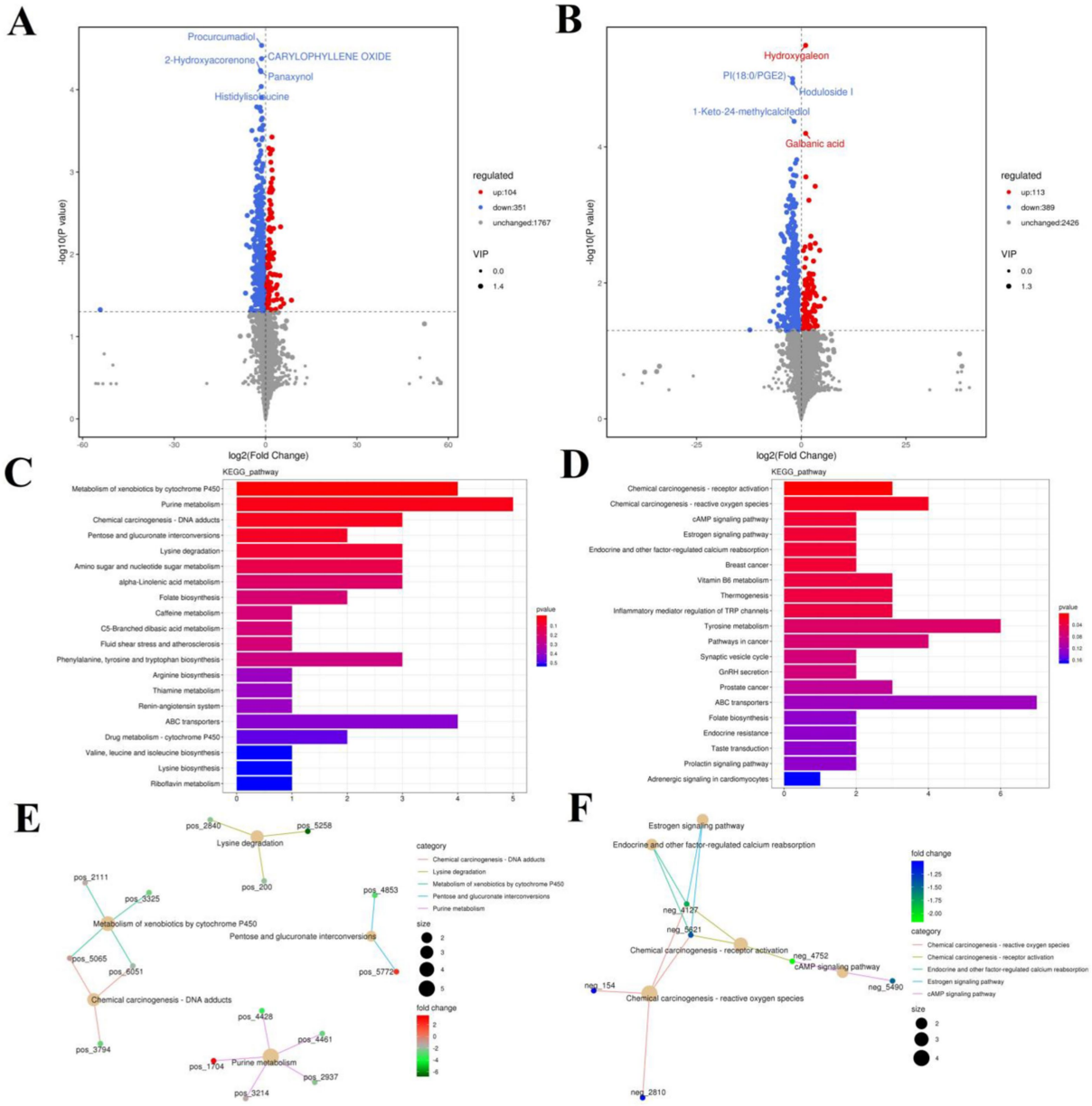

FIGURE 8
Effects of colitis on intestinal metabolism. **(A,B)** Volcano plot of differential metabolites between CON and DSS groups in positive-ion and negative-ion modes. The red dots represent the increased metabolites. The blue dots represent the decreased metabolites. **(C,D)** Intestinal metabolic pathways associated with colitis in positive-ion and negative-ion modes. **(E,F)** The representative network diagram of metabolites and related metabolic pathways between CON and DSS groups in positive-ion and negative-ion modes.

The representative enriched pathways associated with colitis and *Pediococcus acidilactici* administration were present in Figures 8C,D and Figure 9C,D. Among enriched pathways between CON and DSS groups, 13 pathways with a significant difference were the metabolism of xenobiotics by cytochrome P450, purine metabolism, chemical carcinogenesis-DNA adducts, pentose and glucuronate interconversions, chemical carcinogenesis-receptor activation, chemical carcinogenesis-reactive oxygen species, cAMP signaling pathway, estrogen signaling pathway, endocrine and other factor-regulated calcium reabsorption, breast cancer, vitamin B6 metabolism, thermogenesis, inflammatory mediator regulation of TRP channels, which involved in 24 potential biomarkers including L-Noradrenaline, dimethylarsinous acid, oleoylethanolamide, 4-Pyridoxic acid, 2-Oxo-3-hydroxy-4-phosphobutanoate, 2-(Hydroxymethyl)-4-oxobutanoate, estradiol, 5-HETE, histamine, 15(S)-HETE, 5-Amino-4-imidazolecarboxyamide, dGMP, xanthosine, dIMP, Sudan I, digalacturonate, and D-Fructuronate, etc. (Table 1). Moreover, there were 8 pathways that were significantly different between the DSS and RSPQ, namely glutathione metabolism, mTOR signaling pathway, amyotrophic lateral sclerosis, pathways of neurodegeneration-multiple diseases, chagas disease, amoebiasis, arginine and proline metabolism, and arachidonic acid metabolism (Table 2). These pathways are linked to five potential biomarkers: spermine, L-Arginine, 15-Deoxy-Delta12,14-PGJ2, prostaglandin J2, and 15(S)-HETE. The metabolic

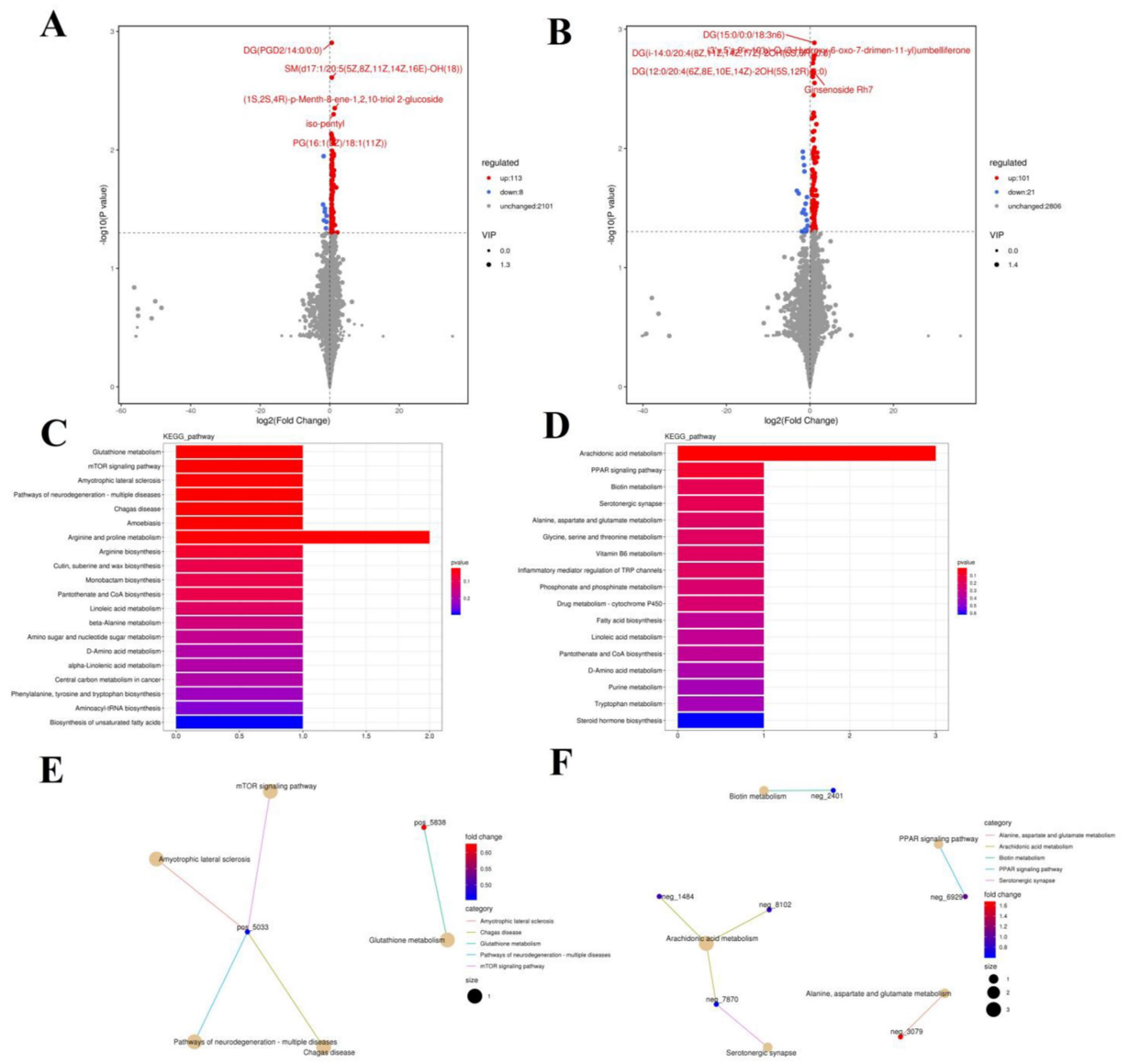

FIGURE 9
Effects of colitis on intestinal metabolism. **(A,B)** Volcano plot of differential metabolites between DSS and RSPQ groups in positive-ion and negative-ion modes. The red dots represent the increased metabolites. The blue dots represent the decreased metabolites. **(C,D)** Intestinal metabolic pathways associated with colitis in positive-ion and negative-ion modes. **(E,F)** The representative network diagram of metabolites and related metabolic pathways between DSS and RSPQ groups in positive-ion and negative-ion modes.

diagrams related to colitis or *Pediococcus acidilactici* administration in the intestine were shown in Figures 8E,F and Figures 9E,F.

Discussion

The adverse effects of colitis on both human and animal health have attracted increasing attention (41). Although the specific pathogenesis of colitis has not yet been fully elucidated, it has been demonstrated to be closely associated with multiple factors such as environment, bacterial infection, oxidative stress, and genetics (42, 43). Recently, some studies involving gut microbiota have reported its important role in the development of colitis (44). Antibiotics remain the most commonly used treatment for colitis. However, antibiotics are no longer recommended for long-term use, due to the negative effects on hots health such as bacterial resistance, drug residues, and gut microbial imbalance. Probiotics have received widespread attention due to their important roles in gut microbiota, immunity, and metabolism (45, 46). Thus, *in vitro* supplementation of probiotics is also considered an effective strategy to alleviate colitis. In this study, we systematically explored the alleviating effect of *Pediococcus acidilactici* isolated from dogs on colitis using microbiome and metabolomics technologies.

To investigate the possible mechanism, we hypothesized that *Pediococcus acidilactici* administration could mediate the gut microbiota and their metabolites to further attenuate the colitis. Gut microbial composition and diversity were previously demonstrated to be associated with multiple intestinal diseases (47). In this study,

TABLE 1 Identification of potential biomarkers associated with differential metabolic pathways between the CON and DSS groups.

Pathway	Biomarkers	*p*	VIP	FC	Trend
Metabolism of xenobiotics by cytochrome P450	2-S-glutathionyl acetate	0.0020	1.76	0.38	Down
	1-Nitro-5-hydroxy-6-glutathionyl-5,6-dihydronaphthalene	0.03	1.41	0.15	Down
	1-(Methylnitrosoamino)-4-(3-pyridinyl)-1,4-butanediol	0.014	1.41	0.53	Down
	4-Oxo-1-(3-pyridyl)-1-butanone	0.027	1.41	0.27	Down
Purine metabolism	2-(Formamido)-N1-(5-phospho-D-ribosyl)acetamidine	0.046	1.39	9.98	Up
	5-Amino-4-imidazolecarboxyamide	0.00016	1.82	0.21	Down
	dGMP	0.049	1.36	0.39	Down
	xanthosine	0.018	1.46	0.095	Down
	dIMP	0.0015	1.77	0.15	Down
Chemical carcinogenesis - DNA adducts	Sudan I	0.048	1.31	0.151	Down
	1-(Methylnitrosoamino)-4-(3-pyridinyl)-1,4-butanediol	0.014	1.41	0.53	Down
	4-Oxo-1-(3-pyridyl)-1-butanone	0.027	1.41	0.27	Down
Pentose and glucuronate interconversions	Digalacturonate	0.015	1.58	0.12	Down
	D-Fructuronate	0.047	1.33	4.22	Up
Primary bile acid biosynthesis	Glycochenodeoxycholate	0.012	1.53	0.22	Down
	3beta,7alpha-Dihydroxy-5-cholestenoate	0.0079	1.69	0.17	Down
	7alpha-Hydroxycholesterol	0.043	1.36	0.61	Down
Neomycin, kanamycin and gentamicin biosynthesis	Nebramycin factor 4	0.010	1.70	0.33	Down
	2′-N-Acetylparomamine	0.026	1.47	1.96	Up
	4′-Oxolividamine	0.040	1.26	0.450	Down
Arachidonic acid metabolism	5-HETE	0.042	1.48	4.03	Up
	Prostaglandin C2	0.033	1.51	0.25	Down
	15(S)-HETE	0.024	1.43	1.60	Up
Valine, leucine and isoleucine degradation	L-Valine	0.0079	1.56	0.39	Down
Valine, leucine and isoleucine biosynthesis	L-Valine	0.0079	1.56	0.39	Down
Polyketide sugar unit biosynthesis	dTDP-4-oxo-5-C-methyl-L-rhamnose	0.044	1.40	0.077	Down
Glycerophospholipid metabolism	CDP-Ethanolamine	0.035	1.48	10.21	Up
Gap junction	L-Noradrenaline	0.018	1.56	0.22	Down
Aldosterone synthesis and secretion	Aldosterone	0.021	1.59	8.84	Up
Mineral absorption	L-Valine	0.0079	1.56	0.39	Down
Linoleic acid metabolism	12,13-DHOME	0.0095	1.68	2.44	Up
	13(S)-HODE	0.010	1.53	1.91	Up

Fold change (FC) was calculated by dividing the normalized means of metabolites in DSS by the CON.

colitis caused intestinal injury and decreased gut microbial alpha diversity, which is consistent with the findings of previous studies (47, 48). Early investigations suggested that intestinal injury inevitably could affecte intestinal environment and microbial survival, which in turn force existing microorganisms to adapt to new intestinal environment and alter the gut microbial composition and diversity, perturbing gut microbial homeostasis (49). The stable gut microbiota is an important biological barrier against the colonization and overgrowth of pathogens and conditioned pathogens (50). Conversely, gut microbial dysbiosis can affect intestinal mucosal barrier and immunologic function, thus increasing susceptibility to pathogens (50, 51). In this study, we observed that *Pediococcus acidilactici* administration could alleviate colon damage and reverse the reduction of microbial index caused by colitis.

We further dissected the relationship between colitis and gut microbiota and observed that colitis could cause changes in some specific bacteria that may play crucial roles in intestinal homeostasis and function. In this research, colitis cause a decline in the relative abundances of *Bacteroidetes*, *Prevotellaceae*, *Alloprevotella*, *Rikenellaceae*, *Alistipes*, and *Roseburia* and an increase in the proportion of *Proteobacteria*, *Turicibacter*, *Bilophila*, *Escherichia_Shigella*, and *Enterococcus*. Previous research indicated that the

TABLE 2 Identification of potential biomarkers associated with differential metabolic pathways between the RSPQ and DSS groups.

Pathway	Biomarkers	*p*	VIP	FC	Trend
Glutathione metabolism	Spermine	0.013	1.90	1.54	Up
mTOR signaling pathway	L-Arginine	0.031	1.72	1.37	Up
Amyotrophic lateral sclerosis	L-Arginine	0.031	1.72	1.37	Up
Pathways of neurodegeneration - multiple diseases	L-Arginine	0.031	1.72	1.37	Up
Chagas disease	L-Arginine	0.031	1.72	1.37	Up
Amoebiasis	L-Arginine	0.031	1.72	1.37	Up
Arginine and proline	Spermine	0.013	1.90	1.54	Up
metabolism	L-Arginine	0.031	1.72	1.37	Up
Arachidonic acid metabolism	15-Deoxy-Delta12,14-PGJ2	0.042	1.86	1.82	Up
	Prostaglandin J2	0.015	2.04	1.53	Up
	15(S)-HETE	0.010	2.21	1.81	Up

Fold change (FC) was calculated by dividing the normalized means of metabolites in DSS by the RSPQ.

gut-residing *Bacteroidetes* is responsible for degrading carbohydrates and proteins (52). Meanwhile, it has been demonstrated to it can facilitate the development of the gastrointestinal immune system (53). As a pro-inflammatory bacterium, the levels of *Turicibacter* is significantly increased during enteritis (54). Earlier investigations showed that the increased *Bilophila* may contribute to the development of appendicitis and colitis (55). *Escherichia_Shigella* has been reported to be associated with diarrhea and intestinal infections (56). *Enterococcus* are common pathogens that can cause sepsis, pericarditis, and meningitis (57). Additionally, *Enterococcus* have been demonstrated to have both intrinsic and acquired drug resistance, which severely affects the treatment of their infections (58). *Prevotellaceae* has been shown to possess the ability to degrade polysaccharide and high-carbohydrate substrates (59). Thus, the decreased abundance of *Prevotellaceae* in the intestine may negatively impact host nutrient uptake. *Alloprevotella* has been demonstrated to be closely related to the decreased lifetime cardiovascular disease risk due to its ability to produce acetate and succinate (4, 5). As a common beneficial intestinal bacteria, *Rikenellaceae* could degrade plant-derived polysaccharides and alleviate the colitis by mediating T-regulatory cell differentiation (60). *Alistipes* and *Roseburia* are potential producers of SCFAs. Previous investigations involving SCFAs have indicated their vital roles in immune system, cell proliferation, energy intake and intestinal metabolism (61, 62). Additionally, SCFAs also participate in the positive regulation of gut microbiota and intestinal barrier, which are essential for host health (63). However, *Pediococcus acidilactici* administration can improve the gut microbial composition of patients with colitis. Notably, *Pediococcus acidilactici* administration can increase the relative abundances of *Akkermansia*. *Akkermansia* has long been recognized as a beneficial intestinal bacterium, and its abundance gradually decreases with the development of enteritis (64). Numerous studies indicated that *Akkermansia* can alleviate intestinal inflammation and prevent intestinal cancer by regulating the immune response in the spleen, intestines, and mesenteric lymph nodes (65, 66). Moreover, *Akkermansia* has been demonstrated to be negatively related to obesity and diabetes (67, 68). These results showed the vital roles of *Pediococcus acidilactici* administration in regulating gut microbiota, which contributed to maintaining intestinal colonization resistance and homeostasis.

Previous studies indicated that the gut microbiota can systematically regulate host health by producing metabolites. Therefore, we also explored the changes in intestinal metabolism. In this study, we observed that eight metabolic pathways (glutathione metabolism, arginine and proline metabolism, arachidonic acid metabolism, etc.) and 5 (spermine, L-Arginine, 15-Deoxy-Delta12,14-PGJ2, prostaglandin J2, and 15(S)-HETE) metabolites were involved in the alleviating effect of *Pediococcus acidilactici* administration. These significantly changed metabolites and metabolic pathways may play a key role in *Pediococcus acidilactici* alleviating colitis. Previous studies have demonstrated that arachidonic acid can alleviate oxidative stress by increasing the levels of superoxide dismutase (SOD) and catalase (CAT) (69). Furthermore, arachidonic acid has been shown to inhibit oxidative stress by reducing mitochondrial membrane potential and blocking reverse electron transport (RET) through uncoupling, which in turn inhibits RET-dependent reactive oxygen species (ROS) generation (70). As an important intracellular metabolic regulator and antioxidant, glutathione can participate in the tricarboxylic acid cycle and sugar metabolism in the body (71). It can also activate multiple enzymes, thereby facilitating the metabolism of carbohydrates, fats and proteins. Additionally, glutathione play a crucial role in maintaining the function of the immune system and the stability of the red blood cell membrane structure (72). Recent research indicates that glutathione can rectify the imbalance of acetylcholine and cholinesterase, exert an anti-allergic effect, and enhance the skin's antioxidant capacity (73). Previous research has indicated that oxidative stress is a significant factor contributing to the development of colitis. Thus, *Pediococcus acidilactici* may alleviate the development of colitis by mediating arachidonic acid metabolism and glutathione metabolism.

Conclusion

Taken together, this study investigated the alleviating effect of *Pediococcus acidilactici* on colitis. Results indicated that *Pediococcus acidilactici* could alleviate colonic injury and reverse the decline in gut microbial diversity and abundance associated with colitis. Additionally, we also observed a positive effect of *Pediococcus acidilactici* on intestinal metabolism in patients with colitis.

Arachidonic acid metabolism and glutathione metabolism may be potential pathways for *Pediococcus acidilactici* to exert its effects. This study is an important exploration of whether *Pediococcus acidilactici* isolated from dogs can alleviate colitis. Meanwhile, it also contributes to expanding the probiotic application and provide a theoretical basis for alleviating colitis from the microbial and metabolic perspective. However, it is important to acknowledge the limitations of this study, particularly the small sample size.

Data availability statement

The original sequence data was submitted to the Sequence Read Archive (SRA) (NCBI, USA) with the accession no. PRJNA1179910.

Ethics statement

The animal study was approved by the Animal Welfare and Ethics Committee of Anqing Normal University. The study was conducted in accordance with the local legislation and institutional requirements.

Author contributions

LW: Writing – review & editing. LX: Writing – review & editing. XD: Writing – review & editing. HJ: Writing – review & editing. RZ: Writing – review & editing. AZ: Writing – review & editing. YZ: Writing – review & editing. ST: Writing – review & editing. XW: Writing – review & editing. ZL: Writing – original draft, Writing – review & editing.

Funding

The author(s) declare that financial support was received for the research, authorship, and/or publication of this article. This work was supported by the Engineering Technology Research Center for Aquatic Organism Conservation and Water Ecosystem Restoration in University of Anhui Province topics open to the outside world (No. AO202301), Anhui Provincial Higher Education Key Scientific Research Project (2023AH050504 and 2024AH051130), and Key Lab. of Biodiversity Conservation and Characteristic Resource Utilization in Southwest Anhui topics open to the outside world (Wxn202402).

Conflict of interest

The authors declare that the research was conducted in the absence of any commercial or financial relationships that could be construed as a potential conflict of interest.

Generative AI statement

The authors declare that no Gen AI was used in the creation of this manuscript.

Publisher's note

Supplementary material

The Supplementary material for this article can be found online at: https://www.frontiersin.org/articles/10.3389/fvets.2025.1520678/full#supplementary-material

References

1. Li A, Liu B, Li F, He Y, Wang L, Fakhar-E-Alam KM, et al. Integrated bacterial and fungal diversity analysis reveals the gut microbial alterations in diarrheic giraffes. *Front Microbiol*. (2021) 12:712092. doi: 10.3389/fmicb.2021.712092

2. Li A, Wang Y, He Y, Liu B, Iqbal M, Mehmood K, et al. Environmental fluoride exposure disrupts the intestinal structure and gut microbial composition in ducks. *Chemosphere*. (2021) 277:130222. doi: 10.1016/j.chemosphere.2021.130222

3. Liao J, Liu Y, Yi J, Li Y, Li Q, Li Y, et al. Gut microbiota disturbance exaggerates battery wastewater-induced hepatotoxicity through a gut-liver axis. *Sci Total Environ*. (2022) 809:152188. doi: 10.1016/j.scitotenv.2021.152188

4. Han B, Shi L, Bao MY, Yu FL, Zhang Y, Lu XY, et al. Dietary ellagic acid therapy for cns autoimmunity: targeting on alloprevotella rava and propionate metabolism. *Microbiome*. (2024) 12:114. doi: 10.1186/s40168-024-01819-8

5. Han Y, Zhang Z, Yang H, Zhang N, Lin C, Raza A, et al. Protective effects of shlo on lps-induced lung injury via tlr4/myd88-erk signaling pathway and intestinal flora regulation. *Pak Vet J*. (2024) 44:776–84. doi: 10.29261/pakvetj/2024.255

6. Li A, Liu F, Si W, Wang Y, Wang D, Yuan Z, et al. Pesticide butachlor exposure perturbs gut microbial homeostasis. *Ecotoxicol Environ Saf*. (2024) 281:116646. doi: 10.1016/j.ecoenv.2024.116646

7. Li J, Jia J, Teng Y, Xie C, Li C, Zhu B, et al. Gastrodin alleviates dss-induced colitis in mice through strengthening intestinal barrier and modulating gut microbiota. *Food Secur*. (2024) 13:2460. doi: 10.3390/foods13152460

8. Wang D, Zeng J, Ma H, Fouad D, Su Z. Comparative analysis of the gut microbiota between two horse species. *Pak Vet J*. (2024) 44:449–57. doi: 10.29261/pakvetj/2024.151

9. Wang L, Nabi F, Zhang X, Zhou G, Shah QA, Li S, et al. Effects of *Lactobacillus plantarum* on broiler health: integrated microbial and metabolomics analysis. *Probiotics Antimicrob Proteins*. (2024):1–19. doi: 10.1007/s12602-024-10336-x

10. Wang R, Yang X, Liu J, Zhong F, Zhang C, Chen Y, et al. Gut microbiota regulates acute myeloid leukaemia via alteration of intestinal barrier function mediated by butyrate. *Nat Commun*. (2022) 13:2522. doi: 10.1038/s41467-022-30240-8

11. Li A, Wang Y, Kulyar MF, Iqbal M, Lai R, Zhu H, et al. Environmental microplastics exposure decreases antioxidant ability, perturbs gut microbial homeostasis and metabolism in chicken. *Sci Total Environ*. (2023) 856:159089. doi: 10.1016/j.scitotenv.2022.159089

12. Luo M, Han Y, Chen Y, Du H, Chen B, Gao Z, et al. Unveiling the role of gut microbiota in curcumin metabolism using antibiotic-treated mice. *Food Chem*. (2024) 460:140706. doi: 10.1016/j.foodchem.2024.140706

13. Liang X, Wang R, Luo H, Liao Y, Chen X, Xiao X, et al. The interplay between the gut microbiota and metabolism during the third trimester of pregnancy. *Front Microbiol*. (2022) 13:1059227. doi: 10.3389/fmicb.2022.1059227

14. Meng A, Zhang X, Pubu P, Ali M, Wang J, Xu C, et al. Protective effect of lentinan against LPS-induced injury in mice via influencing antioxidant enzyme activity, inflammatory pathways, and gut microbiota. *Pak Vet J*. (2024) 44:647–56. doi: 10.29261/pakvetj/2024.225

15. Sasahara Y, Uchida T, Suzuki T, Abukawa D. Primary immunodeficiencies associated with early-onset inflammatory bowel disease in southeast and east asia. *Front Immunol*. (2021) 12:786538. doi: 10.3389/fimmu.2021.786538

16. Wang L, Shao L, Chen MY, Wang L, Yang P, Tan FB, et al. Panax notoginseng alleviates colitis via the regulation of gut microbiota. *Am J Chin Med*. (2023) 51:107–27. doi: 10.1142/S0192415X23500076

17. Yu H, Zhang S, Li R, Ma C, Zhang Q, Xia F, et al. Berberine alleviates inflammation and suppresses pla2-cox-2-pge2-ep2 pathway through targeting gut microbiota in dss-induced ulcerative colitis. *Biochem Biophys Res Commun*. (2024) 695:149411. doi: 10.1016/j.bbrc.2023.149411

18. Cardenas VR, Lozzi RD, Roman HO, Arco M, Moreno FR, Pastorino M. Cat scratch lesions as a manifestation of chronic colitis due to spirochetosis. *Rev Esp Enferm Dig*. (2022) 114:693–4. doi: 10.17235/reed.2022.9078/2022

19. King AP, Donovan TA, Cohen E, Marin J, Le Roux AB. Short colon syndrome in cats. *J Vet Intern Med*. (2024) 38:2138–50. doi: 10.1111/jvim.17103

20. Lyu B, Wang Y, Fu H, Li J, Yang X, Shen Y, et al. Intake of high-purity insoluble dietary fiber from okara for the amelioration of colonic environment disturbance caused by acute ulcerative colitis. *Food Funct*. (2022) 13:213–26. doi: 10.1039/d1fo02264d

21. Jiang P, Zhang Y, Li X, Chen J. Geniposidic acid attenuates dss-induced colitis through inhibiting inflammation and regulating gut microbiota. *Phytother Res*. (2023) 37:3453–66. doi: 10.1002/ptr.7819

22. Xie Q, Zhang Y, Zhang Z, Gong S, Mo Q, Li J. Characteristics and dynamic changes of gut microbiota in cats with colitis. *Pak Vet J*. (2024) 44:414–22. doi: 10.29261/pakvetj/2024.175

23. Zhou G, Zhang N, Meng K, Pan F. Interaction between gut microbiota and immune checkpoint inhibitor-related colitis. *Front Immunol*. (2022) 13:1001623. doi: 10.3389/fimmu.2022.1001623

24. Li S, Jin Y, Fu W, Cox AD, Lee D, Reddivari L. Intermittent antibiotic treatment accelerated the development of colitis in il-10 knockout mice. *Biomed Pharmacother*. (2022) 146:112486. doi: 10.1016/j.biopha.2021.112486

25. Ozkul C, Ruiz VE, Battaglia T, Xu J, Roubaud-Baudron C, Cadwell K, et al. A single early-in-life antibiotic course increases susceptibility to dss-induced colitis. *Genome Med*. (2020) 12:65. doi: 10.1186/s13073-020-00764-z

26. Fu R, Wang L, Meng Y, Xue W, Liang J, Peng Z, et al. Apigenin remodels the gut microbiota to ameliorate ulcerative colitis. *Front Nutr*. (2022) 9:1062961. doi: 10.3389/fnut.2022.1062961

27. Fu W, Chen C, Xie Q, Gu S, Tao S, Xue W. *Pediococcus acidilactici* strain alleviates gluten-induced food allergy and regulates gut microbiota in mice. *Front Cell Infect Microbiol*. (2022) 12:845142. doi: 10.3389/fcimb.2022.845142

28. Meng Z, Sun W, Liu W, Wang Y, Jia M, Tian S, et al. A common fungicide tebuconazole promotes colitis in mice via regulating gut microbiota. *Environ Pollut*. (2022) 292:118477. doi: 10.1016/j.envpol.2021.118477

29. Jadhav A, Jagtap S, Vyavahare S, Sharbidre A, Kunchiraman B. Reviewing the potential of probiotics, prebiotics and synbiotics: advancements in treatment of ulcerative colitis. *Front Cell Infect Microbiol*. (2023) 13:1268041. doi: 10.3389/fcimb.2023.1268041

30. Chandhni PR, Pradhan D, Sowmya K, Gupta S, Kadyan S, Choudhary R, et al. Ameliorative effect of surface proteins of probiotic lactobacilli in colitis mouse models. *Front Microbiol*. (2021) 12:679773. doi: 10.3389/fmicb.2021.679773

31. Cordeiro BF, Alves JL, Belo GA, Oliveira ER, Braga MP, Da SS, et al. Therapeutic effects of probiotic minas frescal cheese on the attenuation of ulcerative colitis in a murine model. *Front Microbiol*. (2021) 12:623920. doi: 10.3389/fmicb.2021.623920

32. Cho H, Lee GY, Ali MS, Park S. Effects of dietary intake of heat-inactivated Limosilactobacillus reuteri PSC102 on the growth performance, immune response, and gut microbiota in weaned piglets. *Pak Vet J*. (2024) 44:819–25. doi: 10.29261/pakvetj/2024.224

33. Luo C, Wang L, Chen Y, Yuan J. Supplemental enzyme and probiotics on the growth performance and nutrient digestibility of broilers fed with a newly harvested corn diet. *Animals (Basel)*. (2022) 12:2381. doi: 10.3390/ani12182381

34. Yang Y, Yan G, Meng X, Wang X, Zhao Z, Zhou S, et al. Effects of Lactobacillus plantarum and *Pediococcus acidilactici* co-fermented feed on growth performance and gut microbiota of nursery pigs. *Front Vet Sci*. (2022) 9:1076906. doi: 10.3389/fvets.2022.1076906

35. Xu W, Liu Q, Fan S, Wang X, Lu S, Liu J, et al. Effect of ginsenoside fermented by *Pediococcus acidilactici* XM-06 on preventing diarrhea in mice via regulating intestinal barrier function and gut microbiota. *J Funct Foods*. (2024) 123:106594. doi: 10.1016/j.jff.2024.106594

36. Liu J, Wang Y, Li A, Iqbal M, Zhang L, Pan H, et al. Probiotic potential and safety assessment of Lactobacillus isolated from yaks. *Microb Pathog*. (2020) 145:104213. doi: 10.1016/j.micpath.2020.104213

37. Hu J, Nie Y, Chen J, Zhang Y, Wang Z, Fan Q, et al. Gradual changes of gut microbiota in weaned miniature piglets. *Front Microbiol*. (2016) 7:1727. doi: 10.3389/fmicb.2016.01727

38. Chen Y, Tian P, Li Y, Tang Z, Zhang H. Thiram exposure: disruption of the blood-testis barrier and altered apoptosis-autophagy dynamics in testicular cells via the bcl-2/bax and mtor/atg5/p62 pathways in mice. *Pest Biochem Physiol*. (2024) 203:106010. doi: 10.1016/j.pestbp.2024.106010

39. Wu S, Liu K, Huang X, Sun Q, Wu X, Mehmood K, et al. Molecular mechanism of mir-203a targeting runx2 to regulate thiram induced-chondrocyte development. *Pest Biochem Physiol*. (2024) 200:105817. doi: 10.1016/j.pestbp.2024.105817

40. Kasimir M, Behrens M, Schulz M, Kuchenbuch H, Focke C, Humpf HU. Intestinal metabolism of alpha-and beta-glucosylated modified mycotoxins t-2 and ht-2 toxin in the pig cecum model. *J Agric Food Chem*. (2020) 68:5455–61. doi: 10.1021/acs.jafc.0c00576

41. Sidaway P. Faecal transplantation reverses colitis. *Nat Rev Clin Oncol*. (2019) 16:66. doi: 10.1038/s41571-018-0139-3

42. Hwang J, Jin J, Jeon S, Moon SH, Park MY, Yum DY, et al. Sod1 suppresses pro-inflammatory immune responses by protecting against oxidative stress in colitis. *Redox Biol*. (2020) 37:101760. doi: 10.1016/j.redox.2020.101760

43. Moradipoor F, Jivad N, Asgharzadeh S, Zare E, Amini-Khoei H. Neuroimmune response and oxidative stress in the prefrontal cortex mediate seizure susceptibility in experimental colitis in male mice. *J Biochem Mol Toxicol*. (2024) 38:e23755. doi: 10.1002/jbt.23755

44. Zhang S, Sun Y, Nie Q, Hu J, Li Y, Shi Z, et al. Effects of four food hydrocolloids on colitis and their regulatory effect on gut microbiota. *Carbohydr Polym*. (2024) 323:121368. doi: 10.1016/j.carbpol.2023.121368

45. Gao R, Zhang X, Huang L, Shen R, Qin H. Gut microbiota alteration after long-term consumption of probiotics in the elderly. *Probiotics Antimicrob Proteins*. (2019) 11:655–66. doi: 10.1007/s12602-018-9403-1

46. Wang X, Zhang P, Zhang X. Probiotics regulate gut microbiota: an effective method to improve immunity. *Molecules*. (2021) 26:6076. doi: 10.3390/molecules26196076

47. Guo S, Geng W, Chen S, Wang L, Rong X, Wang S, et al. Ginger alleviates dss-induced ulcerative colitis severity by improving the diversity and function of gut microbiota. *Front Pharmacol*. (2021) 12:632569. doi: 10.3389/fphar.2021.632569

48. Li F, Han Y, Cai X, Gu M, Sun J, Qi C, et al. Dietary resveratrol attenuated colitis and modulated gut microbiota in dextran sulfate sodium-treated mice. *Food Funct*. (2020) 11:1063–73. doi: 10.1039/c9fo01519a

49. Li C, Wang M, Chen X, Chen W. Taraxasterol ameliorates dextran sodium sulfate-induced murine colitis via improving intestinal barrier and modulating gut microbiota dysbiosis. *Acta Biochim Biophys Sin*. (2022) 54:340–9. doi: 10.3724/abbs.2022019

50. Chen Y, Mai Q, Chen Z, Lin T, Cai Y, Han J, et al. Dietary palmitoleic acid reprograms gut microbiota and improves biological therapy against colitis. *Gut Microbes*. (2023) 15:2211501. doi: 10.1080/19490976.2023.2211501

51. Shen B, Wang J, Guo Y, Gu T, Shen Z, Zhou C, et al. Dextran sulfate sodium salt-induced colitis aggravates gut microbiota dysbiosis and liver injury in mice with non-alcoholic steatohepatitis. *Front Microbiol*. (2021) 12:756299. doi: 10.3389/fmicb.2021.756299

52. Pan X, Raaijmakers JM, Carrion VJ. Importance of bacteroidetes in host-microbe interactions and ecosystem functioning. *Trends Microbiol*. (2023) 31:959–71. doi: 10.1016/j.tim.2023.03.018

53. Sequeira RP, McDonald J, Marchesi JR, Clarke TB. Commensal bacteroidetes protect against *klebsiella pneumoniae* colonization and transmission through il-36 signalling. *Nat Microbiol*. (2020) 5:304–13. doi: 10.1038/s41564-019-0640-1

54. Gerges P, Bangarusamy DK, Bitar T, Alameddine A, Nemer G, Hleihel W. Turicibacter and catenibacterium as potential biomarkers in autism spectrum disorders. *Sci Rep*. (2024) 14:23184. doi: 10.1038/s41598-024-73700-5

55. Feng Z, Long W, Hao B, Ding D, Ma X, Zhao L, et al. A human stool-derived *bilophila wadsworthia* strain caused systemic inflammation in specific-pathogen-free mice. *Gut Pathog*. (2017) 9:59. doi: 10.1186/s13099-017-0208-7

56. Bin P, Tang Z, Liu S, Chen S, Xia Y, Liu J, et al. Intestinal microbiota mediates enterotoxigenic *escherichia coli*-induced diarrhea in piglets. *BMC Vet Res*. (2018) 14:385. doi: 10.1186/s12917-018-1704-9

57. Karasawa Y, Kato J, Kawamura S, Kojima K, Ohki T, Seki M, et al. Risk factors for acute cholangitis caused by enterococcus faecalis and *enterococcus faecium*. *Gut Liver*. (2021) 15:616–24. doi: 10.5009/gnl20214

58. Toc DA, Pandrea SL, Botan A, Mihaila RM, Costache CA, Colosi IA, et al. *Enterococcus raffinosus*, enterococcus durans and *enterococcus avium* isolated from a tertiary care hospital in Romania-retrospective study and brief review. *Biology Basel*. (2022) 11:598. doi: 10.3390/biology11040598

59. Cuevas-Sierra A, Riezu-Boj JI, Guruceaga E, Milagro FI, Martinez JA. Sex-specific associations between gut prevotellaceae and host genetics on adiposity. *Microorganisms*. (2020) 8:938. doi: 10.3390/microorganisms8060938

60. Seo SH, Unno T, Park SE, Kim EJ, Lee YM, Na CS, et al. Korean traditional medicine (jakyakgamcho-tang) ameliorates colitis by regulating gut microbiota. *Meta*. (2019) 9:226. doi: 10.3390/metabo9100226

61. Liu XF, Shao JH, Liao YT, Wang LN, Jia Y, Dong PJ, et al. Regulation of short-chain fatty acids in the immune system. *Front Immunol*. (2023) 14:1186892. doi: 10.3389/fimmu.2023.1186892

62. Schwarz A, Bruhs A, Schwarz T. The short-chain fatty acid sodium butyrate functions as a regulator of the skin immune system. *J Invest Dermatol*. (2017) 137:855–64. doi: 10.1016/j.jid.2016.11.014

63. Liu M, Peng R, Tian C, Shi J, Ma J, Shi R, et al. Effects of the gut microbiota and its metabolite short-chain fatty acids on endometriosis. *Front Cell Infect Microbiol*. (2024) 14:1373004. doi: 10.3389/fcimb.2024.1373004

64. He KY, Lei XY, Wu DH, Zhang L, Li JQ, Li QT, et al. *Akkermansia muciniphila* protects the intestine from irradiation-induced injury by secretion of propionic acid. *Gut Microbes*. (2023) 15:2293312. doi: 10.1080/19490976.2023.2293312

65. Ansaldo E, Slayden LC, Ching KL, Koch MA, Wolf NK, Plichta DR, et al. *Akkermansia muciniphila* induces intestinal adaptive immune responses during homeostasis. *Science*. (2019) 364:1179–84. doi: 10.1126/science.aaw7479

66. Ghotaslou R, Nabizadeh E, Memar MY, Law W, Ozma MA, Abdi M, et al. The metabolic, protective, and immune functions of *akkermansia muciniphila*. *Microbiol Res*. (2023) 266:127245. doi: 10.1016/j.micres.2022.127245

67. Huwart S, de Wouters DA, Rastelli M, Van Hul M, de Vos WM, Luquet S, et al. Food reward alterations during obesity are associated with inflammation in the striatum in mice: beneficial effects of *akkermansia muciniphila*. *Cells*. (2022) 11:2534. doi: 10.3390/cells11162534

68. Zhou Q, Zhang Y, Wang X, Yang R, Zhu X, Zhang Y, et al. Gut bacteria akkermansia is associated with reduced risk of obesity: evidence from the American gut project. *Nutr Metab*. (2020) 17:90. doi: 10.1186/s12986-020-00516-1

69. Wang ZJ, Liang CL, Li GM, Yu CY, Yin M. Neuroprotective effects of arachidonic acid against oxidative stress on rat hippocampal slices. *Chem Biol Interact*. (2006) 163:207–17. doi: 10.1016/j.cbi.2006.08.005

70. Schonfeld P, Wojtczak L. Fatty acids decrease mitochondrial generation of reactive oxygen species at the reverse electron transport but increase it at the forward transport. *Biochim Biophys Acta*. (2007) 1767:1032–40. doi: 10.1016/j.bbabio.2007.04.005

71. Lopez-Huertas E, Palma JM. Changes in glutathione, ascorbate, and antioxidant enzymes during olive fruit ripening. *J Agric Food Chem*. (2020) 68:12221–8. doi: 10.1021/acs.jafc.0c04789

72. Lu C, Jiang Y, Yue Y, Sui Y, Hao M, Kang X, et al. Glutathione and neodiosmin feedback sustain plant immunity. *J Exp Bot*. (2023) 74:976–90. doi: 10.1093/jxb/erac442

73. Gunderson MP, Nguyen BT, Cervantes RJ, Holden LL, French J, Smith BD, et al. Response of phase i and ii detoxification enzymes, glutathione, metallothionein and acetylcholine esterase to mercury and dimethoate in signal crayfish (*pacifastacus leniusculus*). *Chemosphere*. (2018) 208:749–56. doi: 10.1016/j.chemosphere.2018.05.183

frontiers | Frontiers in Microbiology

TYPE Original Research
PUBLISHED 01 April 2025
DOI 10.3389/fmicb.2025.1558802

OPEN ACCESS

EDITED BY
Qinghong Li,
Nestle Purina Research, United States

REVIEWED BY
Yanfen Cheng,
Nanjing Agricultural University, China
Tales Fernando da Silva,
Institute of Biological Sciences, Brazil

*CORRESPONDENCE
Holly H. Ganz
holly@animalbiome.com

RECEIVED 11 January 2025
ACCEPTED 04 March 2025
PUBLISHED 01 April 2025

CITATION
Dione N, Mlaga KD, Liang S, Jospin G, Marfori Z, Alvarado N, Scarsella E, Uttarwar R and Ganz HH (2025) Comparative genomic and phenotypic description of *Escherichia ruysiae*: a newly identified member of the gut microbiome of the domestic dog.
Front. Microbiol. 16:1558802.
doi: 10.3389/fmicb.2025.1558802

Comparative genomic and phenotypic description of *Escherichia ruysiae*: a newly identified member of the gut microbiome of the domestic dog

Niokhor Dione, Kodjovi D. Mlaga, Siyi Liang, Guillaume Jospin, Zara Marfori, Nancy Alvarado, Elisa Scarsella, Ruchita Uttarwar and Holly H. Ganz*

AnimalBiome, Oakland, CA, United States

Introduction: *Escherichia ruysiae* is a newly identified species within the *Escherichia genus*, yet its presence in domestic animals remains largely unexamined. This study characterizes four isolates detected for the first time in the domestic dog (Canis lupus familiaris), focusing on their phenotypic and genomic features.

Methods: We used culturomic methods to isolate four *E. ruysiae* isolates that were initially identified as *Escherichia coli* using MALDI-TOF mass spectrometry. Whole-genome sequencing confirmed that the isolates belonged to *E. ruysiae*, not *E. coli*. Phenotypic characterization included enzymatic activity assays and antimicrobial susceptibility testing. Comparative genomic analyses were performed on these four isolates, along with 14 additional *E. ruysiae* and representative genomes from the five other *Escherichia species* in order to assess genetic diversity and functional gene distribution.

Results and discussion: All strains exhibited similar enzymatic activities and resistance to clindamycin, erythromycin, and metronidazole. The pangenome analysis revealed that most missing gene orthologs are related to motility followed by metabolism, including synthetases, reductases, phosphatases, permeases, transferases, and epimerases, as well as structural genes like efflux pumps and transporters. Phylogroup typing using the ClermonTyping method identified two main groups within the *E. ruysiae* species, Clade III and IV. Typical virulence genes associated with *E. coli* are absent in these strains. The multiple approaches used in this study expand our understanding of the diverse aspects of the recently described species, *E. ruysiae*.

KEYWORDS

***Escherichia ruysiae*, canine microbiome, culturomics, whole genome sequencing, taxono-genomic**

Introduction

The gut microbiota of humans and animals comprises a diverse array of microbes that play critical roles in digestion, immune system function, and overall health. Advances in sequencing technologies, particularly metagenomics, have greatly enhanced our understanding of microbiome composition, enabling the discovery and characterization of new microorganisms and elucidating their roles in host biology. However, the identification of novel microorganisms remains largely dependent on existing databases of known species, limiting the scope of metagenomics. Only culture-based methods can recover live and previously unknown microorganisms (Ju et al., 2022).

Culturomics has emerged in the last decade as a powerful tool to culture and identify unknown bacteria in humans, animals, and the environment. The method consists of diversifying the culture media and conditions for the same sample by modifying parameters such as incubation time, temperature, pH, and atmosphere, or by adding inhibitory or growth factors such as antibiotics, promoters such as blood, and rumen fluid to culture low abundant and or fastidious populations, followed by the rapid identification by MALDI-TOF mass spectrometry. It enables the culture of enormous numbers of new microorganisms, including new species and genera associated with animal and human health and diseases, providing new perspectives on host–microbe interactions (Lagier et al., 2018, 2024).

We are conducting a major effort to identify and characterize the microbiome of domestic dogs. As part of this initiative we have identified over 400 *E. coli* isolates, through different steps: MALDI-TOF for initial screening, qPCR for species confirmation, multiplex PCR for phylogrouping (Dogan et al., 2020) and Whole Genome Sequencing (WGS) to classify serotype and pathogenicity groups. Following WGS we discovered a subset of isolates with a distinct core genome compared to the rest. Further analysis using the Average Nucleotide Identity (ANI) confirmed that these isolates represent a different species within the *Escherichia* genus: *E. ruysiae*.

Non-*Escherichia coli* encompasses cryptic *clades I, II, III*, and *IV*, and *E. ruysiae* is the latest species described within the *Escherichia genus*. This genus also includes four other species: *Escherichia coli*, *Escherichia albertii*, *Escherichia fergusonii*, and *Escherichia marmotae*. The first *E. ruysiae* strain was isolated from a fecal sample collected in the Netherlands from a human (*Homo sapiens*) who may have acquired the strain while traveling internationally for a month in Asia and developed traveler's diarrhea (van der Putten et al., 2021). So far, its dissemination and potential role in human and animal health is not well characterized. *Escherichia ruysiae* was subsequently isolated from a fecal sample collected from a Lohmann Brown layer hen (*Gallus gallus domesticus*) on a farm in England (Thomson et al., 2022) and from a fecal sample collected from an urban dwelling large-billed crow (*Corvus macrorhynchos*) in Japan (Sakaguchi et al., 2023).

In this context of wide dissemination, it is important to understand the genomic features that underline their spread, mechanisms of acquisition of antimicrobial and virulence genes, and the genomic characteristics that support their evolution. Here we describe the phenotypic and genomic features of these new isolates from the domestic dog and perform a comparative genomics analysis with representative species of other *Escherichia* available in the public repository NCBI.

Materials and methods

Sample information, culture, and identification

The stool sample used in this study was collected from a healthy spayed female 9-year-old Shepherd-Husky mix living in Oakland, California, United States. After collection, the samples were transported to the laboratory and homogenized using BIOME-Preserve AS-930 (Anaerobe Systems, Morgan Hill, CA) in a one-to-one ratio. This sample was processed as part of our culturomics efforts to characterize the microbiome of companion pets by culturing, isolating, identifying, and characterizing bacteria. The *E. ruysiae* strains that are the focus of this study were isolated following culturomics protocols as previously described by Lagier et al. (2012). Briefly, 100 µL of the aliquoted sample was serially diluted (10^{-1}–10^{-10}) in Dilution Blank AS-9183 (Anaerobe Systems, Morgan Hill, CA) then 70 µL of each dilution was inoculated into a MacConkey agar plate (Becton Dickinson, Franklin Lakes, NJ 07417), and incubated aerobically at 37°C for 24 h. Following standard procedures, grown colonies were first identified using the MALDI–TOF mass spectrometer (MS). A scrapped colony is deposited on a disposable MALDI-TOF MS target plate (Bruker Daltonics, Bremen, Germany) and covered first with 2 µL of 70% formic acid solution and dried before being covered by 2 µL of a MALDI matrix solution (saturated α-cyano acid-4- hydroxycinnamic in 50% acetonitrile, 47.5% HPLC water, and 2.5% trifluoroacetic acid). After drying, analysis was performed using MALDI Biotyper smart System RUO microflex LT/SH smart with the BIDAL database v12 (Bruker Daltonics, Bremen, Germany). A triplex PCR was carried out using the Clermont typing method (Clermont et al., 2000) followed by whole genome sequencing using the Pacific Biosciences Sequel IIe.

Phenotypic characterization

The newly isolated bacterial strains were identified first using the MALDI-TOF MS instrument (Bruker Daltonics, Bremen, Germany) as per a previous study (Asare et al., 2023). Additionally, bacterial characterization was conducted utilizing the Gram staining technique (Sigma Aldrich, MA, United States), while motility was observed using the hanging drop method under a light microscope (Accu-Scope, NY, United States), as described in earlier studies (Jain et al., 2020). The catalase, oxidase (bioMérieux, Marcy-l'Étoile, France), and biochemical tests API ZYM (bioMérieux, Marcy-l'Étoile, France) were conducted to study the bacterial phenotypic characteristics. Furthermore, these strains were also visualized to characterize their morphology and structure. Fixed bacteria were placed on a 400 mesh Formvar-coated copper grid that had been previously subjected to glow discharge (Electron Microscopy Sciences, PA, United States). Following a settlement period of 2 min for the bacteria, the grids were thoroughly rinsed with UranyLess EM Stain (Electron Microscopy Sciences, PA, United States) and the remaining UranyLess EM Stain was removed. Once dried, the grids were imaged at a voltage of 120 kV using a Tecnai 12 (Thermo Fisher Scientific, Waltham, MA, United States) Transmission Electron Microscope (TEM), located in the Electron Microscope Lab at the University of California, Berkeley.

Antimicrobial susceptibility testing

We used the disk diffusion method to screen the antimicrobial susceptibility of all bacteria isolates. We screened the *E. ruysiae* isolates against 11 antibiotic drugs, sourced from Thermo Fisher Scientific (Waltham, MA, United States), using the following disks: Metronidazole 50 µg, Cefpodoxime 10 µg, Enrofloxacin 5 µg, Erythromycin 15 µg, Amoxicillin/Clavulanic acid 30 µg, Tetracycline 30 µg, Sulfamethoxazole/Trimethoprim 25 µg, Doxycycline 30 µg, Clindamycin 2 µg, Gentamicin 10 µg, and Chloramphenicol 30 µg. We inoculated *E. ruysiae* isolates onto Columbia agar plates and

incubated them at 37°C for 24 h. Pure colonies were introduced into Dilution Blank AS-9183 (Anaerobe Systems, Morgan Hill, CA) to prepare a 0.5 McFarland bacterial suspension. This suspension was then used to inoculate Mueller Hinton agar plates Becton Dickinson BBL™ (Franklin Lakes, NJ, United States) using a wet swab following the SLCI guidelines. Antibiotic disks were then placed on the surface of the plates with the aid of a Sensi-disk self-tamping 8-place dispenser Becton Dickinson BBL™ (Franklin Lakes, NJ, United States). The plates were incubated at 37°C for 24 h and inhibition zones were read by BIOMIC V3 (Giles Scientific in Santa Barbara, CA, United States). Each isolate was tested in triplicate.

DNA extraction and whole genome sequencing

We extracted DNA using the ZymoBIOMICS™ DNA Miniprep Kit for bacterial cells (Zymo Research, Irvine, CA, United States). The samples were first prepared by inoculating a bacterial colony into a 2 mL microcentrifuge tube containing 1,000 µL phosphate buffered saline (PBS) (Thermo Fisher Scientific, Waltham, MA, United States) and centrifuging at 5,000 RPM for 10 min. The PBS was removed without dislodging the pellet. Twenty µl of 20 mg/mL lysozyme & 750 µL ZymoBIOMICS lysis solution was then added and incubated at 37°C for 40 min. The samples were then transferred to ZR BashingBead™ Lysis tubes and secured in a Vortex-Genie® 2 mixer fitted with a 2 mL tube holder adapter and vortexed at full speed for 40 min. DNA concentration was measured using a Qubit 4 Fluorometer (Thermo Fisher Scientific, Waltham, MA, United States). Genomic DNA was sheared to a 7–12 kb fragment length on a Megaruptor 3 (Diagenode LLC., Denville, NJ, United States). The quality of the DNA was examined on a 2% agarose gel. The sequencing library was prepared following the manufacturer's protocol using the SMRTbell prep kit 3.0 and and the isolates were barcoded using the SMRTbell barcoded adapter plate 3.0 (Pacific Biosciences, Menlo Park, CA, United States). We loaded 115 µL of the pooled library onto a 96-well sample plate and prepared it for a sequencing run on a Sequel IIe sequencer using Binding kit 3.2, Sequencing kit 2.0, and SMRT Cell 8 M (Pacific Biosciences, Menlo Park, CA, United States). The library was sequenced using a 15-h movie. HiFi data was obtained from the raw subreads using the circular consensus sequencing process.

Comparative genomics

Genome assembly and annotation

All sequencing reads were screened for quality control using Fastqc v0.12.1 (Andrews, 2010). The sequencing reads were filtered with a Phred score > 30, renamed by sample ID, and assembled using Canu assembler v2.3 (Koren, et al. 2017) with default parameters. The final scaffold files produced were screened for level of contamination and purity using CheckM2 v1.0.2 (Chklovski et al., 2023) and taxonomically classified using GTDB-Tk v2.4.0 (RefDB version r220) (Chaumeil et al., 2022). We annotated the four genomes using Prokka v1.14.6 (Seemann, 2014) with an *e*-value set to 0.00001, a minimum coverage of 95%, using the specific database of the genus *Escherichia* (Supplementary Table S1). In addition, 14 genomes of *E. ruysiae* (Supplementary Table S2) and one representative genome of each other species in the *Escherichia* genus (Supplementary Table S3) were also retrieved from the NCBI Refseq database for comparative analysis purposes and re-annotated using the same methods.

Isolate sequence typing, serogrouping and phylogrouping

We performed an *in silico* Multi-Locus Sequence Type (MLST) analysis using MLST package, version 2.23.0,[1] adapted from https://pubmlst.org (Jolley and Maiden, 2010) using these seven housekeeping genes: *adk, fumC, gyrB, icd, mdh, purA,* and *recA*. *Escherichia ruysiae* species are part of the cryptic clades I, II, III, and IV (Walk, 2015). We used the software ClermonTyping version 1.4.0 (Beghain et al., 2018) to determine the phylogroups of all the genomes.

Pangenome analysis

We performed a pangenome analysis, searching for clusters of ortholog genes using get_homologues v22082022 (Contreras-Moreira and Vinuesa, 2013; Vinuesa and Contreras-Moreira, 2015). We used two approaches to search for ortholog genes, namely OrthoMCL v1.4 (OMCL) (Li et al., 2003) and Clusters of Orthologous Genes (COG) triangles v2.1 (Kurtz et al., 2004; Kristensen et al., 2010) clustering algorithm. Sequence similarity requires an equal Pfam domain, and all clusters detected were reported. The processes were performed locally using default parameters. First we calculated the Average Nucleotide Identity (ANI) and the Percentage of Conserved Proteins (POCPs) of the *Escherichia* genus in order to determine the level of delineation and to determine the relatedness of the newly isolated four strains to publicly available *E. ruysiae* genomes. Then in order to support the ANI-based species delineation, we constructed a core genome midpoint-rooted Maximum Likelihood phylogenetic tree of 23 species, including 18 *E. ruysiae* strains and five representative genomes from other *Escherichia* species, using 1,000 bootstrap replicates. We computed the core and pan-genomes, including their evolution, composition, and the parsimony tree of *E. ruysiae* strains using the intersection of both OMCL and COG approaches. In addition, we queried the pangenome to determine accessory (shell) and specific (cloud) ortholog genes of our strains versus others.

Phylogenetic reconstruction, genomics markers, resistome and virulome

We performed a whole and a core genome alignment of all 18 genomes of *E. ruysiae* using *scapper*,[2] a simple and fast SNP alignment tool that uses mummer v4.0.0 (Kurtz et al., 2004) and Trimal v1.4.rev22 (Capella-Gutiérrez et al., 2009). We reconstructed the phylogenetic evolution of the core genome using FastTree v2.1 (Price et al., 2009). We screened the resistome profile by mapping the full genome of *E. ruysiae* to various resistance gene databases including NCBI (Feldgarden et al., 2019), and ARGANNOT (Gupta et al., 2014), ResFinder (Zankari et al., 2012), CARD (McArthur et al., 2013) and MEGARes 2.0 (Bonin et al., 2023) to determine genes associated to antimicrobial resistance using ABRicate software.[3]

1 https://github.com/tseemann/mlst
2 https://github.com/tseemann/scapper
3 https://github.com/tseemann/abricate

Results

Culture, isolation, and phenotypic characterization

Strains AB134, AB135, AB136, and AB137 were isolated in July 2022 after 24 h of incubation on a MacConkey Agar plate (BD) following the culturomics process. A pure colony of each isolate was tentatively identified using MALDI-TOF mass spectrometry (MBT Sirius One RUO; Bruker Daltonics, Bremen, Germany). The four strains were identified as *E. coli* with a score of 1.8 which is the identification threshold at the genus level. This result was due to the absence of a reference spectrum of *E. ruysiae* in the Bruker BIDAL database v12 used in the analysis. The triplex PCR also did not allow clear identification of *E. ruysiae* We performed whole genome sequencing using PacBio sequencing technology and identified the strains *AB134, AB135, AB136*, *AB137* as *E. ruysiae* with Gtdbtk based on the Average Nucleic Identity (ANI), which were 98.94, 98.93, 98.92, and 97.1%, respectively. Gram staining performed using the Sigma Aldrich Gram Staining Kit (St. Louis MI, United States) showed Gram-negative bacilli rod-shaped (Figure 1A). After identification, we performed a protein extraction as recommended by Bruker to generate a reference spectrum (Figure 1B) using 12 individual colonies of strains AB134 grown on in-house LB agar (Waltham, MA, United States) made from a dehydrated medium.

The rod-shaped bacilli form was confirmed by electron microscopy, where strain *AB134* exhibited a mean length of 1.8 µm and width of 0.6 µm (Figure 1C). When grown on MacConkey agar plates, *E. ruysiae* exhibit irregular dark white colonies with a diameter of about 0.3–0.8 mm (Figure 1D). Evaluation of enzymatic activity of *E. ruysiae* strains AB134, AB135, AB136, and AB137 using API ZYM revealed that all strains exhibited similar enzymatic activities with positive reactions observed with alkaline phosphatase, leucine arylamidase, acid phosphatase, naphthol-AS-BI-phosphohydrolase α-galactosidase, ß-galactosidase, and α-glucosidase. All *E. ruysiae* show negative activity on the other hand with the following enzymes: esterase (C4), esterase lipase (C8), lipase (C14), valine arylamidase, cystine arylamidase, trypsin, α-chymotrypsin, α-galactosidase, ß-glucuronidase, ß-glucosidase, N-acetyl-ß-glucosaminidase, α-mannosidase, and α-fucosidase (Table 1). The API 20E profile evaluating amino acids, salts, activity, and carbon source shows Positive activity for 2-nitrophenyl-üD galactopyranoside, L-ornithine, sodium pyruvate, D-glucose, D-mannitol, D-sorbitol, L-rhamnose, and L-arabiose, and negative activity for L-arginine, L-lysine, trisodium citrate, sodium thiosulfate, urea, L-tryptophan, gelatin (bovine origin), D-saccharose, D-melibiose, and amygdalin (Table 1).

From the disk diffusion method, these *E. ruysiae* strains exhibited susceptibility to cefpodoxime, enrofloxacin, chloramphenicol, tetracycline, doxycycline, trimethoprim-sulfamethoxazole, and gentamicin. The strains exhibited resistance to clindamycin, erythromycin, and metronidazole, while showing an intermediate response for amoxicillin-clavulanate (Table 2; Figure 2).

Genome features, taxono-genomics, and genomic description

Genomes of the four strains were submitted and referenced in the NCBI database with the respective accession numbers: *E. ruysiae* strain AB134 (JAVIWR000000000), *E. ruysiae* strain AB135 (JAVIWS000000000), *E. ruysiae strain* AB136 (JAVIWT000000000), and *E. ruysiae strain* AB137 (JAVIWU000000000). The genomes were assembled, annotated, and genome features described (Table 3). All genomes are circularized in one contig of 4.5 Mb average size and

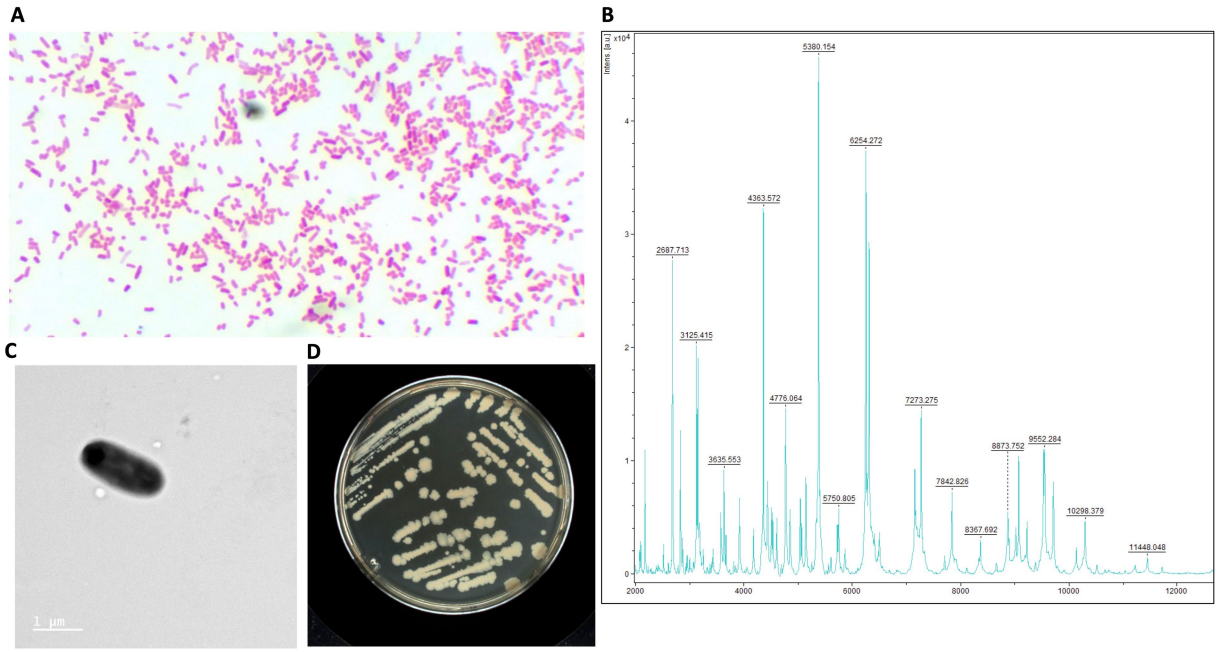

FIGURE 1
Structural and phenotypic characterization of *E. ruysiae* (strain AB135). **(A)** Gram stain of colonies under 100X light microscopy, **(B)** MALDI-TOF spectrum, **(C)** Electronic microscopy with rod-shape bacterium, **(D)** Colony morphology and color on LB agar.

10.3389/fmicb.2025.1558802

TABLE 1 Structure, morphology, and phenotypic characteristics of *E. ruysiae*, strains AB134, AB135, AB136, and AB137. The type strain OPT1704T is listed here to indicate that it was not characterized phenotypically.

Substrates tested	*E. ruysiae* AB134	*E. ruysiae* AB135	*E. ruysiae* AB136	*E. ruysiae* AB137	*E. ruysiae* OPT1704T
Basic characteristics					
Oxygen requirement	Facultative anaerobe	Facultative anaerobe	Facultative anaerobe	Facultative anaerobe	Facultative anaerobe
Gram stain	–	–	–	–	
Motility	Non-motile	Non-motile	Non-motile	Non-motile	
Endospore formation	–	–	–	–	
Enzyme					
Alkaline phosphatase	+	+	+	+	NA
Esterase (C 4)	–	–	–	–	NA
Esterase Lipase (C 8)	–	–	–	–	NA
Lipase (C 14)	–	–	–	–	NA
Leucine arylamidase	+	+	+	+	NA
Valine arylamidase	–	–	–	–	NA
Cystine arylamidase	–	–	–	–	NA
Trypsin	–	–	–	–	NA
α-chymotrypsin	–	–	–	–	NA
Acid phosphatase	+	+	+	+	NA
Naphthol-AS-BI-phosphohydrolase α-galactosidase	+	+	+	+	NA
α-galactosidase	–	–	–	–	NA
ß-galactosidase	+	+	+	+	NA
ß-glucuronidase	–	–	–	–	NA
α-glucosidase	+	+	+	+	NA
ß-glucosidase	–	–	–	–	NA
N-acetyl-ß-glucosaminidase	–	–	–	–	NA
α-mannosidase	–	–	–	–	NA
α-fucosidase	–	–	–	–	NA
Amino acids/salts/carbon source					
2-Nitrophenyl-üD galactopyranoside	+	+	+	+	NA
L-Arginine	–	–	–	–	NA
L-Lysine	–	–	–	–	NA
L-Ornithine	+	+	+	+	NA
Trisodium citrate	–	–	–	–	NA
Sodium thiosulfate	–	–	–	–	NA
Urea	–	–	–	–	NA
L-Tryptophan	–	–	–	–	NA
L-Tryptophan	+	+	+	+	NA
Sodium pyruvate	+	+	+	+	NA
Gelatin (bovine origin)	–	–	–	–	NA
D-Glucose	+	+	+	+	NA
D-Mannitol	+	+	+	+	NA
Inositol	–	–	–	–	NA
D-Sorbitol	+	+	+	+	NA

(Continued)

TABLE 1 (Continued)

Substrates tested	*E. ruysiae AB134*	*E. ruysiae AB135*	*E. ruysiae AB136*	*E. ruysiae AB137*	*E. ruysiae OPT1704T*
L-Rhamnose	+	+	+	+	NA
D-Saccharose	–	–	–	–	NA
D-Melibiose	–	–	–	–	NA
Amygdalin	–	–	–	–	NA
L-Arabiose	+	+	+	+	NA
Origin	Canine gut	Canine gut	Canine gut	Canine gut	NA

TABLE 2 Antimicrobial Susceptibility testing results of *E. rusyiae* strains AB134, AB135, AB135, AB136 compared to *E. ruysiae* strains S1-IND-07-A (Campos-Madueno et al., 2023).

Antibiotics	ZD (mm) value for new isolates				MIC value (mg/mL)
	AB134	AB135	AB136	AB137	S1-IND-07-A
Cefpodoxime	25(S)	25(S)	22(S)	26(S)	2(S)
Enrofloxacin	34(S)	30(S)	34(S)	34(S)	NA
Chloramphenicol	22(S)	21(S)	22(S)	22(S)	NA
Tetracycline	22(S)	22(S)	22(S)	22(S)	NA
Trimethoprim-sulfamethoxazole	29(S)	26(S)	28(S)	29(S)	>4/76(S)
Clindamycin	6(R)	6(R)	6(R)	6(R)	NA
Doxycycline	21(S)	20(S)	22(S)	21(S)	16
Amoxicillin-clavulanate	19(S)	19(S)	19(S)	19(S)	NA
Erythromycin	10(R)	10	10(R)	10(R)	NA
Gentamicin	21(S)	22(S)	21	21(S)	≤1(S)
Metronidazole	6(R)	6(R)	6(R)	6(R)	NA

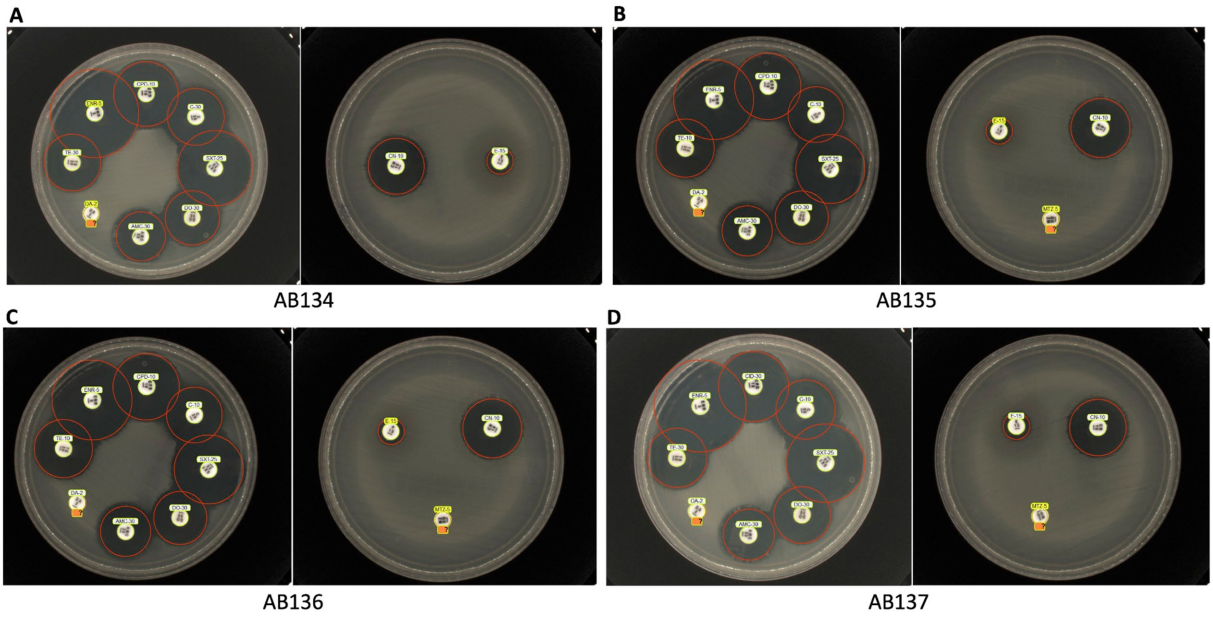

FIGURE 2
Antimicrobial susceptibility testing of *E. ruysiae* isolates. The figure shows results for multiple isolates AB134 **(A)**, AB135 **(B)**, AB136 **(C)**, and AB137 **(D)** against trimethoprim-sulfamethoxazole, cefpodoxime, enrofloxacin, chloramphenicol, tetracycline, doxycycline, amoxicillin-clavulanate, gentamicin, clindamycin, erythromycin, and metronidazole (with the exception that metronidazole susceptibility was not tested for AB134).

TABLE 3 *E. ruysiae* genomes features from genome assembly and annotation.

Isolate ID	Contigs	Genome size*	N50	Susp. Plasmids	Completeness	CDS	genes	Repeat regions	rRNA	tRNA	mRNA	GC%
AB134	2	4,635,588	4,540,385	95,207	100	4,252	4,367	3	22	92	1	50.67
AB135	2	4,632,218	4,537,266	94,952	100	4,253	4,368	3	22	92	1	50.68
AS136	2	4,635,326	4,540,375	94,951	100	4,248	4,363	3	22	92	1	50.67
AB137	2	4,635,425	4,540,363	95,062	100	4,261	4,376	3	22	92	1	50.67

95 kb of circularized plasmid. We checked the quality of the assemblies with CheckM which indicated 100% completeness with an average GC% of 50.6%. Genomic accession numbers, bioproject number, and links for the four new *E. ruysiae* genomes are provided in Supplementary material (Supplementary Table S1). The genomes were taxonomically classified using Gtdbtk and the results indicated that all four genomes are identified as *E. ruysiae* with a minimum of 97.1% of Average Nucleotide Identity (ANI) and 0.95 of Alignment Fraction (AF) with *E. ruysiae* GCF_902498915.1 (Supplementary material). We computed the overall ANI of all the available genomes of *E. ruysiae* including reference genomes of *E. coli*, *E. marmotae*, *E albertii*, *E. fergusonii*, and *E. whittamii* using the OMCL ortholog finding algorithm in get_homologes with default parameters. The heatmap (Figure 3A) indicates that all the *E. ruysiae* (red square) forms a distinct cluster, separate from other *Escherichia* species (white to blue). Additionally, *E. ruysiae* are clustered in two distinct groups, with a minimum of 97.47% and a maximum of 98.6% ANI. The four strains sequenced in this study AB134, AB135, AB136, and AB137 belong to the same group with ANI ranging from 98.94 to 97.6%. The closest related species is *E. coli* NC000913 with 95% on average and the most distant species is *E. fergusonii strain* FDAARGOS 1499 (ANI: 92.41–92.51%). The core genome midpoint-rooted Maximum Likelihood tree indicates that all *E. ruysiae* strains are closely related, forming two distinct clusters separate from the other species (Figure 3B). In contrast, *E. coli*, *E. marmotae*, *E. whittamii*, *E. albertii*, and *E. fergusonii* exhibit more distant relationships.

Pangenome description of *E. ruysiae* species

We clustered the genes from all genomes into ortholog genes using get homolog. From the 18 publicly available genomes (Supplementary Table S2), we identified 6,714 total genes from both OMCL (173 specifics) and COG (186 specifics) with 3,231 genes included in the hard core genes (present in all 18 genomes) and 3,330 genes in the soft core (at least 17 genomes possess these genes). One thousand four hundred eighty-five genes were shared across 10 to 95% of the genomes (accessory or shell genes) and 1899 genes are specific to each genome (cloud genes). The hard core genome estimation using the Tettelin fit converged with residual standard error = 100.76 and fitting value from 4,105 genes to 3,284 following the equation:

$$C(g) = 3284 + 1324 * e^{(-g/2.10)}$$

Using the Willenbrock method, the residual error was estimated to be 95.08 with the fitting value from 4,142 to 3,256 following the equation (Figure 4A):

$$C(g) = 3217 + 18362 * e^{\left(-\sqrt{\{()\sqrt{g}\}}/0.33\right)}$$

Tettelin fitting methods revealed that the variation in gene numbers from the 16th genome onwards is negligible, with only four additional genes identified after the 11th genome. This suggests that the hard core genome has reached a stable state and undergoes minimal variation. The

10.3389/fmicb.2025.1558802

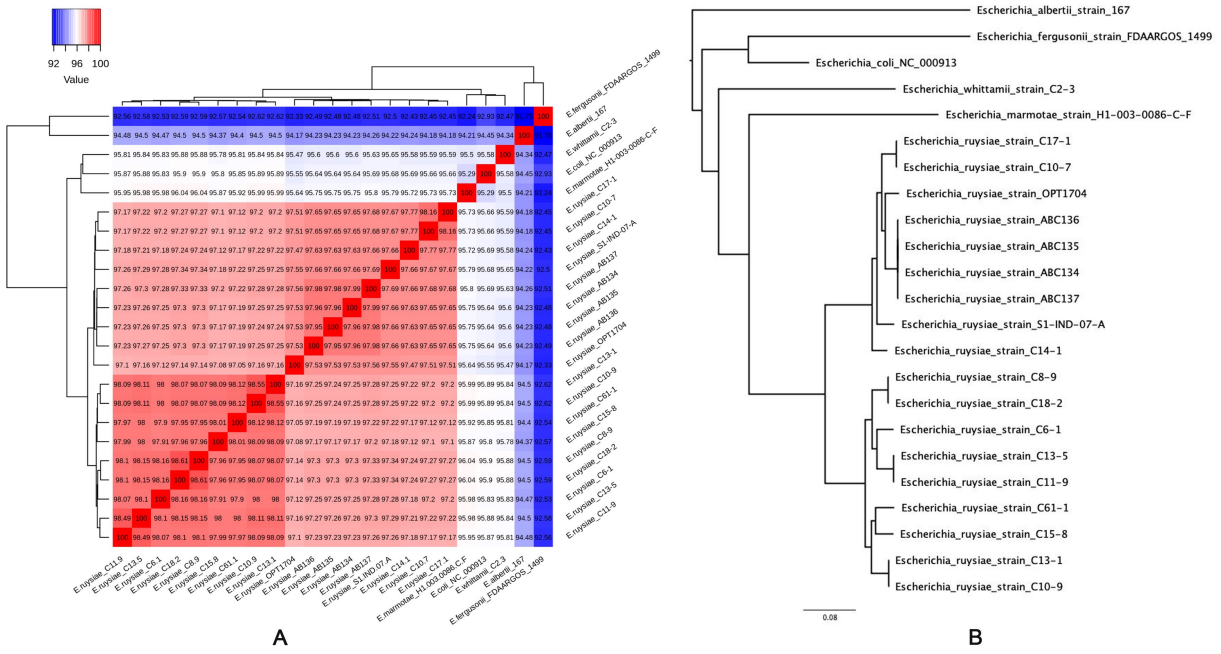

FIGURE 3
Average Nucleotide Identity (ANI) of *E. ruysiae*, *E. coli*, *E. marmotae*, *E. whittami*, *E. albertii*, and *E. fergusonii*. **(A)** Heatmap with overall ANI of all the available genomes of *E. ruysiae*. **(B)** Midpoint rooting maximum likelihood tree based on core genome alignment (RAxML best tree).

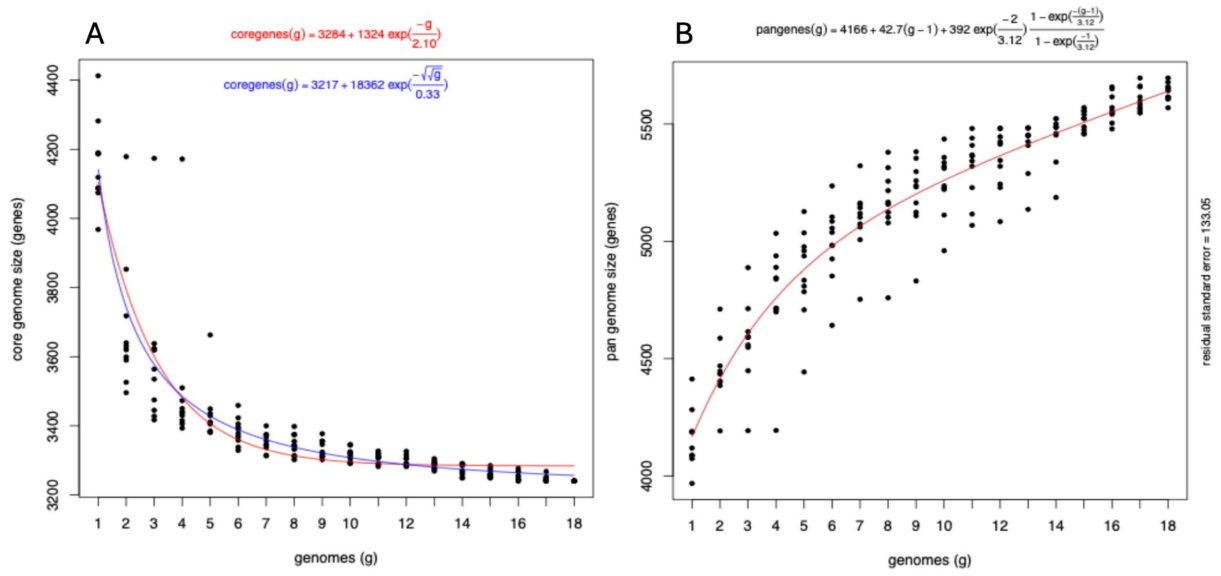

FIGURE 4
Evolution of the pangenome of *E. ruysiae*. **(A)** Hard core genome estimation using the Tettelin fit with residual error estimated using the Willenbrock method. **(B)** Pangenome fit is consistent with an open pangenome.

pan-genome also fit converged with the estimated residual error of 133.05 following the curve equation of

$$P(g) = 4166 + 42.7 * (g-1) + 392 * e^{(-2/3.12)} * \left(1 - e^{(-(g-1)/3.12)}\right) / \left(1 - e^{(-1/3.12)}\right)$$

This equation shows the pangenome size keeps increasing indefinitely when adding a new genome, hence is interpreted as representing an open pangenome (Figure 4B). The four genomes sequenced for this study: AB134, AB135, AB136, and AB137 have altogether 147 unique groups of genes including accessory and unique genes, and are missing 923 groups of genes. The unique group of genes includes genes associated with virulence such as

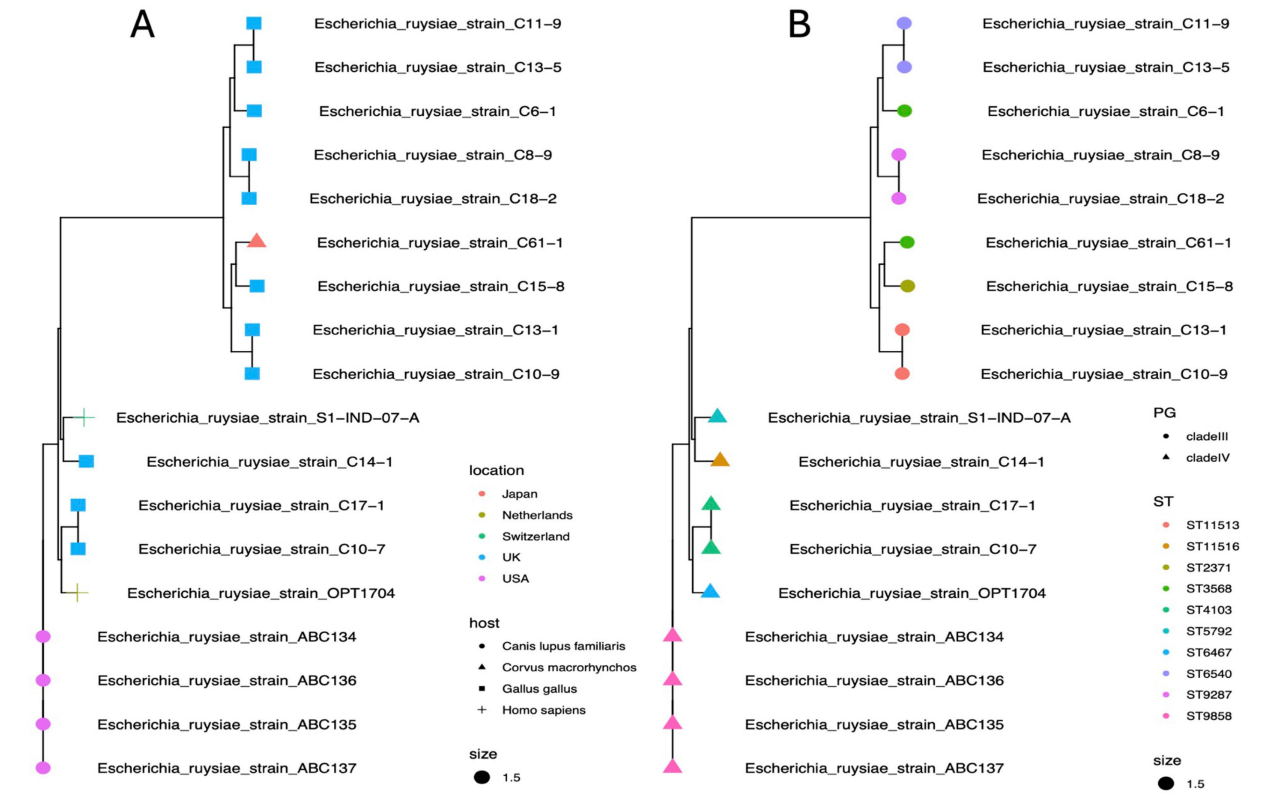

FIGURE 5
Maximum likelihood phylogenetic reconstruction of *E. ruysiae* using core genome alignment. **(A)** Tree showing diversity by geographical location (tip colors) and host (tip shapes). **(B)** Tree showing diversity by phylogroups (tip shapes) and sequence types (ST, tip colors).

invasin (group 1,338), type II secretion system protein J, G, F, and E (*xcpW, epsG, epsF*, and *epsE* respectively), flagella-associated system genes (*flgL, flgH, flgG, flgH, flgE, flgC, tagD, fliI, fliE, vnfA, fliP, flihB*), *flagellin*, and *adhesin BmaC*. we also identified groups of genes associated with evolution mechanisms that include transposon and phage transfer and acquisition [Insertion sequence family transposase (*ISSen1* and *ISEc48* among many others), *endonuclease* and *endoribonuclease, recombinase, prophage integrase (IntS)*]. The majority of missing groups of genes are motility-associated genes and metabolism-associated genes including synthetases, reductases, phosphatases, permeases, transferases, and epimerases, as well as structural-related genes such as efflux pumps and transporters (Supplementary Figure S1).

Phylogenetic analysis and evolution of *E. ruysiae* species

Phylogroup typing using the ClermonTyping method showed that there are two main groups within the *E. ruysiea* species, namely *Clade III* characterized by genes *trpA, trpBA*, and *chuIII* and *Clade IV* characterized by the genes *trpBA, chuIV*, and facultatively *trpAgpC*. All typical genes for *E. coli* typing were absent (*arpA, chuA, yjaA*, and *TspE4.C2*). All genomes sequenced for this study belong to *Clade IV*. The topology of the estimated phylogenetic tree, based on the core genome, shows two distinct clades positioned on separate branches with a midpoint rooting layout (Figure 5A). The phylogenetic distribution and the clade type are neither geographically- nor host-dependent. Strains isolated from chicken occur in both *Clades III* and *IV* while the human and dog strains isolated to date only occur in *Clade IV* (Figure 5B). All *Clade III* strains including the sequencing type (ST): *ST6540, ST3568, ST9287, ST2371*, and *ST11513* are located on the top branch, and the *Clade IV* with ST: *ST6467, ST11516, ST4103, ST5792, ST9858* on the bottom branch (Figure 5B). Analysis of the 18 *E. ruysiae* isolates suggests that phylogenetic distribution and clade type are not strongly associated with geography or host species. However, this pattern likely reflects the limited number of isolates identified to date, given that *E. ruysiae* is a recently described cryptic species. Expanding efforts to isolate *E. ruysiae* from diverse hosts across a broad geographical range may provide deeper insights into the evolution of these clades and their adaptations to different environments.

Resistome and virulome description

We identified genes associated with antimicrobial resistance in all genomes. Aminoglycoside resistance genes *Agly-aadA (aminoglycoside-3-adenyltransferase)* and penicillin-binding protein (*Bla-Pbinding protein*) occurred in all strains. Beta-lactamase *BlaCTX-14, Bla-CTX-8*, and *Bla-CTX-15* can be identified among both clades. The strain *C6-1* isolated from chicken feces possesses some virulence genes but lacks common resistance genes, suggesting

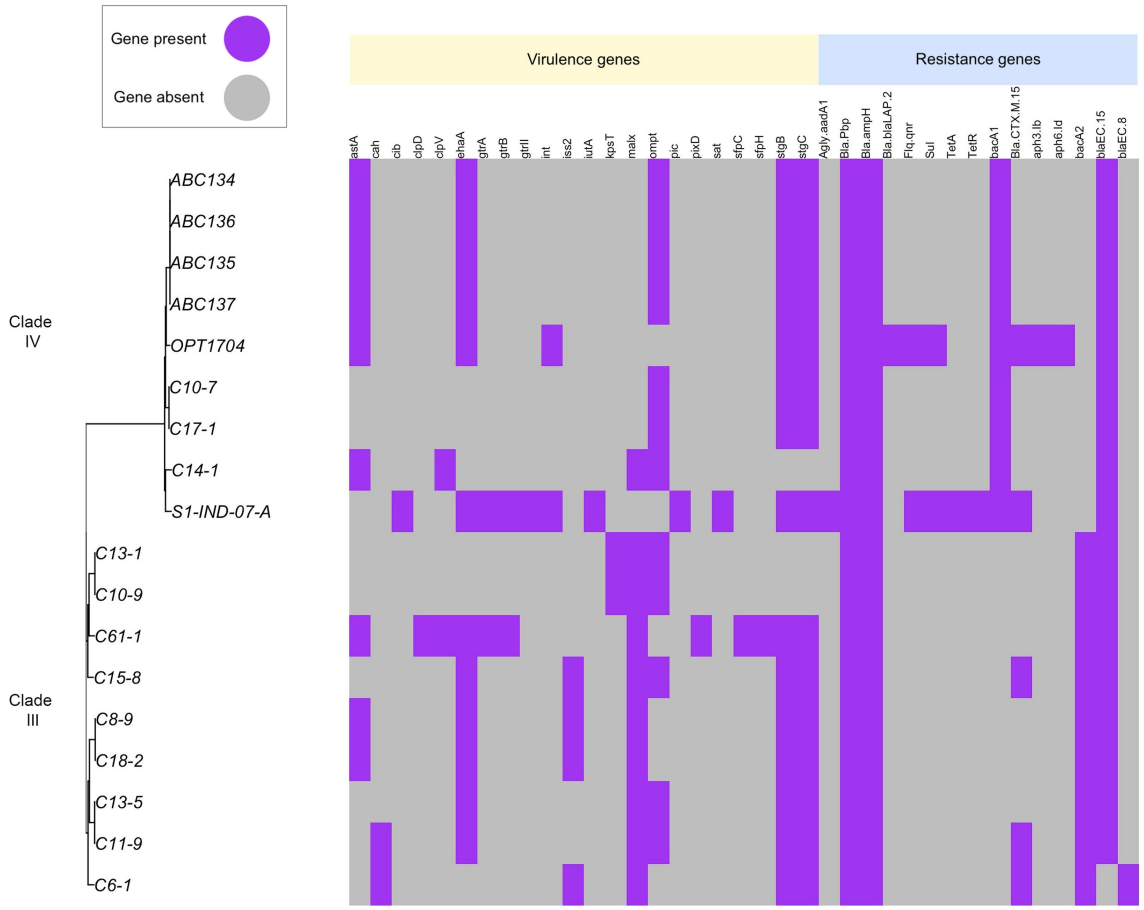

FIGURE 6
Distribution of virulence genes and antimicrobial resistance genes across *E. ruysiae*. Strain C6-1 isolated from chicken feces possesses some virulence genes but lacks common resistance genes, suggesting potential for infection but possibly treatable with a relatively wide range of antibiotics. Strains from humans (OPT1704, S1-IND-07-A) harbor both virulence genes and multiple resistance genes, indicating a potentially high risk for antibiotic-resistant infections. Aminoglycoside resistance genes Agly-aadA (aminoglycoside-3-adenyltransferase) and penicillin-binding protein (Bla-Pbinding protein) were found in all strains. Beta-lactamase BlaCTX-14, Bla-CTX-8, and Bla-CTX-15 were identified in both clades.

potential for infection but possibly treatable with a wider range of antibiotics. Human strains (*OPT1704, S1-IND-07-A*) harbor both virulence genes and multiple resistance genes, indicating a potential risk for antibiotic-resistant infections (Figure 6).

Discussion

The first successful isolation and culturing of *E. ruysiae* from the fecal microbiome of a healthy domestic dog in western United States expands our understanding of its host range and geographic distribution. The reported isolation of *E. ruysiae* from a diversity of animal hosts (a human traveler (van der Putten et al., 2021), an urban wild crow (Sakaguchi et al., 2023), a domestic chicken (Thomson et al., 2022), and now a domestic dog) on three different continents (Europe, Asia, North America) underscores the adaptability of this species and suggests a global distribution. Using culturomic and genomic techniques, we gained new insights into the previously elusive growth requirements and metabolic capabilities of *E. ruysiae*, findings that may help facilitate future isolation efforts.

All strains isolated in this study grew on MacConkey Agar plates, forming colonies with distinct size and color after 18–24 h aerobic incubation at 37°C, following the culturomics process (Lagier et al., 2018). Previous studies reported that *E. ruysiae* forms circular, gray-white colonies on a Columbia sheep blood agar plates after overnight incubation at 37°C (Van Der Putten et al., 2021). MALDI-TOF was unable to distinguish between *E. coli* and *E. ruysiae* because the spectral profile for *E. ruysiae* had not yet been included in the databases of both the MALDI-TOF (Bruker Daltonics, Bremen, Germany) and VITEK2 (BioMérieux, Marcy-l'Étoile, France) systems (van der Putten et al., 2021). The differences between these species became apparent only when we compared the genomes of the isolates with those of *E. coli*. Whole genome sequencing, which confirmed the identification of *E. ruysiae*, remains the gold standard for accurate taxonomic identification, and highlights the limitations of MALDI-TOF when using an incomplete database. Nonetheless the MALDI-TOF remains an excellent identification tool, particularly for well characterized species and is invaluable for culturing-based microbiome analysis (Demir and Hazırolan, 2024).

A detailed phenotypic characterization of *E. ruysiae* strains revealed distinctive features that may contribute to the bacterium's ecological niche. Analysis of biochemical properties and antibiotic susceptibility profiles highlighted the species' phenotypic diversity. Notably, reduced motility and probable loss of flagella were consistent with the initial description of *E. ruysiae* (van der Putten et al., 2021) and may represent an adaptation to a commensal lifestyle. Similar loss of flagellar motility was observed in an experimental evolution study where non-symbiotic *E. coli* evolved into an insect mutualist (Koga et al., 2022). Additional virulence-associated traits warrant further investigation to better understand the ecological relevance and potential pathogenicity of *E. ruysiae* across different environments.

Comparative analysis of the antimicrobial susceptibility of our strains and *E. ruysiea* strain S1-IND-07-A from Campos-Madueno et al. (2023), revealed similar susceptibility to gentamicin, cefpodoxime, and trimethoprim-sulfamethoxazole., Importantly, the antimicrobial resistance findings in our study are not too concerning from a public health perspective because only the Bla-CTX-15 gene was detected in the genomes of the four isolates. However, all four strains exhibited resistance to clindamycin (lincosamide), erythromycin (macrolide), and metronidazole (nitroimidazole) in the *in vitro* disk diffusion AST profiles.

Pangenome analysis provided further insights into the genomic diversity and adaptive potential of *E. ruysiae*. The expansive accessory genome and the exponential pangenome evolution underscore the species' genomic plasticity and its ability to acquire and integrate genetic materials from diverse sources, thereby shaping its evolutionary trajectory. This plasticity likely supports the organism's capacity to live and adapt to various environments and niches. Additionally, phylogrouping based on core genome analysis allowed us to categorize *E. ruysiae* strains into two distinct phylogenetic groups, providing a useful framework for understanding their evolutionary relationships and tracking the geographical and ecological distribution of the species.

In conclusion, our study integrates culturomic, phenotypic, pangenomic, and phylogenetic analyses to provide a robust foundation for further exploration of the ecological, evolutionary, and clinical significance of the recently described species *E. ruysiae*.

Data availability statement

All four genomes sequenced for the study were submitted and referenced in the NCBI database (https://www.ncbi.nlm.nih.gov/bioproject/PRJNA1010808/) with the respective accession numbers *E. ruysiae* strain AB134 (JAVIWR000000000), *E. ruysiae* strain AB135 (JAVIWS000000000), *E. ruysiae* strain AB136 (JAVIWT000000000), and *E. ruysiae* strain AB137 (JAVIWU000000000).

Ethics statement

The stool sample used to isolate *E. ruysiae* was obtained non-invasively with the informed consent of the pet owner.

Author contributions

ND: Conceptualization, Data curation, Formal analysis, Investigation, Methodology, Project administration, Supervision, Validation, Writing – original draft, Writing – review & editing. KM: Data curation, Formal analysis, Investigation, Methodology, Software, Validation, Visualization, Writing – original draft, Writing – review & editing. SL: Investigation, Writing – review & editing. GJ: Data curation, Software, Writing – review & editing. ZM: Investigation, Writing – review & editing. NA: Investigation, Writing – review & editing. ES: Investigation, Methodology, Writing – review & editing. RU: Investigation, Writing – review & editing. HG: Conceptualization, Funding acquisition, Project administration, Resources, Supervision, Writing – original draft, Writing – review & editing.

Funding

The author(s) declare that financial support was received for the research and/or publication of this article. This research was funded by AnimalBiome.

Acknowledgments

The authors thank the pet parents for their consent and contributions to our research on the microbiota in companion animals, including *Escherichia* spp. In particular, we thank Cindy S. for providing Rosie's donations, which yielded these interesting findings.

Conflict of interest

The authors declare that the research was conducted in the absence of any commercial or financial relationships that could be construed as a potential conflict of interest.

Generative AI statement

The author(s) declare that no Gen AI was used in the creation of this manuscript.

Publisher's note

Supplementary material

The Supplementary material for this article can be found online at: https://www.frontiersin.org/articles/10.3389/fmicb.2025.1558802/full#supplementary-material

References

Andrews, S. (2010). FastQC: a quality control tool for high throughput sequence data. Available online at: http://www.bioinformatics.babraham.ac.uk/projects/fastqc/.

Asare, P. T., Lee, C.-H., Hürlimann, V., Teo, Y., Cuénod, A., Akduman, N., et al. (2023). Corrigendum: a MALDI-TOF MS library for rapid identification of human commensal gut bacteria from the class Clostridia. *Front. Microbiol.* 14:1208177. doi: 10.3389/fmicb.2023.1208177

Beghain, J., Bridier-Nahmias, A., Le Nagard, H., Denamur, E., and Clermont, O. (2018). ClermonTyping: an easy-to-use and accurate *in silico* method for Escherichia genus strain phylotyping. *Microb. Genom.* 4:e000192. doi: 10.1099/mgen.0.000192

Bonin, N., Doster, E., Worley, H., Pinnell, L. J., Bravo, J. E., Ferm, P., et al. (2023). MEGARes and AMR++, v3.0: an updated comprehensive database of antimicrobial resistance determinants and an improved software pipeline for classification using high-throughput sequencing. *Nucleic Acids Res.* 51, D744–D752. doi: 10.1093/nar/gkac1047

Chklovski, A., Parks, D. H., Woodcroft, B. J., and Tyson, G. W. (2023). CheckM2: a rapid, scalable and accurate tool for assessing microbial genome quality using machine learning. *Nature methods*, 20, 1203–1212.

Clermont, O., Bonacorsi, S., and Bingen, E. (2000). Rapid and simple determination of the Escherichia coli phylogenetic group. *AEM*, 66, 4555–4558.

Campos-Madueno, E. I., Aldeia, C., Sendi, P., and Endimiani, A. (2023). *Escherichia ruysiae* may serve as a reservoir of antibiotic resistance genes across multiple settings and regions. *Microbiol. Spectr.* 11:e0175323. doi: 10.1128/spectrum.01753-23

Capella-Gutiérrez, S., Silla-Martínez, J. M., and Gabaldón, T. (2009). trimAl: a tool for automated alignment trimming in large-scale phylogenetic analyses. *Bioinformatics* 25, 1972–1973. doi: 10.1093/bioinformatics/btp348

Chaumeil, P.-A., Mussig, A. J., Hugenholtz, P., and Parks, D. H. (2022). GTDB-Tk v2: memory friendly classification with the genome taxonomy database. *bioRxiv*. doi: 10.1101/2022.07.11.499641

Contreras-Moreira, B., and Vinuesa, P. (2013). GET_HOMOLOGUES, a versatile software package for scalable and robust microbial pangenome analysis. *Am. Soc. Microbiol.* 79, 7696–7701. doi: 10.1128/AEM.02411-13

Demir, M., and Hazırolan, G. (2024). Rapid bacterial identification from positive blood cultures by MALDI-TOF MS following short-term incubation on solid media. *Infect. Dis. Clin. Microbiol.* 6, 141–146. doi: 10.36519/idcm.2024.319

Dogan, B., Zhang, S., Kalla, S. E., Dogan, E. I., Guo, C., Ang, C. R., et al. (2020). Molecular and phenotypic characterization of Escherichia coli associated with granulomatous colitis of boxer dogs. *Antibiotics*, 9, 540.

Feldgarden, M., Brover, V., Haft, D. H., Prasad, A. B., Slotta, D. J., Tolstoy, I., et al. (2019). Validating the AMRFinder tool and resistance gene database by using antimicrobial resistance genotype-phenotype correlations in a collection of isolates. *Antimicrob. Agents Chemother.* 63:e00483-19. doi: 10.1128/AAC.00483-19

Gupta, S. K., Padmanabhan, B. R., Diene, S. M., Lopez-Rojas, R., Kempf, M., Landraud, L., et al. (2014). ARG-ANNOT, a new bioinformatic tool to discover antibiotic resistance genes in bacterial genomes. *Antimicrob. Agents Chemother.* 58, 212–220. doi: 10.1128/AAC.01310-13

Jain, A., Jain, R., and Jain, S., (2020). Basic techniques in biochemistry, microbiology and molecular biology (pp. 181–183). New York, NY, USA: Springer.

Jolley, K. A., and Maiden, M. C. J. (2010). BIGSdb: scalable analysis of bacterial genome variation at the population level. *BMC Bioinformatics* 11:595. doi: 10.1186/1471-2105-11-595

Ju, Y., Wang, X., Wang, Y., Li, C., Yue, L., and Chen, F. (2022). Application of metagenomic and culturomic technologies in fecal microbiota transplantation: a review. *Sheng Wu Gong Cheng Xue Bao* 38, 3594–3605. doi: 10.13345/j.cjb.220573

Kristensen, D. M., Kannan, L., Coleman, M. K., Wolf, Y. I., Sorokin, A., Koonin, E. V., et al. (2010). A low-polynomial algorithm for assembling clusters of orthologous groups from intergenomic symmetric best matches. *Bioinformatics* 26, 1481–1487. doi: 10.1093/bioinformatics/btq229

Koga, R., Moriyama, M., Onodera-Tanifuji, N., Ishii, Y., Takai, H., and Mizutani, M., et al. (2022). Single mutation makes Escherichia coli an insect mutualist. *Nature Microbiology*, 7, 1141–1150.

Koren, S., Walenz, B. P., Berlin, K., Miller, J. R., Bergman, N. H., and Phillippy, A. M., (2017). Canu: scalable and accurate long-read assembly via adaptive k-mer weighting and repeat separation. *Genome research*, 27, 722–736.

Kurtz, S., Phillippy, A., Delcher, A. L., Smoot, M., Shumway, M., Antonescu, C., et al. (2004). Versatile and open software for comparing large genomes. *Genome Biol.* 5:R12. doi: 10.1186/gb-2004-5-2-r12

Lagier, J. C., Armougom, F., Million, M., Hugon, P., Pagnier, I., Robert, C., et al. (2012). Microbial culturomics: paradigm shift in the human gut microbiome study. *Clin. Microbiol. Infect*, 18, 1185–1193.

Lagier, J.-C., Dubourg, G., Million, M., Cadoret, F., Bilen, M., Fenollar, F., et al. (2018). Culturing the human microbiota and culturomics. *Nat. Rev. Microbiol.* 16, 540–550. doi: 10.1038/s41579-018-0041-0

Lagier, J.-C., Khelaifia, S., Alou, M. T., Ndongo, S., Dione, N., Hugon, P., et al. (2024). Retraction note: culture of previously uncultured members of the human gut microbiota by culturomics. *Nat. Microbiol.* 10:601. doi: 10.1038/s41564-024-01894-5

Li, L., Stoeckert, C. J. J., and Roos, D. S. (2003). OrthoMCL: identification of ortholog groups for eukaryotic genomes. *Genome Res.* 13, 2178–2189. doi: 10.1101/gr.1224503

McArthur, A. G., Waglechner, N., Nizam, F., Yan, A., Azad, M. A., Baylay, A. J., et al. (2013). The comprehensive antibiotic resistance database. *Antimicrob. Agents Chemother.* 57, 3348–3357. doi: 10.1128/AAC.00419-13

Price, M. N., Dehal, P. S., and Arkin, A. P. (2009). FastTree: computing large minimum evolution trees with profiles instead of a distance matrix. *Mol. Biol. Evol.* 26, 1641–1650. doi: 10.1093/molbev/msp077

Sakaguchi, K., Tanabe, M., Takizawa, S., Kasahara, S., Denda, T., Koide, S., et al. (2023). Zoonotic potential and antimicrobial resistance of Escherichia spp. in urban crows in Japan-first detection of E. Marmotae and E. Ruysiae. *Comp. Immunol. Microbiol. Infect. Dis.* 100:102040. doi: 10.1016/j.cimid.2023.102040

Seemann, T. (2014). Prokka: rapid prokaryotic genome annotation. *Bioinformatics* 30, 2068–2069. doi: 10.1093/bioinformatics/btu153

Thomson, N. M., Gilroy, R., Getino, M., Foster-Nyarko, E., van Vliet, A. H. M., La Ragione, R. M., et al. (2022). Remarkable genomic diversity among *Escherichia* isolates recovered from healthy chickens. *PeerJ* 10:e12935. doi: 10.7717/peerj.12935

Van Der Putten, B. C. L., Matamoros, S., Mende, D. R., Scholl, E. R., Consortium, C., and Schultsz, C. (2021). *Escherichia ruysiae* sp. nov., a novel gram-stain-negative bacterium, isolated from a faecal sample of an international traveller. *Int. J. Syst. Evol. Microbiol.* 71:004609. doi: 10.1099/ijsem.0.004609

Vinuesa, P., and Contreras-Moreira, B. (2015). Robust identification of orthologues and paralogues for microbial pan-genomics using GET_HOMOLOGUES: a case study of pIncA/C plasmids. *Methods Mol. Biol.* 1231, 203–232. doi: 10.1007/978-1-4939-1720-4_14

Walk, S. T. (2015). The "cryptic" Escherichia. *EcoSal Plus* 6, 10–1128. doi: 10.1128/ecosalplus.ESP-0002-2015

Zankari, E., Hasman, H., Cosentino, S., Vestergaard, M., Rasmussen, S., Lund, O., et al. (2012). Identification of acquired antimicrobial resistance genes. *J. Antimicrob. Chemother.* 67, 2640–2644. doi: 10.1093/jac/dks261

Frontiers in Microbiology

Explores the habitable world and the potential of microbial life

The largest and most cited microbiology journal which advances our understanding of the role microbes play in addressing global challenges such as healthcare, food security, and climate change.

Discover the latest Research Topics

See more →

Frontiers

Avenue du Tribunal-Fédéral 34
1005 Lausanne, Switzerland
frontiersin.org

Contact us

+41 (0)21 510 17 00
frontiersin.org/about/contact